Carbonate facies, diagenesis and sequence stratigraphy of an eocene nummulitic seservoir interval (jdeir formation), offshore NW Libya

Abdelhakim S. Alhnaish

Carbonate Facies, Diagenesis and Sequence Stratigraphy of an Eocene Nummulitic Reservoir Interval (Jdeir Formation), Offshore NW Libya

Abdelhakim. S. Alhnaish

Supervisor: Dr. Moyra Wilson

A thesis submitted to the University of Durham of degree of Masters in carbonate sedimentology

Department of Earth Science

January, 2006.

Declaration

The contents of this thesis are the original work of the author and have not previously been submitted for a degree at this or any other university. The work of other people is acknowledged by reference.

Abdelhakim. S. Alhnaish
Department of Earth Science
University of Durham
January, 2006.

Carbonate Facies, Diagenesis and Sequence Stratigraphy of an Eocene Nummulitic Reservoir Interval, (Jdeir Formation) Offshore NW Libya

ABSTRACT

This study investigates the sedimentology, petrology and depositional environments of a major Early Eocene nummulitic reservoir unit: the Jdeir Formation, from offshore NW Libya in the Mediterranean Sea. This formation is a prolific hydrocarbon-producing unit that was deposited as part of the Mesozoic-Cenozoic stratigraphic fill of the Sabratah Basin. The Sabratah Basin is an elongate ESE/WNW trending fault-bounded basin that originated as a left lateral pull-apart basin during the Late Triassic-Early Jurassic. Presented in this thesis is a review of the tectonostratigraphic setting of the Jdeir Formation, an evaluation of the facies and an interpretation of the depositional environment of the platform. During this Master project, diagenesis was also evaluated with the aim of better understanding reservoir development of the Jdeir Formation.

On the basis of detailed core description and petrographic study eight facies have been distinguished. These are: (1) Planktonic Foraminifera Facies, (2) *Discocyclina*-Nummulite Facies, (3) Nummulite Facies, (4) *Alveolina* Facies, (5) Peloidal-Bioclastic Facies, (6) Mollusc Facies, (7) Echinoderm Facies and (8) Sandy-Bioclastic Facies. These are interpreted as having been deposited in open-marine, fore-bank, bank, lagoonal (back-bank) and restricted lagoonal environments. Nummulitic rudstones, dominated by B-forms with minor A-forms, comprise the upper part of bank, and float/rudstones form the lower part of the bank. Abrasion and fragmentation of bioclasts resulted from the transport of sediment from palaeohighs and their reaccumulation into intra-, or back-bank environments. *Discocyclina* and planktonic foraminifera-rich facies formed in open-marine environments, with the former accumulating towards the base of the photic zone. The back-bank or lagoonal deposits are highly variable, were sometimes affected by siliciclastic influx, and may be dominated by molluscs, echinoderm debris or imperforate foraminifera. Facies and thickness variations between the three wells were controlled by the

palaeotopography and palaeoenvironments of the Sabratah Basin. It is appears that the depositional settings of the shallow platform deposits were more variable than has been previously documented.

The carbonates of the Jdeir Formation have been altered by a variety of diagenetic processes as inferred from petrography, cathodoluminescence, SEM and stable isotope analysis. The diagenetic sequence involved initial marine diagenesis including micritization, which has obliterated much of the original fabric of many skeletal grains, and the formation of micrite envelopes also occurred at this time. Leaching of bioclasts and the matrix has created vuggy and mouldic porosity, which is now commonly partially or completely filled by drusy and minor blocky calcite cements and rare kaolinite cement. Recrystallization of micrite to microspar and pseudospar is attributed to meteoric diagenesis, which has occluded some of the original porosity. The final diagenetic features include development of dissolution seams, stylolites and fractures, coarse calcite spar, dolomitization, silicification and pyrite. All these later diagenetic features are inferred to have occurred in a burial environment. As a result of these diagenetic processes, Nummulitic limestones of the Jdeir Formation have lost most of their primary porosity. Secondary porosity formed through the dissolution of aragonitic skeletons and micritic matrix during meteoric diagenesis, and possible also late burial diagenesis.

The overall sequence stratigraphic interpretation of the Jdeir Formation would most likely be transgressive deposits (transgressive system tract) based on underlying early dolomite which is associated with tidal flat deposits and overlying deep marine deposits. Intra-formation smaller-scale trends most likely formed under transgressive, stillstand and regressive conditions. The incomplete well data through the Jdeir Formation and different numbers of transgressive and regressive cycles in each well makes formation-wide correlation problematic.

Acknowledgements

Firstly I must thank my parents, my wife and my children. This thesis could have not been completed without their continued encouragement and support.

I must thank also my supervisor, Dr. Moyra Wilson, for her continued encouragement through all stages of this project. She has guided me through the world of carbonate sedimentology and diagenesis. The exhaustive reviews of the drafts by Dr. Moyra Wilson have greatly improved this thesis. Her patience and generosity are greatly appreciated.

I would like to thank Prof. Maurice Tucker and Dr. Tony Adams for their constructive comments and suggestions, which greatly improved the quality of this thesis.

I acknowledge the support of Petroleum Research Centre in providing the funds for the project; special thanks must go the General manger of PRC Dr Bourima Ali Belgassem for his ongoing support. I wish to thank to all the staff of Petroleum Research Centre, particularly the Exploration Department for their support and encouragement, many thanks also to staff of Exploration Department in Agip Oil Company for providing me with all the data needed for this project.

I would like to thank all the staff in Earth Science department: Carole Blair, Karen Atkinson and Janice Oakes for their general helpfulness and Dave Stevenson and Gary Wilkinson for their support and help with the computer and Colin Macpherson for his time spent helping with the isotope analysis.

Finally, I wish to thank my brother and my sisters for their help and encouragement.

Table of contents

List of Figures

Chapter 1:

Chapter 2:

Chapter 3:

Chapter 4:

Chapter 5:

List of Tables

CHAPTER ONE

1. THESIS INTRODUCTION

INTRODUCTION:

This study investigates the sedimentology, diagenesis and sequence stratigraphy of the Early Eocene Jdeir reservoir interval (Upper part of the Farwah Group) in the Sabratah Basin, offshore Northwestern Libya. The study presented in this thesis concentrates on the Jdeir Formation, and includes the analysis and interpretation of data from three exploration wells drilled by Agip Company within the NC41 Concession (Tables 1.1 and 1.2). The focus of this study, the Jdeir Formation, is the main reservoir target in the Sabratah Basin. The Bouri field is one of the largest fields offshore north-west Libya (40000-80000 bbl/day), discovered by Agip-ENL in 1976, which has proven reserves of 2 billion barrels and a possible 5 billion barrels of oil reservoired in the Jdeir Formation. This work has implications for reservoir development in other Paleogene limestones containing abundant larger foraminifera.

1.1- AIMS OF THE STUDY:

These are four main aims of this study:

- To study the main facies of the Jdeir Formation (Upper unit of the Farwah Group) in the A2, B7 and E1-NC41 wells of the north-western Libya offshore area (Figure 1.1) and to determine their depositional environment. The wells have been carefully chosen to allow variations from the platform to the basin margin to be evaluated.
- To undertake a detailed investigation of petrography and diagenesis and to evaluate the influence of depositional texture and diagenesis on reservoir characteristics.
- To apply sequence stratigraphic methods of analysis to the Jdeir Formation using the variation in facies tracts and stacking patterns and to relate them to changes in relative sea level.
- To compare the depositional models, diagenesis and reservoir development of the Jdeir Formation with other comparable units rich in larger benthic foraminifera to better understand global variations in Paleogene limestones and their reservoir quality.

Well Name	Formation	Core No	Top (ft)	Bottom (ft)	Thickness	Thin-sections No
A2-NC41	Jdeir	10	9060.0	9300.0	240	28
B7-NC41	Jdeir	13	8248.0	8650.0	402	36
E1-NC41	Jdeir	11	8257.0	8575.0	318	28

Table 1.1. Conventional core data and thin-sections studied from the three oil wells selected from the Jdeir Formation.

Well Name	Formation	Top (ft)	Bottom (ft)	Thickness (ft)
A2-NC41	Jdeir	9041.0	9300.0	259
B7-NC41	Jdeir	8222.0	8812.0	590
E1-NC41	Jdeir	8225.0	8825.0	600

Table 1.2. Well log data from the three oil wells selected from the Jdeir Formation.

1.2-LOCATION OF THE STUDIED AREA:

The study area is located offshore north-western Libya, situated on the extreme north-western margin of the Africa shield, within the Sabratah Basin (Figure 1.1).

1.3-METHODOLOGY:

Data available for this study is core, thin-section and wireline data from three subsurface wells in the offshore Libya area (Figure 1.1). The cores were described in detail, logged and photographed at the geological labs in Agip Company. On the basis of core analyses 28 thin-sections from cores A2-NC41 well were prepared in the geological labs at Petroleum Research Centre, Libya. In addition, 36 thin-sections from B7-NC41 Well and 28 thin-sections from E1-NC41 Well were prepared in the Earth Science labs at Durham University. These thin-sections were examined petrographically in order to observe rock fabric and to determine the presence and abundance of constituent grains, matrix and cements. The prepared thin-sections were

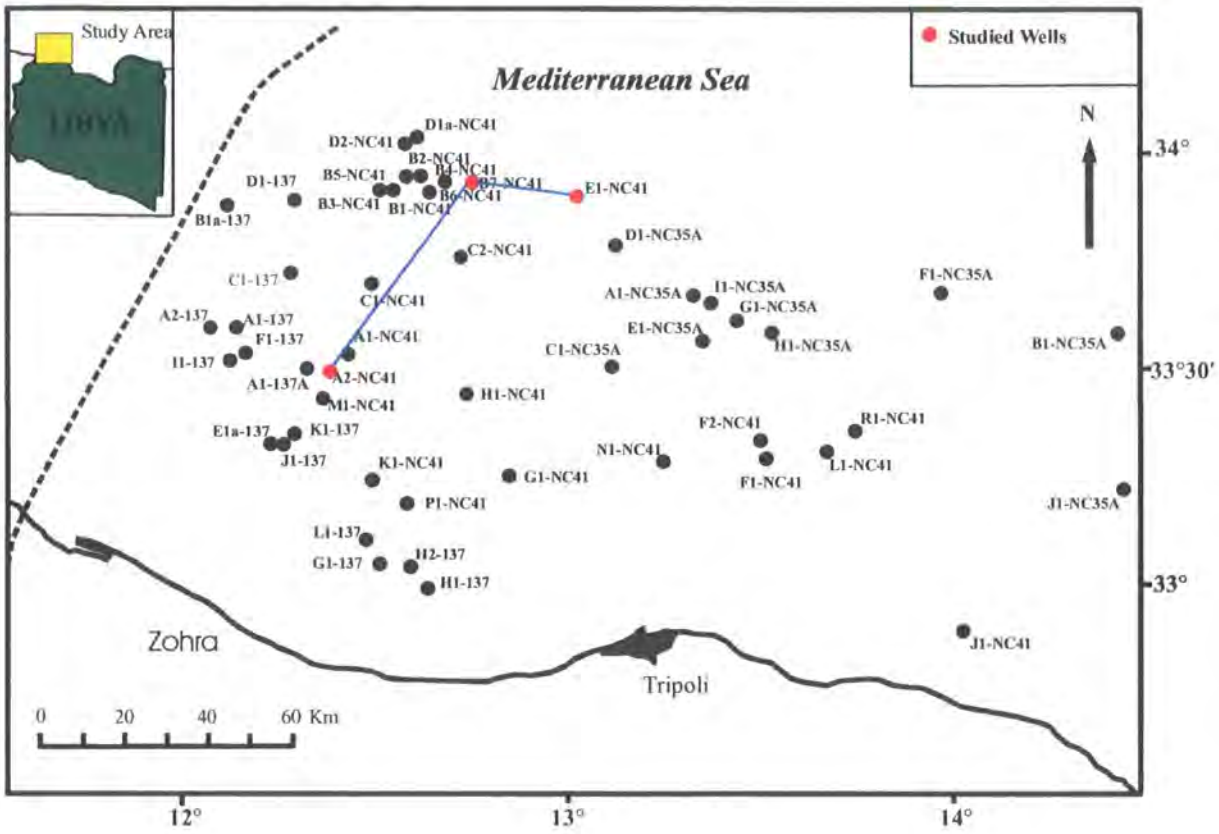

Figure 1.1. Location map of the study area showing offshore Libya wells. Wells in red are those analysed in this study.

stained with Alizarin Reds and Potassium ferricyanide following the methodology of Dickson (1966) to distinguish between ferroan-, non-ferroan calcite, dolomite and iron-rich dolomite. The stained thin-sections were covered to protect the sections from damage. Percentages of constituents within the sections were determined using Point Counting. The terms employed in crystallization fabric follow Friedman (1965), and those employed in carbonate classification, in principle, follow Dunham (1962). The terms employed in carbonate grain-size measurements follow Wentworth (1922). Determination of the type of porosity uses the descriptive and identification scheme established by Choquette and Pray (1970). Four samples for scanning electron microscopy (SEM) and four samples for cathodoluminescene (CL) were chosen to describe and interpret diagenetic features (see chapter 5).

1.4. LAYOUT OF THESIS.

This thesis is presented in seven chapters. The first chapter introduces the study area, study objectives and methods of study. The second chapter summarizes data from previous studies on the regional geological setting of the Pelagian Block and Sabratah Basin, offshore western Libya. This chapter also includes the stratigraphy and depositional environments for the formations in the Sabratah Basin. Chapter 3 describes the general palaeoenvironments of Eocene nummulitic accumulations and presents some facies models that have been proposed for nummulites deposits and their reservoir quality. Chapter 4 discusses the sedimentology of the Jdeir Formation and includes a section on previous work. This chapter also describes main facies in the Jdeir formation on the basis of core descriptions and petrographic analysis of thin-sections under the transmitted light microscope. A comparison between the Jdeir Formation and other Eocene nummulitic deposits, particularly from Tunisia was undertaken at the end of this chapter and in chapter 5 to better understand global variations in Paleogene limestones and their reservoir quality. Chapter 5 focuses on the main diagenetic features and reservoir quality of the Jdeir Formation. Different analyses used in this study include scanning electron microscopy (SEM), cathodoluminescence (CL) and oxygen and carbon stable isotopes ($\delta^{18}O$ & $\delta^{13}C$). The interpretation of sequence stratigraphy for the Jdeir formation is presented in chapter 6. The final chapter (7) presents the conclusion for this study. The list of references and then appendix 1 (Terminology) follow.

CHAPTER TWO:

2. TECTONIC SETTING

2.1. INTRODUCTION

2.2. REGIONAL TECTONIC SETTING OF THE PELAGIAN BLOCK

2.3. SABRATAH BASIN

2.4. PREVIOUS STUDIES

2.5. NOMENCLATURE OF THE SABRATAH BASIN

2.5.1. ALALGAH FORMATION

2.5.2. MAKHBAZ FORMATION

2.5.3. JAMIL FORMATION

2.5.4. BU ISA FORMATION

2.5.5. AL JURF FORMATION

2.5.6. EHDUZ FORMATION

2.5.7. FARWAH GROUP

2.5.7.1. BILAL FORMATION

2.5.7.2. JIRANI MEMBER

2.5.7.3. JDEIR FORMATION

2.5.8. TALJAH FORMATION

2.5.9. TAJOURA FORMATION

2.5.10. TELIL GROUP

2.5.11. GHALIL FORMATION

2.5.12. NUMMULITES VASCUS MARKER BED

2.5.13. DIRBAL FORMATION

2.5.14. RAS ABD JALIL FORMATION

2.5.15. AL MAYAH FORMATION

2.5.16. SIDI BANNOUR FORMATION

2.5.17. TUBTAH FORMATION

2.5.18. BIR SHAFUF FORMATION

2.5.19. MARSA ZOUAGHAH FORMATION

2.6. SUMMARY

2.1. INTRODUCTION:

The study area is located offshore of western Libya. The western Libya offshore area encompasses the southern part of the Pelagian Block and the eastern portion of the Sabratah Basin. This chapter summarises previous work on the main tectonic events that have influenced the Pelagian Block and Sabratah Basin. In addition, the formations in the study area are briefly described.

2.2. REGIONAL TECTONIC SETING OF THE PELAGIAN BLOCK:

The western offshore region of Libya forms part of the Pelagian Block, which represents the northern margin of the Africa Plate. The Pelagian Block is Mesozoic to Cenozoic in age, and is located between Sicily, the Ionian Sea, the Libya coast, and Tunisia (Figure 2.1). From north to south the Pelagian Block is divided into the following tectonic elements: the Ragusa-Malta Plateau, the Pantelleria Rift Zone, the Malta Plateau and the Lampedusa- Medina Plateau Arch. The Sabratah Basin lies between the Pelagian Block and the present day Libyan coast (Figure 2.1). The Pelagian Block is terminated to the east by the Medina Escarpment (Don Hallett, 2002). The Pelagian Block has been affected by a series of extensional tectonic events that have occurred from the Middle-Upper Triassic to the Quaternary. According to Finetti (1982) the basin has been affected by four main events. The first phase was extensional, causing major rifting, and occurred coevally with opening of the Central Atlantic Ocean during Middle-Upper Triassic time. Volcanic activity is inferred from basalts found in wells drilled in the Ragusa-Malta area. In the Mid-Jurassic, the second event commenced with the rifting of Tethys and led to fragmentation of the old Pelagian carbonate platform that had been created during the Triassic (Mengoli and Spinicci, 1984). The third extensional tectonic event started during the Late Cretaceous. At this time a widespread transgression affected all parts of the north African continent. This event is associated with considerable volcanic activity and tectonic subsidence. The last phase was from the Middle-Late Miocene up to the Quaternary with rifting of the Sicily Channel in the Pantelleria, Linosa and Malta areas (Finetti, 1982).

2.3. SABRATAH BASIN:

The Sabratah Basin is located west-northwestwards just offshore Libya, along the southern side of the Pelagian Block and extends into onshore Tunisia (Figure 2.1).

The Sabratah Basin has an elongate oval shape extending in an ESE to WNW direction. The Basin measures approximately 500 km in length and 250 km in width. It is bounded to the north by the Lampedusa Plateau; to the south by the Jifarah fault system; to the east by the Misratah – Medina scarp (an extension of the Jifarah arch to the north) (Hammuda et al. 1985). The Sabratah Basin is thought to have originated as a left-lateral pull-part basin during the Late Triassic- Early Jurassic between the WNW Libyan Coastal Fault System and Southern Graben Fault Zone; both believed to have been originally Hercynian fault system (McCrossan, 1988). After basin initiation, strike-slip motion ceased in the Middle Jurassic and the basin continued to thermally subside. Reactivation involving dextral strike-slip motion occurred in the Cretaceous and Tertiary (Anketell, 1993).

2.4. PREVIOUS STUDIES:

Previous studies involving tectonic subsidence histories have been reported especially from the North Atlantic Passive Continental margin (Pitman and Talwani, 1972; Jansa and Wade, 1975; Montadert et al., 1979; Keen, 1979; Keen and Barrett, 1981) and to a lesser extent form the Mediterranean region (Gvirtzman and Buchbinder, 1976; Ben Avraham, 1978). Most of the studies mentioned, determined the tectonic subsidence due to crystal thinning. Bernasconi et al. (1991) studied the petrography and diagenesis of the Farwah Group in the Bouri Oil Field and divided the group into three main lithofacies i.e. Nummulitic, Dolomitic and Micritic facies and proposed a model for the Nummulitic bank facies. Sbeta (1984) conducted a comprehensive sedimentological study of the Eocene sequence in the north-western Libya offshore area, investigating the lithofacies and interpreting their depositional environment according to the standard facies model of Wilson (1975). Most of Sbeta's work was concentrated on the Middle and Upper Eocene sequences. Hammuda et al. (1985) proposed a new stratigraphic nomenclature for the sedimentary sequence in the northwestern Libya offshore region. Mriheel and Anketell (1995) studied dolomitization of the Early Eocene Jirani dolomite formation and presented preliminary depositional and diagenetic models for the dolomites based on sedimentological, stratigraphical and petrographic characteristics. They concluded that dolomite formation in the Jirani Dolomite developed in three stages. Stage I involved penecontemporaneous/early diagenetic dolomitisation of the precursor

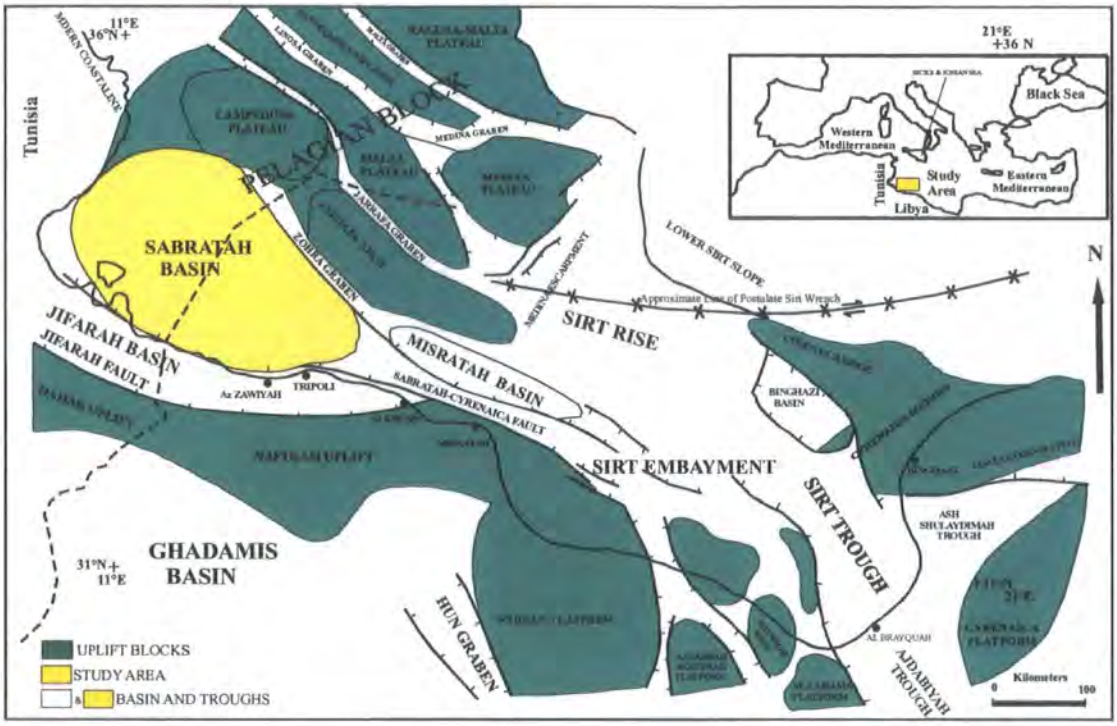

Figure 2.1. Major structural elements of Offshore Western Libya (Source, Don Hallett, 2002)

limestones with gypsum/anhydrite under hypersaline seepage reflux conditions. Stage. II dolomitisation, mainly confined to the non-anhydritic dolomite facies, was probably formed in the mixing zone between meteoric and sea water, probably at shallow depths of burial. Stage III dolomitisation occurred at depth in the late stage of basin evolution, causing some infilling of mouldic and vuggy porosity by coarsely crystalline, saddle dolomite. Hammuda et al. (1992) used geohistory analysis results from fourteen wells in the central and southern Sabratah Basin to produce subsurface maps, stratigraphic and geosynthetic cross-sections. Most of the previous work remains as unpublished and confidential internal reports by the working Oil Companies i.e. Aquitaine, Sirt, and Agip.

2.5. NOMENCLATURE OF THE SABRATAH BASIN:

The oldest rocks encountered offshore Libya are of Triassic age but rocks of Permian age present in well A1-38, drilled along the coast near Sabratah (Sbeta 1991), (Figure 2.2). Overlying these Triassic and Permian beds, successions of Cretaceous

and Tertiary rocks are encountered in many wells drilled in the Sabratah Basin. At the end of 1980, the National Oil Corporation of Libya set up a stratigraphic committee with the task of reviewing the stratigraphic nomenclature used by the Oil Companies Operating in the Libyan offshore area and to establish a stratigraphic scheme in accordance with the rules of the International Code of Stratigraphic Nomenclature. In northwestern offshore Libya the operators were using stratigraphic terminology that was originally defined in onshore eastern and southern Tunisia. The stratigraphic committee consisting of Hammuda, Sbeta, Mouzughi and Eliagoubi, found that some of these terms were ill defined, while others were based on time equivalency rather than lithology. To avoid stratigraphic confusion due to the misuse of terminology originally defined in distant areas, the committee established a new stratigraphic nomenclature for the northwestern offshore of Libya (Hammuda et al, 1985) (Figure 2.2 & 2.3). Briefly described in the sections below are the formations found in the Sabratah Basin of Cretaceous and Cenozoic age.

2.5.1. ALALGAH FORMATION

The Alalgah Formation, a term introduce by Hammuda et al. (1985), is a sequence predominantly of dolomites and anhydrites with streaks of black shale, confined to the southwestern margin of Sabratah Basin. The type section of the formation, the 9578-10164 feet interval in K1-137 well, overlies volcanics. The **Alalgah Formation** unconformably overlies the **Kikala Formation** and is overlain by the **Makhbaz Formation**. The Formation is unfossiliferous, but its stratigrahpic position suggests a Cenomanian age.

2.5.2. MAKHBAZ FORMATION

The **Makhbaz Formation** is formed of often argillaceous, locally peloidal and oolitic limestone with occasional shaly and marly interbeds. The type section is located in the I1-137 well at 8326-8928 feet. The **Makhbaz Formation** is overlain by the **Jamil Formation.** The formation extends across the whole of the Sabratah Basin but is much thicker (over 600 feet), in the west than in the east where it measure less than 100 feet. The foraminifera assemblages suggest a Turonian-Santonian age.

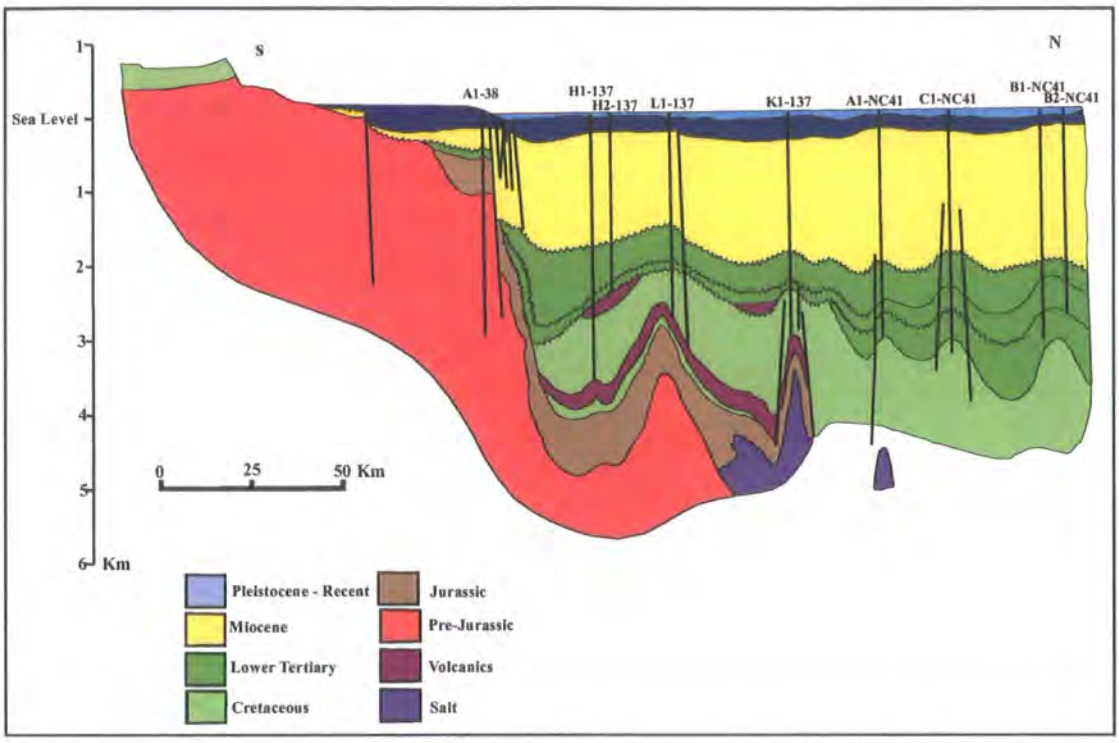

Figure 2.2. Cross Section of the Sabratah Basin (After Sbeta, 1991).

2.5.3. JAMIL FORMATION

The **Jamil Formation** consists mainly of calcareous shale grading to marl and occasionally interbedded with argillaceous limestone. Hammuda et al. (1985) selected the 7908-9150 feet sequence in the K1-137 well as the type section for this formation. The **Jamil Formation** overlies the **Makhbaz Formation** and is overlain with a probable unconformable contact by the **Bu Isa Formation**. The **Jamil Formation** is rich in planktonic foraminifera, suggesting open marine, relatively deep-water conditions. The microfossils indicate an uppermost Turonian to Santonian age for the **Jamil Formation**.

2.5.4. BU ISA FORMATION

The **Bu Isa Formation** is characterised by a thick succession of fossiliferous, argillaceous, chalky limestone, locally grading to marl. Its type section is in the H1-137 well at 9150-10102 feet. The **Bu Isa Formation** underlies the **Al Jurf Formation** and overlies, probably unconformably the **Jamil Formation**. The **Bu Isa**

Formation is rich in planktonic foraminifera, which indicate a Campanian to early Maastrichtian age.

2.5.5. AL JURF FORMATION

The **Al Jurf Formation** consists predominantly of shale with thin beds of argillaceous limestone. Locally a few sandstone lenses occur. The type section is located in the C1-NC41 well at 9208-10565 feet. The **Al Jurf Formation** is rich in planktonic foraminifera indicative of a deep marine depositional environment. The formation is Campanian to Thanetian age.

2.5.6. EHDUZ FORMATION

The **Ehduz Formation** is interpreted as a limestone succession overlying and partly contemporaneous with the **Al Jurf Formation** (Figure.2.3) and overlain by the **Farwah Group** or the **Ajaylat Formation**. Palaeontological evidence indicates a shallowing of the depositional environment from middle neritic to shallow inner neritic. Biostratigraphic evidence indicates a Palaeocene to possibly earliest Eocene age for the **Ehduz Formation**.

2.5.7. FARWAH GROUP

Hammuda et al. (1985) defined the **Farwah Group** as a carbonate sequence bounded at the top by shale and argillaceous limestone of the **Ghalil** and at the base by the shale and marl of the **Al Jurf Formation**. The **Farwah Group** is Early Eocene (Ypresian) age. The group is subdivided into: **Bilal Formation, Jirani Member and Jdeir Formation**. It is the Group that the current study is focused on.

2.5.7.1. BILAL FORMATION

The type section of the formation was encountered at a depth 8786-8937 feet in B2-NC41 well (Figure 2.4). The formation consists of fossiliferous wackestone to packstone and lime-mudstone at the top giving way to argillaceous packstone and globigerinid mudstone below. It is reported as conformably underlying the **Jirani Dolomite** in the north and centre of the Sabratah Basin.

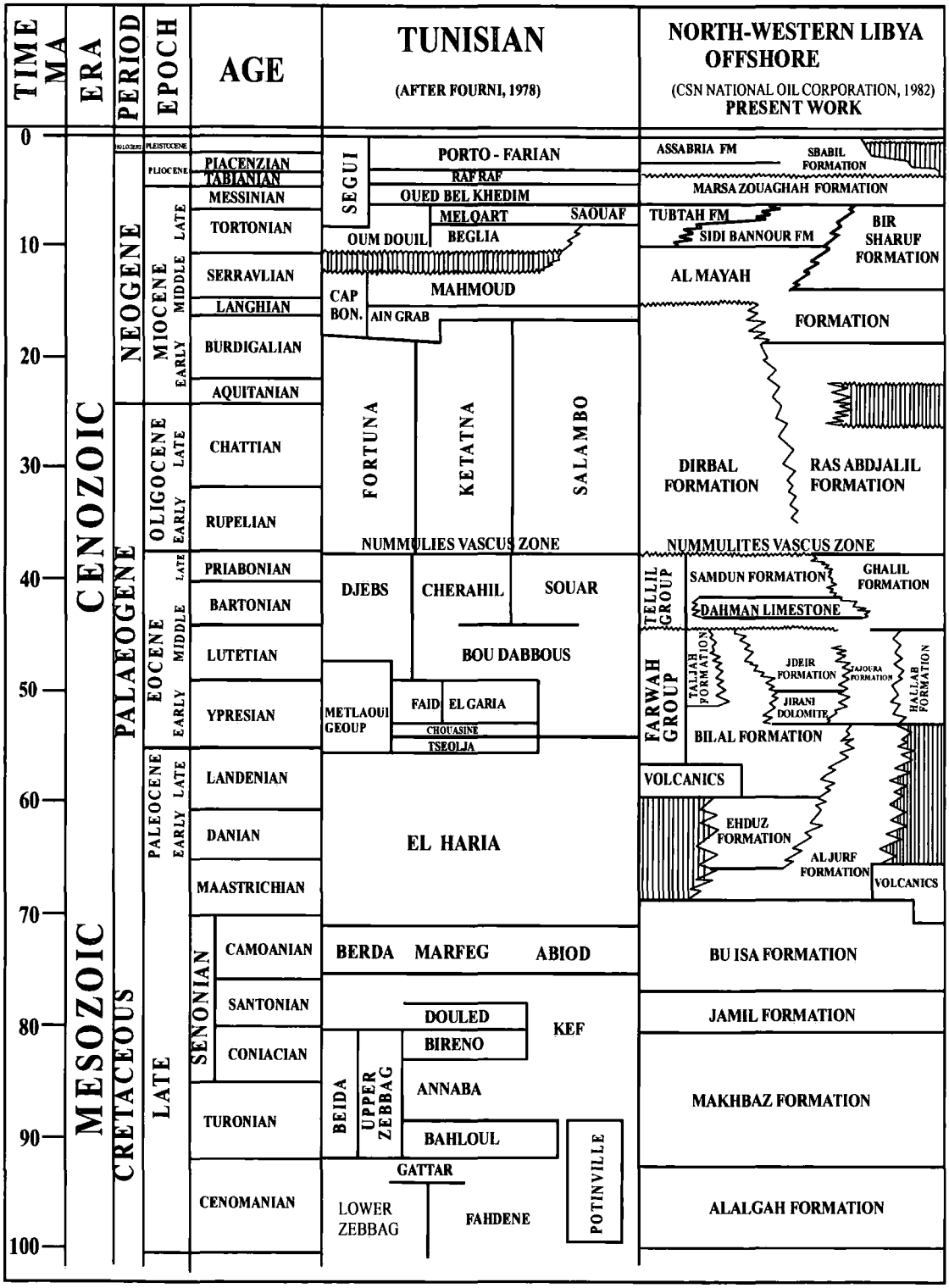

Figure 2.3. Correlation Chart of Upper Cretaceous and Cenozoic Rocks in the NW Offshore of Libya.

2.5.7.2. JIRANI MEMBER

The type section of the Jirani member is present at a depth 8514 - 8638 feet in B2-NC41 well (Figure 2.4). The Jirani Member is composed largely of dolostone with minor limestone interbeds and is often known as the Jirani Dolomite. The dolostone is brown to dark brown with black laminae, very finely crystalline, locally argillaceous and fossiliferous. Anhydrite nodules are common with kaolinite present at the top of the section. Dolomitic limestone and chalky pelletal, fossilifierous limestone becomes more common towards the base. The lower contact is taken at the lowest dolomite bed and where limestone becomes dominant. The formation grades southwards into the transitional facies of the **Bilal** and to the **Tajoura** and **Hallab Formations** eastward (Figure 2.3). The age is designated as Early Ypresian.

2.5.7.3. JDEIR FORMATION

The type section of the formation was encountered at a depth of 8084 - 8514 feet in B2-NC41 well (Figure 2.4). The formation includes light brown, nummulitic wackestone and packstone locally grading to argillaceous grainstone and lime-mudstone. Two units were recognised in the type section, well B2-NC41, an upper 354 feet thick light brown to light grey nummulite-rich, foraminiferal, bioclastic packstone to wackestone, and a lower 76 feet thick interval of light grey to brown *Alveolina-Orbitolites* rich foraminiferal, bioclastic packstone to grainstone. The upper contact with the **Ghalil Formation** is unconformable; the lower contact is conformable and is taken at the top of the uppermost dolostone of the **Jirani Dolomite**. Where the latter is not present the lower limit is taken at the top of the argillaceous limestone of the **Bilal Formation**. The age is given as Late Ypresian to Early Lutetian. Equivalent strata include the **Taljah Formation** to the south of the **Bilal Formation** in the Sabratah basin centre, the upper part of the **Tajoura** and **Hallab Formations** in the west and the **El Garia Formation** of the Tunisian Metlaoui Group (Figure 2.3).

2.5.8. TALJAH FORMATION

The **Taljah Formation** was first defined by Hammuda et al (1985) in the H1-137 well on the southern flank of the Sabratah Basin. The **Taljah Formation** is equivalent to the **Jdeir Formation**. In type section it consists of micritic dolomite, sandy at the base, anhydritic in the middle and argillaceous toward the top. The

Taljah Formation lies above the **Bilal Formation**. The Formation is limited in extent and is confined to the southern margin of the Sabratah Basin, where it represents a southern facies of the **Farwah Group**.

2.5.9. TAJOURA FORMATION

The **Tajoura Formation** was established by Hammuda et al (1985) with the type section in the F1-NC41 well. The lower part of the Formation is composed of bioherms containing abundant bryozoan fragments. The middle part is composed of skeletal and oolitic limestone, with bryozoa, ostracods, bivalves, echinoids, algae and foraminifera. The upper part is predominantly dolomitic with some brecciated zones, interbedded with marl and shale. The lower contact is conformable with the underlying **Bilal Formation**. On the basis of stratigraphic position the formation is assumed to be Ypresian in age.

2.5.10. TELLIL GROUP

The **Tellil Group** was established by Hammuda et al. (1985). It consists of a variety of interbedded lithologies including shale, limestone, siltstone and locally dolomite, anhydrite and sandstone. The sequence overlies the **Farwah Group** and is overlain by the **Nummulites Vascus Marker Bed**. Both contacts are unconformable. The Tellil Group occurs only in the western and southern parts of the Sabratah Basin. The type section of the Tellil Group is located in the H1-137 well at 6142-8080 feet. The group is subdivided into three formations: the **Harshah Formation,** the **Dahman Formation and** the **Samdun Formation**. Palaeontological evidence indicates a Middle to Late Eocene age and a shallow marine to marginal marine environment of deposition.

2.5.11. GHALIL FORMATION

Hammuda et al. (1985) defined the **Ghalil Formation** as a deep-water equivalent of the **Tellil Group**. This formation consists of silty shale grading to marl, with lenses of limestone in its lower part and sandy lenses it its upper part. The type section chosen was the 7680-8231 feet interval in the D2-NC41 well. The **Ghalil Formation** overlies **the Farwah Group** and underlies the **Dirbal** or **Ras Abd Jalil Formation** and sometimes below the intervening **Nummulites Vascus Bed.** Both

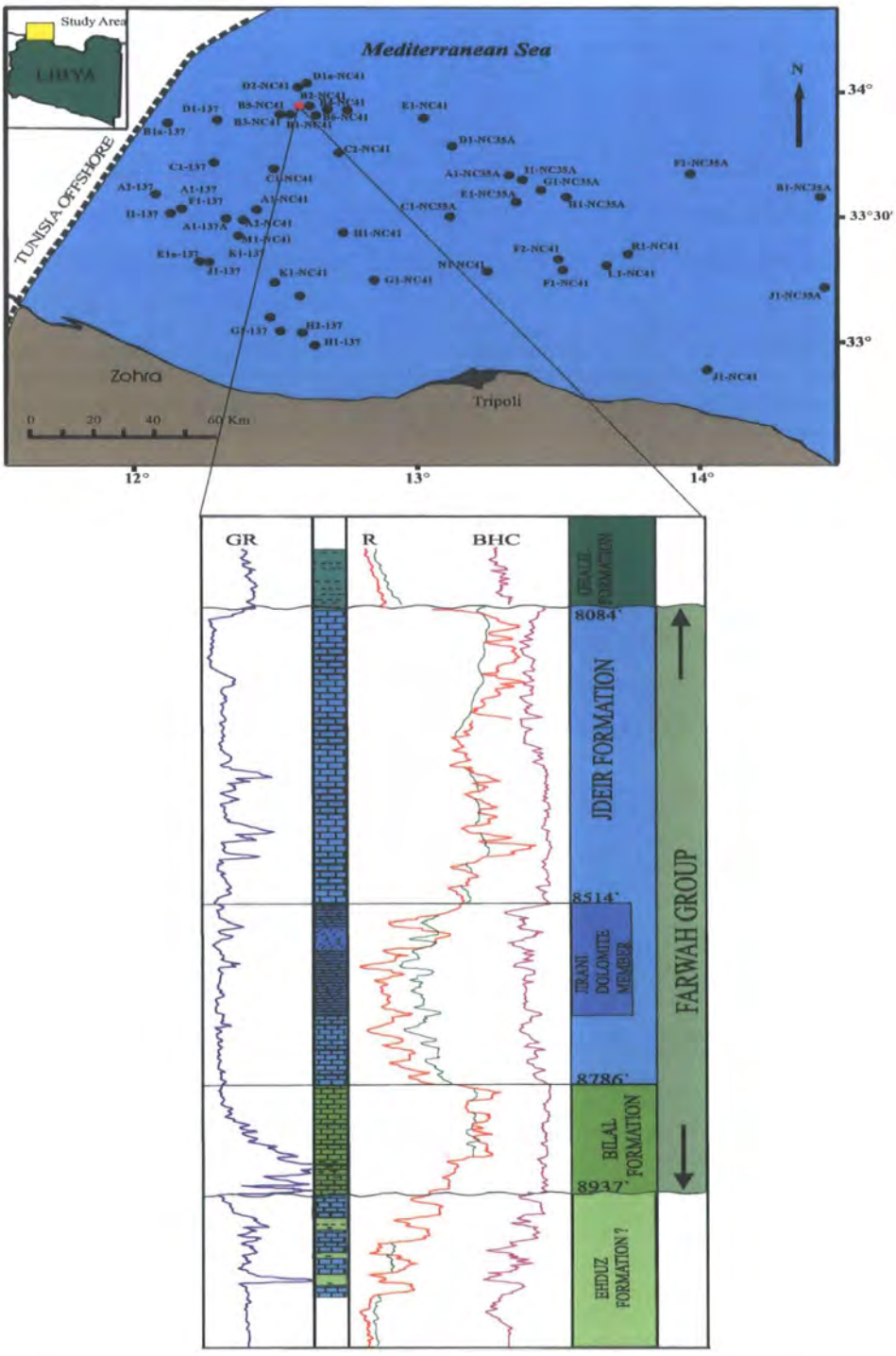

Figure 2.4. Farwah Group type section (B2-NC41) (after Hammuda et al., 1985).

upper and lower contacts are unconformable. The **Ghalil Formation** is confined to the northeastern part of the Sabratah Basin. The formation is of Middle to Late Eocene age.

2.5.12. NUMMULITES VASCUS MARKER BED

The **Nummulitic Vascus Marker Bed** is a distinctive limestone unit in the southwestern part of the Libyan offshore area, separating the **Tellil Group** from the **Dirbal or Ras Abd Jalil Formation**. It is variously described as a nummulitic grainstone, wackestone, packstone, occasionally slightly dolomitic and glauconitic. Characteristic is the presence of the larger foraminifera species *Nummulites vascus*. The thickness of this marker bed varies from 22 feet (A1-137) to 57 feet (F1-137). The age is Early Oligocene.

2.5.13. DIRBAL FORMATION

The **Dirbal Formation** is a fossiliferous, shallow water limestone succession developed locally in the western part of the Libyan offshore area and laterally equivalent to the **Ras Abd Jalil Formation**. The **Dirbal Formation** overlies the **Nummulites Vascus Marker Bed**, the **Samdun Formation** or portions of the **Lower Ras Abd Jalil Formation**. The **Dirbal Formation** varies in thickness from 2862 feet (A1-NC41) to 282 feet (K1-137). Hammuda et al. (1985) divided this section into two units: a lower unit consisting of grainstones and boundstones, interbedded with dolomite, and an upper unit with alternations of wackestones and packstones and streaks of shale and marl. The **Dirbal Formation** is rich in fossils, including larger foraminifera, bryozoa and coralline algae. The formation is of Oligocene to Early Miocene age.

2.5.14. RAS ABD JALIL FORMATION

The **Ras Abd Jalil Formation** is the deeper water equivalent of the **Dirbal Formation**. It consists of shale (often silty or sandy), marl, argillaceous limestone and stringers of siltstone and sandstone. The **Ras Abd Jalil Formation** extends over most of the Sabratah Basin. It overlies, with an unconformable contact, the **Ghalil Formation, Samdun Formation** or the **Nummulites Vascus Marker Bed**, and underlies the **Al Mayah Formation**. Hammuda et al. (1985) selected the 4890-7848 feet interval in the E1-NC41 well as the type section for the **Ras Abd Jalil Formation**. It is of Oligocene to Early Miocene age.

2.5.15. AL MAYAH FORMATION

The **Al Mayah Formation** is a succession of shale and sandstone with rare limestone interbeds. The sandstones predominate in the upper part of the formation. Hammuda et al. (1985) designated the 3079-5886 feet interval in the G1-NC41 well as the type section for the **Al Mayah Formation**. They recognised five units, from top to bottom: 320 feet of predominantly sandstone interbedded with clay; 900 feet of shale and clay with minor sandstone interbeds; about 40 feet of argillaceous wackestone/packstone; about 380 feet of sandy shale and clay; 1170 feet of alternating shale and sandstone. The **Al Mayah Formation** underlies the Tabtah Formation and overlies the **Ras Abd Jalil Formation**. The formation extends across the entire Sabratah Basin, decreasing in thickness from over 3000 feet in the north (3495 feet in D2-NC41) to less than 1000 feet in the south (201 feet in the F1-NC41). The **Al Mayah Formation** is Early to Middle Miocene.

2.5.16. SIDI BANNOUR FORMATION

Hammuda et al (1985) introduced the term **Sidi Bannour Formation** for a sequence of sandy clay with levels of mudstone and sandstone overlying and partly laterally equivalent to **Al Mayah Formation**. The type section is in E1-NC41 well from 2420-3868 feet. The formation is of Late Miocene (Tortonian) age.

2.5.17. TUBTAH FORMATION

The **Tubtah Formation** is a sequence of limestone and shale or clay. Hammuda et al. (1985) subdivided its type section, the 1661-2838 feet interval in the C1-137 well, into three units. These are: a lower unit (512 feet) composed of mudstone interbedded with wackestone and commonly containing pellets, a middle unit (250 feet) consisting of clay with thin beds of wackestone/packstone, sandy in its lower most part and upper unit (406 feet) composed of wackestone/packstone, occasionally oolitic, with rare mudstone. The **Tubtah Formation** is overlain by the **Marsa Zouaghah Formation** and underlain by **Al Mayah Formation**. The formation extends over most the Sabratah Basin. The formation is of Late Miocene age.

2.5.18. BIR SHARUF FORMATION

Hammuda et al. (1985) introduced the **Bir Saurf Formation** as the deep water equivalent of the Tubtah Formation. Three units were recognised in the type section (B1a-137) from 1410-2568 feet. These are: a lower unit (478 feet) composed of pelleted micrite and biomicrite; a middle unit (255 feet) of interbedded shale and micrite, becoming sandy in the lower part and an upper unit (431 feet) consisting of pelletal micrite and biomicrosparite, locally chalky and argillaceous, with rare clay interbeds and some gypsum near the top. The **Bir Sharuf Formation** is overlain by the **Marsa Zouaghah Formation** and underlain by the **Sidi Bannour Formation**. The formation is of Middle to Late Miocene age.

2.5.19. MARSA ZOUAGHAH FORMATION

The **Marsa Zouaghah** Formation is a predominantly evaporitc sequence. Its type section, the 1355-1661 feet interval in the C1-137 well, contains interbeds of gypsum, glauconitic marl, gypsiferous clay and dolomitic micrite. It overlies the **Tubtah Formation** and is overlain by the sandy **Assabria Formation** or the marly **Sbabil Formation**. The **Marsa Zouaghah Formation** yielded non-age-diagnostic, restricted microfossil assemblages. Regional biostratigraphic evidence from overlying and underlying strata suggests a Late Messinian age.

2.6. SUMMARY:

The Sabratah Basin forms part of the Pelagian Block and is thought to have originated as a left-lateral pull-part basin during the Late Triassic–Early Jurassic. The oldest rocks in the area are Late Triassic in age in L1-137, located in the southern Sabratah Basin. The stratigraphic sequence in the offshore area is dominated by limestones, dolomites, evaporates and shales, ranging in age from Triassic to Recent. During the Late Triassic-Early Jurassic, when the Sabratah Basin formed, shallow-marine carbonates and restricted evaporates were laid down. From Middle Jurassic until the Late Miocene, the southern parts of the offshore were dominated by restricted marine carbonates, grading northward into shallow-marine carbonates (including the Jdeir Formation of this study) that passed into deep-water deposits in north.

CHAPTER THREE

3. EOCENE NUMMULITIC ACCUMULATIONS AND PALAEOENVIRONMENTS:

3. EOCENE NUMMULITIC ACCUMULATIONS AND PALAEOENVIRONMENTS

3.1. INTRODUCTION:

The aim of this chapter is to describe the Eocene Nummulitids and other larger benthonic foraminifera and throw the light on the main factors which controlled their distribution and the test size and shape of these foraminifera. The significance of the environmentally influenced life cycle of larger benthonic foraminifera, and the symbiotic relationship between many larger foraminifera and photosynthetic symbionts is discussed. In addition other physical and chemical influences on larger foraminifera are summarized including nutrient supply, substrate, water energy, salinity, temperature and taphonomic processes. This chapter also includes a description of some of the facies models that have been proposed for Nummulitic deposits and a brief discussion of their reservoir quality.

3.2. GENERALITIES ABOUT EOCENE NUMMULITIC DEPOSITS.

According to Racey (2001), *Nummulites* are Tertiary (Late Palaeocene to middle-Oligocene) benthic rotaliid foraminifera, which are particularly common throughout the Tethyan region. The morphology of *Nummulites* is characterised by large, lenticular and flat to subglobular tests, which comprise a single planispirally-coiled layer subdivided into numerous simple chambers, separated by septa (Figure 3.1). The test size and species diversity of Nummulites decreased across the Eocene/Oligocene boundary and most Eocene taxa become extinct at this time (Brasier, 1995). *Nummulites* accumulations or "Banks" commonly develop in platform or shelf-margin areas and mid to outer ramp settings. These accumulations are particularly abundant in the circum-Mediterranean region, the Middle East and the Indian Subcontinent (Figure 3.2) (Racey, 2001) and form hydrocarbon reservoirs or targets in countries such Tunisia, Egypt, Italy, Oman and Pakistan as well as Libya. Racey (2001) also noted that large flat *Nummulites* tend to be associated with large flat *Assilina* and *Discocyclina* in "deeper" more outer platform/shelf/ramp settings (50-80m water depth), whereas small and medium sized lenticular *Nummulites* are more often associated with *Alveolina* and occur in shallower inner platform/shelf/ramp settings. In general, *Nummulites* have alternating asexual and

sexual generations. The asexual generation has a large proloculus (initial chamber) and small test diameter, and is referred to as the megalospheric form, or the A-form. The sexual generation with a small proloculus and large test diameter, is known as the microspheric form, or B-form (Figure 3.3) (Beavington-Penney and Racey, 2004). Many authors have assumed that the asexual and sexual generations alternate, and give rise to an assemblage with an A-to B-form ratio of approximately 10:1 (Blondeau, 1972). However, departures from this ratio may result from environmental differences and have been used to define a "degree of winnowing". Beavington–Penney, and Racey (2004) observed that A-forms dominate fossil communities which result from repeated asexual reproduction and are likely to have formed in the shallowest or deepest parts of the depth range of a particular species. In comparison, sexually produced B-forms are most common in intermediate intervals of a specific depth range. The distribution is partly because sexual reproduction is less likely to be successful in shallow, turbulent water, and the large sexual forms are restricted to deeper environments, below fair weather wave base. They noted that these two environments (shallow and deep) could be distinguished on the basis of test shape and analysis of associated biota, matrix and sedimentary structures.

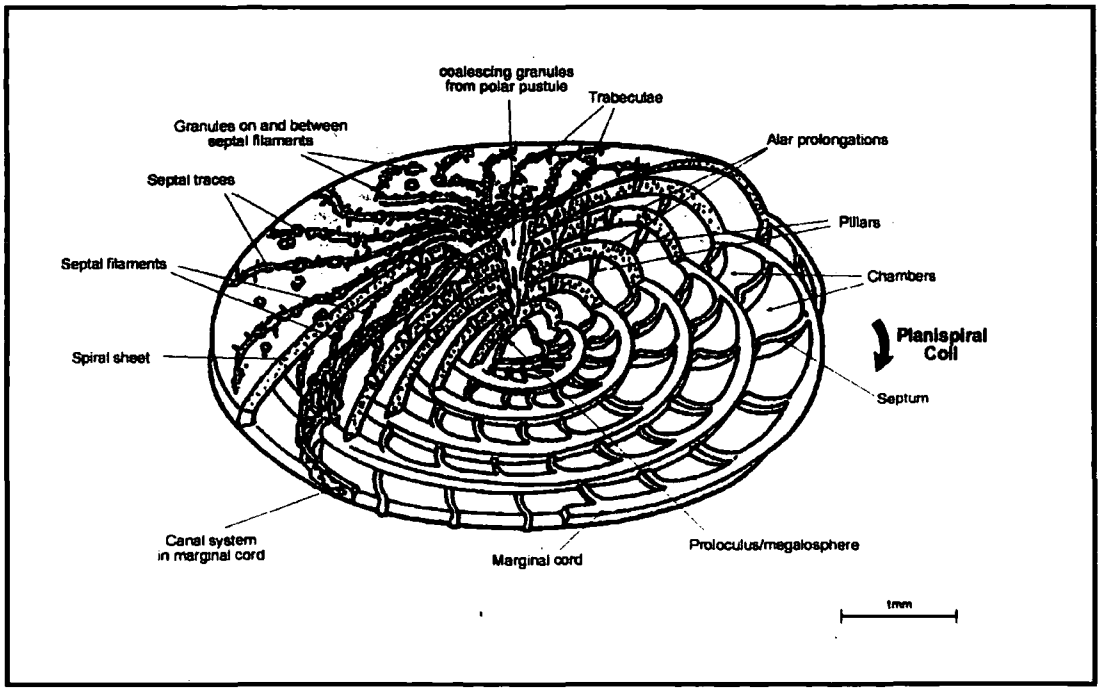

Figure 3.1. A-form (megalospheric) nummulite morphology (after Racey, 2001).

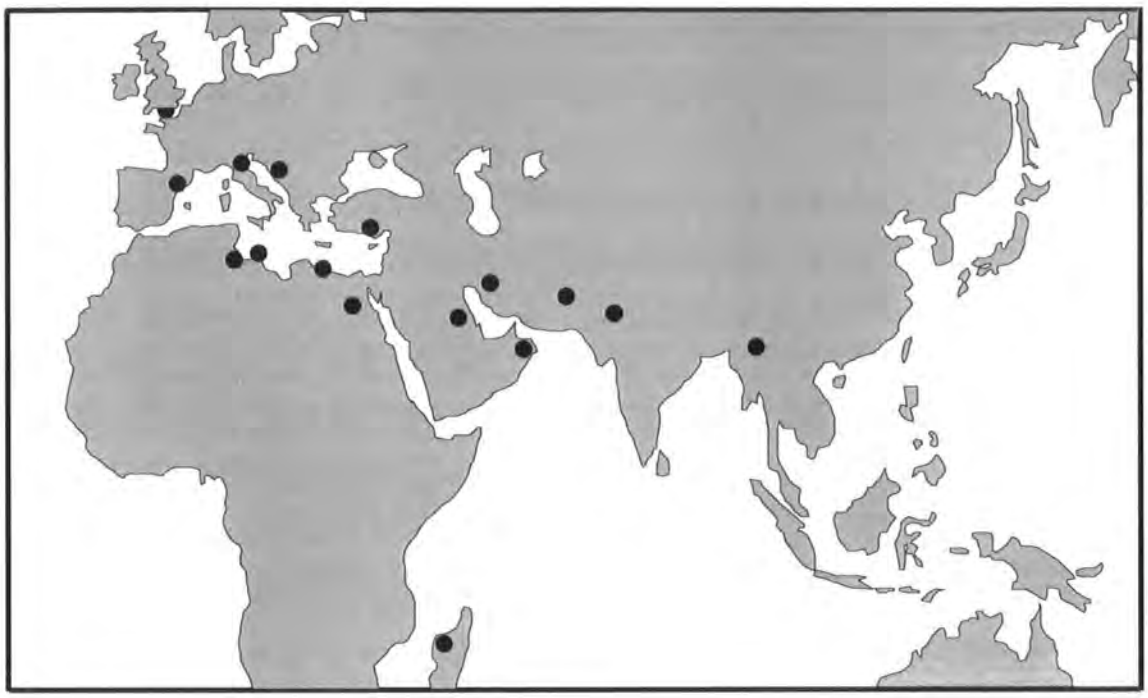

Figure 3.2. Geographic distribution of principle Eocene nummulitic accumulations (after Racey, 2001).

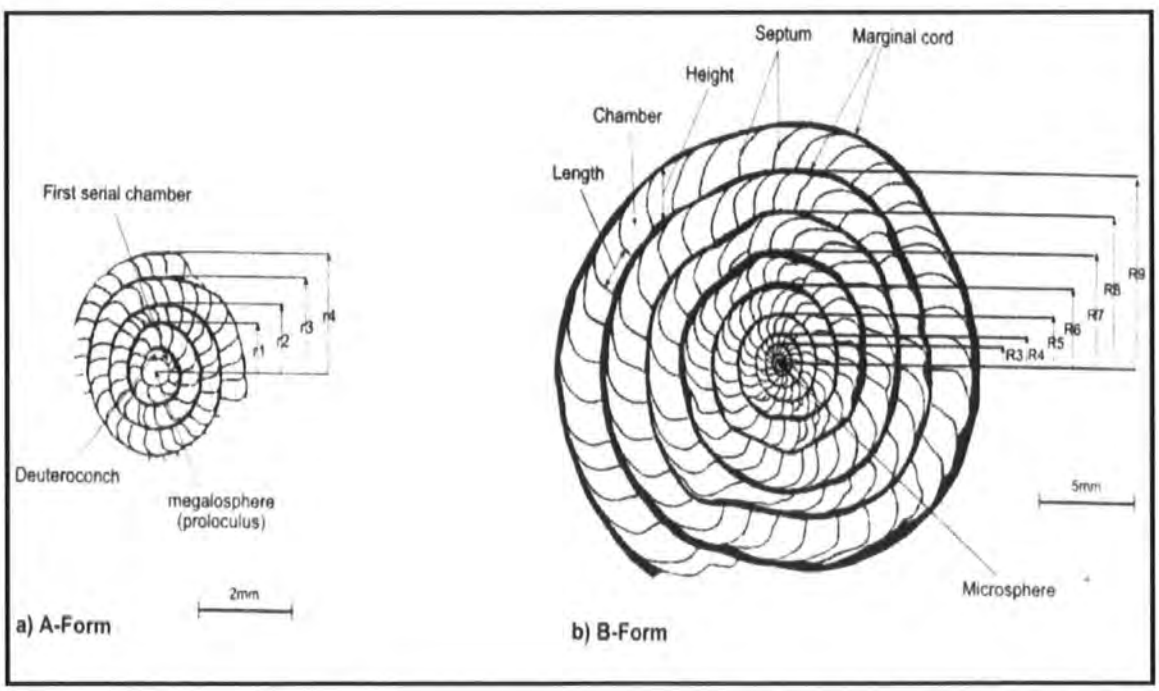

Figure 3.3. Difference between nummulites A-forms (megalospheric generation) and B-forms (microspheric) (after Racey, 2001).

3.3. ECOLOGICAL CONTROLS ON NUMMULITES ACCUMULATIONS:

3.3.1. SYMBIOTIC PROCESSES:

Nummulites with many other larger foraminifera including nummulitids and alveolinids are characterized by complex internal morphologies. Haynes (1965) related this complexity to the presence of photosynthetic, symbionts within the test of many species. This host-symbiont relationship means that most living larger foraminifera are restricted to shallow seas, and if untransported, their presence is generally indicative of water depth less than 130m, i.e., within photic zone (Hottinger, 1983; Hallock,1984). Ross (1972) suggested that algal symbiosis in larger foraminifera is comparable in terms of growth stimulation and calcium carbonate fixation to that found in hermatypic corals. Reiss and Hottinger (1984) concluded that Nummulites and other larger foraminifera have lived symbiotically with photosynthetic algae and are therefore thought to have been restricted to warm (25°C), clear, shallow (<120m) waters within the euphotic zone. In the symbiotic relationship, the Nummulites provide shelter for the algae while the algae, produced oxygen and nutrients for the Nummulites as a bi-product of photosynthesis (Racey, 2001).

3.3.2. LIGHT INTENSITY AND WATER ENERGY:

Haynes (1965) proposed that test shape is a compromise between the metabolic requirements associated with algal symbiosis, hydrodynamic factors and light. Many authors have suggested that light availability controls test morphology through symbiotic interaction as illustrated in Figure 3.4 (Haynes, 1965; Hottinger and Dreher, 1974; Hallock and Hansen, 1979). As light intensity decreases with increasing water depth there is a tendency for the test to thin and flatten resulting in a larger surface area for the photosynthetic symbionts to available light. Hallock (1979) observed that more oblate and thicker tests are found in species inhabiting shallow water where they are more able to withstand higher energies associated with wave or current activity. Trevisani and Papazzoni (1996) identified two Nummulite subspecies which occur in the upper and lower facies of shallowing-upwards cycles, with the flatter form occurring in base-cycle marls, and the more `robust` form being restricted to shallower, cycle-top limestones. These differences were attributed to the effects of water energy, light intensity and substrate.

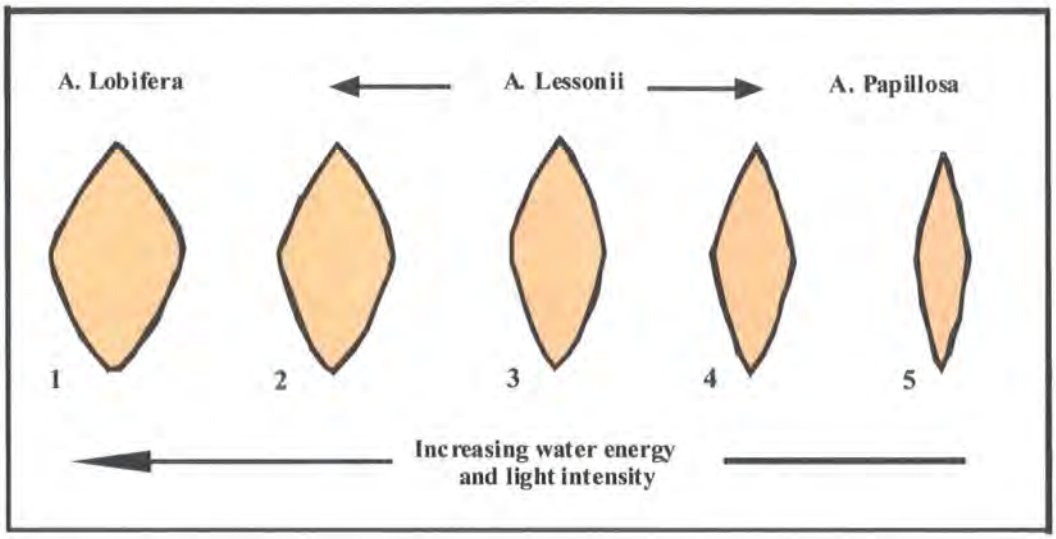

Figure 3.4. The range of shape in three Indo-Pacific species of Amphistegina related to water energy and light intensity:

(1) A. Lobifera, high-energy, high-light environment; (2) A. Lessonii, moderate-energy, high-light environment; (3) A. Lessonii, low-energy, moderate-light environment; (4) A. Lessonii, low-energy, low-light environment; and (5) A. Papillosa, low-energy, very low-light environment (after Beavington-Penny, Racey, 2004).

3.3.3. SUBSTRATE:

Hohenegger et al. (2000) noted that extant Nummulitids from the west Pacific prefer coarse sandy substrates below fair weather wave base, whilst the deep-dwelling *Planoperculina Heterosteginoides* is restricted to poorly illuminated areas of 0.3 to 2.5 % surface light intensity and preferred medium- to fine- grained sand substrates and calm water. Several authors have attributed variations in test size of fossil Nummulites to changes in substrate (often related to changes in water depth). Pomerol (1981) noted that the size of Nummulites was inversely proportional to clay content of the surrounding sediments, while Nemkov (1962) concluded that Nummulites were larger in shallow-water calcareous and sandy deposits than in deeper water clay-rich sediments. Beavington-Penny (2002) identified two A-form dominated Nummulites populations associated with seagrass-vegetated environments in the Middle Eocene Seeb Formation of Oman. Both contained a highly diverse biota typical of shallow marine, protected environments (including micritic peloids, soritid foraminifera orbitolites, alveolinids, miliolids, peneroplids, texulariids, probable encrusting foraminifera and dasycladacean green algae), many of which are common in seagrass environments.

3.3.4. WATER MOTION:

Hallock (1979) indicated that water motion may influence test shape (Figure 3.4). Hallock et al. (1986) observed in their study that increased light saturation and water motion produced a thicker wall, and therefore a thicker test. They also noted that, as water motion increased the test thickens (through increased calcification). Slower growth rates were also noted by Röttger (1972) in *Heterostegina depressa* under conditions of increased water motion.

3.3.5. SALINITY:

Reiss and Hottinger (1984) report that larger foraminifera are abundant and diverse in the Gulf of Aqaba at salinities of 40-41%. The rotalliid larger foraminifera are typically stenohaline, with tolerance limits in the range of 30-45% (Hallock and Glenn, 1986).

3.3.6. TEMPERATURE:

Temperature strongly affects many physical and chemical properties and biological processes within the marine environment (Beavington-Penney and Racey, 2004). Murray, (1987), Adams et al. (1990), and Jones, (1999) observed that temperature also appears to control the diversity of larger foraminifera assemblages: tropical to subtrobical, shallow-water assemblages are characterized by more than 10 species, whilst very warm (greater than approximately 31°C) and warm-temperate (less than approximately 20°C) shallow-water environments generally contain fewer species. Hollaus and Hottinger (1997) suggest that the larger benthonic foraminifera distribution limit of 16-18°C is related to the minimum temperature required for the growth of their endosymbionts. Of the larger benthonic foraminifera, amphisteginoids and soritids display the widest latitudinal distribution, related to their tolerance of a relatively wide temperature range (Murray, 1991; Langer and Hottinger, 2000), as shown in (Figure 3.5).

3.4. TAPHONOMIC PROCESSES:

Beavington-Penney (2004) concluded that possible candidates responsible for the damage observed in Eocene nummulites include predation by large bioeroders, such as fish and echinoids, and transport within turbidity currents. Other taphonomic

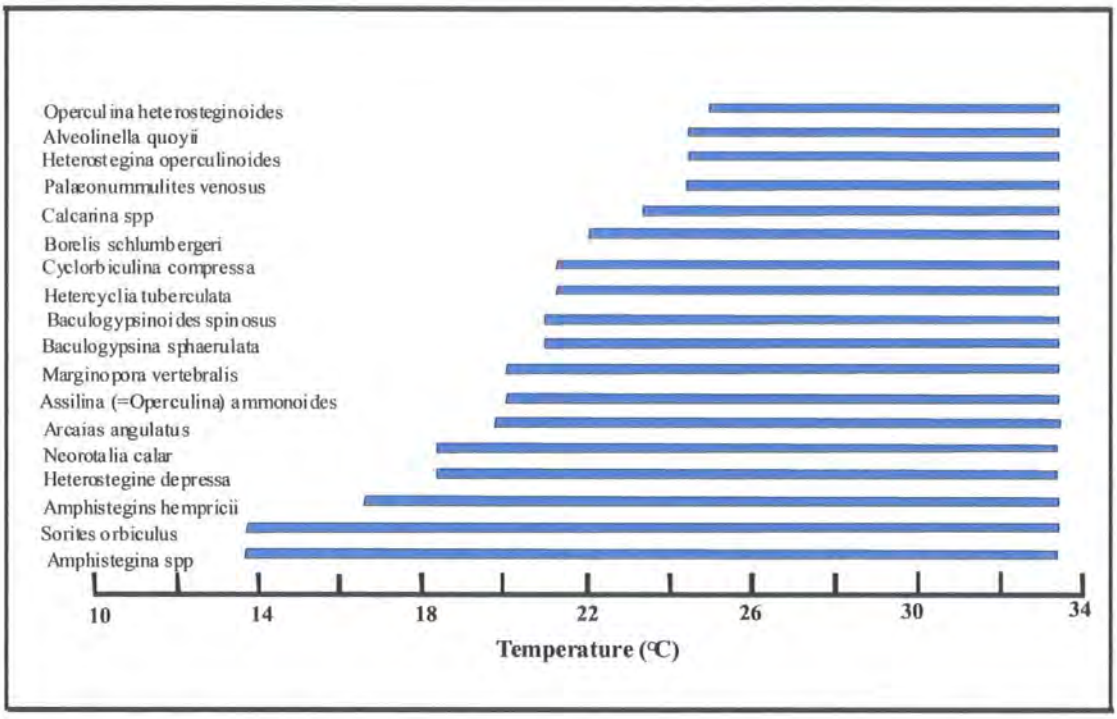

Figure 3.5. Sea surface temperature ranges of selected larger benthic foraminifera (after Beavington-Penny, Racey, 2004).

factors that have produced or contributed to extra damage (such as micro-scale bioersion, dissolution, and compaction) are considered to have played only a minor role. Beavintgon-Penney (2004) observations were used to aid identification of in-situ versus transported fossil nummulites tests in thin-section are illustrated in Figure 3.6.

3.5. MODELS OF LARGER FORAMINIFERA DEPOSITS:

In term of depositional environment, several facies models have been proposed to characterise nummulite-rich deposits. Different palaeowater depths are proposed, from 10-60m-depth, and different morphologies of sedimentary bodies are described (Figure 3.7).

- **Nummulite banks**: form convex-up structures. These so-called "bank" structures were described first by Nemkov (1962) and then named by Arni (1965). This sedimentary body is usually characterised by a mono-specific association of Nummulites, separating a restricted area (back-bank environment) from an open marine zone (fore-bank settings). This model has been applied for the Eocene Tatra Formation of Poland (Kulka, 1985), for the

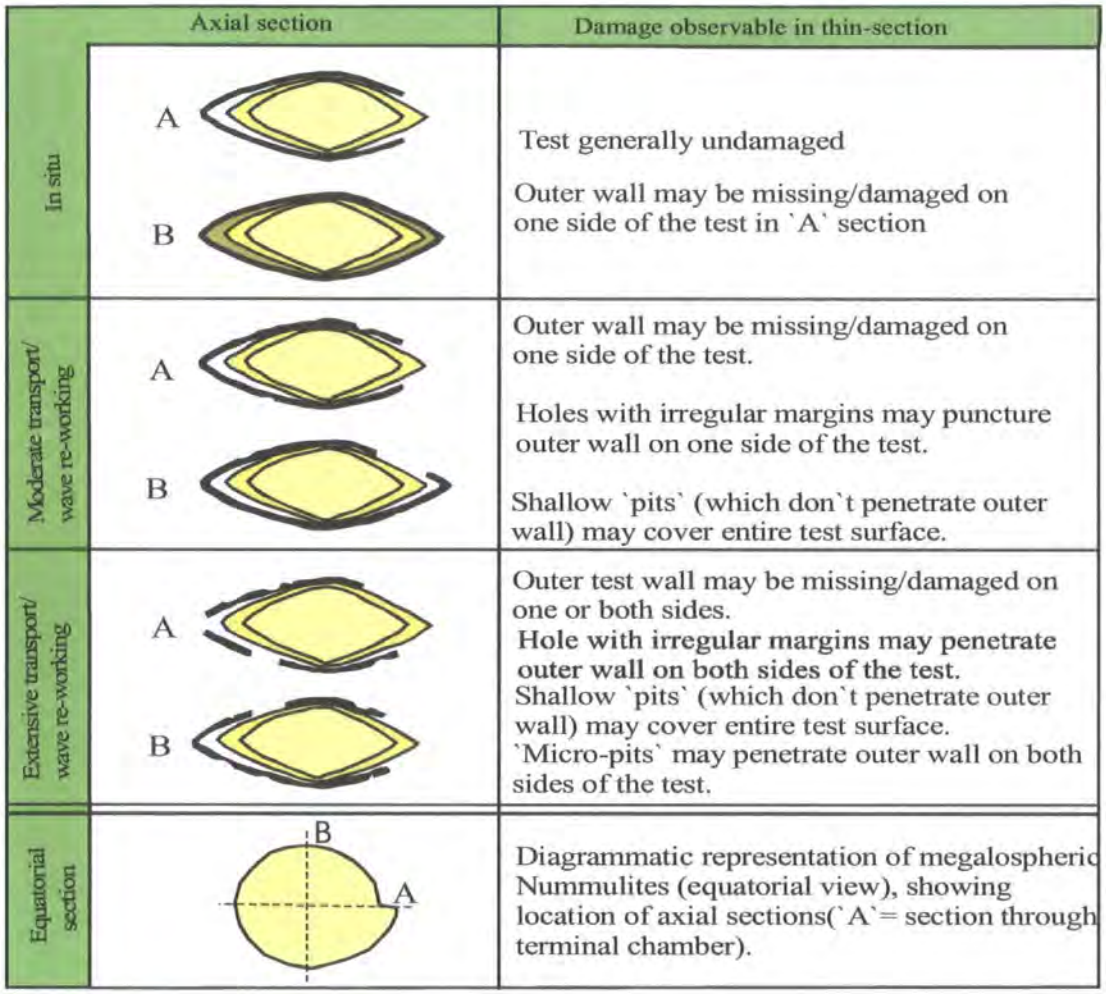

Figure 3.6. Test breakage patterns in Palaeonummulites venosus as a guide to the Autochthonous /allochthonous nature of fossil nummulites in thin-section (after Beavington-Penney, 2004).

Middle Eocene build-ups in Egypt (Aigner, 1983), for the El Garia Formation in central Tunisia (Moody et al., 1987) and for the Jdeir Formation in offshore Libya (Anketell and Mriheel, 2000).

- **Shoals:** may form in proximal up-ramp settings or as re-deposited Nummulitic material in deep-water environment (Racey et al., 2001). Nummulites were reworked from the proximal up-ramp areas and transported by turbidity or storm currents into deep-waters.
- **Nummulite "bars":** developed in very shallow environments, in front of coralgal reef bordering a carbonate ramp system (Eichenseer and Luterbacher, 1992). This model has been proposed for the Ager Formation in south Pyrenees

foreland basin (Spain). High-energy hydrodynamic structures forming Nummulite bars can be observed in Central Tunisia (after Jorry, 2004).

Nummulite-rich sediments are considered as autochthonous deposits or para-autochthonous to allochthonous deposits, the later resulting from landward or seaward transportation. Autochthonous deposits are characterised by packstone to wackestone textures, in which macrospheric forms (A-form) are much more frequent than microspheric ones (B-form). Tests are rarely abraded and are encrusted on only one side (Jorry, 2004). The fauna associated with Nummulite accumulations often includes coralline algae, echinoderms, molluscan debris, small benthonic foraminifera and larger benthonic foraminifera such as *Discocyclina* and *Assilina* (Racey, 2001). In contrast para-autochthonous and allochthonous deposits resulting from transportation or in-situ winnowing are characterized by more or less monospecific assemblages and grain-supported patterns. Sedimentary structures, which should be omnipresent in high-energy deposits, have been rarely documented in field or core studies (Jorry, 2004). Jorry et al (2003) mentioned the presence of large-scale cross bedding in the Eocene El Garia Formation in Central Tunisia but most of the grain-supported facies show a rather chaotic pattern and no obvious sedimentary structures.

4.6. NUMMULITE ACCUMULATION RESERVOIRS:

Nummulitic limestones are important hydrocarbon reservoir in Tunisia and Libya and represent exploration targets in other parts of north Africa, the Mediterranean and the Middle East. Nummulite accumulations may have high porosity ranging from 10-26% and permeabilities ranging from 10-50 md (Racey, 2001). In the Jdeir Formation, Offshore northwestern Libya porosities reaches to 40% (Anketell and Mriheel, 2000). According to Racey (2001) the best reservoir development is in Nummulite accumulations where there has been little compaction and where Nummulithoclastic debris and lime-mud are absent. In these deposits Nummulite tests are generally moderately to well sorted and there is minimal or no precipitation of late burial cements. Diagenesis (such as dissolution, dolomitization, cementation and compaction) is the main control on enhancing or destroying the porosity in Nummulite accumulations (Anketell and Mrihell, 2000 and Racey, 2001).

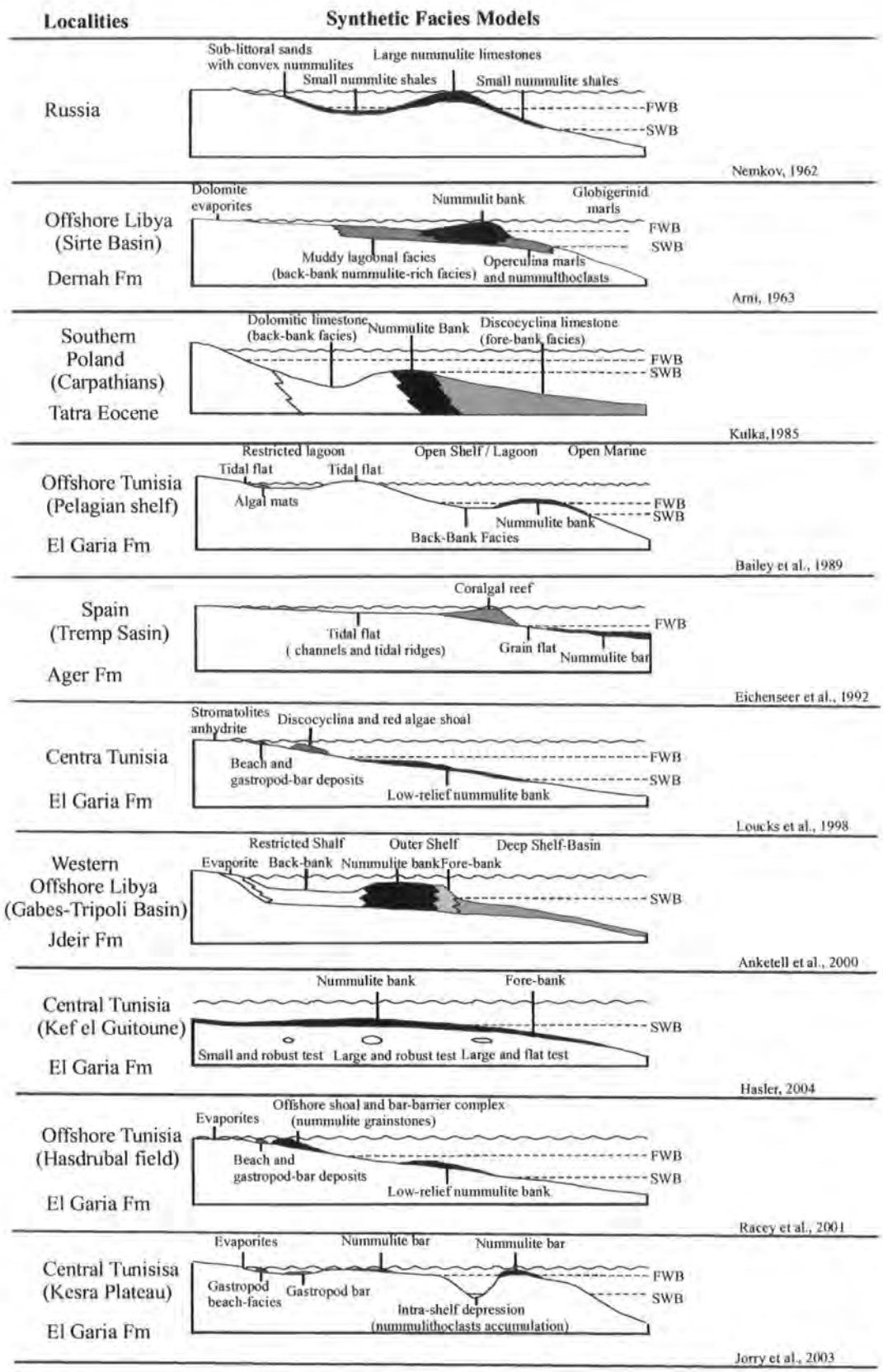

Figure 3.7.Comparison between different models characterizing the nummulite paleoenvironment (modified by Jorry. 2004).

3.7. SUMMARY:

Larger benthonic foraminifera are important contributors to modern and ancient tropical, shallow–marine sediments. Nummulites with other larger foraminifera including nummulitids and alveolinids are believed to have lived symbiotically with photosynthetic algae and are therefore thought to have been restricted to warm (25°C), clear, shallow waters (<120m) within the euphotic zone. Nummulites had alternating asexual and sexual generations, characterised respectively by small A-forms and larger B-forms. In nummulitic banks, B-forms are often dominant in high-energy settings, whereas the A-forms and larger *Discocyclina* are dominant in deeper-water, lower energy settings. The distribution of these two morphotypes is in general controlled by the hydrodynamics of the depositional system. Nummulite tests may display breakage ranging from external damage to complete fragmentation (commonly referred to as nummulithoclastic debris). Studies of modern larger benthonic foraminifera suggest that transport-induced abrasion is a likely candidate for the test damage.

CHAPTER FOUR

4. FACIES AND DEPOSITIONAL ENVIRONMENT OF THE JDEIR FORMATION:

4. FACIES AND DEPOSITIONAL ENVIRONMENT OF THE JDEIR FORMATION

4.1. INTRODUCTION:

This chapter contains results and interpretations of a detailed petrographic study of ninety-two core samples selected from the Jdeir Formation in wells E1-NC41, B7-NC41 and A2-NC41, Sabratah Basin, offshore northwest Libya. The main objectives of this chapter are:

- To describe and interpret the different facies of the Jdeir Formation in three wells using both core data and petrographic microscope observations.
- To interpret the depositional environment of facies and to evaluate the spatial variability in carbonate platform development.

4.2. JDEIR FORMATION INTRODUCTION:

The Jdeir Formation is a shallow carbonate platform deposit that developed during the Early-Middle Eocene in the Sabratah Basin. The Formation comprises the upper unit of the Farwah Group and is the main target for hydrocarbon exploration in the offshore area. The Jdeir Formation was formally defined by Hammuda et al (1985) as a skeletal carbonate, rich in nummulites; the type section was selected in well B2-NC41 in the Bouri field (Figure 2.4). In this well, a lower bioclastic limestone rich in nummulites, orbitolites and alveolinids, is overlain by an upper unit consisting of fossiliferous bioclastic and micritc limestone containing numerous nummulites, calcareous algae, gastropods, bivalves and ostracods. The total thickness in the type section is 131 m. The Jdeir Formation is present over a wide area in the Sabratah Basin extending at least 80 km in a N-S direction and in E-W direction. Sbeta (1990) published distribution map of the Jdeir Formation (Figure 4.1), showing a maximum thickness of over 200 m in the E1-NC41 and L1-NC35A wells. The formation thins towards the south-west to only 37 m in well F1-137, and passes into the Taljah Formation south of well P1-NC41. Farther east it averages 180 m in concession NC35A, toward the shelf-edge. It is not present on the Jarrafa Arch in F1-NC35A and B1-NC53, nor in well M1-NC41 and extending toward well L1-137. In general, the Jdeir Formation was bounded by restricted platform deposits of the Taljah Formation

in a southerly landward direction and by deep-platform to basinal facies of the Hallab Formation towards the northern offshore direction.

4.3. PREVIOUS WORK ON THE JDEIR FORMATION:

The Jdeir Formation has been the subject of number of studies during the last decade after a number of wells were drilled (e.g., Bernasconi et al., 1991; Sbeta, 1984; Mriheel, 1991; Mriheel et al. 1993; Anketell and Mriheel, 2000).

-Bernasconi et al. (1991) studied the petrography and diagenesis of the Farwah Group in the Bouri oil field and divided it into three main lithofacies: Nummulitic, dolomitic and micritic deposits and proposed a nummulite bank-model.

-Sbeta (1984) conducted a comprehensive sedimentological study of the Eocene sequence in the north-western offshore Libya area and related the lithofacies to depositional environments according to the standard facies model of Wilson (1975).

-Mriheel (1991) studied the diagenetic history of the Jdeir Formation and recognised that diagenetic alteration had occurred in three environments: Marine phreatic, Meteoric phreatic and Burial.

-Mriheel et al. (1993) studied the Jdeir Formation in B3-09-NC41 well and divided it into four main units: Fore-bank (shelf-slope setting), nummulitic bank, Fore-bank with levels of restricted platform setting and Fore-bank-pelagic facies.

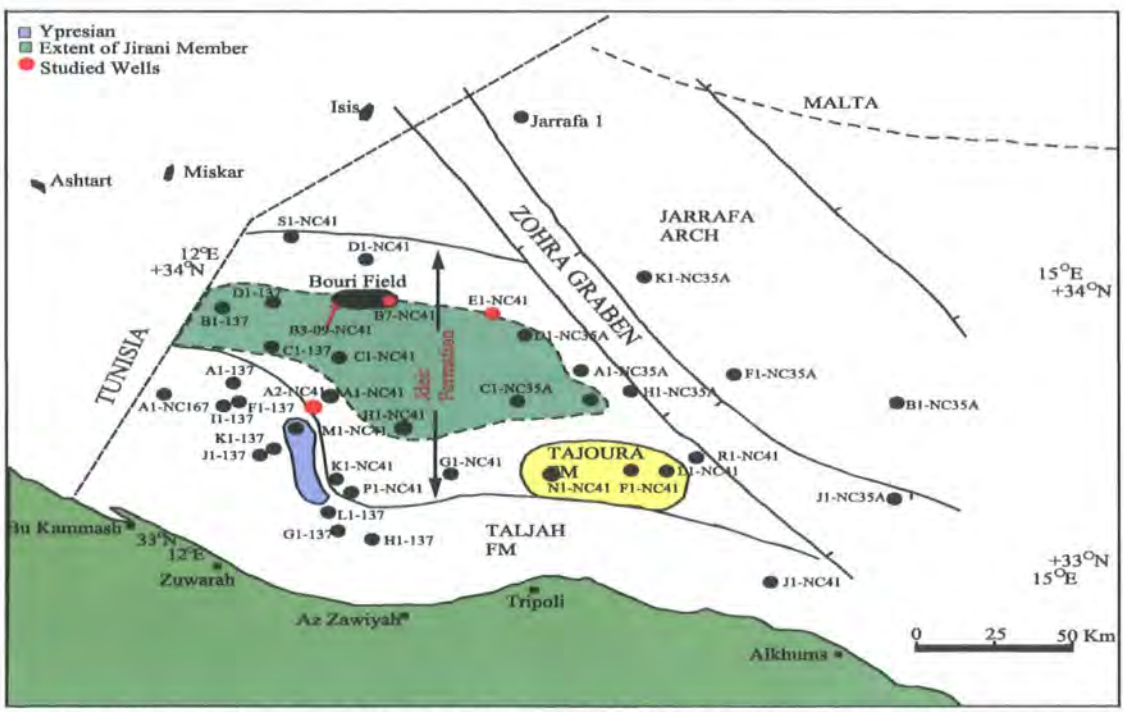

Figure 4.1. Distribution map of the Jdeir Formation Offshore northwest Libya (Sbeta, 1990).

-Anketell and Mriheel (2000) in their study of the Jdeir Formation recognized three major lithofacies: Nummulitic packstone/grainstone, Alveolina-orbitolites wackestone /packstone and foraminiferal-discocylina-assilina wackestone/packstone, deposited in bank, back-bank, and fore-bank environments, respectively. They also noted that lithofacies were structurally controlled by contemporaneous and/or syndepositional tectonic movements, with nummulitic facies tending to develop on uplifted areas.

4.4. FACIES ANALYSIS OF THE JDEIR FORMATION:

Based on the core description of three wells (A2, B7 and E1-NC41) and the petrographic study of 92 thin-sections, eight main facies and twenty-four microfacies within the Jdeir formation have been distinguished during this study. These seven major facies are described and interpreted below, and the facies scheme is summarised on Table 4.1. Although the main diagenetic features of each facies are described here, their interpretation is described in chapter 5.

4.4.1. DISCOCYCLINA -NUMMULITES FACIES (DNF):

Includes:

Microfacies: Discocyclina Nummulites Floatstone/Rudstone (DNF/R)

i-Facies description:

This facies occurs only in the uppermost part of well E1-NC41 (Figures 4.13 and 4.14). The unit is 17 feet thick.

The Discocyclina / Nummulite Facies consist predominantly of coarse- to pebble- sized, poorly sorted, thin, inflated large *Discocyclina* (15%), associated with whole and fragmented nummulites (10 %) (Figures 4.2 and 4.3a). Nummulites are dominated by small B-forms (size ranges from 0.5 to 4mm). Other less common bioclasts are small echinoid fragments. Most of the echinoderm grains are rimmed by syntaxial overgrowths. The matrix is composed of micrite and small fragmented bioclasts. Stylolites and pressure solution seams were the only structures seen in this facies and there was no indication of primary sedimentary structures. Observed porosity is poor (3%) and includes small vuggy and rare intragranular pores. The permeability is poor because the pore spaces are not interconnected.

ii- Facies interpretation:

The bioclasts in this facies indicate open marine conditions. Abundant thin *Discocyclina* and the presence of micrite suggests that these deposits formed in a low to moderate energy, fore-bank environment (Henson, 1950). Whole and fragmented nummulites are interpreted to have been reworked from higher energy areas. Racey (1995) inferred in a study of the Eocene Seeb Formation of Oman that large, elongate Assilina and Discocyclina lived in relatively deep water (50-80 m) on open parts of the ramp. Anketell and Mriheel. (2000) state that the fragmented *Discocyclina-Assilina* facies was only noted the northern part of Jdeir formation and was also interpreted as fore-bank deposits. The presence of abundant elongate *Discocyclina* suggests deposition in the photic zone, but below FWWB (Beavington-Penney et al., 2005).

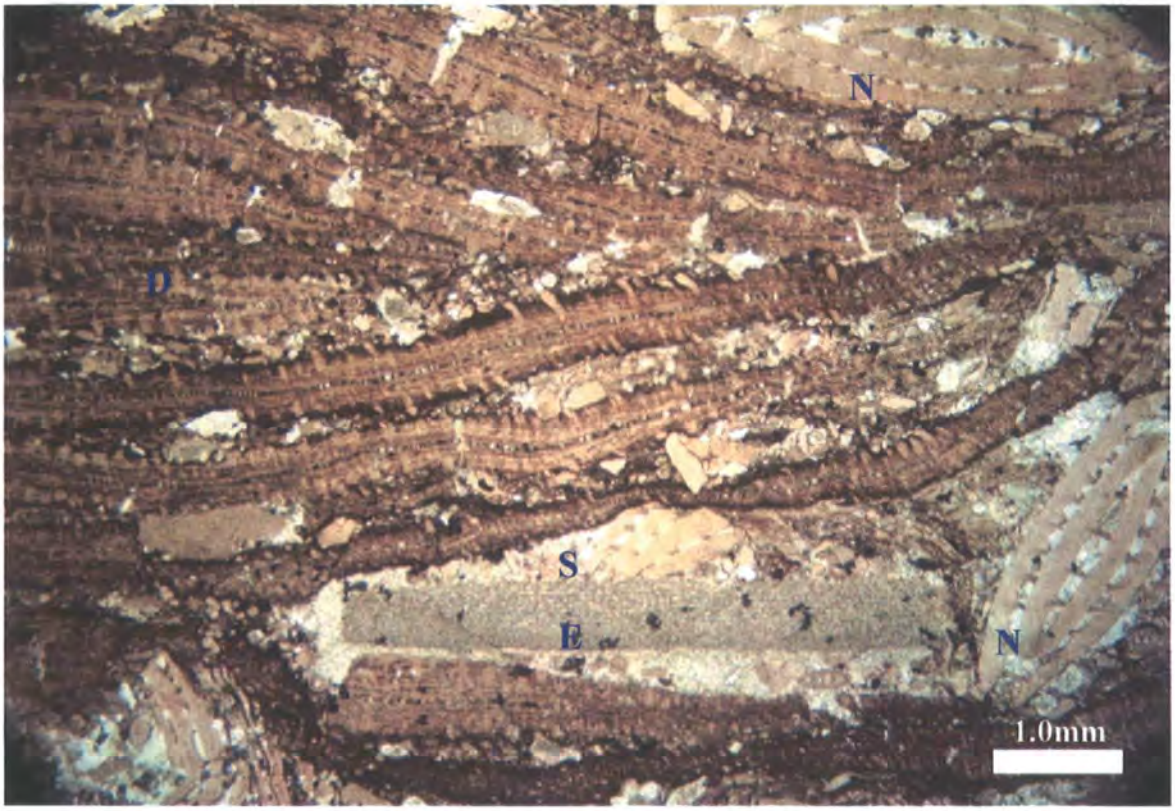

Figure 4.2. Photomicrograph of Discocyclina- Nummulitic floatstone/rudstone microfacies with thin, large *Discocyclina* (D) and scattered robust nummulites (N). Syntaxial cement overgrowth around echinoid fragments (E) has locally occluded intergranular pores (S). Jdeir Formation, E1-NC41 well, 8260.0 feet, PPL.

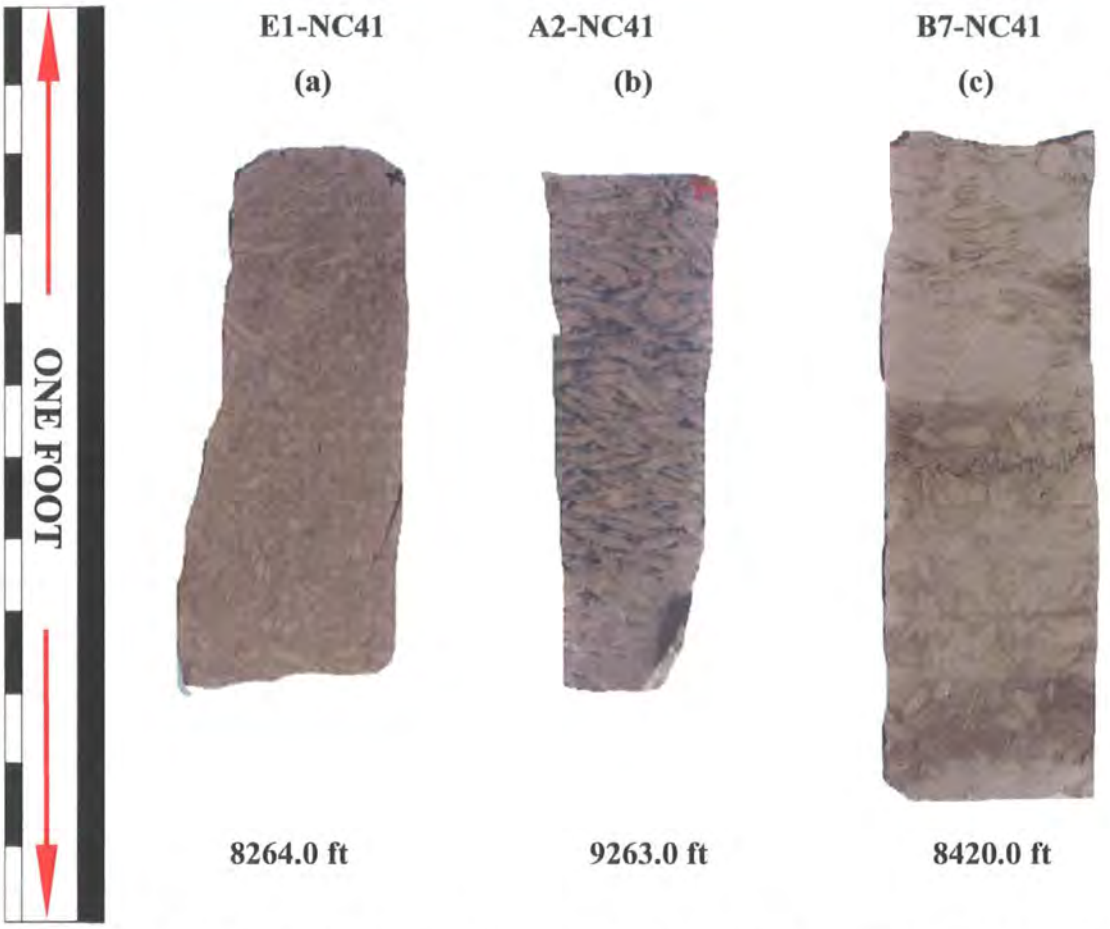

Figure 4.3. Core photographs of Discocyclina-nummulite facies (a) and nummulite facies (b and c) showing Discocyclina fore-bank and nummulitic bank deposits in three wells.

4.4.2. NUMMULITE FACIES (NF):

Includes:

Microfacies:

Nummulitic Rudstone (NR)

Nummulitic Packstone-Grainstone/Rudstone (NP-G/R)

Nummulitic Floatstone/Rudstone (NF/R)

Nummulitic Wackestone/Floatstone (NW/F)

Nummulitic Wackestone-Packstone/Floatstone (NP-W/F)

Nummulithoclastic Wackestone/Floatstone (NCW/F)

Nummulithoclastic Wackestone/Packstone (NCW/P)

Nummulite-Echinoid Wackestone (NEW)

i-Facies description:

This facies occurs in the upper and the lower parts of wells B7-NC41 and A2-NC41, while in E1-NC41 it occurs only in the upper part underlying the Discocyclina

/ nummulite facies (Figures 4.13, 4.14, 4.22, 4.23, 4.26 and 4.27). Unit thickness of this facies varies between 5-72 feet thick.

The Nummulite Facies consists mainly of light grey to light brownish grey, coarse- to pebble-size, small and large nummulites (fragments <42% and whole <38%). Other common components are echinoid and mollusc fragments, all in a fine to coarse skeletal grain wackestone /packstone matrix. Occasionally intervals of mudstone were also observed. The sorting of the bioclasts is moderate to poor. Other skeletal grains are minor smaller foraminifera (rotaliids and miliolids), rare D*iscocyclina*, ostracoda and brachiopod fragments. Very rare fragments of coral and coralline algae are observed only in the upper part of well A2-NC41 (Figure 4.6).

The Nummulitic Packstone-Grainstone/Rudstone microfacies is observed in the upper part of well B7-NC41. It is composed of sub-globular small nummulites (A-forms with scattered large, flattened B-forms). The Nummulite Rudstone microfacies occurs in the lower part of well A2 and the upper part of well B7. This microfacies is dominated by compacted, flattened small and large B-forms and sub-globular small A-forms with very rare scattered small echinoid fragments (Figures 4.3b, 4.3c, 4.4and 4.5). The Nummulitic Floatstone/Rudstone was observed in the upper and lowermost parts of well B7 and only in the upper part of wells E1 and A2. It is composed of a mixture of sub-globular small B and A-forms and scattered flattened large B-forms with minor echinoid, mollusc fragments and scattered miliolids. The Nummulithoclastic Wackestone/Floatstone and Wackestone/Packstone occur in three wells and are composed mainly of small nummulite fragments with high amounts of micrite. The matrix contains a high proportion of Nummulithoclastic debris. The Nummulite Echinoid Wackestone occurs only in the lowermost part of A2-NC41. Most of the echinoid fragments and spines are rimmed by syntaxial overgrowth cements. Molluscan fragments (including: gastropods and bivalves), have been partially to completely dissolved and filled by blocky and drusy calcite cements. Oysters are also observed in some samples. Non-skeletal grains include rare peloids (micritized grain) and intraclasts. The matrix is composed of micrite and fine bioclastic fragments. Authigenic minerals are dominated by non-ferroan calcite cements and pyrite. In some samples chert (microquartz, macroquartz and chalcedony) has partially replaced nummulites and filled primary porosity. Nummulites are tightly packed and occasionally grain contacts are sutured or stylolitic. The stylolite seams are generally <1 cm in amplitude and are commonly infilled by dark black organic

matter or bitumen. Fractures and microfractures are observed. They are generally <1mm in width and up to a few cms in length. When present, they are usually infilled by calcite cement and sometime by oil. Bored mollusc fragments are also rarely present (Figure 4.7). Observed porosity in this facies is poor to very good (ranges from 0-17 %) and includes intragranular, vuggy, mouldic and rare microfracture types. The permeability ranges from poor to good.

ii- Facies interpretation:

The occurrence of well-preserved, abundant large perforate foraminifera and echinoids indicates that normal marine conditions prevailed during the deposition of this facies. The large-size, nature and sorting of the large nummulite tests and grain-supported texture of the nummulite rudstone are all indicative of a moderate to high-energy bank environment. Racey (2001) summarised the complex relationships between large benthoic foraminifera typical of Early Tertiary carbonate platforms, concluding that Nummulites occupied a broad range of open marine environments on the both ramp and shelf and were generally absent from more restricted waters. Large flat Nummulites tend to be associated with similarly shaped *Assilina* and *Discocyclina* in relatively deep-water environments, whilst smaller, lenticular Nummulites occur in shallower, inner ramp/shelf settings, often coexisting with *Alveolina* "banks" including medium- to large-sized Alveoloinids. Lenticular-to globular-shaped Nummulites tend to occupy intermediate environments. Outer wall damage of some nummulites in the nummulithoclastic floatstone/rudstone microfacies may show moderate transport/ wave re-working (Beavington-Penney, 2004). The occurrence of abundant nummulithoclastic debris in NCW/F and NCW/P microfacies indicates extensive transportation. It is suggested that periodic high-energy events resulted in redeposition in inter or back-bank area. Abundant micrite is indicative of deposition in lower energy conditions. Anketell and Mirheel (2000) suggest that high-energy conditions caused fragmentation of Nummulites in the Jdeir Formation, carrying them towards parts of the back-bank setting. Beavington-Penney et al. (2005) concluded from a study of the Al Garia Formation of Tunisia that Nummulites on the palaeohighs were transported into surrounding deeper water. They suggested that ocean and storm currents swept the platform top, producing a nummulitic sediment package that thickened and became increasingly fine-grained and fragmented into outer ramp environments.

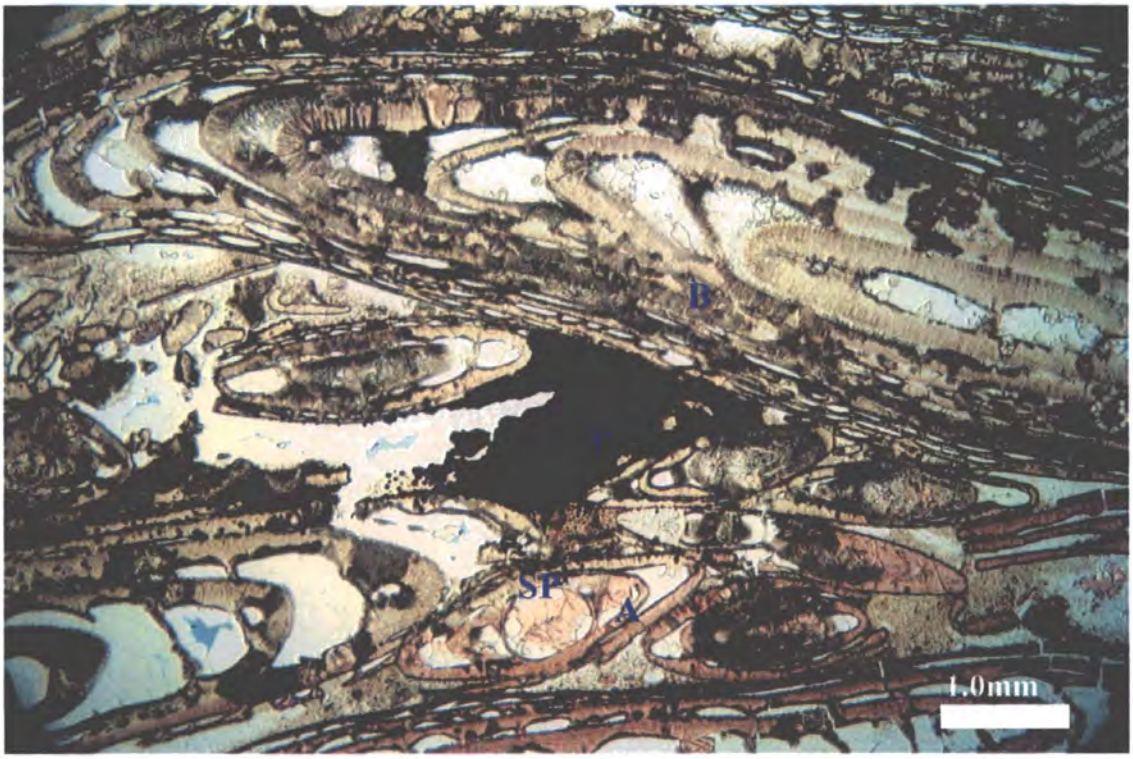

Figure 4.4. Photomicrograph of Nummulite rudstone microfacies shows flattened, large B-form nummulite (B) with rare small A-form (A). Intragranular porosity still preserved within nummulite chamber. Irregular pyrite (P) and blocky to drusy calcite (SP) cements have partially filled porosity. Jdeir Formation, A2-NC41 well, 9262.5 feet, PPL.

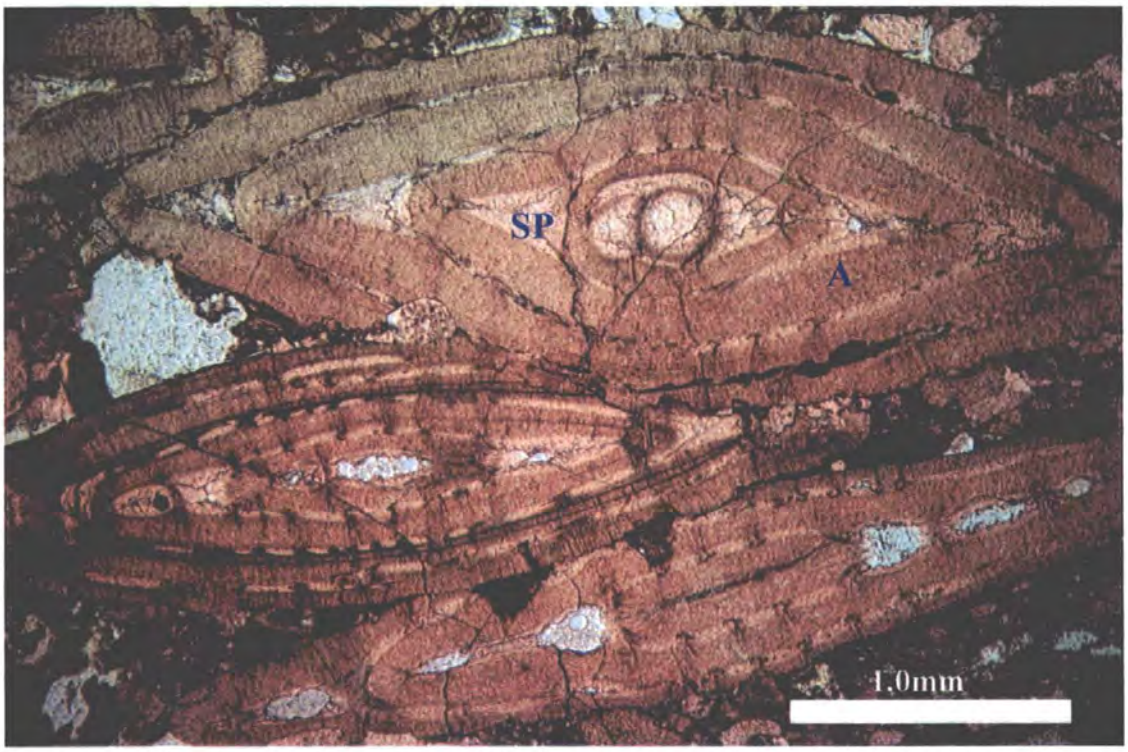

Figure 4.5. Photomicrograph of Nummulite floatstone/rudstone microfacies shows compacted, robust A-form nummulite (A). Intragranular porosity within nummulite chambers has mostly been lost due to calcite cements (SP). Jdeir Formation, B7-NC41 well, 8295.0 feet, PPL.

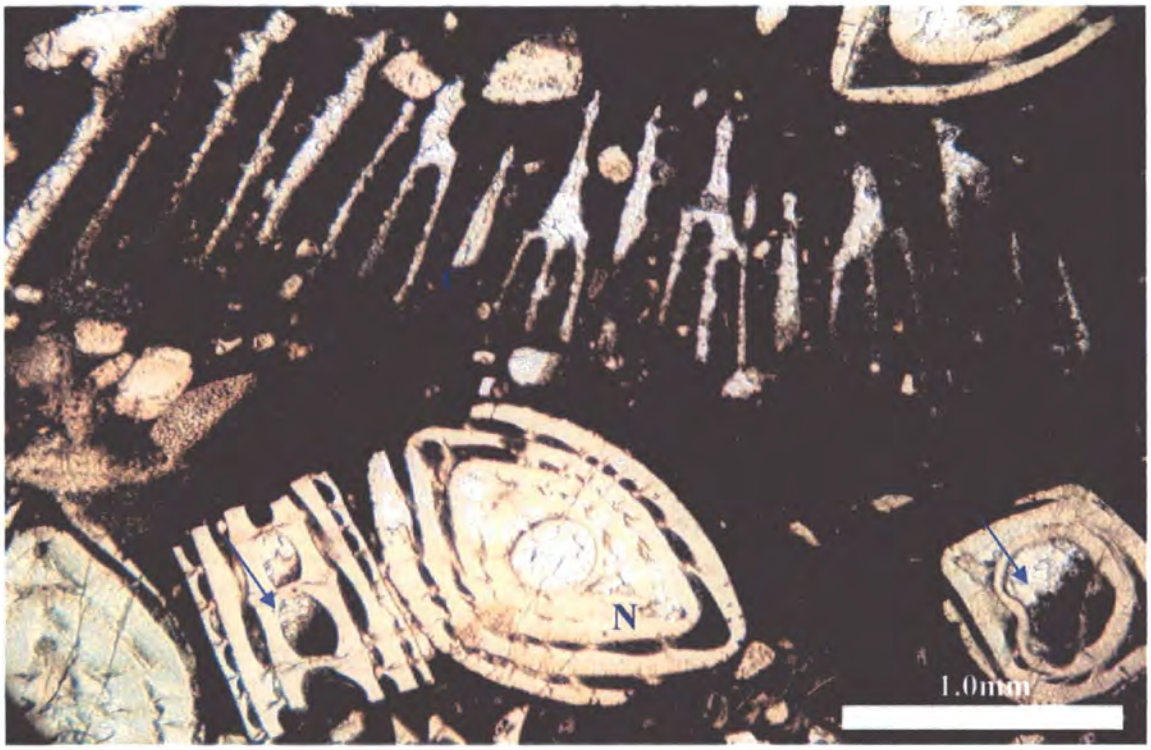

Figure 4.6. Photomicrograph of Nummulite wackestone/floatstone microfacies showing coral (C), and broken nummulites floating in micrite matrix. Geopetal structure occurs within nummulite chamber (arrows). Jdeir Formation, B7-NC41 well, 9067.0 feet, PPL.

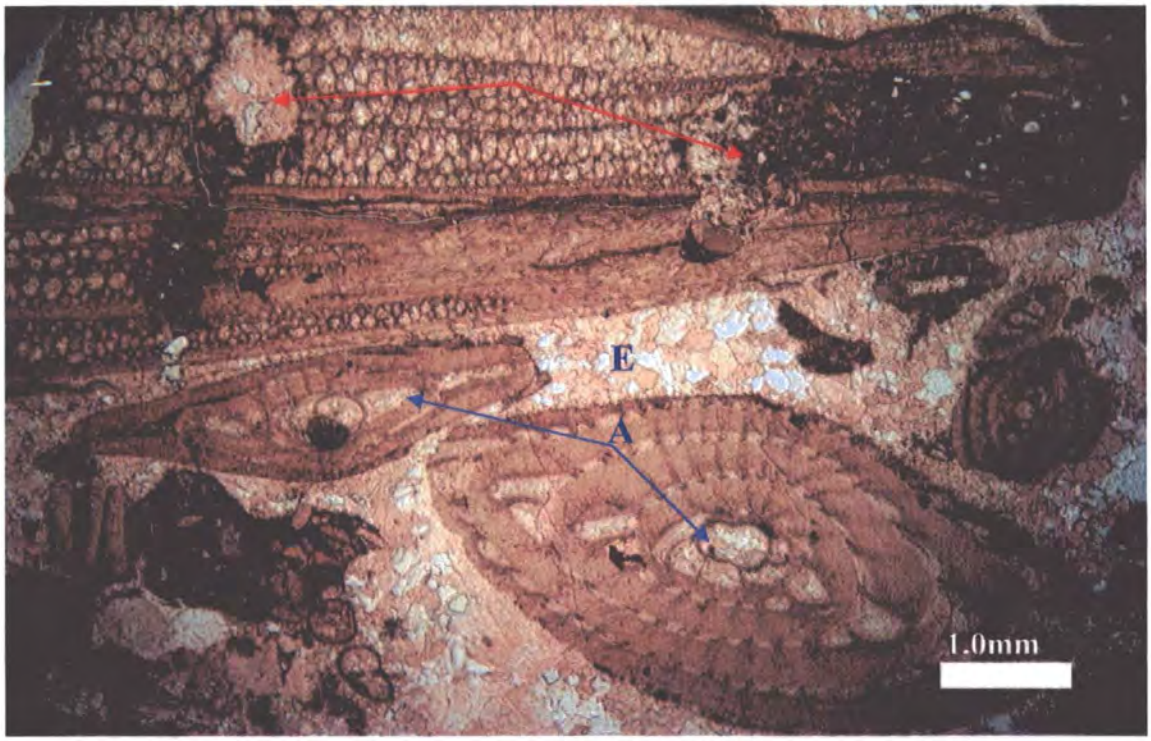

Figure 4.7. Photomicrograph of Nummulite packstone-grainstone/rudstone microfacies with bored mollusc fragment (oyster) (red arrows) and robust nummulite grainstone. Intergranular (E) and intragranular (A) porosity have been completely filled by sparry calcite cement. Jdeir Formation, B7-NC41 well, 8253.0 feet, PPL.

4.4.3. ALVEOLINA FACIES (AF):

Includes:

Microfacies: **Alveolina-Miliolid Wackestone/Packstone (AMIW/P)**
Alveolina-Echinoid Wackestone/Packstone (AEW/P)
Alveolina-Mollusc Wackestone/Packstone AMOW/P)
Alveolina-Nummulitic Packstone (ANP)
Alveolina-Orbitolites Packstone (AOP)

i-Facies description:

This facies is observed in the middle and lower parts of well E1-NC41 (Figures 4.13 and 4.14). Units range in thickness from 10-116 feet thick

The Alveolina Facies is composed of light grey to medium grey, medium – coarse *Alveolina* (up to 15 %) and miliolids (4-10%) with common small echinoid and mollusc fragments (Figures 4.8, 4.9, 4.10 and 4.11). Other less common grains includes peloids, small foraminifera (rotaliids), orbitolites, whole and fragments sub-globular, small nummulites, dasycladacean algae and small coralline algae fragments. Some mollusc fragments have been partially to completely dissolved and filled by blocky and drusy calcite cements. Syntaxial overgrowth cements around echinoid fragments are common in this facies. The groundmass is composed of micrite, fine bioclastic fragments and calcite cements. Micrite is partially recrystallized to microsparite. Structures seen include stylolites, pressure solution seams and fractures. Observed porosity is poor to fair (0-7%), including vuggy and mouldic types. The permeability is poor in this facies because the voids or pore space are isolated or poorly interconnected.

ii-Facies interpretation:

The presence of perforate foraminifera, and echinoids are suggestive of normal marine conditions. On the base of abundant *Alveolina* this sediment may have formed in clear protected lagoonal back-bank environments. The occurrence of well-preserved miliolids suggests deposition in inner shelf settings in water depths of 6-10m (Cushman et al. 1954). Bebout and Pendexter (1975) interpreted the miliolid-micrite facies as forming in shallow shoal or lagoon environments. The presence of calcareous algae (dasycladacean algae) suggests deposition at depth ranging from the low tide level down to 10m (Johnson, 1961). Newell et al. (1953) reported dasycladacean algae from inner platform settings. A moderate-energy depositional

setting is inferred for these lithologies based on the wackestone /packstone texture. The Alveolina-Orbitolites-Miliolid packstone in the Dernah Formation from northeastern Cyrenaica, northern Libya is interpreted as having been deposited in shallow protected environment (Jorry, 2004). In the Jdeir Formation from northwestern Libya, the Orbitolites-Alveolina wackestone/packstone is interpreted as forming in a back-bank setting (Anketell and Mriheel, 2000).

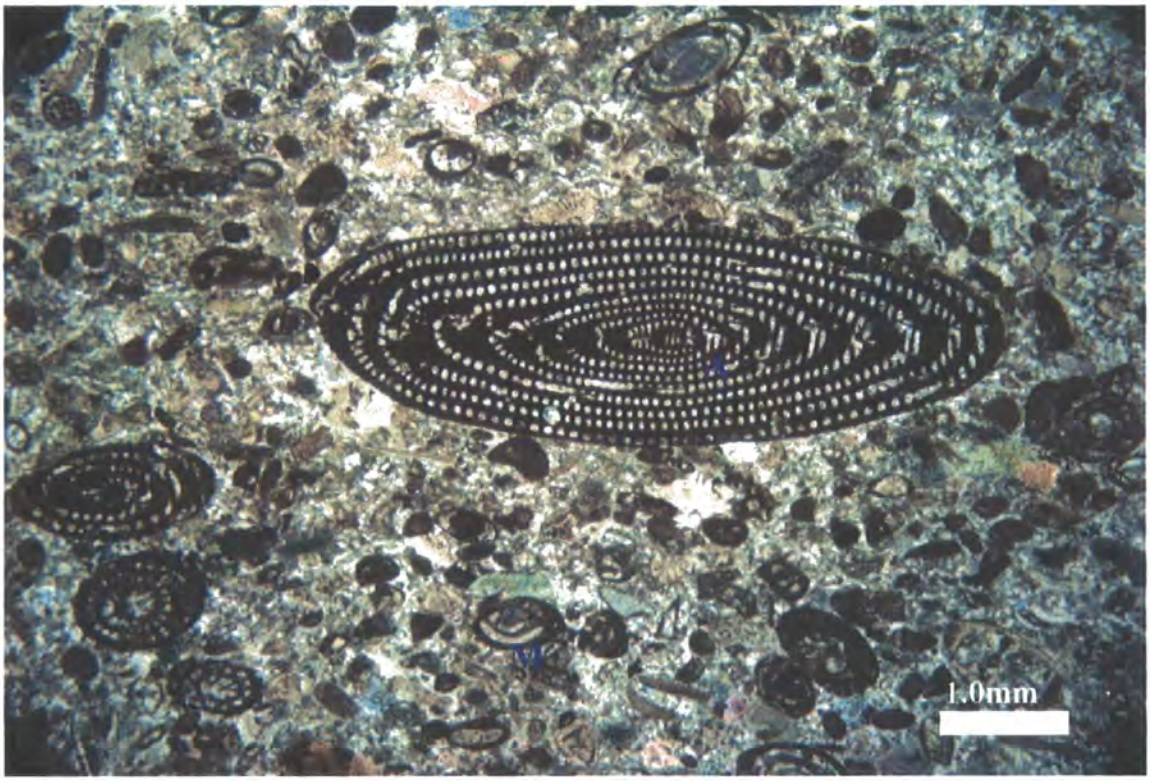

Figure 4.8. Photomicrograph of *Alveolina* –Miliolid wackestone/packstone shows fine to medium-grained packstone /grainstone consisting almost entirely of *Alveolina* (A), with miliolids (M), and small bioclastic debris. Jdeir Formation, E1-NC41 well, 8361.0 feet, XN.

4.4.4. PELOIDAL- BIOCLASTIC FACIES (PBF):

Includes:

Microfacies: **Peloidal Echinoid Packstone grainstone(PEP/G)**

Peloidal Echinoid Coralline algal Packstone (PERP)

i-Facies description:

This facies is observed only in the lower part of well E1-NC41. Units range from 10 to 52 feet thick (Figures 4.13 and 4.14).

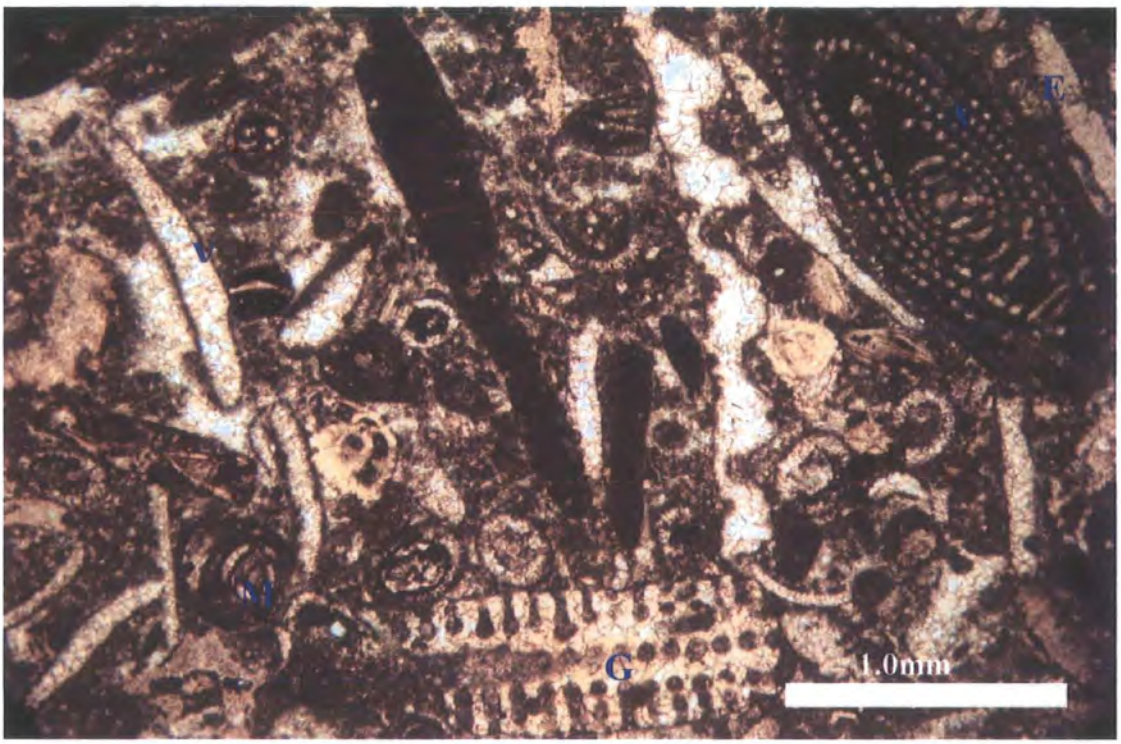

Figure 4.9. Photomicrograph of Alveolina-Molluscan wackestone/packstone microfacies shows a variety of bioclastic grains including *Alveolina* (A), dasycladacean algae (G), miliolid (M), and bivalves (V) and echinoid fragment (E). Bivalves have been completely dissolved and replaced by equant and drusy calcite cements. Jdeir Formation, E1-NC41 well, 8389.0 feet, PPL.

Figure 4.10. Photomicrograph of Alveolina -Echinoid wackestone/packstone microfacies shows coralline algae (R) and echinoid fragment (E). Porosity has been completely filled by equant and drusy calcite cements (SP). Jdeir Formation, E1-NC41 well, 8489.0 feet, PPL.

Figure 4.11. Photomicrograph of Alveolina-Orbitolite packstone microfacies containing a mixture of grains include orbitolites (O), miliolid (M), rotaliids (R), small gastropods (G) and peloids (P). Jdeir Formation, E1-NC41 well, 8564.0 feet, PPL.

The Peloidal-Bioclastic Facies is composed of light grey to light brownish grey, fine-medium grained, moderately sorted, rounded and sub-rounded peloidal (10-15%) and echinoid fragments (8-10%). Other common grains are small foraminifera (Rotaliida and Miliolida) and coralline algae in packstone and wackestone/packstone depositional textures (Figure 4.12). Many of the peloids have heavily micritized margins with some showing original internal structure. The size of the peloids is less than 1mm, but the majority are in the range of 0.1-0.5mm in diameter. Other grain types are mollusc fragments, coralline algae, dasycladacean algae and very rare nummulite fragments. *Alveolina* and orbitolites are also observed in some microfacies. Syntaxial overgrowths around echinoid fragments are common. The matrix is composed of micrite, microsparite and small bioclastic fragments. Structures seen include common stylolites and dissolution seams. Observed porosity is poor to fair (3-8%) and includes mouldic and vuggy types. The permeability is poor.

ii-Facies interpretation:

The presence of echinoids and coralline algae are indicative of normal marine conditions. Common miliolids throughout the facies suggests depositional in shallow water depth of ~ 6-10m in lagoonal or back-bank environments. The occurrence of packstone and wackestone texture suggests that these sediments were deposited in low to moderate energy. Tucker (1981) described peloids as spherical, cylindrical or angular grains composed of microcrystalline carbonate with no internal structure. Most peloids in this facies appear to be micritized grains and possibly minor faecal pellets.

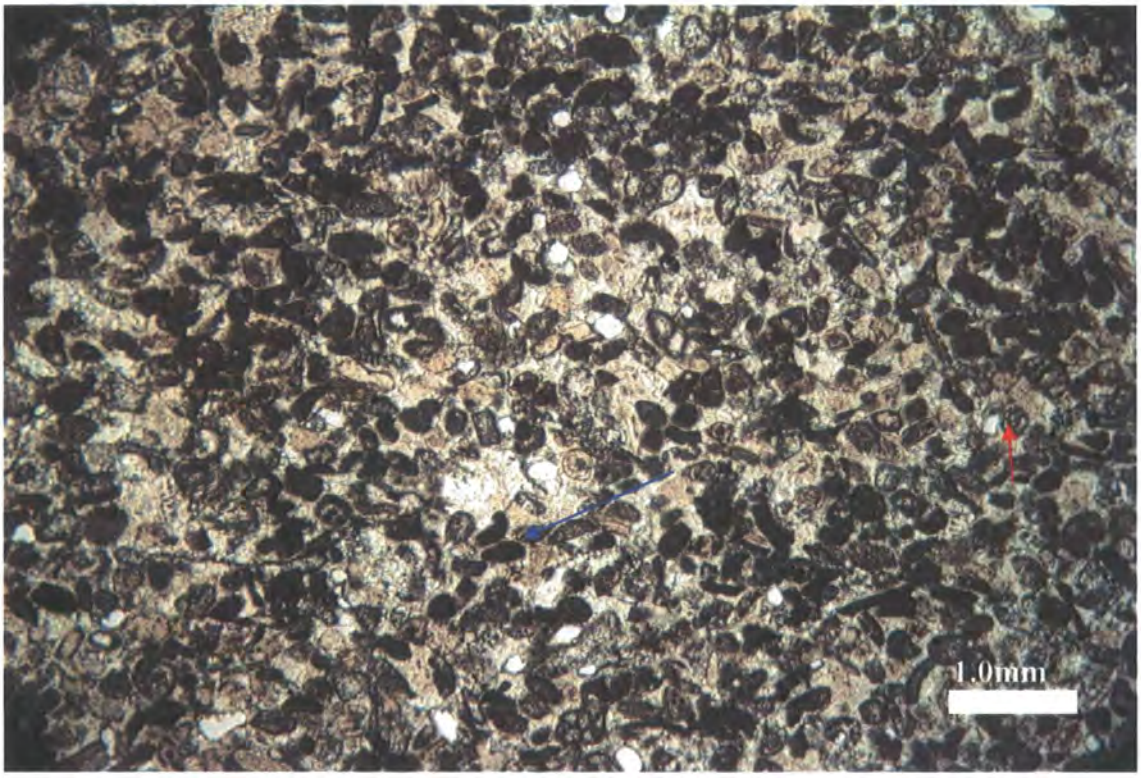

Figure 4.12. Photomicrograph of peloidal-Echinoderm packstone/grainstone showing fine grained, moderately sorted peloids (blue arrows), and small foraminifera (red arrow). Jdeir Formation, E1-NC41 well, 9498.0 feet, PPL.

4.4.5. MOLLUSC FACIES (MOF):

Includes:

Microfacies: Mollusc Wackestone/Packstone (MOWP)

Mollusc Packstone/Grainstone (MOPG)

Mollusc -Foraminfera Mudstone/Wackestone (MOFMW)

Mollusc Wackestone/Floatstone (MWF)

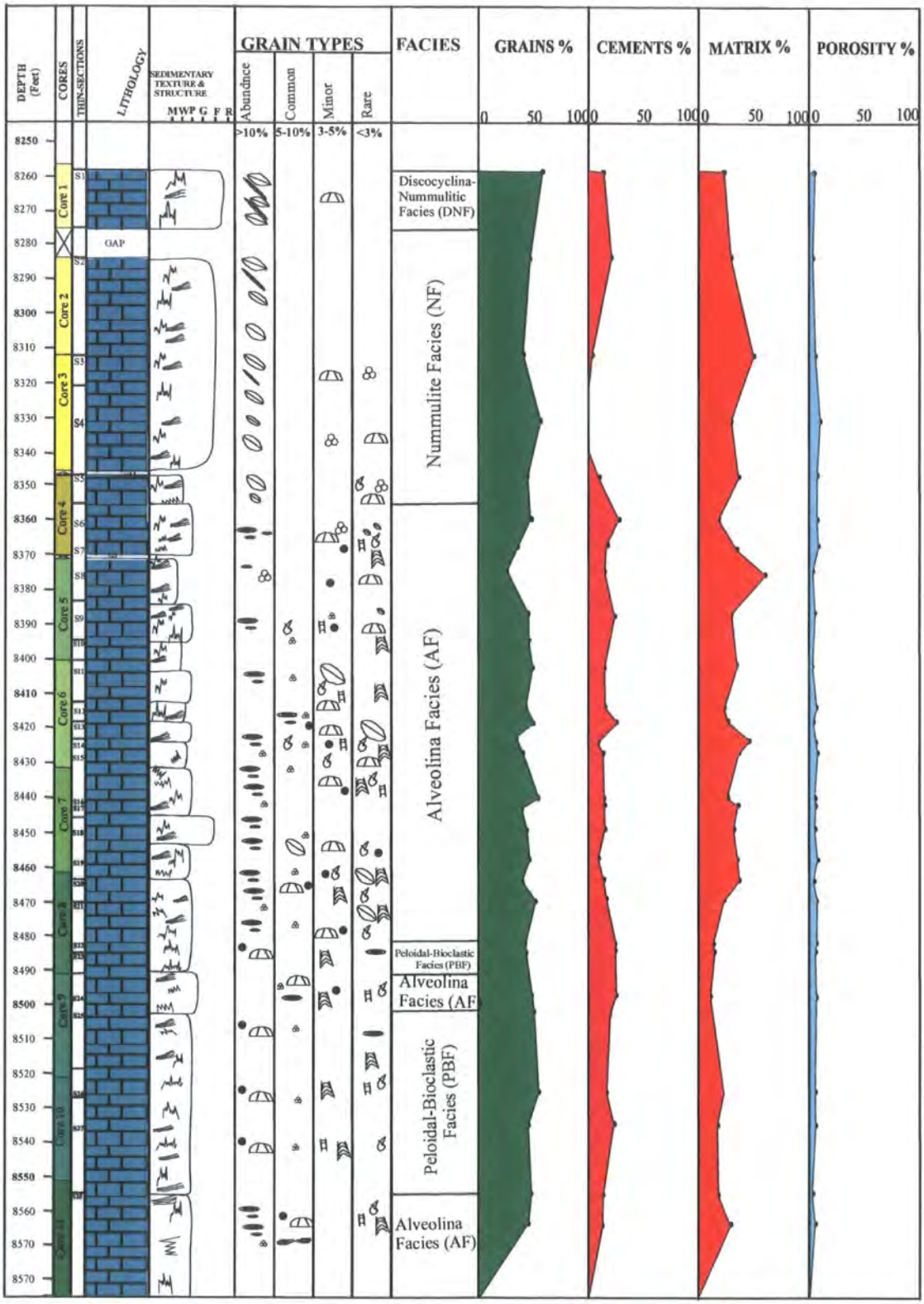

Figure 4.13. Petrographic characteristics of the Jdeir Formation in well E1-NC41, showing the point counting data, grain types, cements, matrix and porosity. (See appendix for key).

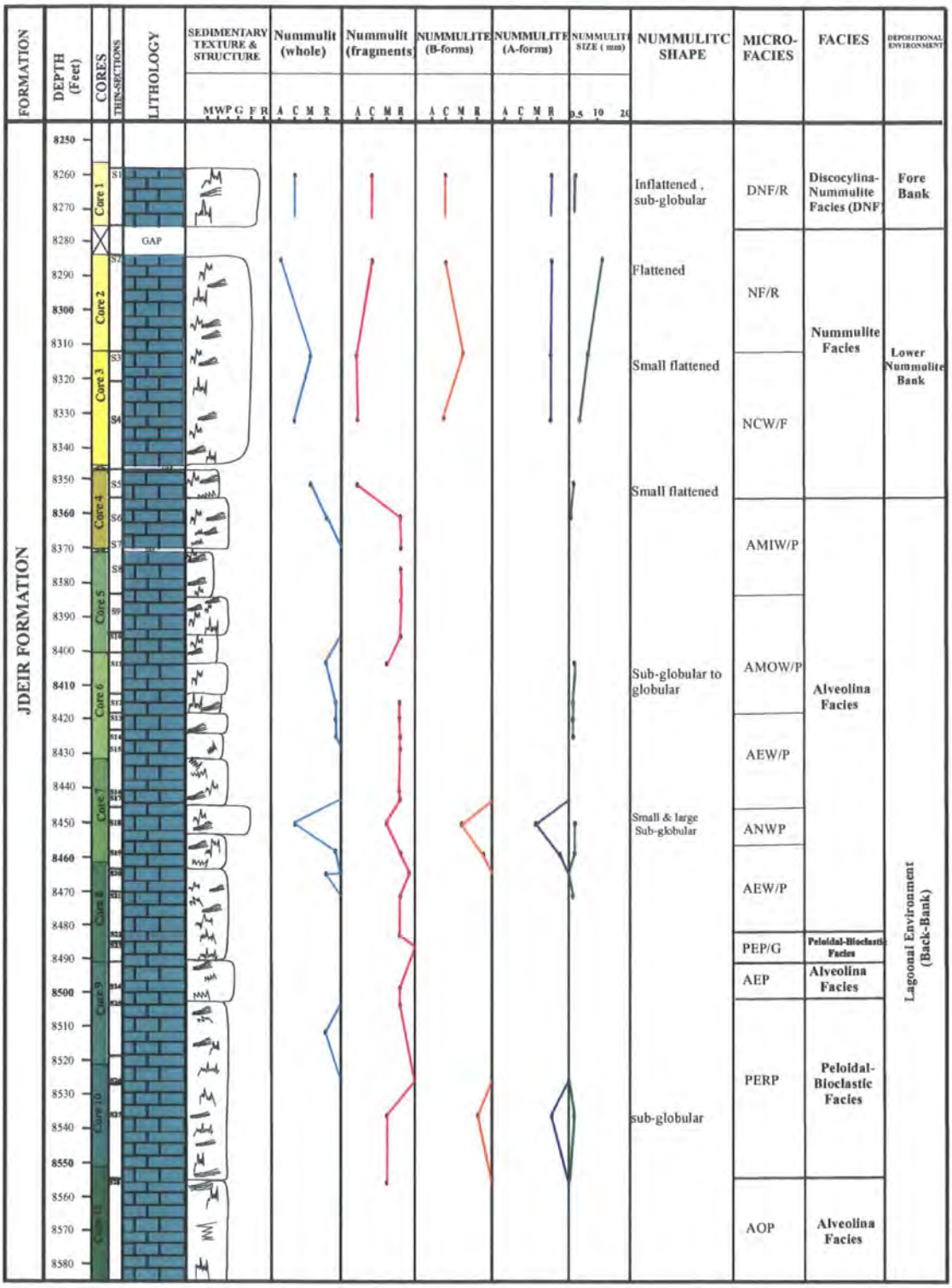

Figure 4.14. Petrographic characteristics of the Jdeir Formation in well E1-NC41, showing the point counting data of nummulites (B-forms, A-forms, whole, fragments and grain size). (See appendix for key).

i-Facies description:

This facies is observed in the lower part of wells A2-NC41 and B7-NC41. Unit thickness varies between 1-82 feet thick (Figures 4.22, 4.23, 4.26 and 4.27).

The Mollusc Facies is composed mainly of light grey to medium grey, fine-coarse grained mollusc fragments (bivalves, gastropod and oyster) (5-40%) and echinoid fragments (1-8%). The facies has wackestone/packstone and grainstone textures sometimes grading to mudstone /wackestone depositional textures (Figures 4.15, 4.16, 4.17 and 4.18). Other bioclasts include small foraminifera (rotaliids & rare miliolids) and whole and fragmented small nummulites. Peloids and very rare intraclasts are also present. Micritic envelopes are occasionally noted. The original mollusc shells have been partially to completely dissolved and only the outer micritic envelope remains especially in grainstone microfacies. Subsequently, these envelopes are infilled by blocky and drusy calcite and original structure of the bioclasts has been lost during diagenesis. Silicification of mollusc and echinoid fragments and other bioclasts is common in the lower and middle parts of well A2-NC41. The matrix in the wackestones is dominantly composed of micrite and very fine crystalline dolomite, the later associated with solution seams. In comparison fine fragmented bioclasts comprise the matrix in the packstone/grainstone. The micrite has partially recrystallized to microsparite (crystals size range from 4-10μm). Some mollusc fragments have been bored. Pressure solution seams and stylolites are common. Porosity is poor to good (0-13%) and includes vuggy and mouldic porosity. The permeability is poor because there is a lack of interconnected pore spaces.

ii-Facies interpretation:

Normal marine conditions are inferred for at least some of this facies from the presence of echinoid grains. The mudstone/wackestone, packstone and grainstone texture of this facies suggests deposition under a range of energy conditions. The limited variety of abundant numbers of gastropod and bivalves suggest conditions may have become restricted at times (Wilson, 1995). The oysters usually inhabit areas of normal marine salinity, but can tolerate brackish conditions. Deposition in lagoonal areas is the inferred environment of formation of these sediments. Sbeta (1991) interpreted the presence of wackestone and packstone facies rich in bivalves, foraminiferas and ostracods within the Harshah Formation (Middle-Upper Eocene) in Offshore Western Libya as having been deposited in a shelf lagoon environment. He

thought that local thick accumulation of biavalves perhaps included the formation of oyster banks.

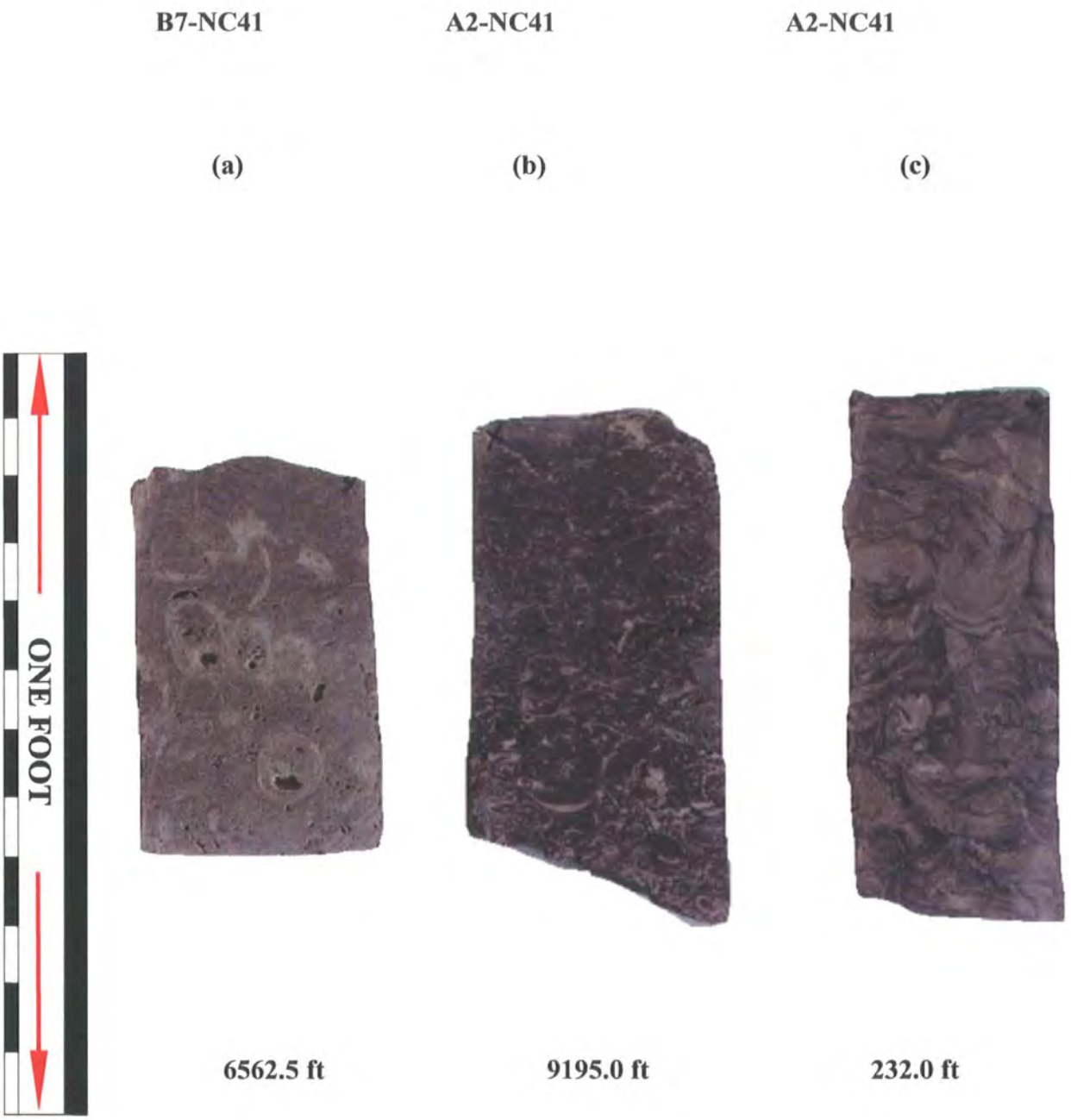

Figure 4.15. Core photographs of mollusc facies showing; (a) large gastropods; partially dissolved or intragranular porosity preserved; (b) small bivalves and (c) large bivalves (oyster).

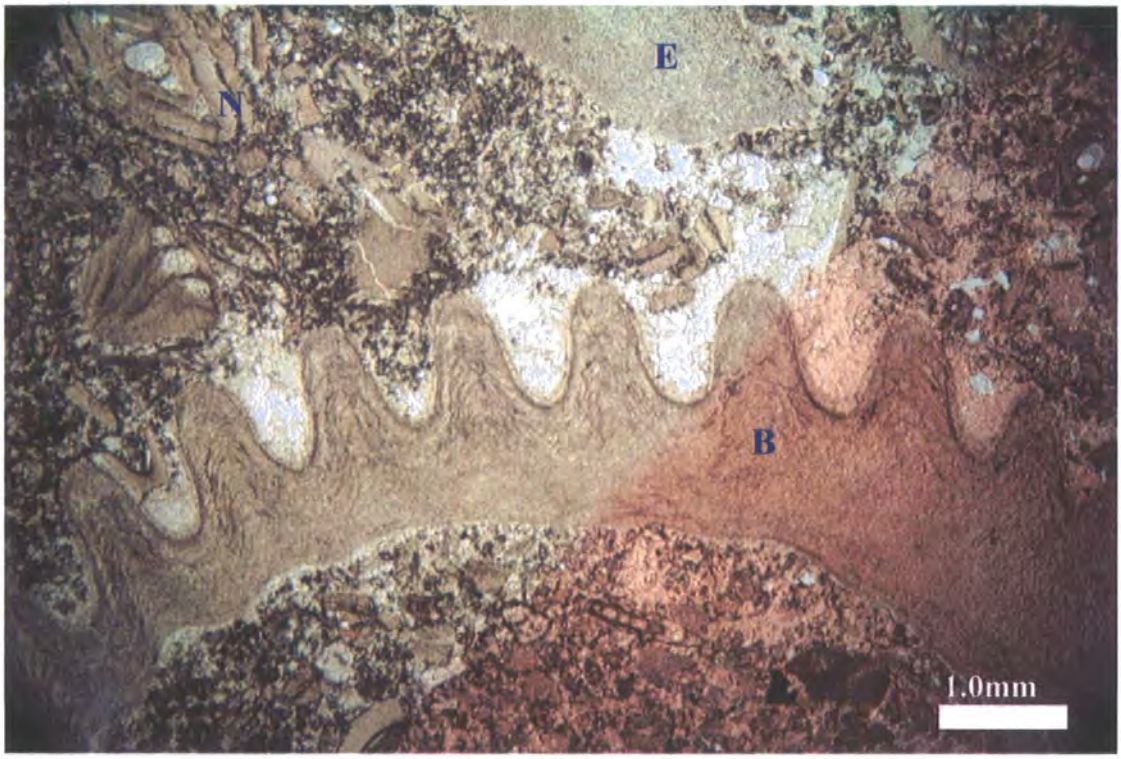

Figure 4.16. Photomicrograph of mollusc wackestone/packstone microfacies showing large brachiopod fragment (B), with echinoid fragment (E), and broken nummulite (N). The surrounding matrix consists of small bioclastic fragments cemented by equant calcite. Jdeir Formation, B7-NC41 well, 8395.0 feet, PPL.

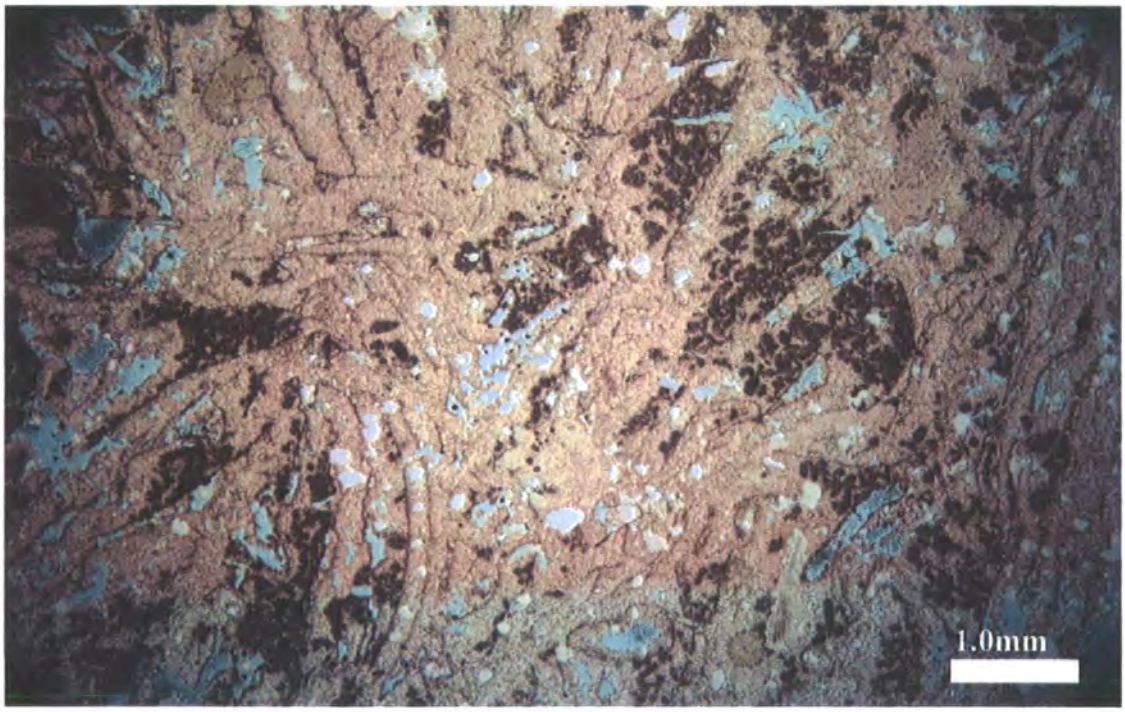

Figure 4.17. Photomicrograph of mollusc packstone/grainstone microfacies shows bioclasts, probably originally molluscs have been completely altered. Bioclasts were micritized, dissolved then infilled with drusy calcite cement. Some vuggy and mouldic porosity is still preserved. Jdeir Formation, A2-NC41well, 9203. 5 feet, PPL.

Figure 4.18. Photomicrograph of mollusc wackestone/floatstone microfacies shows pebble-size mollusc shells (oysters). The red arrow points to a possible wall of a large gastropod replaced by calcite cements. Recrystallization affected the matrix and part of the mollusc shells (oyster). Sutured or styloilted grains boundaries are seen in the upper part of the field of view. Jdeir Formation, A2-NC41 well, 9234.0 feet, PPL.

4.4.6. ECHINODERM FACIES (EF):

Includes:

Microfacies: **Echinoderm Wackestone/Packstone (EW/P)**

Echinoderm Mudstone/Wackestone (EM/W)

i-Facies description:

This facies is observed in the lower part of wells A2 and B7-NC41. Units range from 6-10 feet thick (Figures 4.22, 4.23, 4.26 and 4.27).

The Echinoderm Facies consists of light grey to medium grey, fine- to medium wackestone/packstone. These contain abundant echinoderm fragments (up to 40%) (Figure 4.19). The echinoderm fragments are dominated by echinoids. Some of echinoderm debris is from crinoids since the central hole is through the ossicle visible. Other components include large mollusc fragments, smaller benthonic foraminifera and rare nummulites fragments. In some samples, echinoderm fragments are partially

or completely replaced by silica. A few echinoid fragments are rimmed by syntaxial overgrowths. Scattered phosphatic grains and small pyrite crystals are also present in this facies. The matrix is composed of micrite and very-fine crystalline replacive dolomite. No porosity was observed in this facies.

ii-Facies interpretation:

The high abundance of echinoderm fragments in this facies indicates normal marine conditions. The fragmented echinoderm and molluscan debris is suggestive of reworking perhaps of shallow-water material into relatively deep-water settings. The wackestone and packstone texture suggests that these sediments were deposited in moderate to low energy whilst muddy fabric indicates low energy conditions. This facies can be interpreted as deposited in deep and open lagoon environment. Holocene echinoid-rich muddy facies have been reported from the deeper and inner parts of the Bahamas Bank (Multer, 1977). Phosphate is often associated with nutrient rich areas and this is consistent with deposit feeding habit of echinoderm and molluscs.

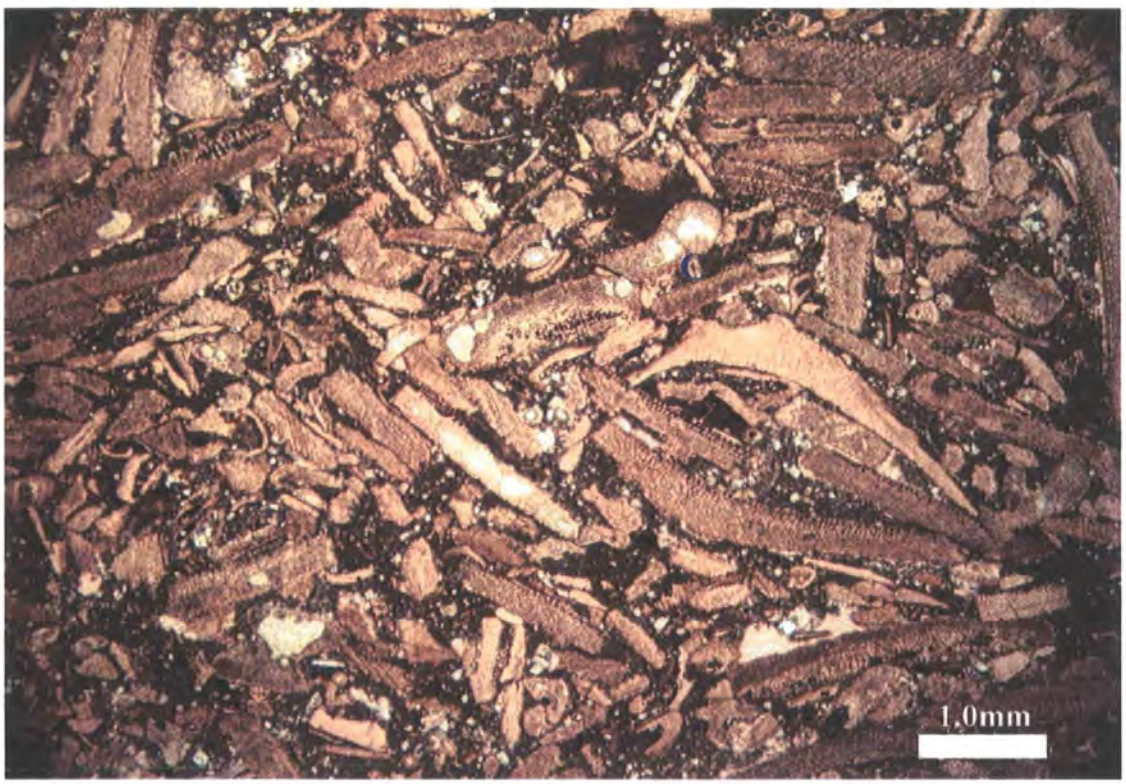

Figure 4.19. Photomicrograph of echinoderm wackestone microfacies dominated by fine to medium, moderately sorted echinoid and crinoid (C) fragments. Jdeir Formation A2-NC41 well, 9249.0 feet, PPL.

4.4.7. PLANKTONIC FORAMINFERA FACIES (PFF)

Includes:

Microfacies: **Planktonic Echinoderm Mudstone/Wackestone (PEM/W)**

i-Facies descripton:

This facies is observed only in the middle part of well A2-NC41 overlying mollusc facies and overlain by nummulitic facies. Bed thickness of this facies is ~32 feet (Figures 4.26 and 4.27).

The Planktonic Facies is composed mainly of medium grey and fine-grained whole planktonic foraminifera (10-20%) and common small echinoderm fragments (15%) in a mudstone/wackestone texture (Figure 4.20). Some of the planktonic foraminifera and echinoderm fragments have been replaced by silica (micro-quartz). The matrix is composed of high amount of micrite and finely fragmented bioclasts, which may be partially replaced by silica. Scattered small pyrite crystals are observed in this facies. Although sedimentary structures are not visible in this facies, rare lamination does occur at a depth of 9180.0 feet in the well A2-NC41. Structures seen include fractures, which may be completely filled with chalcedony (Figure 5.28 in diagenesis chapter). Porosity and permeability are poor, probably due to high percentages of micrite and silica cement.

i-Facies interpretation:

All the bioclasts within this facies are normal marine in character. The fine-grained, slightly laminated and mudstone/wackestone texture indicates that this facies was deposited in a low energy environment. An open marine environment is inferred from the high percentage of planktonic foraminifera (~ 20%). Van Gorsel (1988) reported that the percentage of planktonic foraminifera in assemblages increases from about 20% in middle sublittoral (30-100 m) 40%-80% in outer sublittoral (100-200 m) to 90% or more in bathyal (>200 m) depths. Pyrite commonly forms under reducing conditions replacing organic material or in close proximity to organic material (Flugel, 2004).

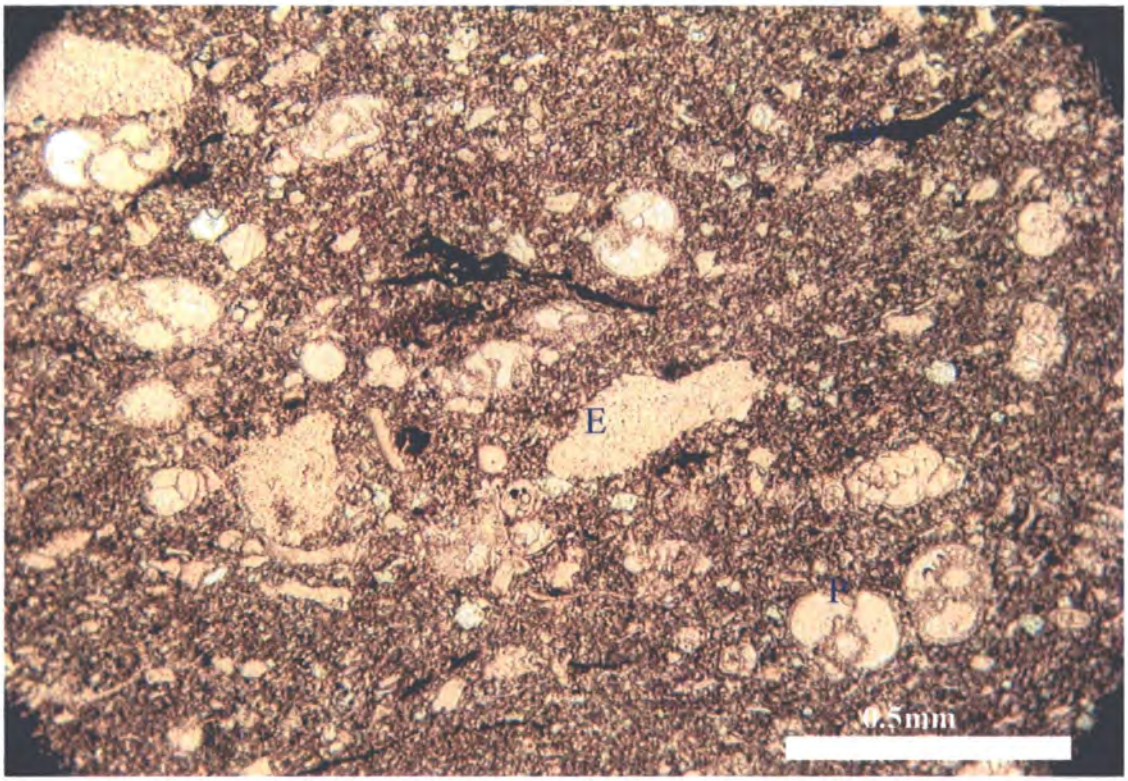

Figure 4.20. Photomicrograph of planktonic-Echinoderm mudstone/wackestone microfacies dominated by planktonic Foraminifera (P) and echinoderm fragments (E). Note sall organic material (O) Jdeir Formation, A2-NC41well, 9180.0 feet, PPL.

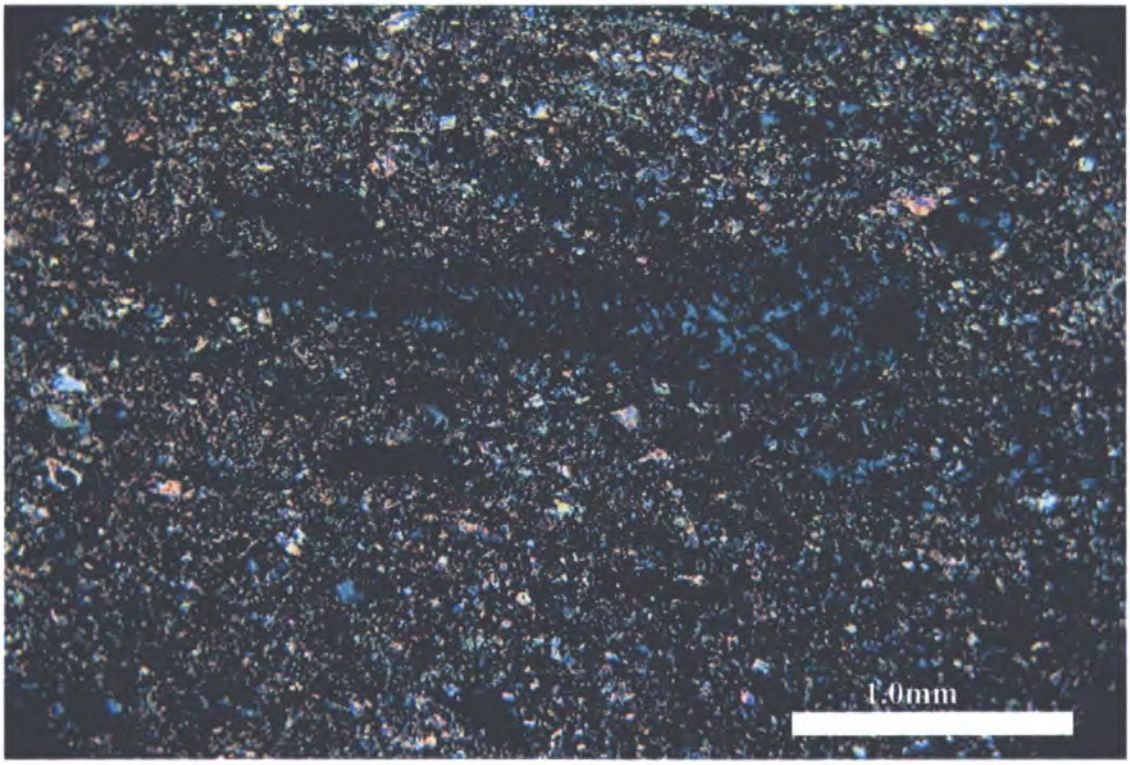

Figure 4.21. Photomicrograph of planktonic-Echinoderm mudstone/wackestone microfacies showing silica replacement of bioclasts and matrix. Jdeir Formation, A2-NC41well, 9180.0 feet, XN.

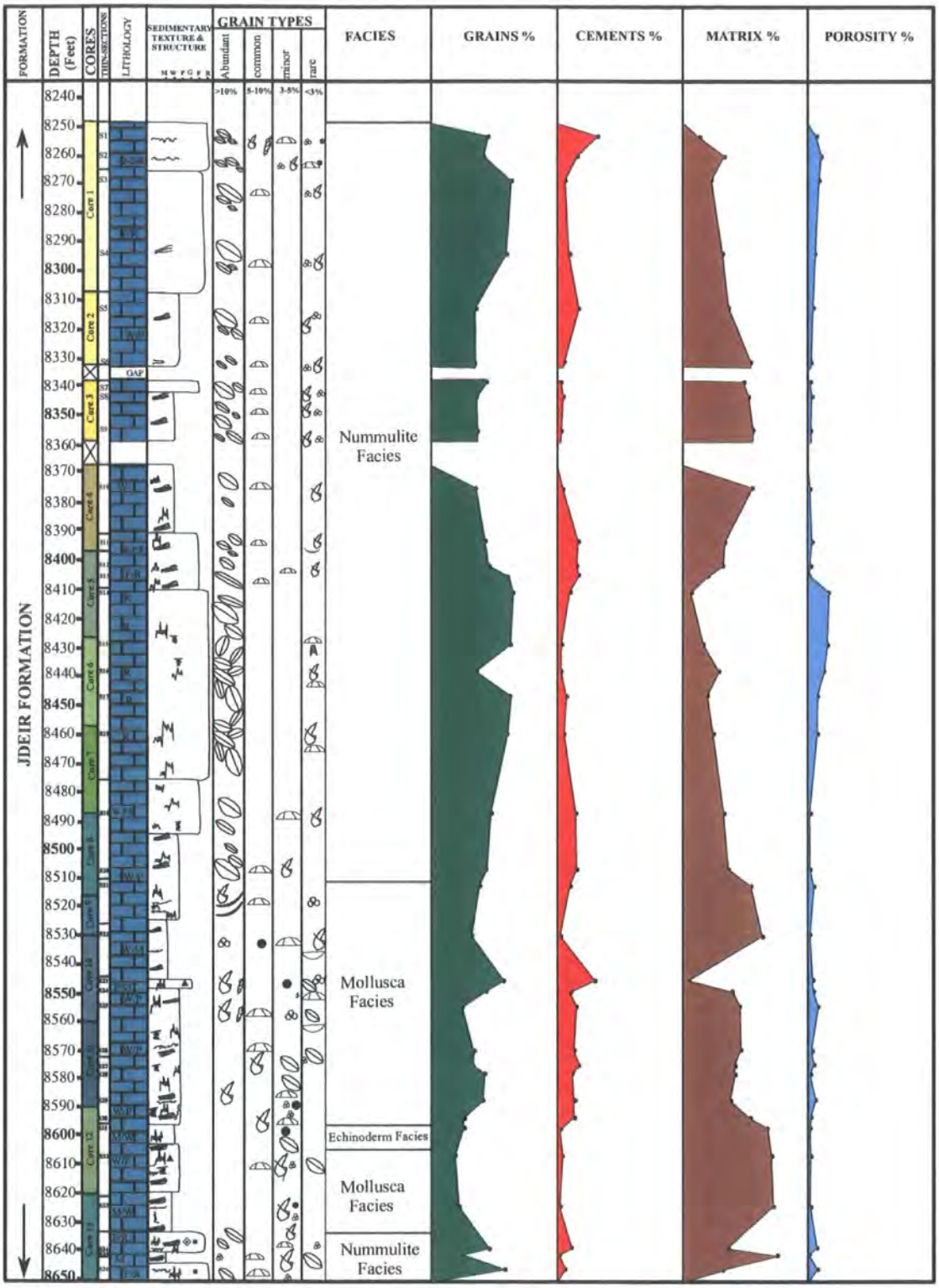

Figure 4.22. Petrographic characteristics of the Jdeir Formation in well B7-NC41, showing the point counting data, grain types, cements, matrix and porosity. (See appendix for key).

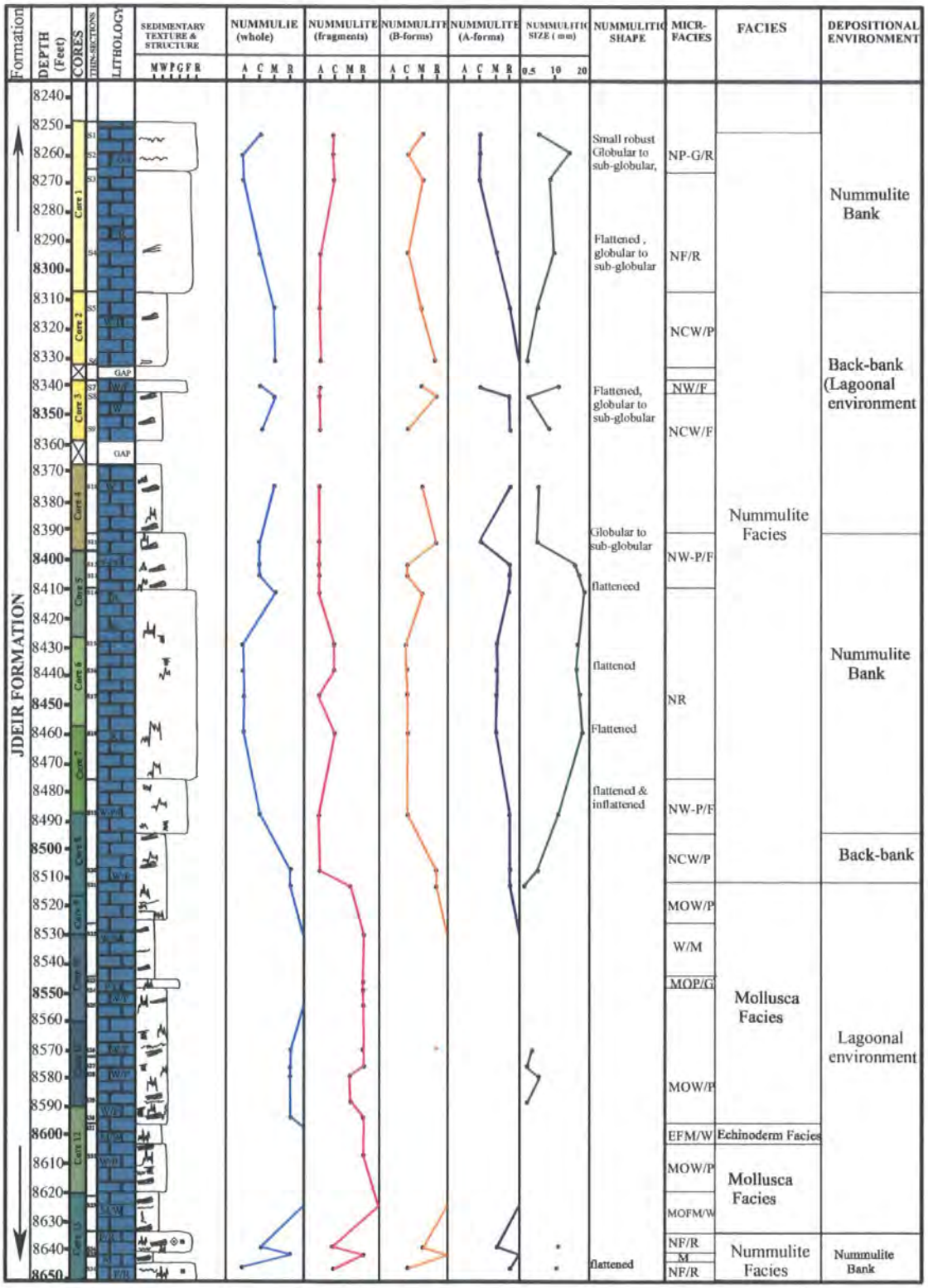

Figure 4.23. Petrographic characteristics of the Jdeir Formation in well B7-NC41, showing the point counting data of Nummulites (B-forms, A-forms, whole, fragments and grain size). (See appendix for key).

4.4.7. SANDY-BIOCLASTIC FACIES (SBF)

Includes:

Microfacies: **Sandy Bioclastic Wackestone/Packstone (SBWP)**

i- Facies description:

This facies occurs only in the lowermost part of well A2-NC41, overlying the Jirani Dolomite. The unit is ~ 45 feet thick (Figures 4.26 and 4.27).

The Sandy Bioclastic Facies consists of light to medium grey, fine to coarse grained and poorly sorted wackestone/packstone texture. The main grain types are very fine-to-fine, monocrystalline, unstrained quartz grains (6-15%), coralline algae and miliolids (Figures 4.24 and 4.25). Other grains present in minor amounts include brachiopod fragments, mollusc fragments, orbitolites, ostracoda and nummulites fragments. Peloids are also present. The matrix is composed of micrite, very-fine crystalline dolomite and small bioclastic fragments. Stylolites and dissolution seams are present. The observed porosity types are mouldic and vuggy. Porosity is restricted mainly to scattered and/or isolated vugs and moulds of different bioclastic. This facies has poor porosity and permeability.

ii-Facies interpretation:

The wackestone /packstone texture of this facies suggests deposition under low to moderate energy conditions. The water depth is inferred to have been ~ 6-10 m based on abundant miliolids (Cushman et al.1954). The size and shape of quartz grains (very fine to fine grained and sub-rounded) suggests they are product of periods of sediment reworking from a siliciclastic source. This facies passes shorewards into tidal flat facies (very-crystalline dolomite and anhydrite) (Mriheel and Anketell, 1995). Deposition in a restricted lagoonal area is the inferred environment of formation of these sediments.

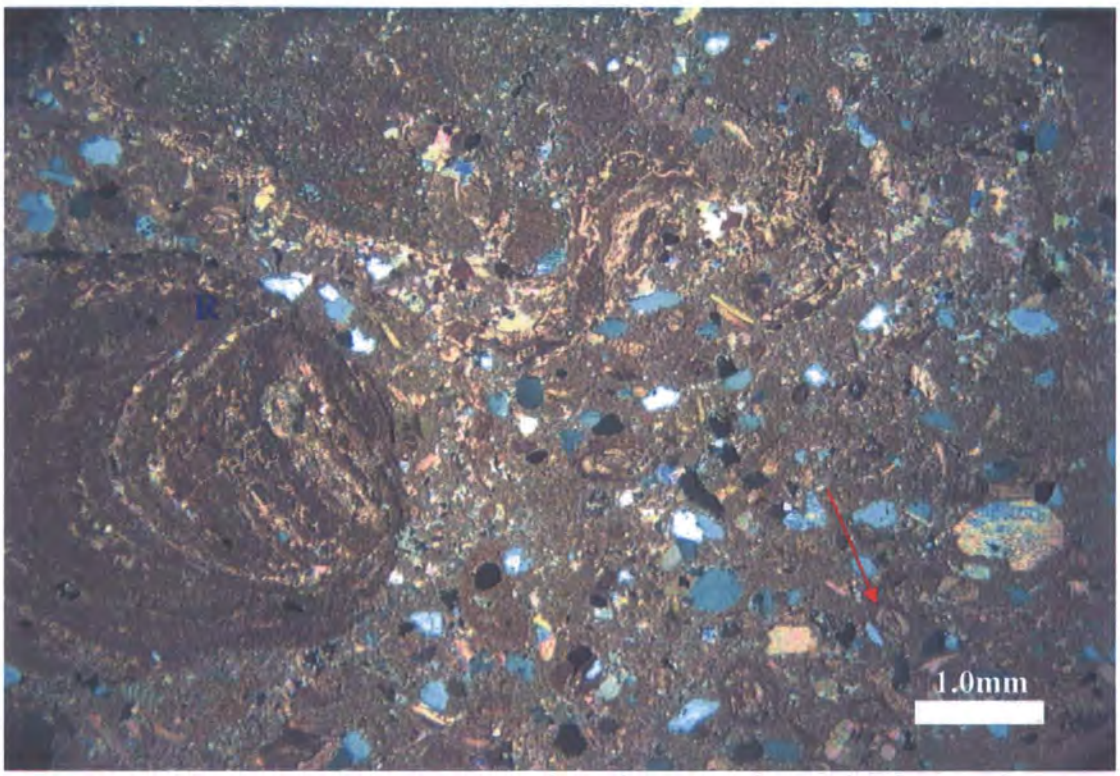

Figure 4.24. Photomicrograph of sandy-bioclastic wackestone/packstone showing very fine to fine quartz grained, coralline algae (R), and miliolids (red arrow). The matrix is of lime-mud and small bioclastic fragments. Jdeir Formation, A2-NC41 well, 9288.5 feet, XN.

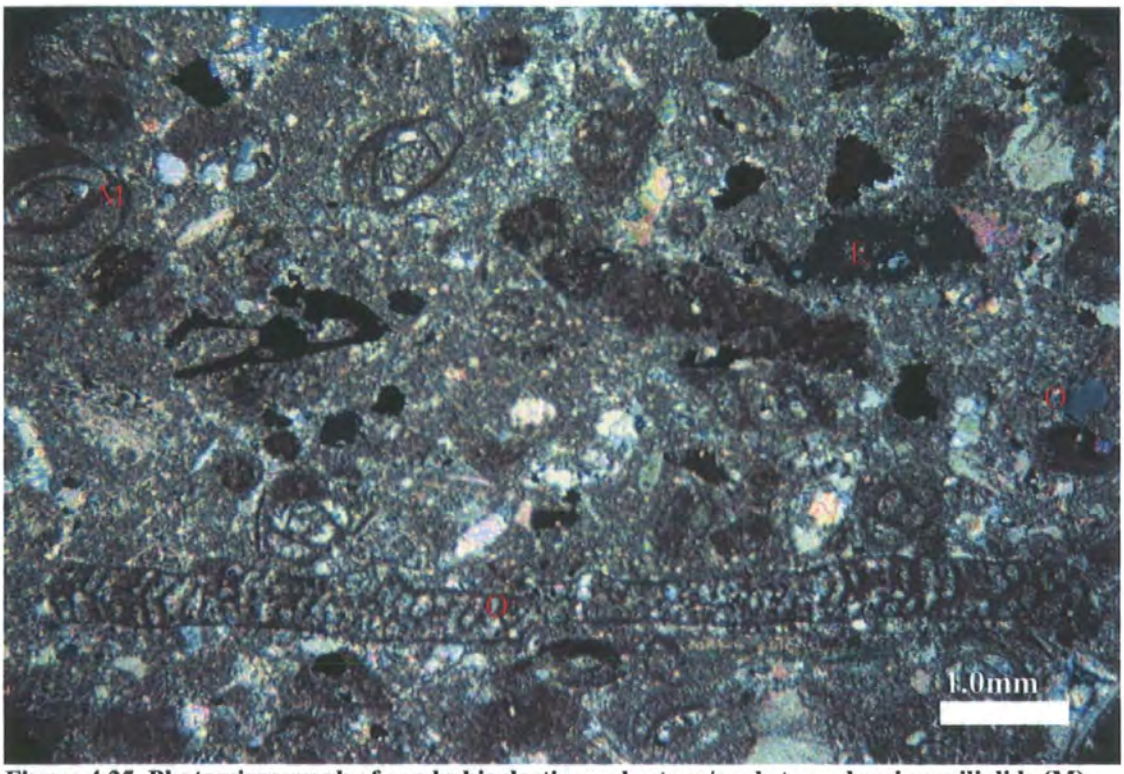

Figure 4.25. Photomicrograph of sandy-bioclastic wackestone/packstone showing miliolids (M), orbitolites (O), echinoid fragments (E) and quartz grains (Q). Jdeir Formation, A2-NC41 well, 9293.5 feet, XN.

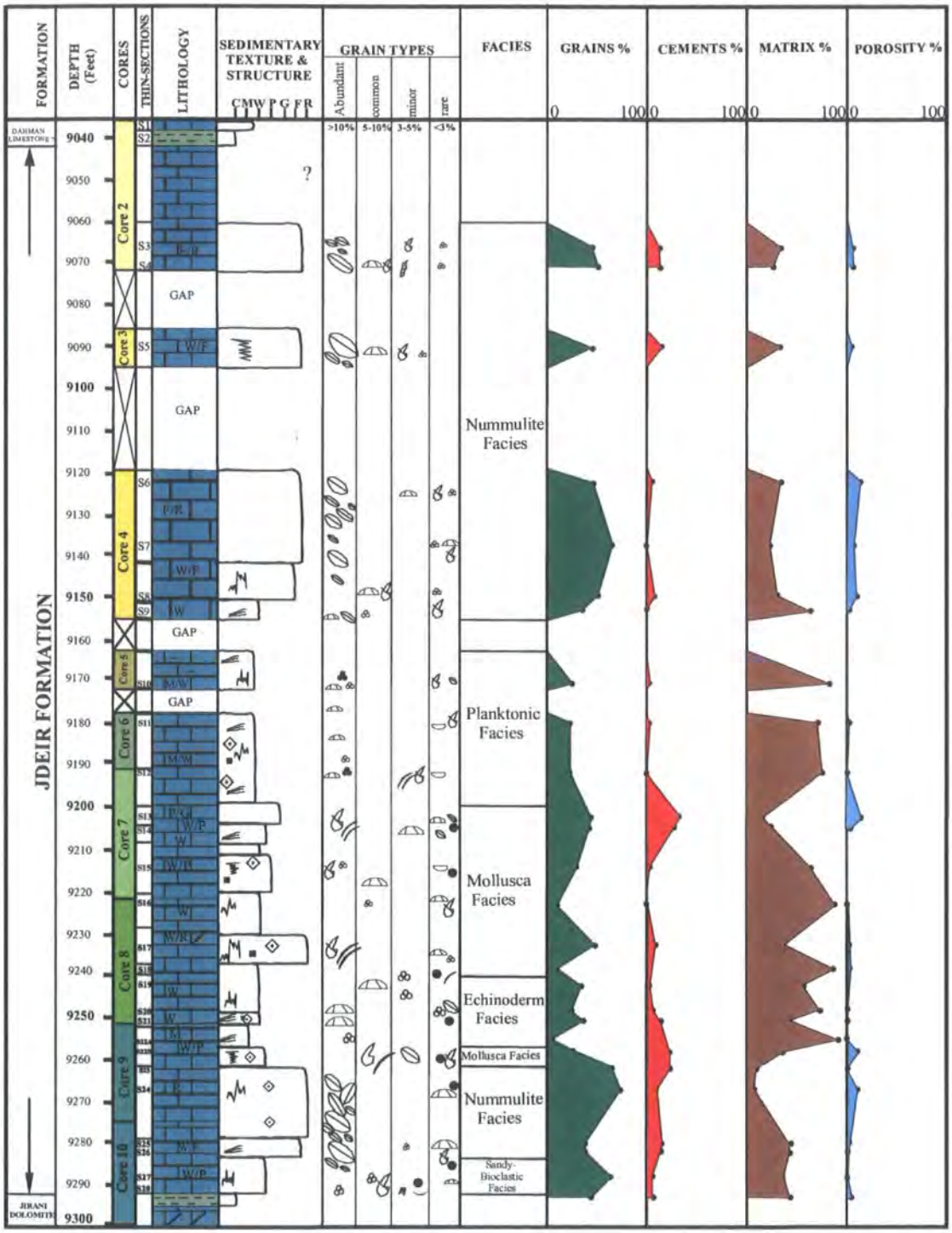

Figure 4.26. Petrographic characteristics of the Jdeir Formation in well A2-NC41, showing the point counting data, grain types, cements, matrix and porosity. (See appendix for key).

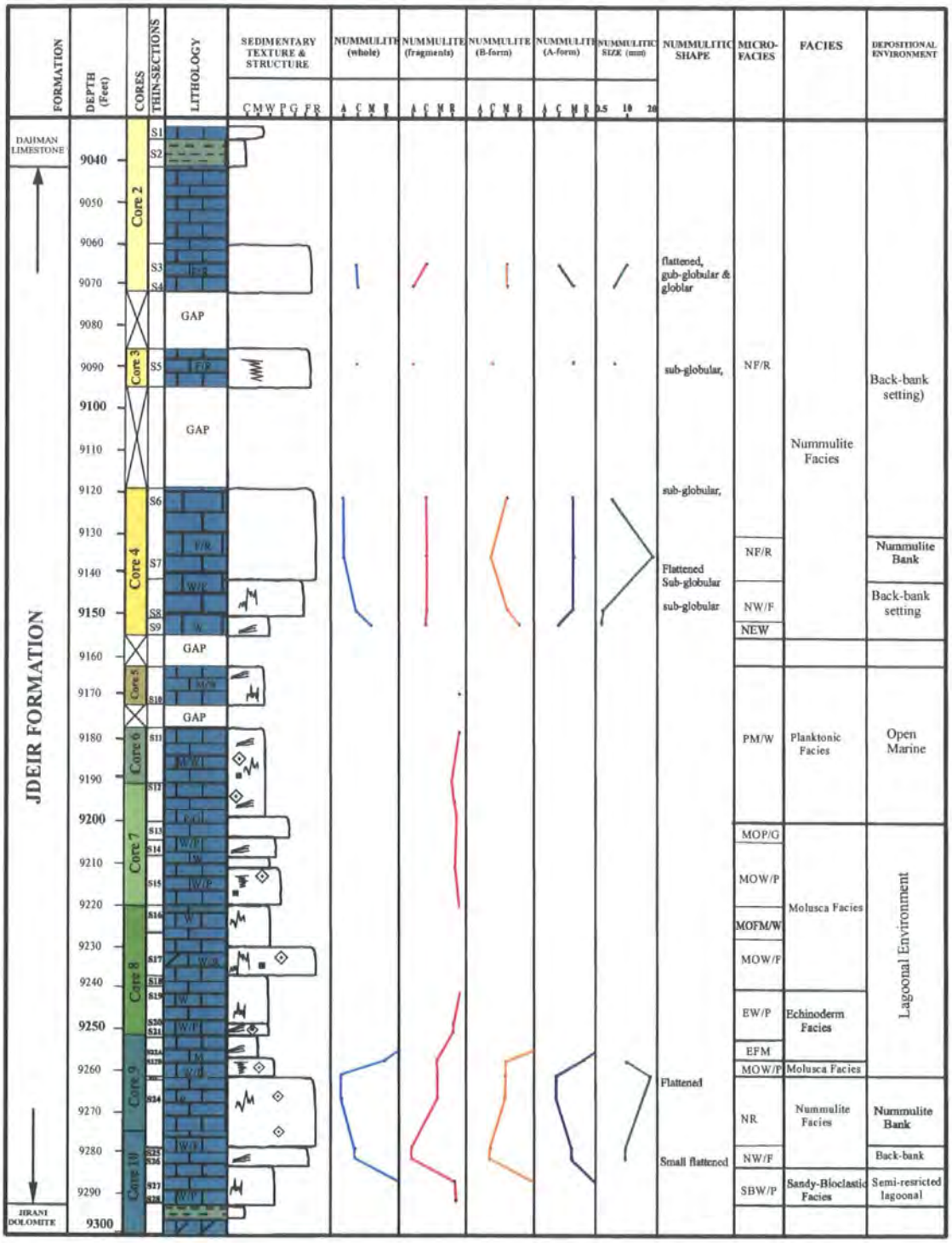

Figure 4.27. Petrographic characteristics of the Jdeir Formation in well A2-NC41, showing the point counting data of nummulites (B-forms, A-forms, whole, fragments and grain size). (See appendix for key).

FACIES	MICROFACIES	Grain Types	ENVIRONMENT
Discocyclina-Nummulite Fcies (DNF)	Discocyclina Nummulites Floatstone/Rudstone (DNF/R)	Discocyclina, Nummulite, Echinoid fragments	Fore-Bank Setting
Nummulite Facies (NF)	Nummulitic Rudstone (NR) Nummulitic Packstone-Grainstone/Rudstone (NP-G/R) Nummulitic Floatstone/Rudstone (NF/R) Nummulitic Wackestone/Floatstone (NW/F) Nummulitic Wackestone-Packstone/Floatstone (NP-W/F) Nummulithoclastic Wackestone/Floatstone (NCW/F) Nummulithoclastic Wackestone/Packstone (NCW/P) Nummulite Echinoid Wackestone (NEW)	Nummulite (A & B-forms) Nummulithoclastic debris Echinoid fragments Mollusc fragments Miliolids, Rotaliids Brachiopod fragments, Intraclasts	bank setting and intra- or back-bank setting
Alveolina Facies (AF)	Alveolina-Miliolid Wackestone/Packstone (AMIW/P) Alveolina-Echinoid Wackestone/Packstone (AEW/P) Alveolina Mollusc Wackestone/Packstone AMOW/P) Alveolina Numulitic Packstone (ANP) Alveolina Orbitolite Packstone (AOP)	Alveolina, Miliolids, Echinoid fragments, Mollusc fragments, Nummulites, Peloids, Rotaliid, dasycladacean algae, coralline algae	Back-Bank Setting
Peloidal-Bioclastic Facies (PBF)	Peloidal Echinoid Packstone (PEP) Peloidal Echinoid Coralline algal Packstone (PERP)	Peloids, Echinoid fragments, Miliolids, Rotaliids, peloids	Lagoonal Environment
Mollusc Facies (MF)	Mollusc Wackestone/Packstone (MOWP) Mollusc Packstone/Grainstone (MOPG) Mollusc Foraminfera Mudstone/Wackstone (MOFMW) Mollusc Wackestone/Floatstone (MWF)	Mollusc fragments, Echinoid fragments, Rotaliid, , Peloids, Intraclasts, Phsphatic grains.	Lagoonal Environment
Echinoderm Facies (EF)	Echinoderm Wackestone (EW/P) Foraminifera Echinoderm Mudstone/Wackestone (FEM/W)	Echinoid fragments, Mollusc fragments, Small foraminifera, Phsphatic grains.	lagoonal Environment With open oceanic influence
Planktonic Facies (PF)	Planktonic Echinoderm Mudstone/Wackestone	Planktonic foraminifera, Echinoderm fragments	Open marine environment
Sandy-Bioclastic Facies (SBF)	Sandy Bioclastic Wackestone/Packstone	Quartz grains, Miliolids, coralline algae, Mollusc fragments, Orbitolites, Brachipod, Ostracoda, Peloids.	Semi-Restricted lagoonal Environment

Table 4.1. Facies of the Jdeir Formation in wells A2, B7 and E1-NC41.

4.5. DISCUSSION AND OVERALL DEPOSTIONAL INTERPRETATION:

The modal analyses of the bioclastic components and composition of foraminifera assemblages, from petrography allowed eight facies and twenty-four microfacies to be recognised. These facies and microfacies can be interpreted as having accumulated in open marine, fore-bank, bank and lagoonal environment (back-bank setting). The distribution of the various facies and microfacies in the three wells is shown in Figures 4.13, 4.14, 4.22, 4.23, 4.26 and 4.27. The Nummulite facies is the main facies in the Jdeir Formation and occupies most of the upper parts of the three wells and the lower parts of wells A2-NC41 and B7-NC41. Its thickness is ~ 261 feet in well B7-NC41. It thins towards the south to only 96 feet in the well A2-NC41 and to the northeast to 76 feet in the E1-NC41 well. The nummulitic rudstone with abundant B-forms and minor A-forms dominates in the upper part of the bank. This microfacies is absent in well E1-NC41. Most of the smaller A-forms can be removed by winnowing leaving a residue enriched in B-forms (Figure 4.4). Sedimentary textures and biofabrics within the bank suggest that the mud has been mainly winnowed away and the test concentrated by physical processes (Racey, 1995). Nummulites tests in the upper bank often show chaotically stacked imbrications (Figure 4.3b,c). Contact edgewise imbrication and chaotically stacked B-forms test have been interpreted as showing an increasing energy and probably shallowing (Racey, 1995).

The Nummulite packstone-grainstone/rudstone is recorded only in well B7-NC41. It is dominated by A-forms with minor large B-forms and common mollusc fragments (gastropods & large bivalves). Miliolids are also observed in this microfacies. This microfacies was interpreted as having been deposited in a high-energy back-bank setting. The Nummulithoclastic debris microfacies consists mainly of wackestone, wackestone/packstone and wackestone /floatstone with fragmented nummulites dominating and minor amount of echinoid fragments. This microfacies is inferred to have been deposited in a low energy intra or back-bank setting. Anketell and Mriheel (2000) suggest that high-energy conditions caused fragmentation of nummulites in the Jdeir Formation, carrying them towards parts of back-bank setting. Beavington-Penney and Racey (2005) conclude that transport of sediment from the palaeohighs resulted in abrasion and fragmentation of nummulites and produced package that gradually thicken and become increasingly fine-grained into mid and outer ramp environments. Experimental and field observation (see Beavington-

Penney, 2004) suggests that the additional damage noted in Eocene Nummulites may be is the result of transportation within turbidity currents and/or predation by relatively large bioeroders, such as fish and echinoids. Processes such as dissolution and microboring are considered to have played only a minor role in the break-down of Nummulites.

The Discocyclina-Nummulite facies is observed in the uppermost part of well E1-NC41 overlain Nummulite facies and has not been recorded in other wells. This suggests that Jdeir formation changes gradually to deeper water deposits in the north and northeast. The presence of elongate *Discocyclina* in this facies may reflect an increase in water depth, although they may also be allochthonous (Beavington-Penney and Racey, 2005).

The Alveolina facies occurs only in the middle and lower parts of well E1-NC41 interbedded with peloid-bioclastic facies and overlain by nummulite facies. Units range in thickness from 10-116 feet thick. This facies is absent in wells B7-NC41 and A2-NC41. The occurrence of *Alveolina* with gastropods suggest close proximity to a lagoonal environment (back-bank setting) whilst miliolids, textulariids, orbitolites, dasycladacean algae accumulated in shallower perhaps restricted environment (Racey, 1995). Anketell and Mriheel (2000) in their study of the Jdeir Formation infer that the orbitolites-alveolina wackestone/packstone facies accumulated in a back-bank lagoonal setting. The Peloid-Bioclastic Facies is concentrated in the lower part of well E1-NC41 interbedded with alveolina facies (ranging in thickens from 10-52 feet). This facies has not been recorded in other wells. The presence of miliolids, coralline algae, dasycladacean algae and mollusc fragments suggest deposition in a back-bank lagoonal setting. Deposition in water depths within the photic zone is inferred from the occurrence of calcareous algae. In well B7-NC41 nummulites facies are underlain by mollusc facies and in the well A2-NC41 underlying by echinoid facies. Mollusc facies is observed in the lower part of wells B7-NC41 and A2-NC21, ranging in thickness between 1-82 feet. Bioclasts and texture within this facies suggest deposition in low energy lagoonal environments. The Echinoderm facies is recorded in the lower part of wells A2-NC41 and B7-NC41 with a thickness ranging from 6-10 feet. The common occurrence of echinoid fragments in this facies suggests normal marine salinities. High amount of carbonate mud in the mudstone/wackestone microfacies indicates deposition in low energy deep lagoonal environment. The Planktonic facies is observed only in the middle part in

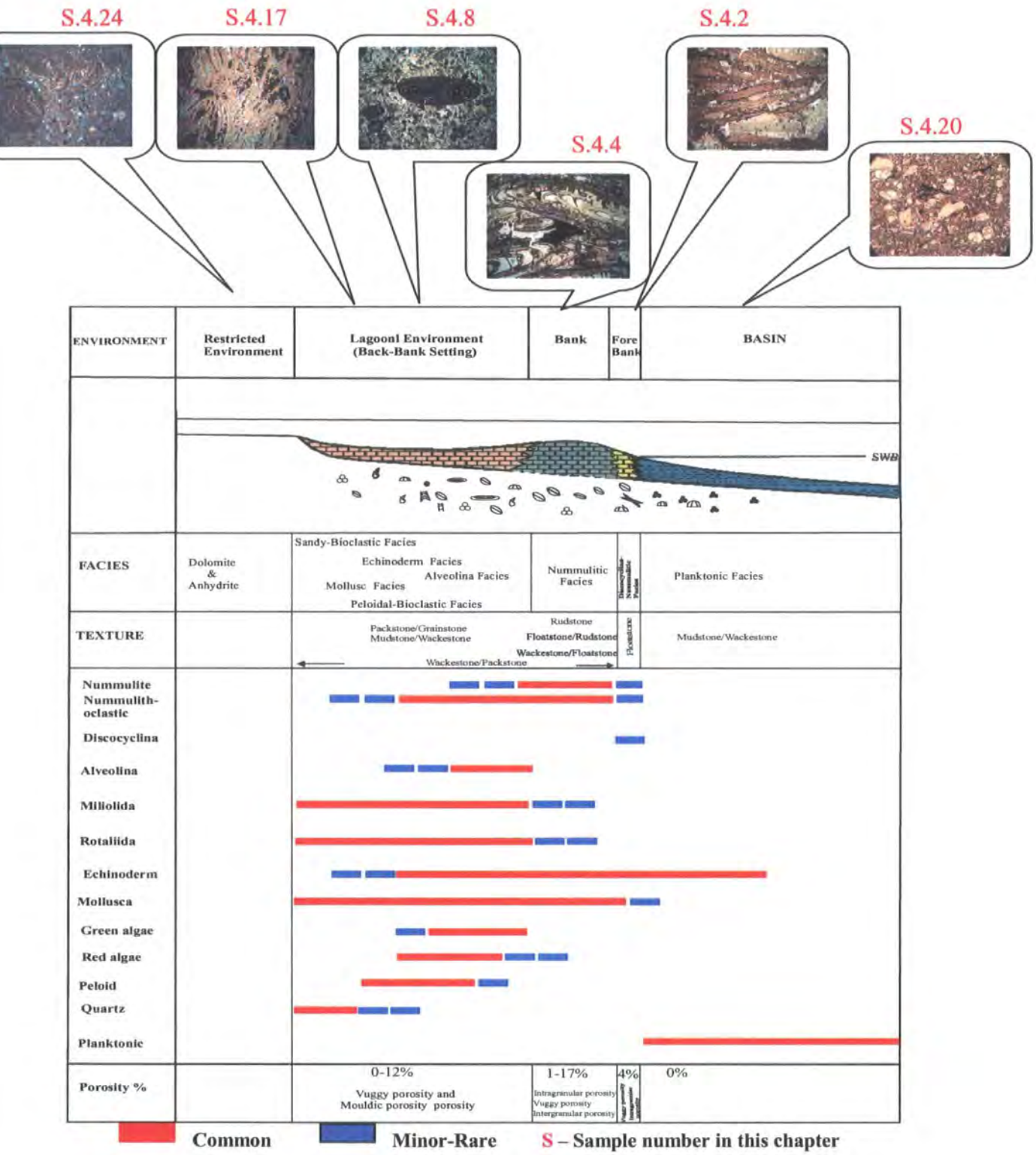

Figure 4.28. Schematic distribution of facies, texture and bioclasts along the facies model for the Jdeir Formation.

well A2-NC41 overlain by Nummulite facies. The presence of planktonic foraminifera suggests deposition in an open marine environment. The Sandy-Bioclastic facies occurs at the base of well A2-NC41 overlain by nummulite facies and overlying by the Jirani Dolomite. This facies has not been recorded in wells E1-NC41 and B7-NC41. The abundance of well-preserved milliards in a wackestone / packstone texture suggests that this facies was deposited in a shallow, moderate energy, lagoonal environment. Very fine-to-fine, monocrystalline, unstrained quartz grains are interpreted as products of periods of sediment reworking. The lowermost Jdeir Formation in well A2-NC41 is interpreted as having been deposited in restricted environment more than other wells on the basis of this facies.

Figure 4.28 shows a schematic reconstruction of the Jdeir Formation based on the environmental interpretation and interrelationships of the facies. Anketell and Mriheel (2000) proposed a rimed shelf model for the Jdeir Formation, western Libya offshore region based on both the geometry and distribution of facies. They concluded that nummulitic facies acted as a barrier separating a lagoonal orbitolites-alveolina back-bank facies from open-marine condition. Reali et al. (2003) proposed a ramp model for Jdeir Formation.

The gradual variation in facies from shallow to deep photic zone deposits in the three wells as shown below is more compatible with a ramp model than a rimmed shelf model. However, there is evidence that the inner facies were deposited in deep open lagoonal to restricted lagoonal conditions for a least part of the platform's history. An extensive open lagoon would be indicative of a rimmed shelf, whereas a restricted lagoon could occur on the inner part of a ramp protected by shoals or on a rimmed shelf. It would be expected that restricted lagoonal facies would have a greater aerial extent on a rimmed shelf. One of the critical factors in determining a rimmed versus a ramp type model, that of a shallow 'rim' and then a steep slope into deeper water, is difficult to infer from the well data. In the most seaward well although the Discocyclina facies accumulated in the deeper part of the photic zone there is no evidence for massive reworking from a platform margin that might be expected for a rimmed shelf. However, this facies could be considered a platform margin facies and no data was available from more basinward facies. If predominant transport directions were onto the platform, and there is evidence for transport into back-bank areas, there may be a limited supply of material available for basinward

transport. Some modern platforms such as the Florida Shelf have both ramp and rimmed shelf

geometries depending on the area of study and it may be that the shelf of the Jdeir Formation also had a complex and variable geometry. The determination of platform type needs more data from other wells in three concessions and further detailed investigation (NC41, NC35A and 137).

4.6. COMPARISON WITH NUMMULITE CARBONATES FROM TUNISIA (EL GARIA FORMATION):

The El Garia Formation has been the subject of a series of studies (e.g. Fournie, 1975 Anz and Ellouz, 1985; Fletcher, 1985; Hmidi and Sadras, 1991; Loucks et al., 1998; Racey, 2001; Jorry et al., 2003; Beavington-Penny et al. 2005). The models have been proposed for El Garia Formation are shown in figure 3.7. The El Garia Formation developed during Lower Eocene similar to Jdeir Formation. In the *Hasdrubal field* (Figure 4.29) two distinct depositional environments are proposed for the El Garia (Figure 3.7). Nummulites accumulated in shallow water-depth, forming nummulite shoals. The reworking of these shallow sediments leads to nummulite-rich sediment transportation downdip the platform, forming low-relief nummulite-banks (Racey et al., 2001). In *Central Tunisia*, Nummulites facies of the El Garia Formation were deposited on a gentle ramp, between the fair-weather and the storm wave base. The formation of a low-relief nummulite bank is induced by storm wave action. Nummulithoclast deposits are exported toward the basin. *Discocyclina* facies were concentrated landward of the nummulitic facies and are interpreted as a shoal deposits (Loucks et al., 1998). In comparison, in the Jdeir Formation the *Discocyclina* facies lies seawards of the nummulite facies and are inferred to have formed in a fore-bank setting. In addition, the lagoonal or inner platform setting in the Jdeir Formation in the well E1-NC41 is characterized by the presence of *Alveolina* and *Orbitolites* back-bank facies. This facies is absent from the El Garia Formation. Jorry et al. (2003) studied the El Garia in *Central Tunisia (Kesra Plateau)* (Figure 4.29) and concluded that nummulites are concentrated in palaeohighs and nummulithoclast-rich facies accumulated within intra-shelf depression and/or within the basin. In *Central Tunisia (Kef el Guitoune)* Nummulite bank facies in the El Garia Formation consist of coarse-grained sediments, poor in muddy matrix, accumulated near SWB. The fore-bank deposits are characterized by an abundance of nummulite debris. Successive storm

events may have contributed to successive stacking of the nummulite bank deposits (Hasler, 2004). These differences in depositional settings are probably the result of a variable palaeogeography and palaeoenvironments setting in the Basin.

Figure 4.29. Location map of the Kesra Plateau, Central Tunisia (Green square) and Hasdrubal field (Yellow square).

4.7. SUMMARY:

The Jdeir Formation consists mainly of shallow-water carbonates. This Formation comprises the upper part of Farwah Group (Lower Eocene, Ypresian age), overlies the Jirani Dolomite and is overlain by the Tellil Group (Middle Eocene). The Jdeir Formation has been studied in three wells in the NC41 concession, Sabratah Basin, northwestern offshore Libya in the Mediterranean Sea. Detailed core description and petrographic study show that Jdeir Formation is characterised by facies and thickness variation between three wells. The maxiumum thickness is ~ 600 feet in well E1-NC41. It decreases towards to 290 feet in well B7-NC41 and to the south to 259 feet in the well A2-NC41. The detailed description of 92 thin-sections

allowed eight facies and twenty-four microfacies to be identified and their different depositional environments to be inferred. The position of the different facies along depositional model has been inferred on basis of the main component (nummulite, *Discocyclina*, *Alveolina* and miliolida). Eight facies are recognized in the Jdeir Formation including discocyclina-nummulite facies, nummulite facies, alveolina facies, peloidal-bioclastic facies, mollusc facies, echinoderm facies, planktonic facies and sandy-bioclastic facies. These are interpreted as having been deposited in open marine, fore-bank, bank and lagoon environment (back-bank setting). The nummulite Rudstone dominated by B-forms with minor A-form forms the upper part of the bank and floatstone/ rudstone form the lower part of the bank. Abrasion and fragmentation of sediments resulted in the transport of sediments from palaeohighs and reaccumulation into intra or back-bank environments. The Discocyclina - Nummulite facies is concentrated only in E1-NC41 well, where it accumulated in a fore-bank setting. Lagoonal deposits in E1-NC41 are characterized by the presence of alveolina, orbitolites and peloids .By contrast, lagoonal deposits in the middle and the lower parts of wells B7-NC41 and A2-NC41 are characterized by abundant mollusc, echinoid and nummulites fragments. In the lowermost part of well A2-NC41, lagoonal deposits are dominated by very fine-to-fine quartz grains, miliolids and mollusc fragments with rare orbitolites and echinoid fragments.

CHAPTER FIVE

5. DIAGENESIS AND RESERVOIR CHARACTERISTICS OF THE JDEIR FORMATION.

5. DIAGENESIS AND RESERVOIR CHARACTERISTICS OF THE JDEIR FORMATION

5.1. INTRODUCTION:

The main objective of this chapter is to describe and interpret the main diagenetic feature which were recognized during petrographic examination of stained thin-sections, cathodoluminescence microscopy (CL), scanning electron microscopy (SEM) and oxygen and carbon stable isotope analysis ($\delta^{18}O$ & $\delta^{13}C$).The influence of the diagenesis on reservoir equality of the Jdeir Formation is discussed and comparisons are made with other known Eocene nummulitic reservoirs.

5.2. A BRIEF INTRODUCTION TO CARBONATE DIAGENESIS:

5.2.1. INTRODUCTION:

There is an extensive literature on carbonate diagenesis, which has been reviewed recently in James & Choquette (1983 and 1984), Moore (1989), McIlreath & Morrow (1990), Tucker & Bathurst (1990), Tucker & Wright (1990) and Tucker (1991 and 1993). Diagenesis encompasses those natural changes which occur in sediments and sedimentary rocks between the time of initial deposition and the time when the changes caused by elevated temperatures and pressures result in metamorphism. For carbonate sediments, diagenesis results in the transformation into stable limestones or dolomites. Diagenetic processes include the dissolution, neomorphism and replacement of unstable minerals, the compaction of grains and lithification by the precipitation of void-filling cements. Carbonate diagenesis operates in three principle environments: the marine, meteoric and burial environments (Figure 5.1). Recognition of the products of a particular diagenetic environment depends upon combined used of petrographic examination and geochemical techniques. This section focuses on the key diagenetic aspects related to this thesis and provides a brief introduction to carbonate diagenesis. The three principle diagenetic environments are briefly discussed in the following sections.

5.2.2. MARINE DIAGENESIS:

Marine diagenesis takes place on and just below the sea floor in both shallow and deep water, and in the intertidal-supertidal zone and the processes operating are most common in low latitude, shallow-marine environments. The main processes involved in sea-floor diagenesis are: (a) the precipitation of cements and (b) the alteration of grains by the biological boring of organisms (James and Choquette, 1990 b). Cementation is most widespread in areas of high current activity, such as along shorelines and shelf margins, where sea-water is pumped through the sediment, but it also occurs in areas of evaporation, such as on tidal flats and beaches. In comparison micritization of grains by algae, fungi and bacteria is more common in quieter-water areas, such as back-reef lagoons (Tucker, 1991). Thus in the shallow-marine, it is possible to distinguish three zones: (1) in the active marine phreatic, pore-waters are

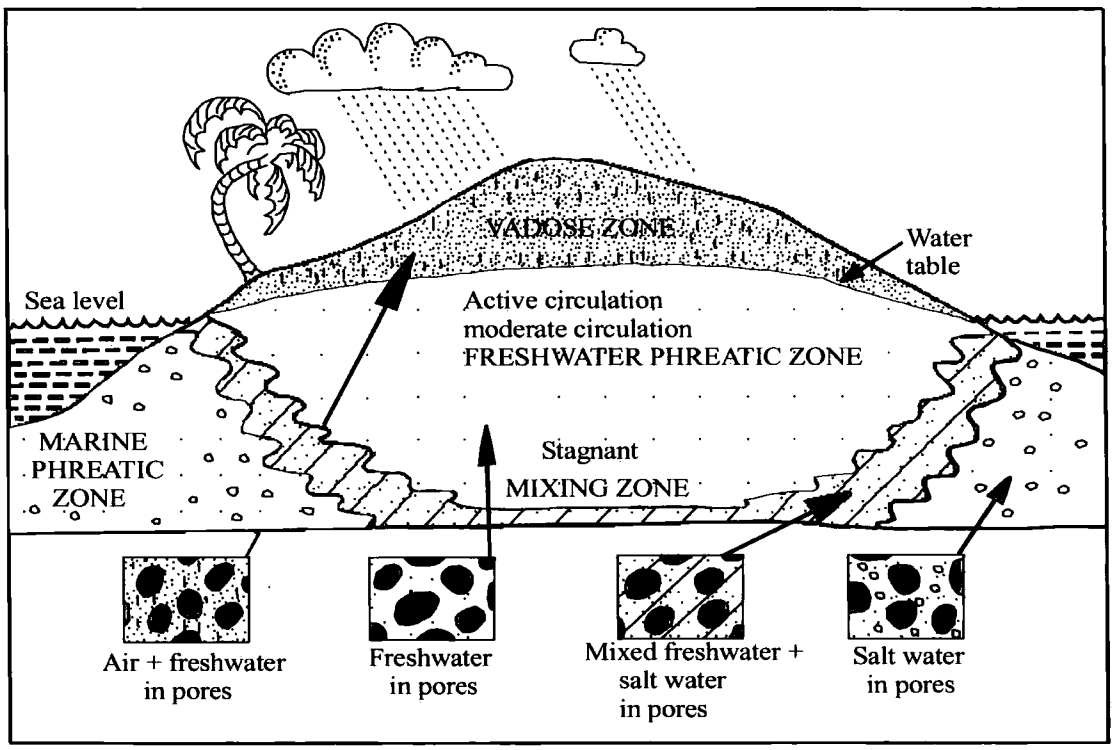

Figure 5.1. Cross-section showing the distribution and relationships of major diagenetic environments in the shallow subsurface (After Longman, 1982).

constantly being replenished and cementation is common (e.g. reefs and shoals); (2) in the stagnant marine phreatic, there is little sediment or pore-fluid movement, microbial micritization of grains is ubiquitous and cementation is limited (e.g. in shelf lagoons), and (3) in the marine vadose, cementation chiefly occurs through

evaporation of sea-water and there may also be some evidence of microbial effects (e.g. beaches and tidal flats) (Tucker and Wright 1990).

In mid to high latitudes, shallow-marine carbonates are rarely cemented. Shallow seawater becomes undersaturated in $CaCO_3$ away from the sub-tropics, and carbonate grains are thus more liable to suffer dissolution (Alexandersson, 1978). Wilson (2002) stated that high equatorial rainfall and low marine salinities make marine cement precipitation less common in the equatorial tropics than in arid-zone tropical setting. The marine cements have a large variety of morphologies and are essentially formed of only two minerals: aragonite and high-Mg calcite (Tucker and Wright, 1990) (Figure 5.2). The common types of aragonite cement crystals are isopachous fringes, needles and botryoids, and micron-sized equant crystals (micrite). High-Mg calcite cements occur as bladed isopachous fringes, equant crystals and micrite (Tucker and Wright, 1990). Aragonite cements from intertidal-shallow subtidal sediments typically contain high strontium contents, up to 10,000 ppm, and Mg content of about 1000 ppm or less. The high-Mg calcite cements are typically between 14 and 19 mole % $MgCO_3$, but Sr is low at around 1000 ppm (Tucker and, Wright, 1990). Stable isotopic studies show that the oxygen isotopic signatures of shallow-marine cements and sediments depend largely on the sea-water $\delta^{18}O$ composition and temperature (Milliman, 1974; James and Ginsburg, 1979; Anderson and Arthur, 1983). With marine cements, the value is commonly those predicted for precipitation in equilibrium with sea-water or they are slightly heavier, or more enriched than would be expected (Gonzalez and Lohmann, 1985). The $\delta^{18}O$ range is typically -0.5 to +3 ‰, and high-Mg calcite cements display a slight enrichment in $\delta^{18}O$ compared to aragonite, due to fractionation effects (Tucker and Wright, 1990).

5.2.3. METEORIC DIAGENSIS:

The meteoric diagenetic environment is the zone where rainfall-derived groundwater is in contact with sediment or rock. Several zones exist within the meteoric diagenetic environment. The main zones are vadose and phreatic. Each zone exhibits distinctive suites of processes and products (Allan and Matthews, 1982). The water table is the surface where atmospheric and hydrostatic pressure is equal (James and Choquette, 1990b). The water table is a critical interface in meteoric diagenesis. It separates the zone of intermittent saturation and drying (vadose zone) from the zone of permanent saturation (phreatic zone). Transitional between the vadose and phreatic

zones is the capillary zone, where water is drawn up by capillary action. In the vadose zone, the pores periodically contain water or air, or both. Water drains under gravity, which can be relatively rapid in the case of conduit flow (water movement via joints and fractures) compared to the case of diffuse flow (water movement through inter-grain pores). Two sub-zones can be identified: the upper zone of infiltration and the lower zone of percolation. The three most important processes in the vadose zone are: (1) gravitation drainage; (2) desiccation by evaporation and (3) evapo-transpiration (James and Choquette, 1990b). Water passing through this zone contains both atmospheric CO_2 and organic acids. Not only does this increase the acidity of the fluid, but also adds dissolved organic carbon to the groundwater, and increase the ability of meteoric fluid to dissolve the limestone wall rocks (Tucker and Wright, 1990).

In contrast to the vadose zone, pores in the phreatic zone are always filled with water; so that calcite crystals can grow unimpeded by water-air interfaces until they come into contact with neighbouring carbonate grains or cement crystals (Morse and Mackenzie, 1990). In the shallow subsurface where the marine and meteoric waters interface, there is a mixing zone (Back et al., 1984). Machel (2004) suggested that mixing zones tend to form caves with or without very small amounts of dolomite. The geometry of the mixing zone varies depending on the hydrostatic head, rock porosity-permeability and presence of confined/unconfined aquifers (Tucker and Wright, 1990).

Cement morphologies in the vadose and phreatic zones are different due to the different nature of the water-wetted surfaces in these regimes. In the case of the vadose zone, downward percolation of water is not uniform and thus cements are distributed irregularly throughout the fractures and pores. These calcite cements are concentrated at grain boundaries and commonly exhibit a curved surface, reflecting growth outwards the curved interfaces of partially water-filled pores (meniscus cement) (Figure 5.2). In deeper regions of the vadose zone, where more fluid is available, droplets of water can accumulate at the bottom of grains, or at the tips of fractures and joints (Pendant cements). The phreatic cements are characterized by crystals increasing in size toward the pore centre (drusy), equidimensional crystals without substrate control (granular) and crystals without a preferred orientation (blocky) (Figure 5.2). The vadose and phreatic cements in carbonate rocks are composed of low-Mg calcite (Morse and Mackenzie, 1990). Observation of the

Acicular: Needle-like crystals, growing normal to substrate. Crystals elongated parallel to the c-axis, exhibiting straight extinction. Width < 10 μm, length about 100 μm and more. Often forming isopachous crust. Predominantly aragonite, but also Mg-calcite. Marine phreatic.

Fibrous: Fibrous crystals, growing normal to the substrate. Crystals show a significant length elongation, usually parallel to the c-axis. Crystal shape is needle- like or columnar (length to width ratio >6:1, width >10 μm). Size commonly fine to medium crystalline common in inter- and intraparticle pores. Aragonite or Mg-calcite. Mostly marine phreatic, but also meteoric-vadose.

Botryoidal: Pore-filling cement consists of individual and compound fans, which in turn are composed of elongate euhedral fibers with a characteristic sweeping extinction in cross-polarized light. Aragonite. Usually marine (commc in cavities of reefs and steep seaward slops), but also known from burial environments.

Radiaxial fibrous: Large, often cloudy and turbid, inclusion-rich calcite crystals with undulose extinction. Size medium to coarse crystalline. Sometimes extending several millimetres in length, usually about 30 to 300 μm. Preatic-marine and burial.

Bladed: Crystals that are not equidimensional and not fibrous. The correspond to elongate crystals somewhat wider than fibrous crystals and exhibiting broad flattened and pyramid-like terminations. Crystal size up to 10 μm in width and between less than 20 and more 100 μm in length. Crystals increase in width along their length. Usually High-Mg but also aragonite. Marine phreatic (abundant in shallow-marine setting).

Meniscus: Calcite cement precipitated in meniscus style at or near grain-to-grain contacts in pores containing both air and water. Exhibits a curved surface below grains. Characteristically formed in the meteoric-vadose zone.

Drusy: Void-filling and pore-lining cement in intergranular and intraskeletal pores, molds and fractures, characterized by equant to elongated, anhedral to subhedral non-ferroan calcite crystals. Size increase toward the centre of the void. Near-surfcae meteoric as well as burial environments.

Blocky: Calcite cement consisting of medium to coarse-grained crystals without a preferred orientation. Characterized by variously sized crystals (tens of micros to several millimetres), often showing distinct crystals boundaries. Xenotopic and hypidiotopic crystals fabric are common. High-Mg calcite or Low-Mg calcite. Typically in meteoric and burial environments. Precipitated after the dissolution of aragonite cements or grains or as late diagenetic cement filling remaining pore spaces.

Syntaxial overgrowth: Subsrtate-controlled overgrowth around a host grain made by a single crystal (Usually High-Mg calcitic echinoderm fragments).Overgrowth cements from near-surface marine and meteoric-phreatic environments are inclusion-rich and cloudy, in contrast to clear overgrowth from burial environments.

Figure 5.2. Sketches of the varieties of marine and meteoric cements (from Flugel, 2004).

composition of waters in modern near-surface sediments and experimental evidence show that low-Mg calcite is the phase anticipated to form from such waters (Morse and Makenzie, 1990). Meteoric waters in carbonate sediment have low salinities, low Mg^{2+} / Ca^{2+} ratios, low SO_4^{2-}concentration, variable, but measurable concentrations of PO_4^{3-} and generally low dissolved organic carbon concentration (Lohmann, 1988). Stable isotopic studies have shown that the $\delta^{18}O$ composition of meteoric groundwater is largely constant at individual geographic sites (Craig, 1961), related to variations in the amount of dissolved soil gas CO_2, and to the extent of rock water interaction products. Since the composition of the meteoric water can vary geographically with individual systems possessing unique values, the $\delta^{18}O$ value of meteoric calcite must be determined individually for each sequence and locality studied (Lohmann, 1988). A recent study of global variations in isotopic values of meteoric waters showed that past changes in the climatic and physiographic parameters controlled the distribution of $\delta^{18}O$ regimes (Bowen and Wilkinson, 2002). The $\delta^{13}C$ composition of meteoric cements are distinctly lower than those of the depositional sediment. The main features are a more negative $\delta^{13}C$ caused by the addition of light carbon (^{12}C) from the soil, although variation is in $\delta^{13}C$ not simply a function of distance below an exposure surface (Tucker and Wright, 1990).

5.2.4. BURIAL DIAGENESIS:

Burial diagenesis begins as soon as a sediment is buried below the reach of near-surface marine and/or meteoric digenetic processes and operates over a considerable range of depth, pressure and temperature under the influence of pore-fluids with variable salinity and chemistry. The most common result of burial diagenesis is the destruction of porosity, through the processes of cementation, compaction and pressure dissolution. However, porosity can also be gained, through either compactional / tectonic fractures or the dissolution of metastable grains. Two categories of compaction are recognized: mechanical and chemical. Mechanical compaction may begin soon after deposition and leads to a closer packing of grains, flattening of elongate bioclasts toward the plane of the bedding and collapse of micrite envelopes, the latter if there has been an earlier phase of dissolution of the aragonitic bioclasts (Tucker, 1991). Chemical compaction requires several hundred metres of burial resulting in of increased solubility at grain contacts and along sediment

interfaces. Three common textures result from chemical compaction: (1) fitted fabric; (2) stylolites and (3) pressure-dissolution seams (Tucker, 1991).

5.3. DIAGENESIS OF JDEIR FORMATION:

5.3.1. INTRODUCTION:

The Jdeir Formation is inferred to have undergone extensive diagenetic alteration in marine, fresh water and burial environments. The diagenetic processes and their relative timing can be divided into three groups: 1) early marine diagenesis, 2) meteoric and early burial diagenesis and 3) late burial diagenesis, occurring prior to, and after lithification (Figure 5.30). Micritization, dissolution, cementation, neomorphism, dolomitization, silicification, compaction, pyrite growth and hydrocarbon migration are the main diagenetic processes which have modified the Jdeir Formation.

5.3.2. METHODOLOGY:

Diagenetic features have been described and interpreted using: petrographic analysis of 92 stained thin sections. Chips from four samples were gold-coated and examined using Scanning Electron Microscopy (SEM). Four polished thin section were studied using Cathodoluminescence (CL) Microscopy. The cold-stage CL instrument (Technosyn 8200 MK II) operated at 15 KV beam energy and about 200-300 mA gun current in a 0.05-0.1 torr vacuum. Ten stable isotopes ($\delta^{18}O$ & $\delta^{13}C$) samples were run on a Thermal MAT253 with preparation run via autosampler and a thermal GasBench. All data were run (and normalised to) NBS-19, which is the primary carbonate standard used to define the V-PDB scale ($\delta^{13}C$= +1.95‰, $\delta^{18}O$= -2.2‰). In addition, 4 replicate analyses of an internal carbonate standard (DCS01) were reproducible to ±0.12‰ (1σ). oxygen and carbon samples. CL. SEM and isotope samples were prepared and analysed in the Earth Science labs at Durham University.

5.3.3. EARLY MARINE DIAGENESIS:

5.3.3.1. MICRITIZATION:

This is one the first stages of diagenesis seen in the Jdeir Formation and it occurred soon after deposition since it predates all other diagenetic features.

Micritization is the process by which skeletal and non-skeletal particles undergo alteration and destruction by boring algae result in the formation of a micrite envelope. This phenomenon was described by Bathurst (1975), Perkins and Haksey (1977), Alexandersson (1972) and Kobluk and Risk (1977). Micritization was only observed in the alveolina facies, peloidal-bioclastic facies and mollusca facies. In this study micritization takes two forms: first is micritzation of the outer portions of grains (Figure 5.3); second is the complete transformation of the skeletal grains into peloids. This process may be responsible for the formation the peloidal-bioclastic facies in the well E1-NC41. It is believed that these processes take place in a marine phreatic zone similar to the interpretations of Bathurst (1966, 1975) and Kobluk and Risk (1977). Micritzation of bioclastic occurs on or just below the sediments-seawater interface and is most prevalent in quieter-water locations where is little movement of sediment (Tucker and Wright, 1992). In this study all the facies where micritization is common are inner shelf deposits. Micritzation is a common process in shallow-water environments and has been interpreted to result from boring by microrganisms including endolithic algae and fungi (Bathurst, 1975; MacIntyre et al., 2000, Reid and MacIntyre, 2000).

5.3.4. METEORIC AND EARLY BURIAL DIAGENESIS:

5.3.4.1. DISSOLUTION:

The diagenetic phenomenon of dissolution has been observed in most facies of the Jdeir Formation, but dominates in the upper part of the units. This process is responsible for the creation of large volumes of secondary porosity within the Nummulitic facies. Secondary porosity greatly enhanced primary intergranular porosity and is mainly responsible for the formation of high reservoir potential (Figures 5.4, 5.5, 5.6 and 5.7). In some samples, 15% of the rock may be porosity due to dissolution. Many of the biomoldic pores are partially or completely infilled by drusy, non-ferroan calcite, particularly in the lower part of the Jdeir Formation (Figures. 5.3 and 5.6). Dissolution of aragonitic bioclasts is most common in platform to or shallow-water deposits. A meteoric origin is inferred for dissolution which post dates micritization and where moulds are infilled by meteoric drusy calcite cement. This early dissolution predates burial features. However, where dissolution vugs have not been infilled by later cements (Figures 5.4 and 5.5) an early meteoric origin is less

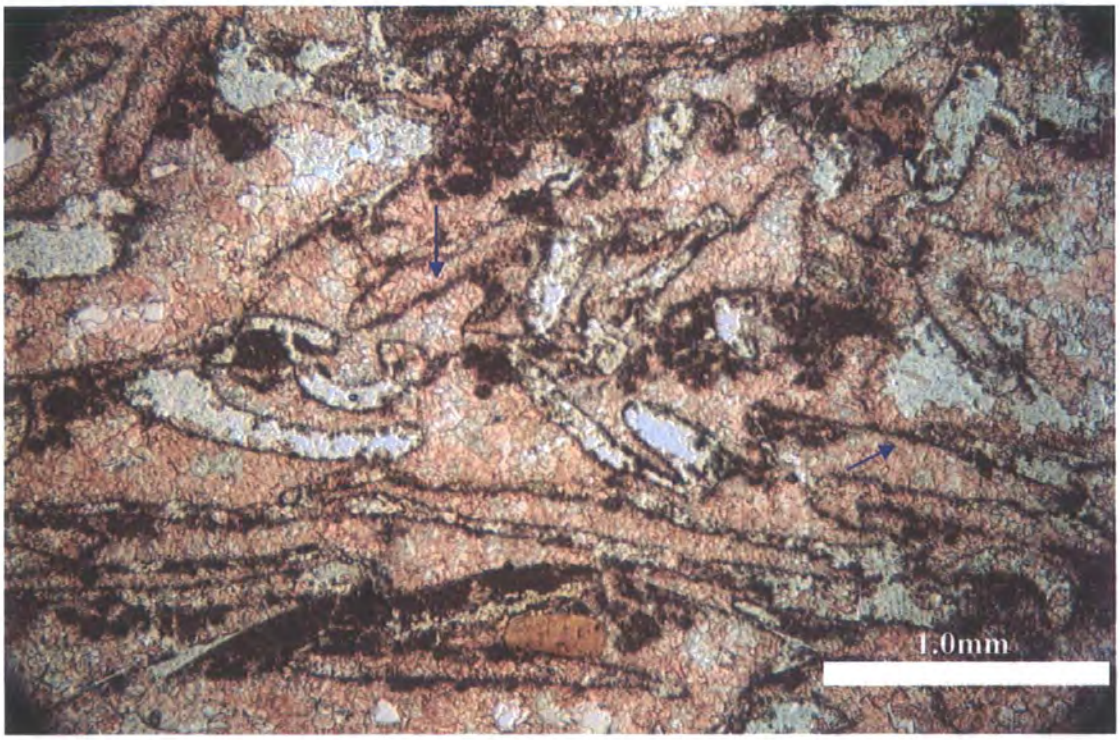

Figure 5.3. Photomicrograph shows mollusc cast, mostly after bivalves. All were originally aragonite that has dissolved and completely filled by drusy calcite cements, only the micrite envelopes remaining to outline the shell shapes (arrows). Note that some dissolution post-dates some cement formation since not all the molds are completely filled whereas the intergranular pore space is totally filled. Jdeir Formation, B7-NC41 well, 8545.5 feet, PPL.

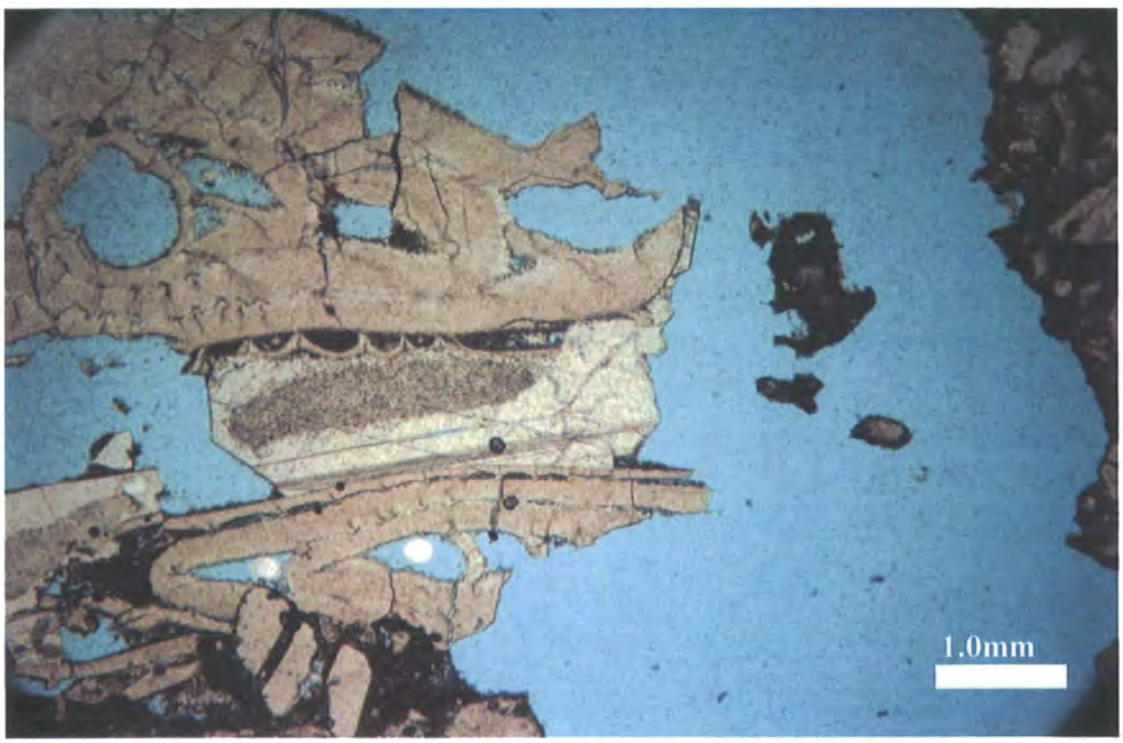

Figure 5.4. Photomicrograph shows extensive dissolution. Note that dissolution postdates syntaxial overgrowth. Jdeir Formation, A2-NC41 well, 9123.5 feet, PPL.

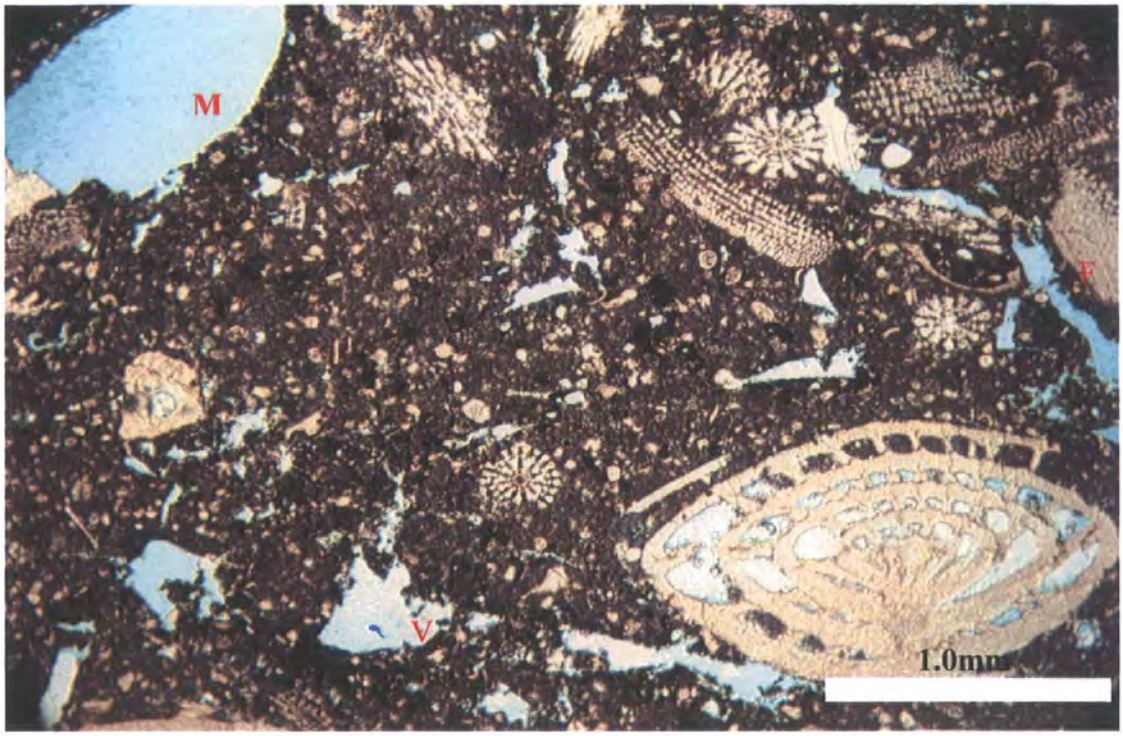

Figure 5.5. Photomicrograph shows mouldic (M), small vuggy (V) and small fracture (F) porosity. Jdeir Formation, A2-NC41 well, 9150.0 feet, PPL.

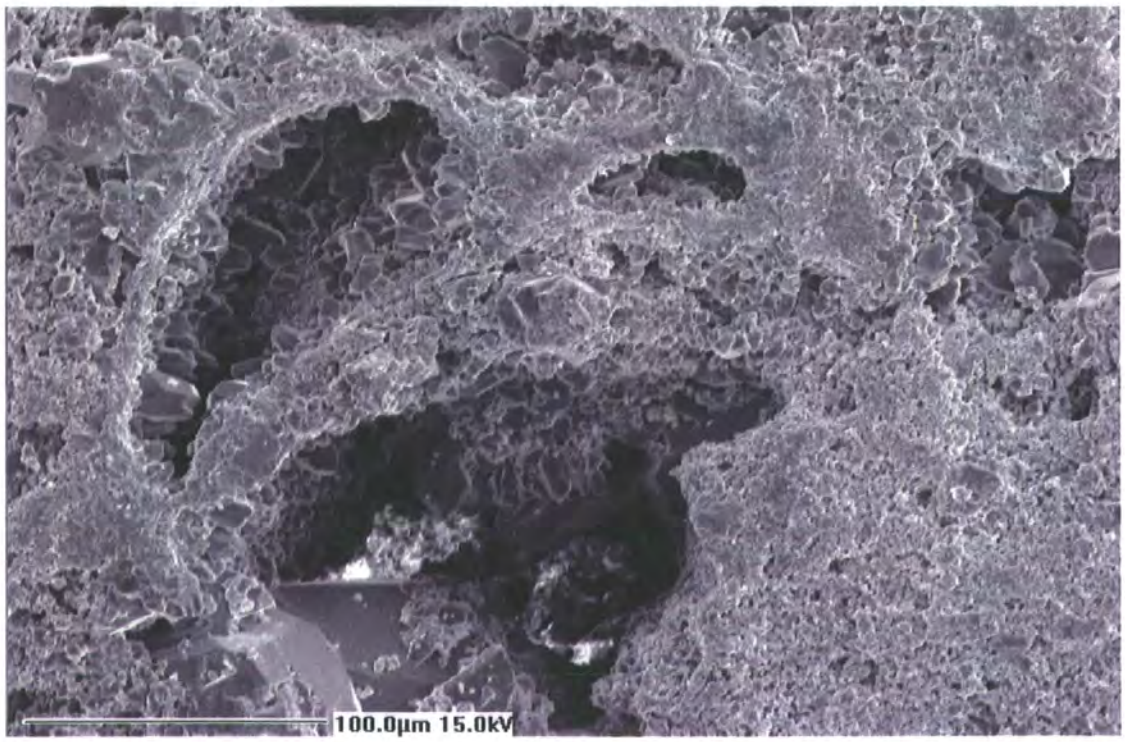

Figure 5.6. SEM Photomicrograph shows partial infill of fully dissolved bioclast by drusy/blocky calcite cement and left mouldic porosity. Jdeir Formation, E1-NC41, 8420.0 feet.

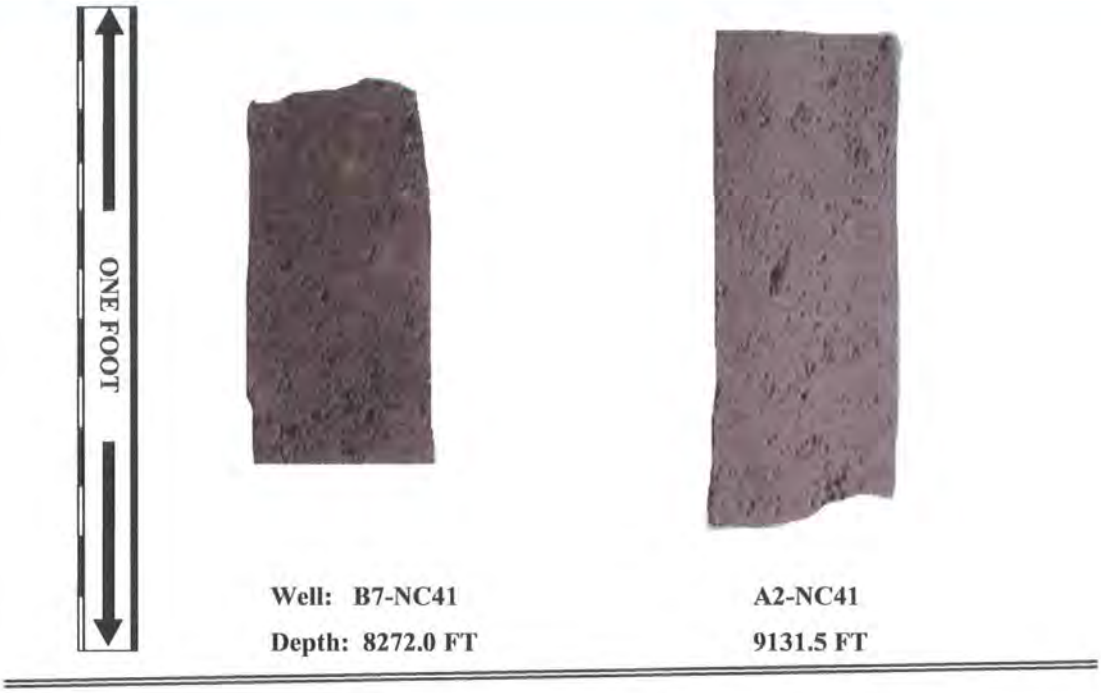

Figure 5.7. Core slab of nummulite facies showing extensive dissolution in the Jdeir Formation.

clear. At least some of the dissolution postdates syntaxial overgrowth formation (Figure 5.4). Where dissolution enhances porosity along fractures (Figure 5.5), it may be related to burial. Multiple phase of dissolution may have affected the Jdeir Formatiom with an early meteoric phase and a possible late burial phase.

5.3.4.2. CEMENTATION:

Drusy calcite, blocky calcite and syntaxial overgrowths around echinoid fragments are the most common cement types observed in the Jdeir Formation. Kaolinite cement occurs only in the lower parts of wells B7-NC41 and E1-NC41, partially filling porosity (Figures 5.14 and 5.15). Drusy calcite cement increases in crystal size regularly towards the centre of the former void-space (Figures 5.8, 5.9, 5.10 and 5.12). The precipitation of non-ferroan drusy calcite spar is the main cause of porosity reduction in the Jdeir Formation. Drusy calcite postdates the formation of micrite envelopes and is commonly reported from meteoric phreatic zone (Wilson, 2002). Drusy calcite cements are often better developed in intergranular space than within moulds derived from solution of skeletal particles. This suggests that the dissolution of bioclasts occurred near contemporaneously or slightly post-dating the precipitation of some drusy cement (Tucker and Wright, 1990 and Wilson and Evans,

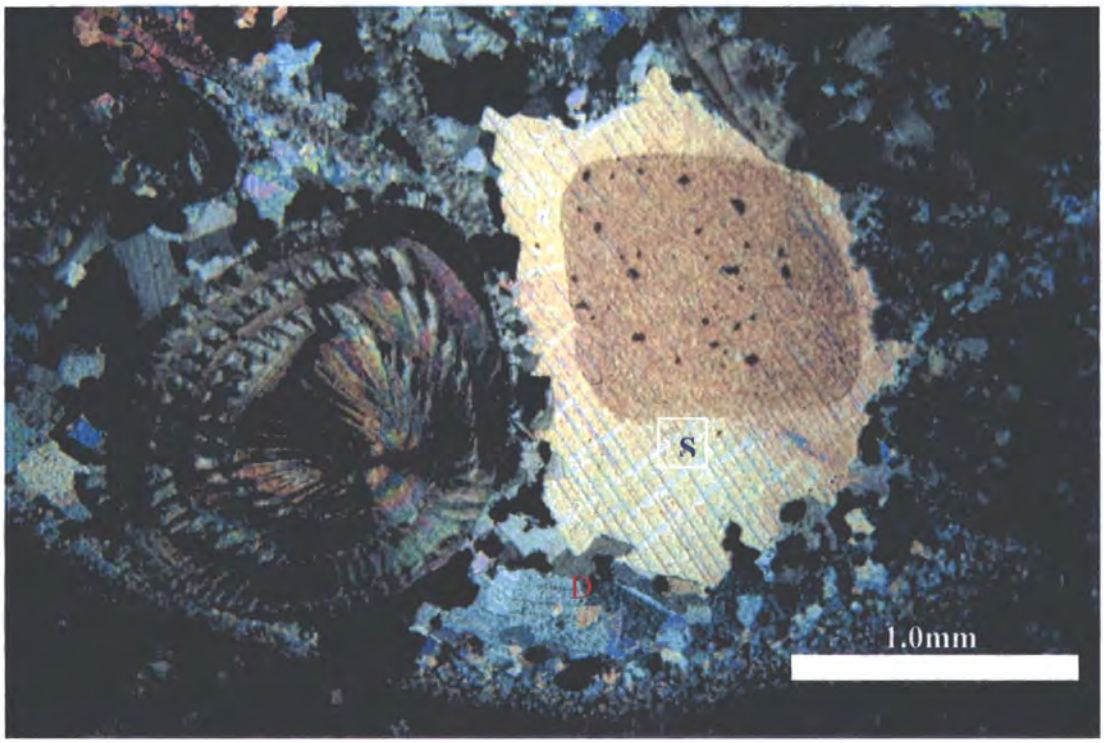

Figure 5.8. Photomicrograph shows syntaxial overgrowth around echinoderm fragments, (S) drusy calcite (D) to equant calcite cements have completely filled porosity. Jdeir Formation, B7-NC41 well, 8253.0 feet, PPL.

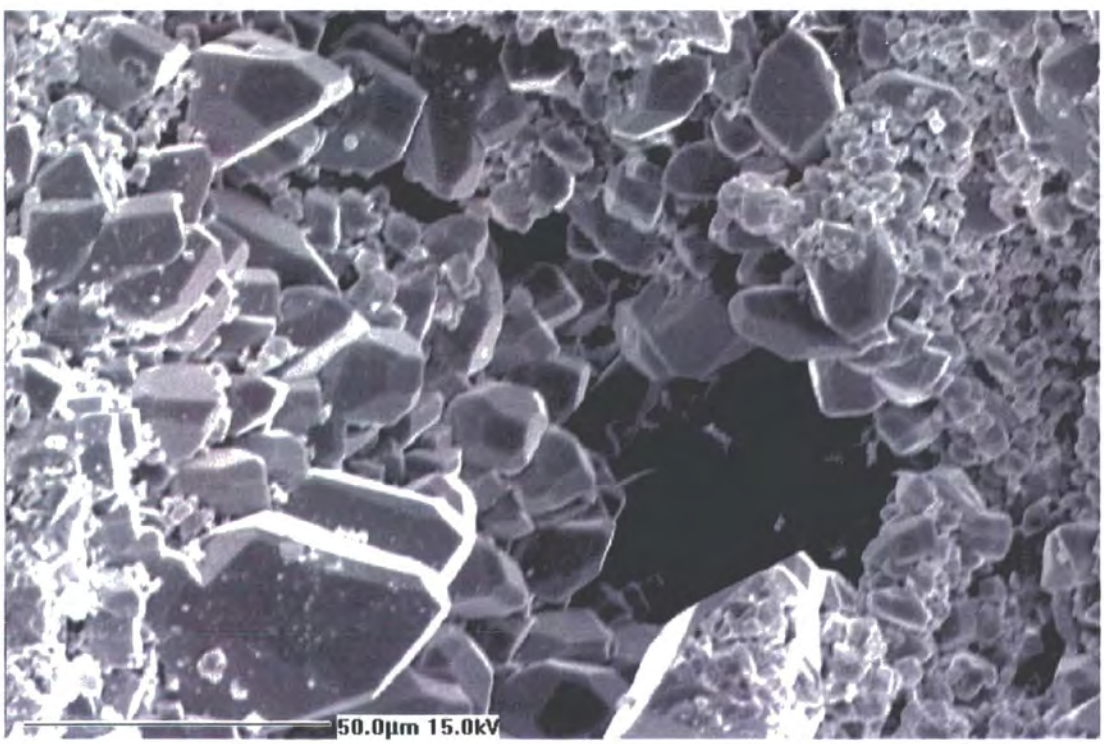

Figure 5.9. SEM Photomicrograph shows blocky to drusy calcite crystals growth within porosity. Jdeir Formation, E1-NC41, 8420.0 feet.

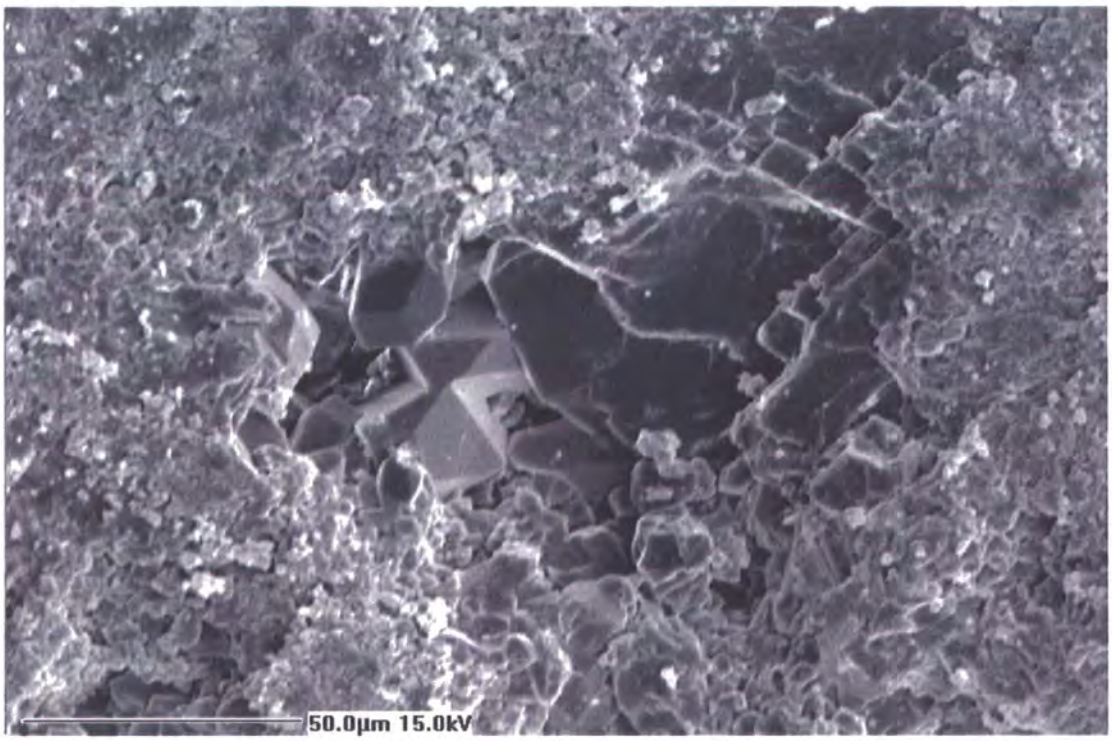

Figure 5.10. SEM Photomicrograph of drusy calcite cement, which has completely filled porosity. Jdeir Formation, E1-NC41, 8420.0 feet.

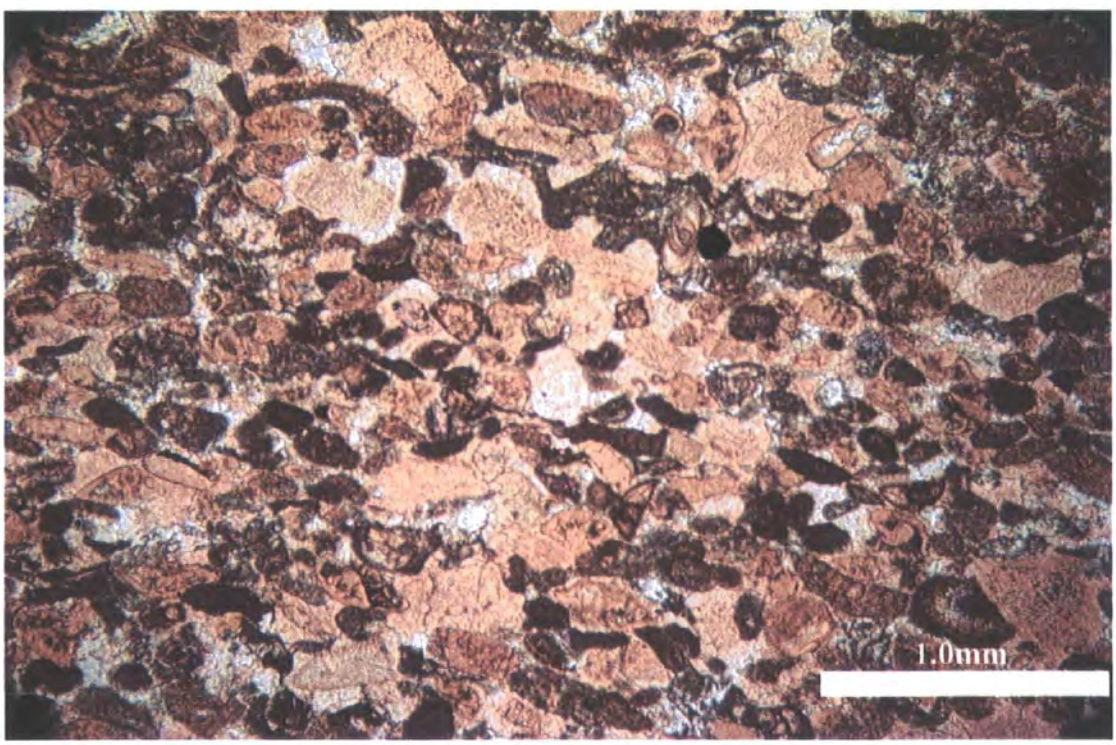

Figure 5.11. Photomicrograph shows syntaxial overgrowth around echinoderms and small foraminifera (rotaliida). Jdeir Formation, E1-NC41 well, 8465.0 feet, PPL.

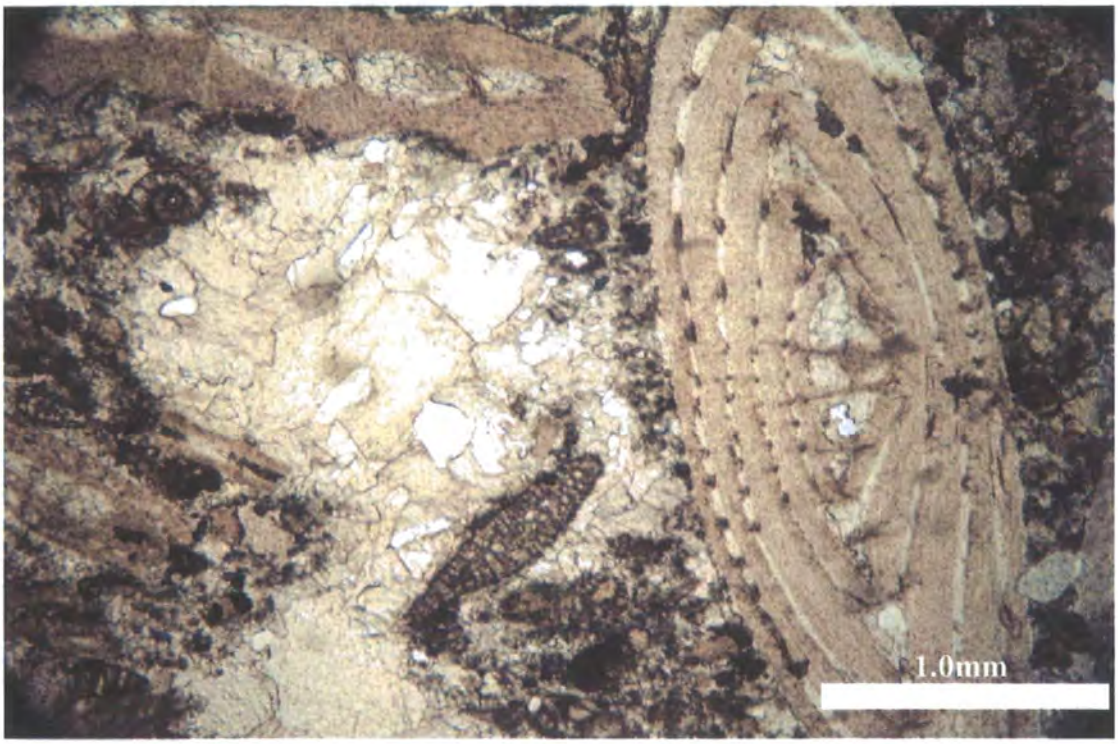

Figure 5.12. Photomicrograph shows drusy calcite has filled porosity. Jdeir Formation, E1-NC41 well, 8286.0 feet, PPL.

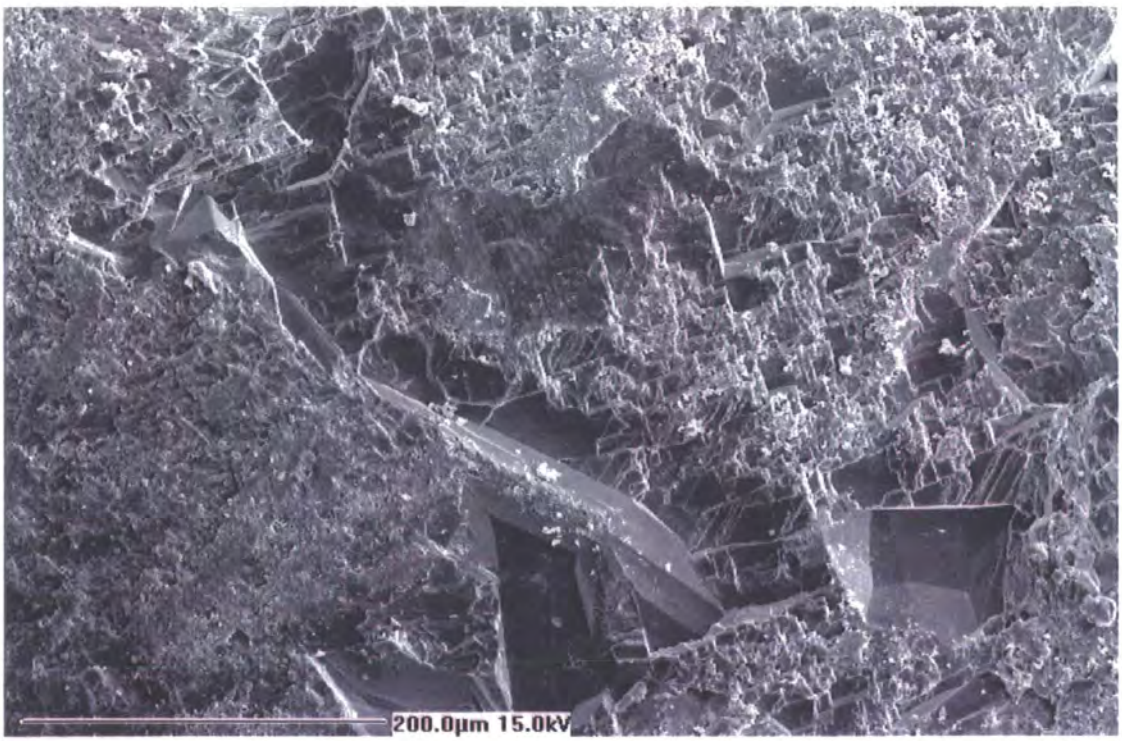

Figure 5.13. SEM Photomicrograph shows blocky calcite cement has completely filled fracture porosity. Jdeir Formation, B7-NC41, 8513.5 feet.

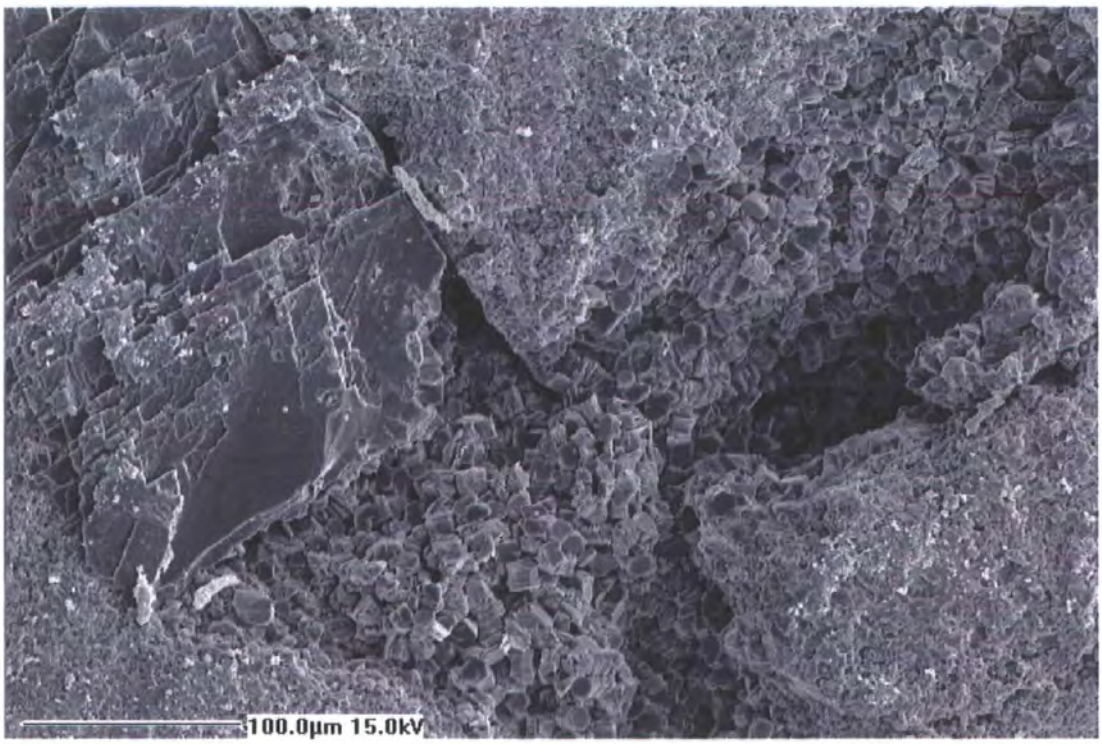

Figure 5.14. SEM Photomicrograph shows kaolinite cement. Jdeir Formation, B7-NC41, 8513.5 feet.

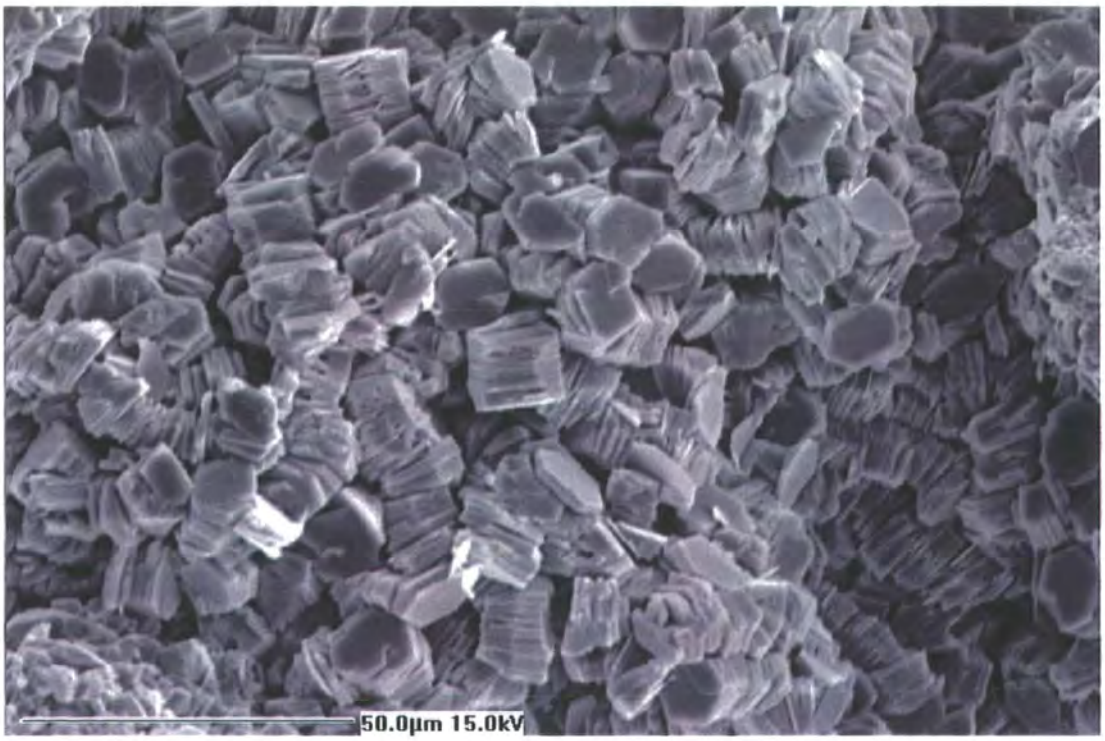

Figure 5.15. Higher magnification of figure 5.20 shows booklet texture of Kaolinite cement. Jdeir Formation, B7-NC41, 8513.5 feet.

2002). Syntaxial overgrowths around echinoid fragments are common within the peloid, echinoderm, and mollusc and nummulite facies but are only a minor feature in the *Discocyclina* and sandy-bioclastic facies. The presence of these syntaxial overgrowths is strongly dependent on the occurrence of echinoid fragments. In some samples within the peloid facies, syntaxial overgrowths alone have reduced porosity by more than 10% (Figure 5.11). Syntaxial overgrowths usually formed after micritization and may pre- or post-date dissolution of aragonite. Some of the syntaxial overgrowths in nummulite facies are clear cements (Figure 5.8), but in other facies are cloudy (Figure 5.11), and may be inclusion-rich. It is possible that the overgrowths formed in different environments. Flugel (2004) points out that overgrowth cements from near-surface marine, vadose-marine and meteoric phreatic environments are cloudy and inclusion-rich, in contrast to clear overgrowth from burial environments. Some authors interpret the syntaxial overgrowth cements to be of meteoric diagenetic origin (e.g. Longman, 1980). However, overgrowth cements on echinoderms are also common in ancient limestones formed in marine environments (Walker et al., 1990). Thin cloudy overgrowth cements often represent the first generation of overgrowth on echinoderm grains followed by a continued growth under meteoric conditions (Flugel, 2004)

5.3.4.3. NEOMORPHISM:

. Neomorphic replacement of micritic matrix by microsparite calcite is observed just in the lower part of well E1-NC41 in the *Alveolina* and peloidal-bioclastic facies (Figure 5.16). The transformation of aragonite and High-Mg calcite grains and mud to low-Mg calcite is one of the most important processes in carbonate diagenesis because it controls the ultimate petrophysical properties of limestones and their geochemical compostion (particularly stable isotopes and Sr content)(Al-Asam and Veizer, 1986). Depending on water chemistry and rates of flow, micrite may recrystallize and neomorphose to coarse grains in a fresh water phreatic environment or in a fresh water vadose environment (Longman, 1980; Flugel, 1982).

5.3.5. LATE BURIAL DIAGENESIS:

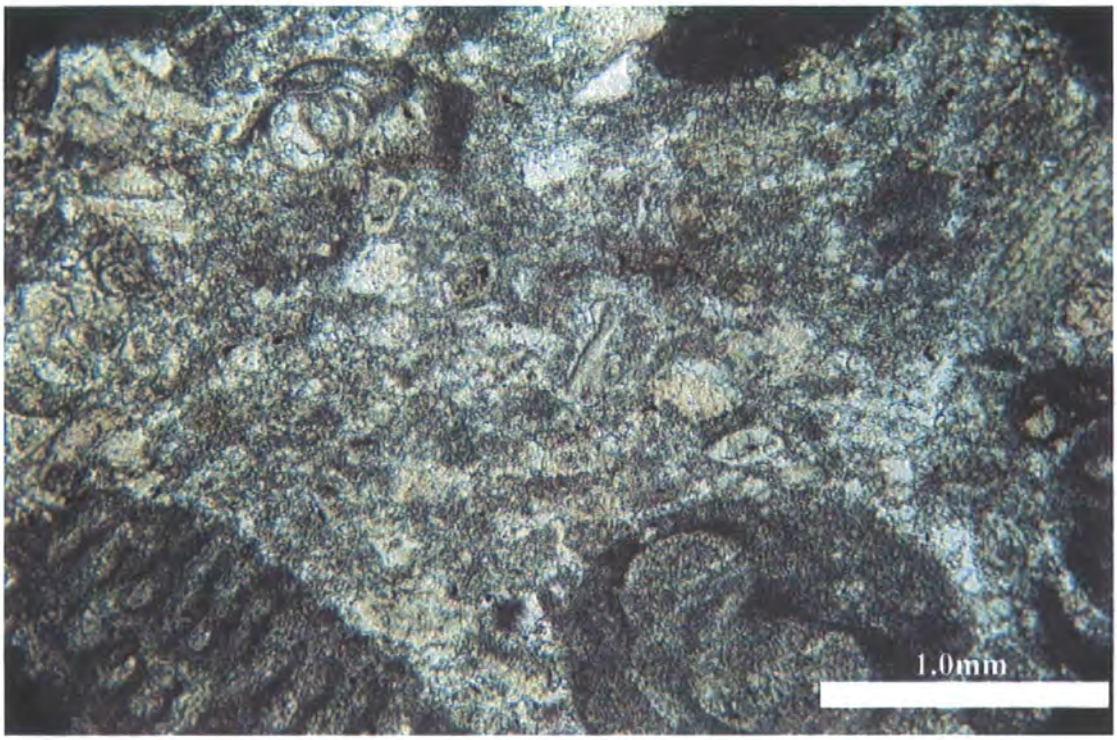

Figure 5.16. Photomicrograph shows aggrading neomorphism of carbonate mud (micrite). Jdeir Formation, E1-NC41 well, 8441.0 feet, PPL.

Figure 5.17. Photomicrograph shows nummulites cut by rectangular or high amplitude stylolite. Jdeir Formation, B7-NC41 well, 8460.0 feet, PPL.

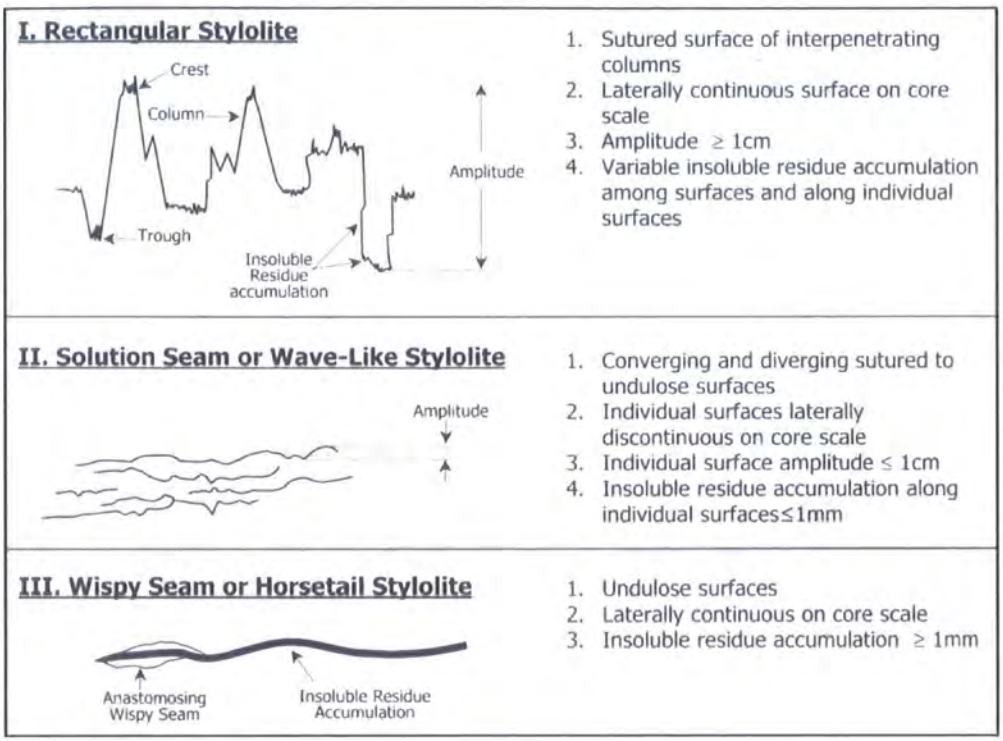

(a)

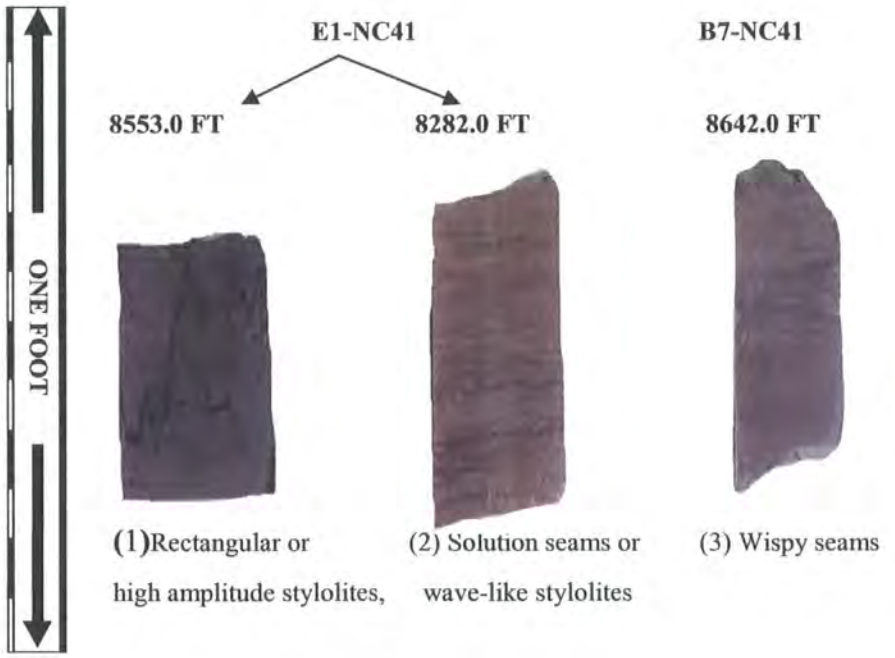

(b)

Figure 5.18. Types of stylolites: (a) modified after Alsharhan et al. 2000; (b) Core photographs of study wells showing three types of dissolution features (stylolites and dissolution seams).

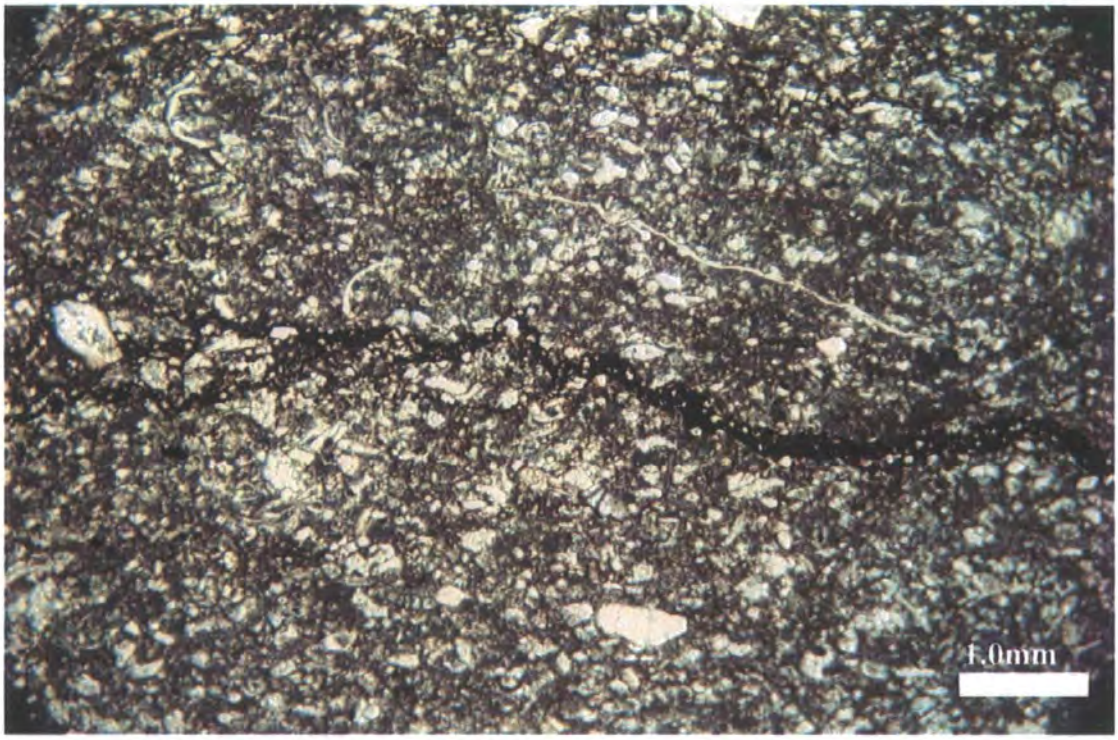

Figure 5.19. Photomicrograph shows solution seams or wave-like stylolites. Dark material (bitumen), is concentrated along the stylolite. Jdeir Formation, B7-NC41 well, 8442.0 feet, PPL.

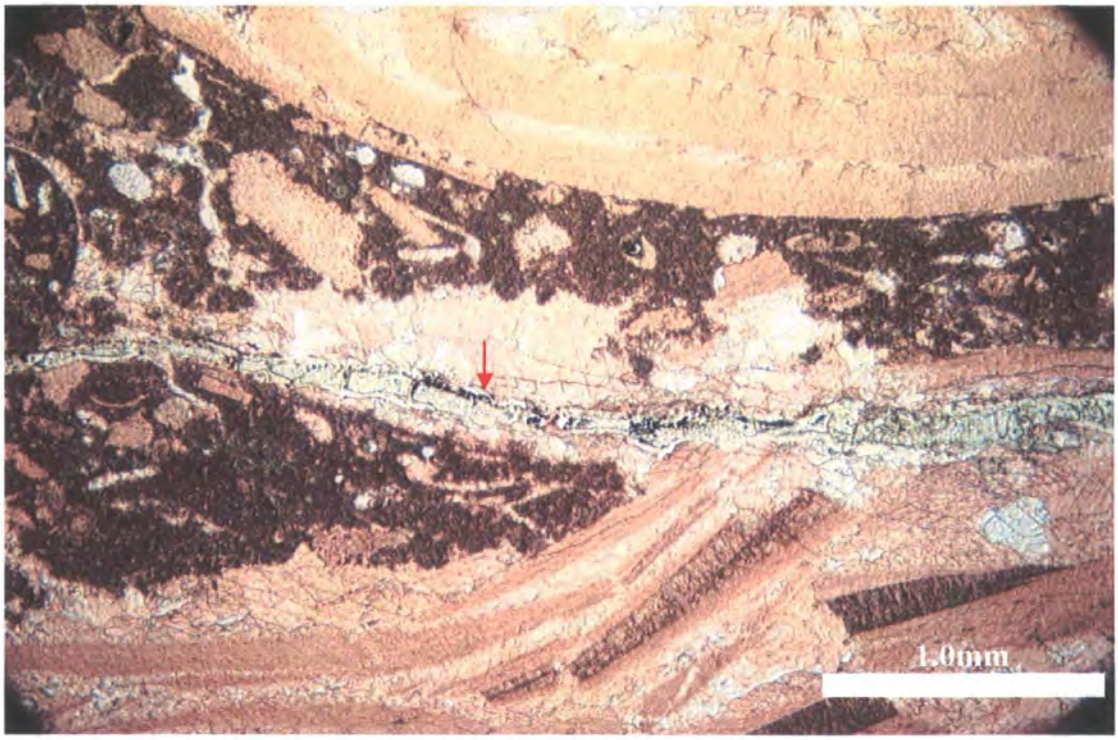

Figure 5.20. Photomicrograph shows fracture cutting large mollusc fragments and other sediments. This fracture is partially filled by bitumen (arrow). Jdeir Formation, B7-NC41 well, 8588.0 feet, PPL.

5.3.5.1. STYLOLITES AND FRACTURES:

The observed compaction features seen throughout most of the studied sections are represented by horizontal stylolites. This study uses the classification scheme of stylolites after Alsharhan et al. (2000). It is based on the amplitude and morphology of the pressure-dissolution surface within stylolites, their lateral continuity, and the thickness of the accumulated insoluble residue in stylolites. The detailed sedimentological and petrographic study for three wells (E1, B7 and A2-NC41) resulted in recognition of three kinds of stylolites or dissolution seams in the Jdeir Formation (Figure 5.18). These are: (1) rectangular or high amplitude stylolites (Figure 5.17), (2) solution seams or wave-like stylolites (Figure 5.19), and (3) wispy dissolution seams. Concentrated along dissolution seams is an insoluble residue of dark organic matter or bituminous substance. Stylolitisation significantly affects carbonate reservoir quality by providing pathways for hydrocarbon migration. The stylolites have clearly acted as pathways for hydrocarbon migration since bitumen is still present as a residue along most stylolites (Figures 5.17 and 5.19). Stylolites are pressure dissolution features formed after burial and their width might have been enhanced by acidic leaching.

The observed fractures within Jdeir Formation have been partially or completely infilled by coarse non-ferroan calcite (Figure 5.23). In the mollusc facies, some fractures are partially filled by black bitumen (Figure 5.20).These fractures are up to centimetres in length and range from less than 1mm to 6mm in width. In the Bouri Field, stylolites are frequently associated with open microfractures (Bernasconi et al. 1984 and Mriheel, 1991).

5.3.5.2. DOLOMITIZATION:

The effect of dolomitisation processes on the Jdeir Formation is very limited. Dolomite has been recognized within lower part of the well A2-NC41, located in the south part of study area, particularly in the mollusc facies (Figures 5.21 and 5.22). The dolomite occurs as fine rhombs (20-100 μm) replacing the matrix. The presence of dolomite along styolites and pressure dissolution seams is suggestive of dolomite forming during burial. Tucker, (2001) pointed out that scattered rhombs, dolomite crystals along stylolites and pressure dissolution seams, and late cavity-filling dolomite cements are all common forms of burial dolomite in many limestones.

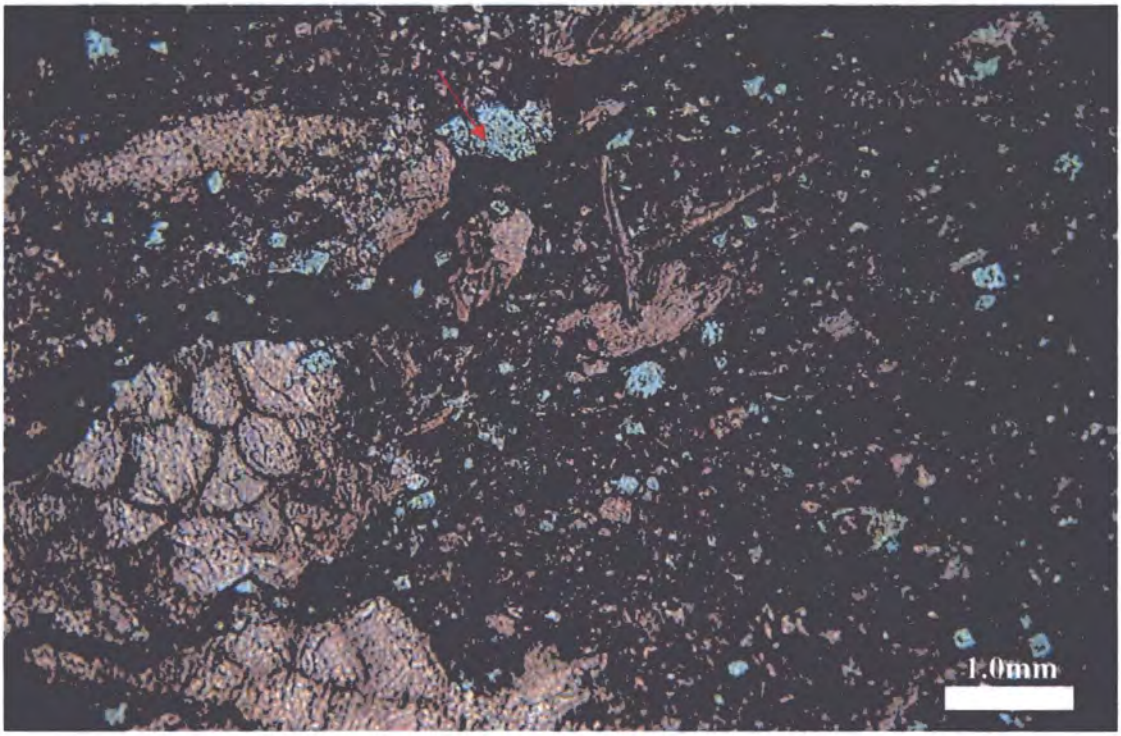

Figure 5.21. Photomicrograph shows scattered very fine crystalline dolomite (unstained) replacing the matrix and concentrated along dissolution seams. Jdeir Formation, A2-NC41 well, 9234.0 feet, PPL.

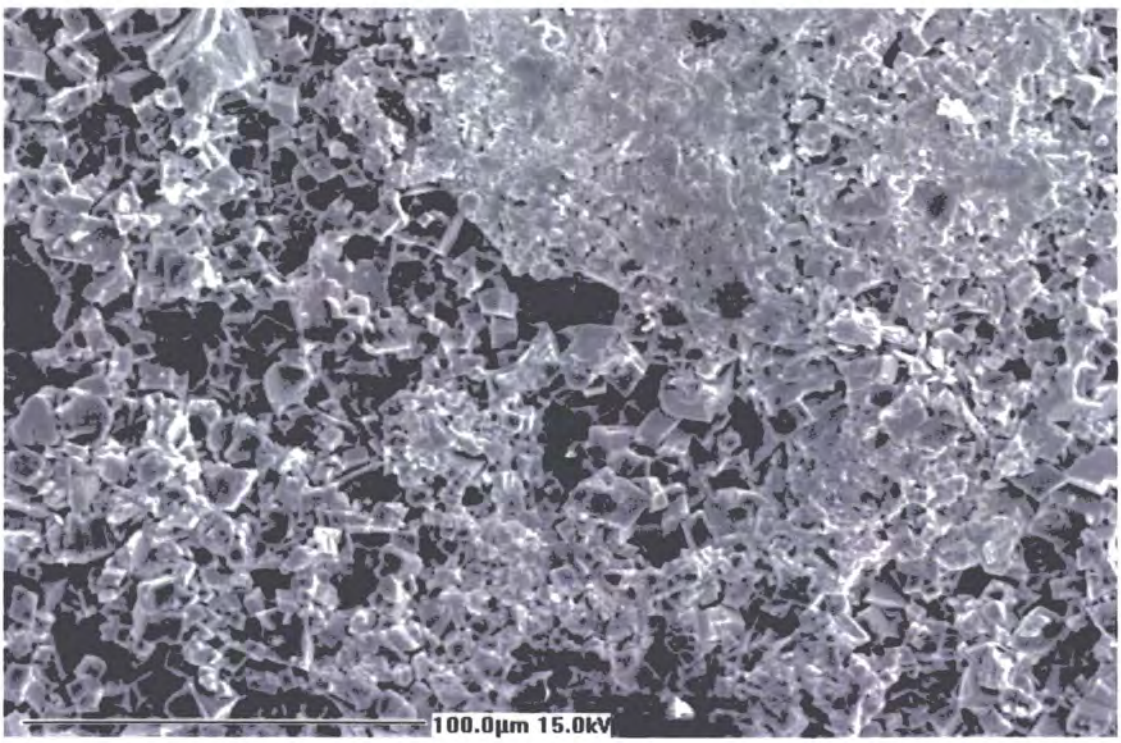

Figure 5.22. SEM Photomicrograph shows very fine crystalline dolomite has replaced micritic matrix. Jdeir Formation, A2-NC41, 9237.5 feet.

5.3.5.3. COARSE CALCITE SPAR:

Coarse calcite spars are found in some facies of the Jdeir Formation as a pore-filling cement in fracture porosity (Figure 5.23).These calcite crystals are commonly euhedral. In the nummulite facies in well A2-NC41, coarse calcite spar is replaced by silica. This suggests that coarse calcite spar probably formed before silicification during burial of sediment at a relatively late stage in their diagenetic history. The bright-dull orange for the coarse calcite suggests precipitation under reducing condition (Figures 5.28).

Figure 5.23. Photomicrograph shows coarse non-ferroan calcite filling the fracture porosity. Jdeir Formation, A2-NC41 well, 9090.0 feet, PPL.

5.3.5.4. SILICIFICATION:

Silicification of some bioclasts and matrix, together with silica filling pore spaces by silica is common in the lower and middle part of well A2-NC41 within the planktonic foraminifera, the echinoderm, nummulitic and mollusc facies, but forms rarely in wells E1-NC41 and B7-NC41. Three different petrographic types of chert are recognized in this study including microquartz, drusy megaquartz and chalcedonic quartz (Flugel, 2004). Microquartz and macroquartz occurs in the echinoderm, the

Figure 5.24. Photomicrograph shows silica has completely filled porosity and may have replaced calcite cements. Jdeir Formation, A2-NC41 well, 9262.5 feet, XN.

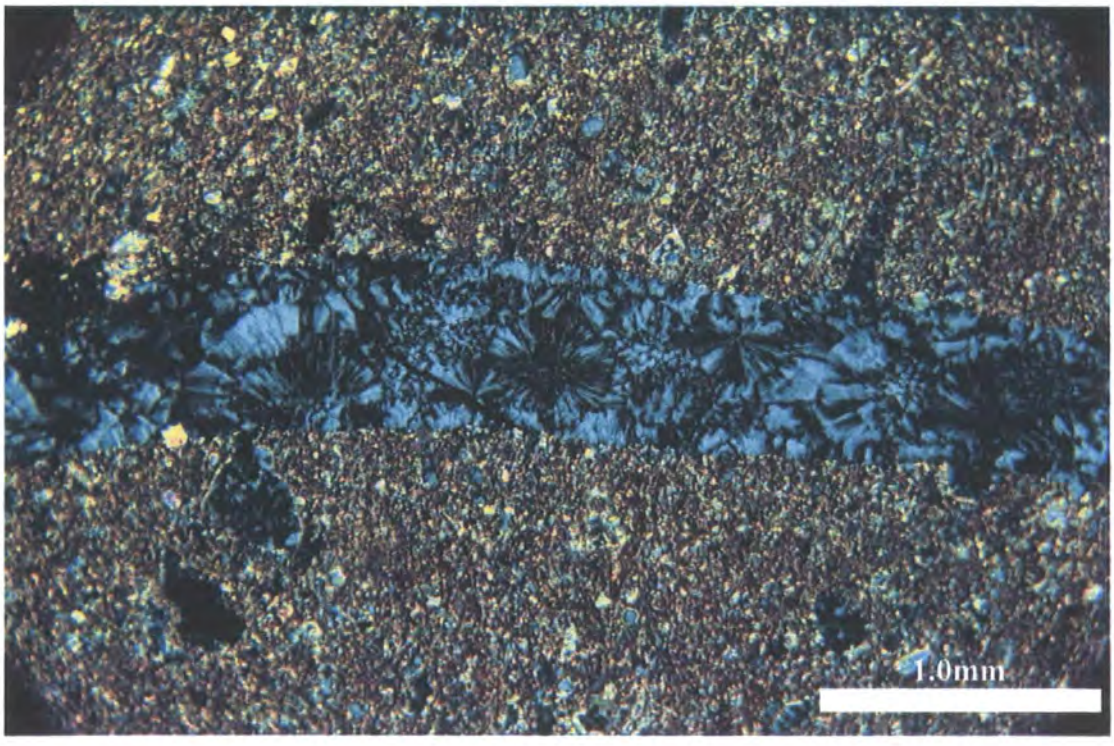

Figure 5.25. Photomicrograph shows chalcedonic quartz has filled fracture porosity. Jdeir Formation, A2-NC41 well, 9180.0 feet, XN.

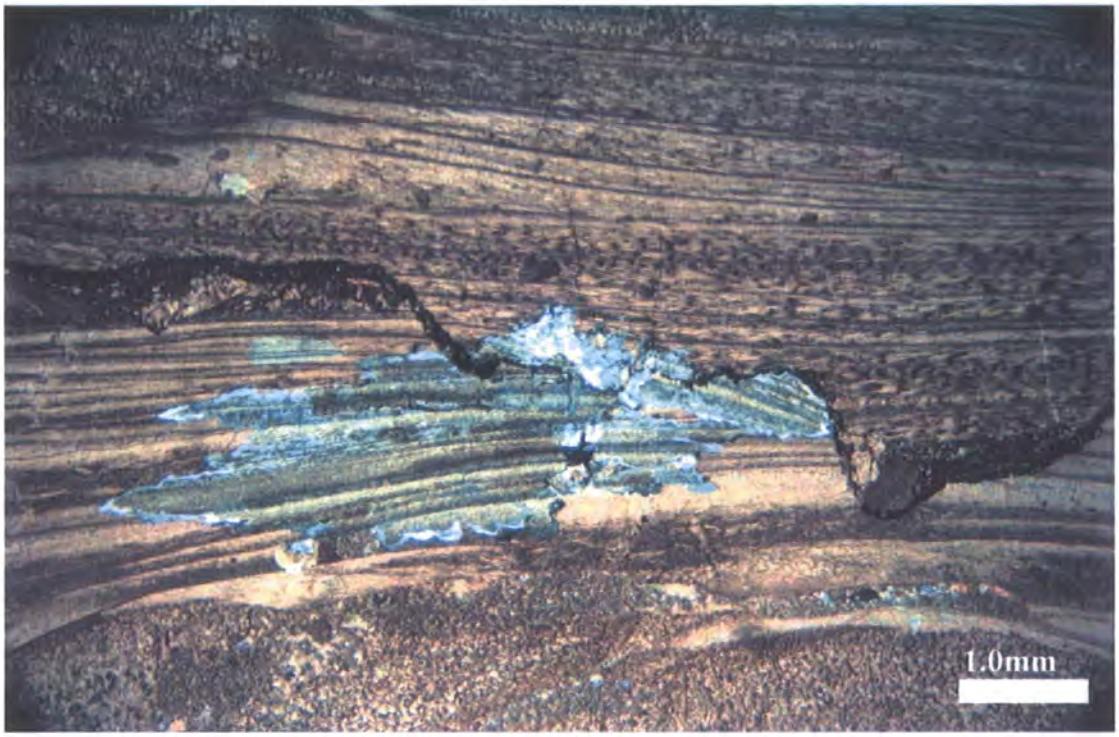

Figure 5.26. Photomicrograph shows silica has partially replaced molluscs and partly follows cross-cutting stylolites. Jdeir Formation, A2-NC41 well, 9234.0 feet, XN.

nummulitic and the mollusc facies, but is most common in the planktonic foraminifera, the nummulitic (Figure 5.24) and the echinoderm facies in well A2-NC41. Chalcedonic quartz is common in the echinoderm facies, particularly in mudstone/wackestones. Some fractures within echinoderm facies in well A2-NC41 predate chalcedony quartz precipitation, since they have been infilled by this cement. (Figure 5.25).In the mollusc rudstone, silica has replaced mollusc fragment and cuts pressure dissolution seams (Figure 5.26). This suggests that silicification is likely to have taken place during burial diagenesis.

5.3.5.5. PYRITE:

Pyrite is observed in most facies of the Jdeir Formation, but it most common in mudstone/wackestones of the echinoderm facies in the lower part of A2-NC41. Pyrite is usually scattered and replaces bioclasts and silica cements (Figure 5.27). This suggests that pyrite formed after silicification. Authigenic pyrite commonly forms under reducing conditions replacing organic material, or in close proximity to organic material (Flugel, 2004). In modern sediments the sulphur required for pyrite formation

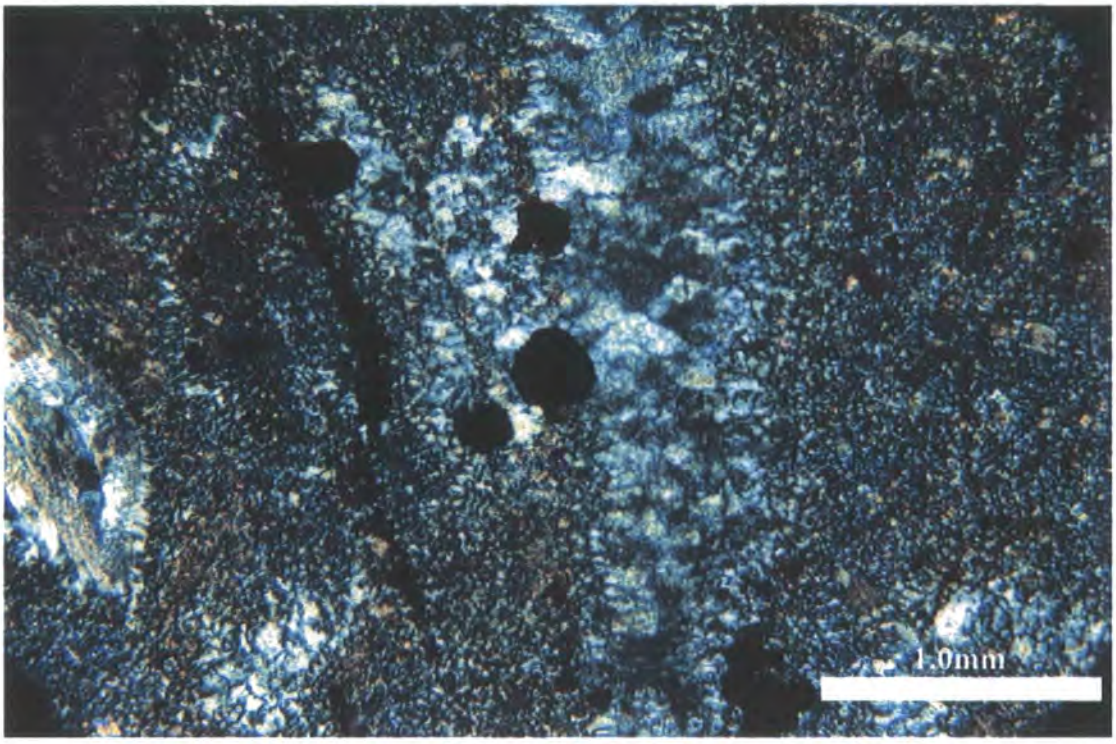

Figure 5.27. Photomicrograph shows pyrite crystals have partially replaced silica. Jdeir Formation, A2-NC41 well, 9252.0 feet, XN.

is derived from the seawater (Hudson and Palframan, 1969), whereas iron is usually transported to the basin as clay minerals then released in a reducing environment (Carroll, 1958). According to Berner (1970) the sulphide for the precipitation of pyrite comes mainly from bacterial reduction of dissolved sulphate in pore waters, producing H_2S which reacts with Fe^{2+} in solution. Other sources of H_2S are from thermal maturation of kerogen or crude oil (Machel et al. 1995).

5.3.5.6. HYDROCARBONS:

The hydrocarbon accumulations in the north western Libya offshore have mainly been discovered in carbonate reservoirs ranging in age from Late Cretaceous to Early Tertiary (Mriheel, 1991). Oil generation in the offshore basin commenced after the Miocene and is still continuing (after Mriheel et al., 1993). A late phase of migration postdating burial diagenesis is consistent with residual bitumen along stylolites and in fractures in the study wells. It is suggested that the decrease in CO_2 during thermal maturation of organic matter with the source rocks increased the

potential for dissolution and consequently enhanced the formation the secondary porosity (after Mriheel et al., 1993).

5.4. CATHODOLUMINESCENCE (CL)

Cathodoluminescence (CL) is a petrographic tool widely used in studies of diagenesis. The most common application of CL in carbonate rocks is in revealing successive stages or zones of void filling cements that could not be seen using transmitted light microscopy (Miller, 1988). CL features of calcite have generally been attributed to variation in Mn concentration as the main activator and to Fe as the main quencher (Machel and Burton, 1991). According to Miller (1988) the intensity of luminescence during CL analysis in calcite is usually grouped into three categories: non-luminescent (dead, extinguished or black), dull (brown) and luminescent (bright yellow, orange and moderate). The variation between bright and dull cement luminescence indicates a change from oxidizing to more reducing condition of fluid (Meyers, 1991). Non-luminescent calcite or dolomite is normally the result of low content of an activator (Fairchild, 1983). Non-luminescent calcite is suggested to be precipitated from oxidizing pore-water, whereas bright and dull luminescent indicates more reducing pore-fluid (Meyers, 1978 and Tucker 1991). In this study four uncovered and polished thin-sections from the Jdeir Formation have been studied by using CL in order to investigate the effect of the chemistry pore-fluid on the cementation. The results studied indicate two different types of CL zones in the studied limestone. These are non-luminescent and bright-dull orange. The non-luminescent zone includes microcrystalline calcite (micrite), microsparite calcite and silica cements between grains (Figures 5.28, 5.32 and 5.33). Bright –dull orange luminescence is present in drusy calcite, syntaxial overgrowths and coarse calcite cements (Figures 5.28, 5.29, 5.30, 5.32 and 5.33). The cathodoluminescence behaviour of micrite, microsparite calcite and silica cements which show non-luminescent reflects the apparently oxidizing nature of the shallow meteoric waters whereas drusy calcite, syntaxial overgrowths and coarse calcite cements which show the bright-dull orange luminescence reflect reducing conditions. Bright –dull luminescence of the drusy calcite and syntaxial overgrowths is indicative of precipitation from waters of varying chemistry (Wilson and Evans 2002).

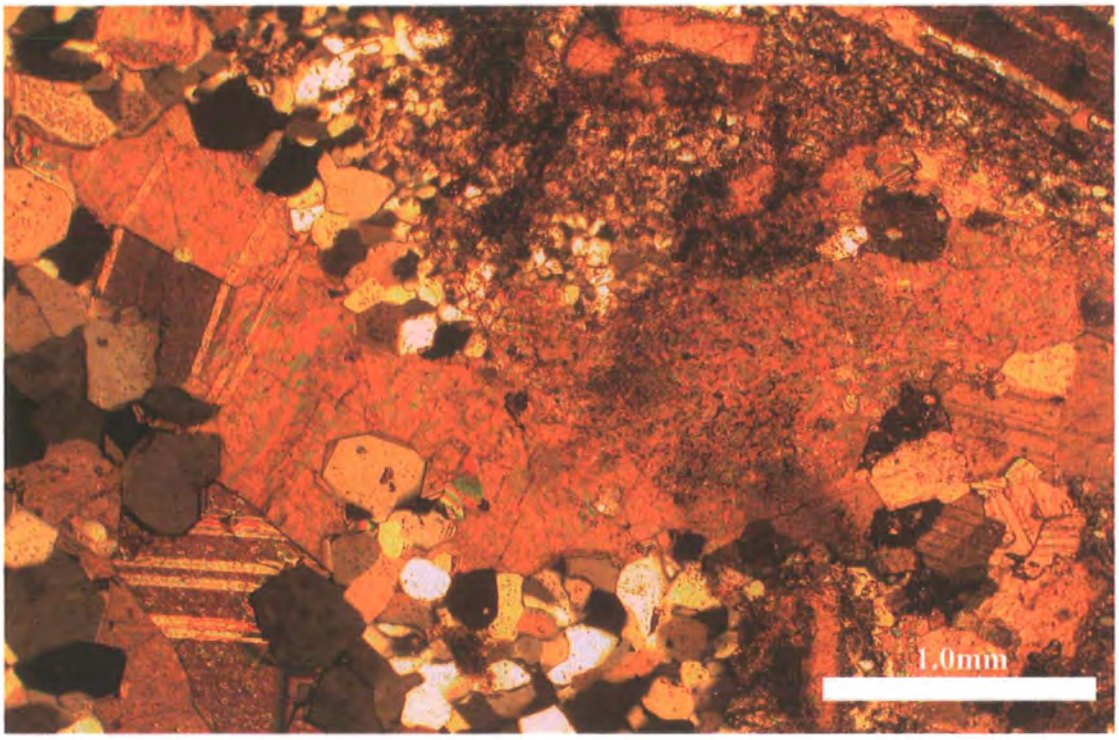

(a)

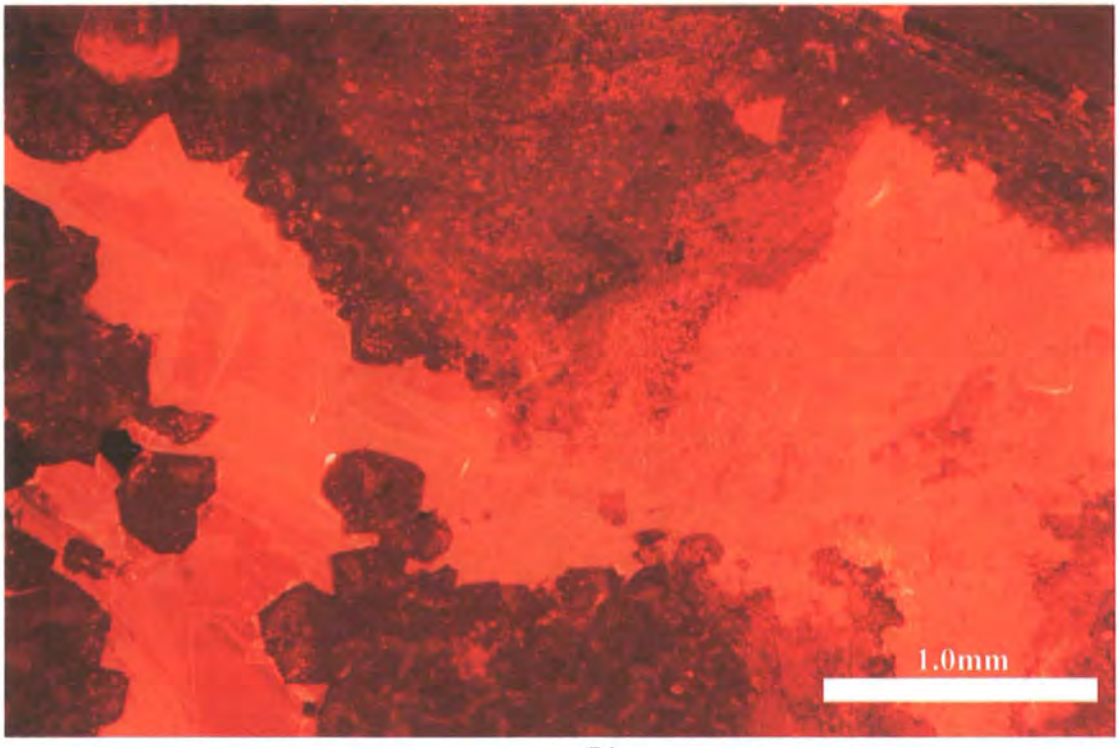

(b)

Figure 5.28. Paired photomicrographs taken under normal light (XN) (a) and CL (b), showing coarse calcite cement has completely filled primary porosity. Later, the calcite cement has been replaced by micro-macroquartz (silica). Under CL (b), the coarse calcite cement shows bright-dull orange for the calcite and non-luminescent properties for the silica. Jdeir Formation, A2-NC41 well, 9262.5 ft feet.

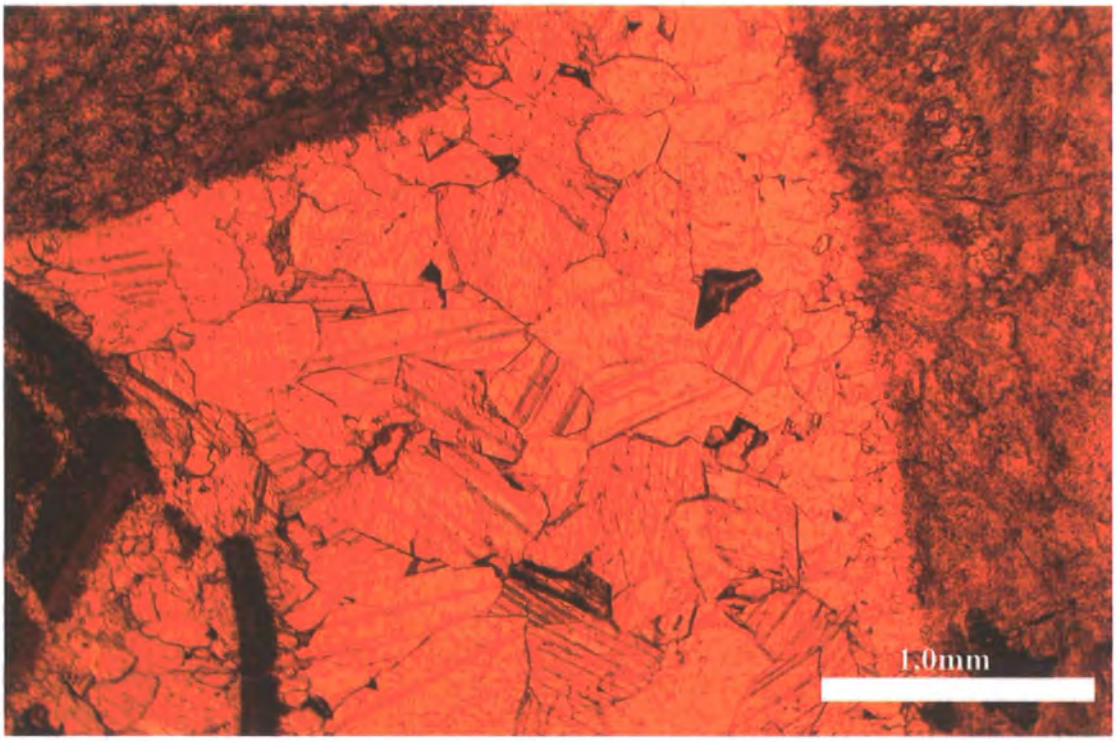

(a)

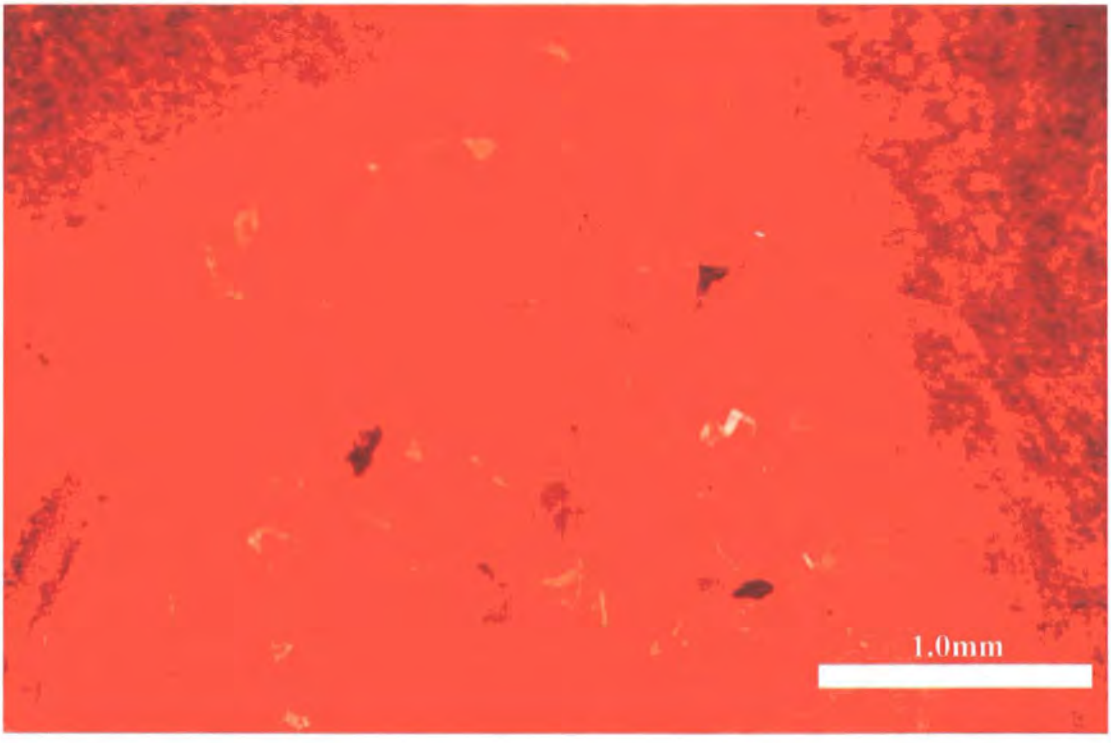

(b)

Figure 5.29. Paired photomicrographs taken under normal light (PPL) (a) and CL (b), showing drusy calcite spar has filled porosity. Under CL (b), the drusy calcite cement is generally has bright-dull orange luminescene. Jdeir Formation, B7-NC41well, 8253.0 feet.

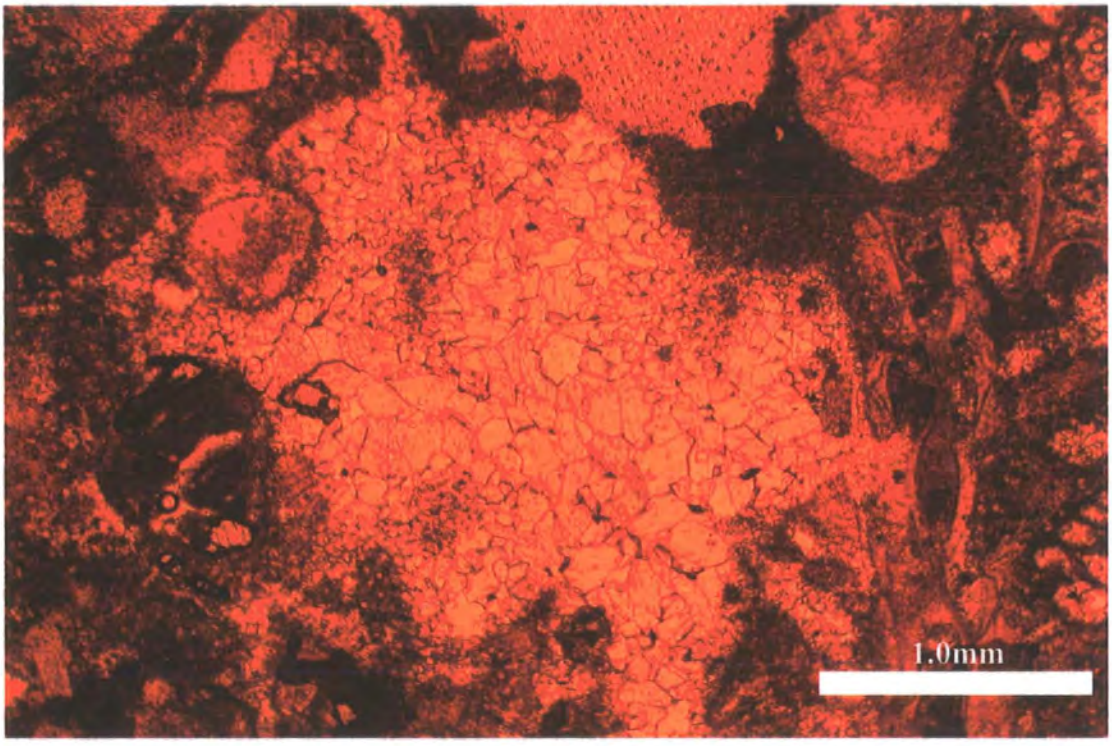

(a)

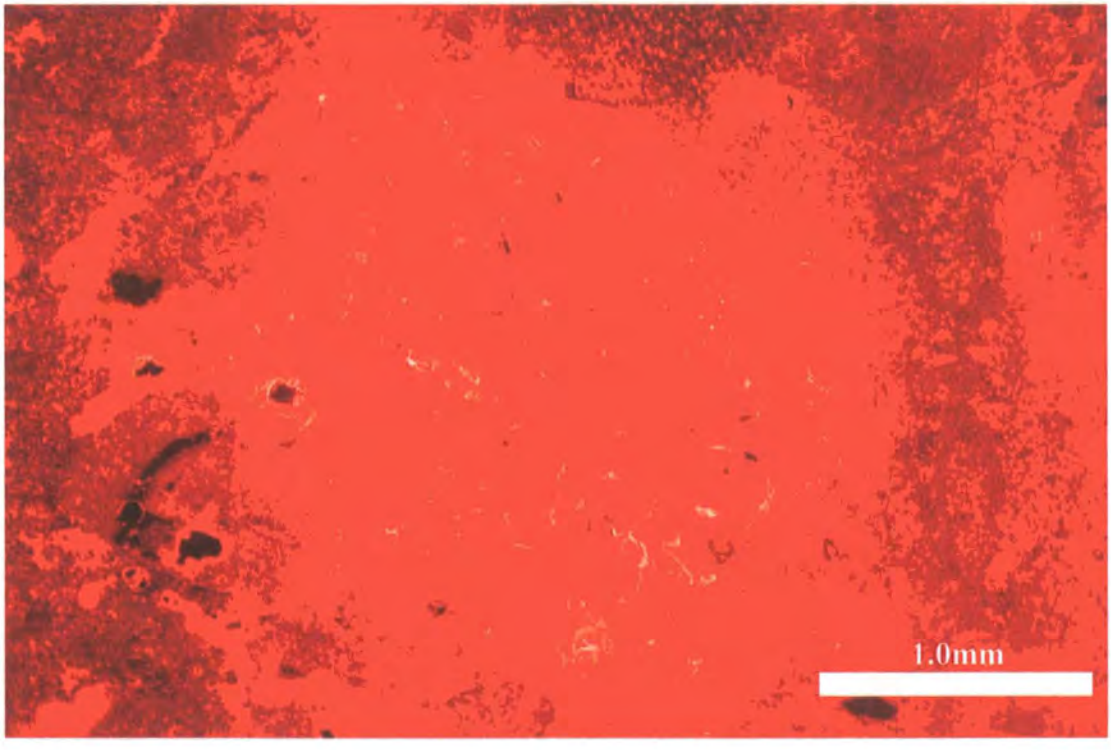

(b)

Figure 5.30. Paired photomicrographs taken under normal light (PPL) (a) and (b), showing drusy calcite cements within secondary porosity. CL image shows orange luminescent for the drusy calcite. Jdeir Formation, B7-NC41 well, 8253.0 feet.

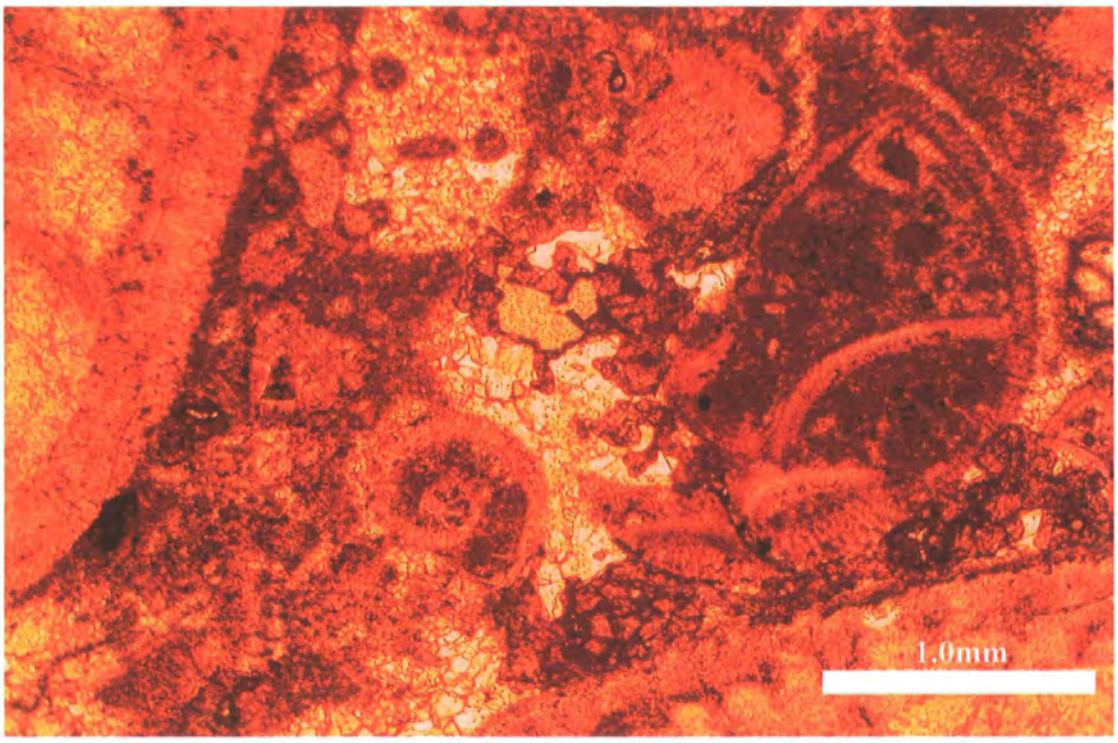

(a)

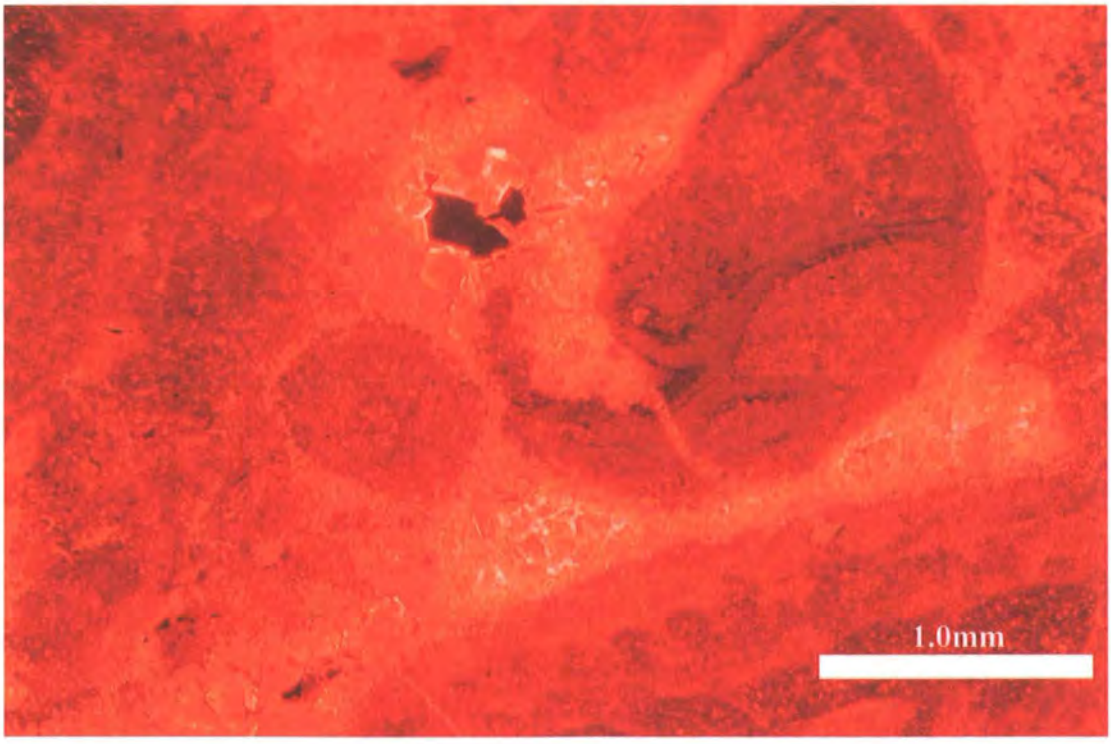

(b)

Figure 5.31. Paired photomicrographs taken under normal light (PPL) (a) and CL (b), showing drusy microsparite calcite has filled primary porosity. Under CL (b), the microsparite shows bright orange luminescent. Jdeir Formation, B7-NC41 well, 8253.0 feet.

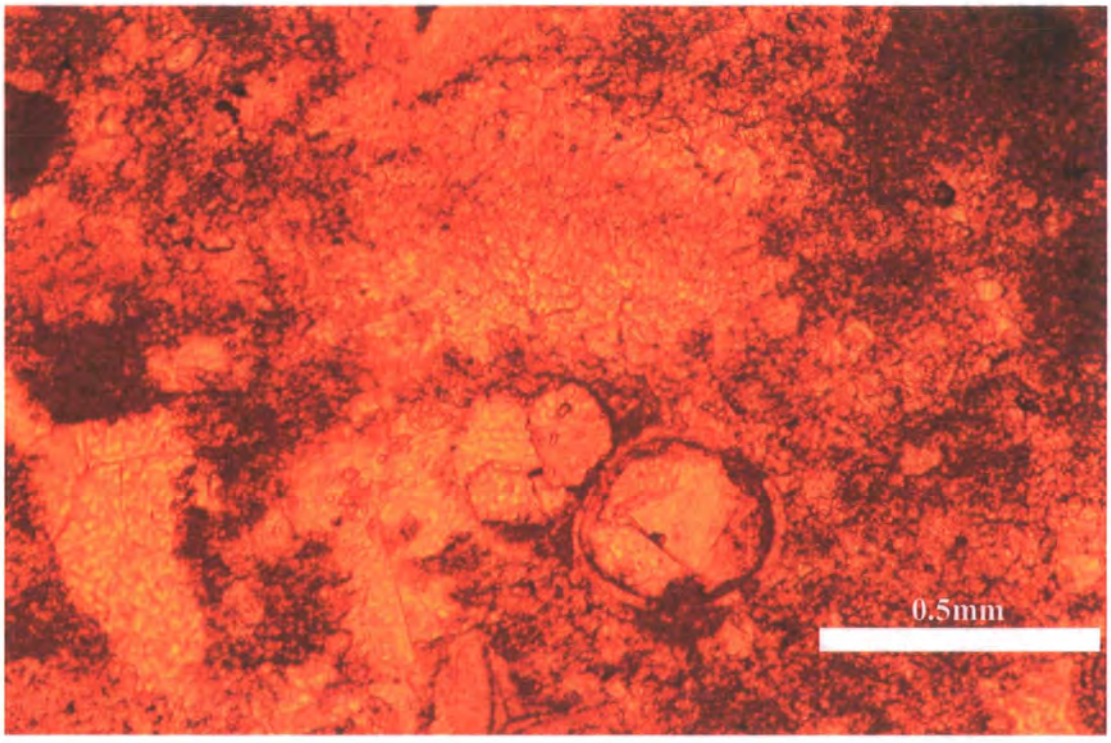

(a)

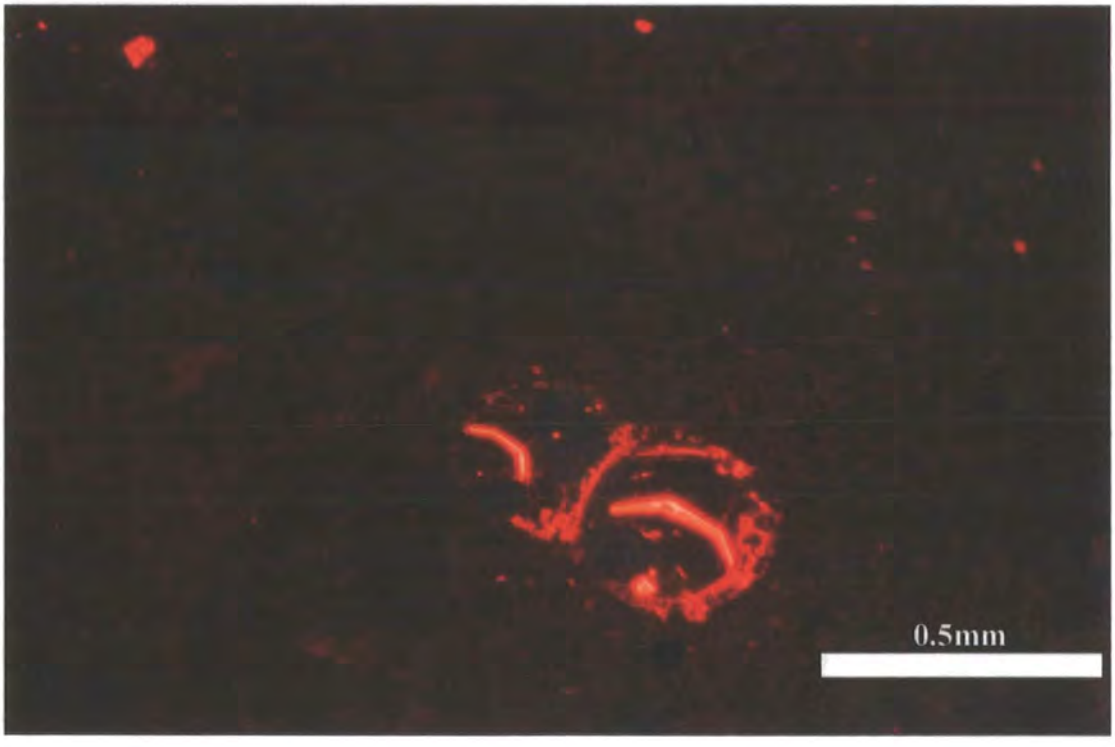

(b)

Figure 5.32. Paired photomicrographs taken under normal light (PPL) (a) and CL (b), showing partial recrystallization of fine-grained matrix to microsparite. Under CL (b) the micrite and microsparite are non-luminescent whereas bright and dull orange lumincence occurs only in pore filing cements within bioclasts. Jdeir Formation, E1-NC41 well, 8361.0 feet.

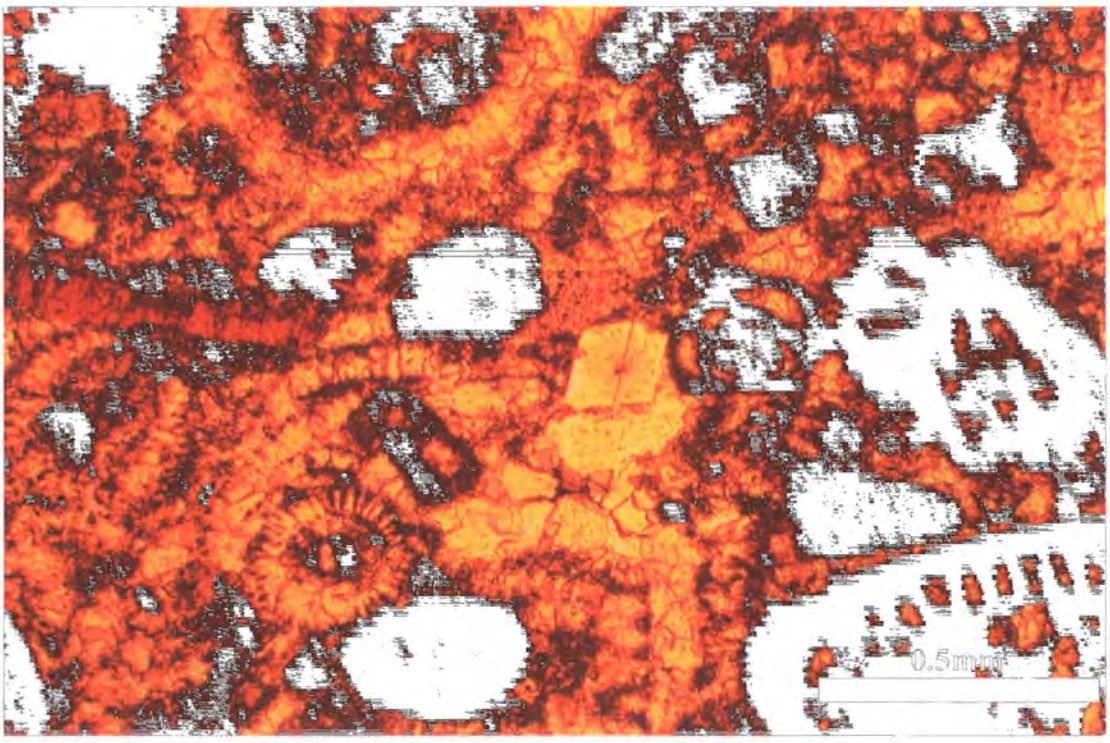

(a)

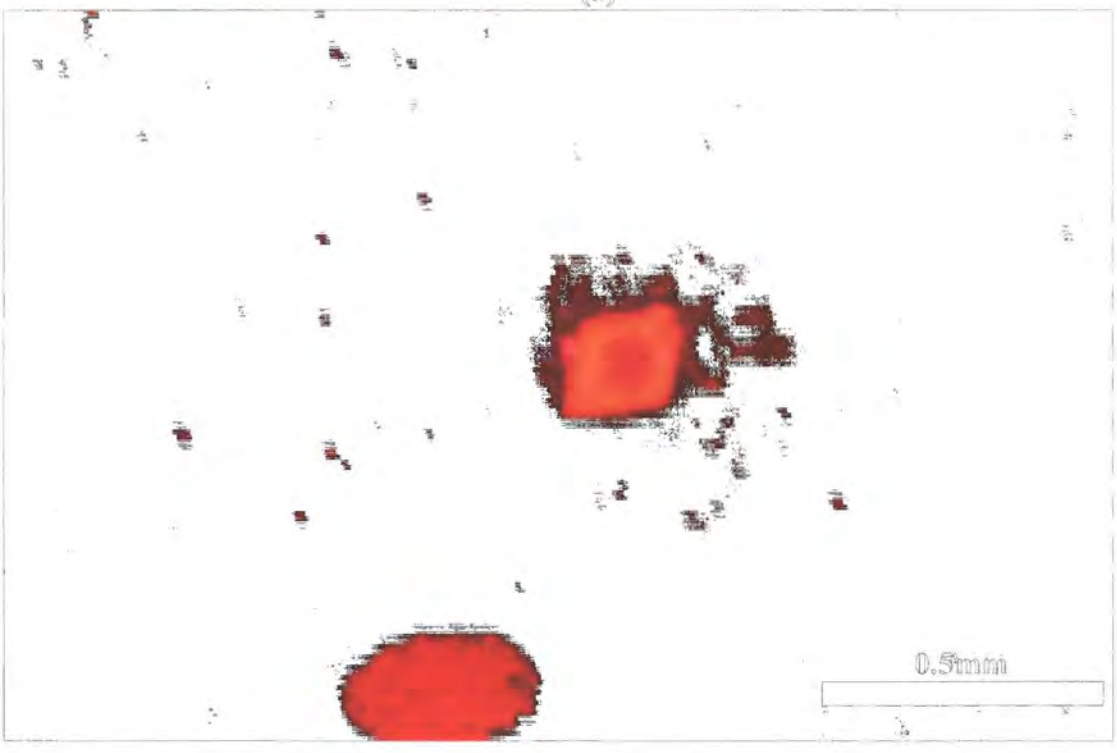

(b)

Figure 5.33. Paired photomicrographs taken under normal light (PPL) (a) and CL (b), showing non-luminescent microsparite calcite and concentric bright and dull orange zonation of syntaxial overgrowth. Note that peloid also shows bright luminescence. Jdeir Formation, E1-NC41 well, 8429.0 feet.

5.5. CARBON AND OXYGEN STABLE ISOTOPES ($\delta^{18}O$ & $\delta^{13}C$):

Stable isotopes of oxygen and carbon are one of the various geochemical techniques employed for assisting with the interpretation of sedimentary and diagenetic conditions and environments (Hudson, 1977; Anderson and Arthur, 1983; Marshall, 1992 and Corfield, 1995). The two most naturally abundant isotopes of oxygen, ^{18}O and ^{16}O and of carbon, $^{13}C/^{12}C$ ratios, are normally used. Variations in $^{18}O/^{16}O$ and $^{13}C/^{12}C$ ratios between samples being measured by high-precision mass

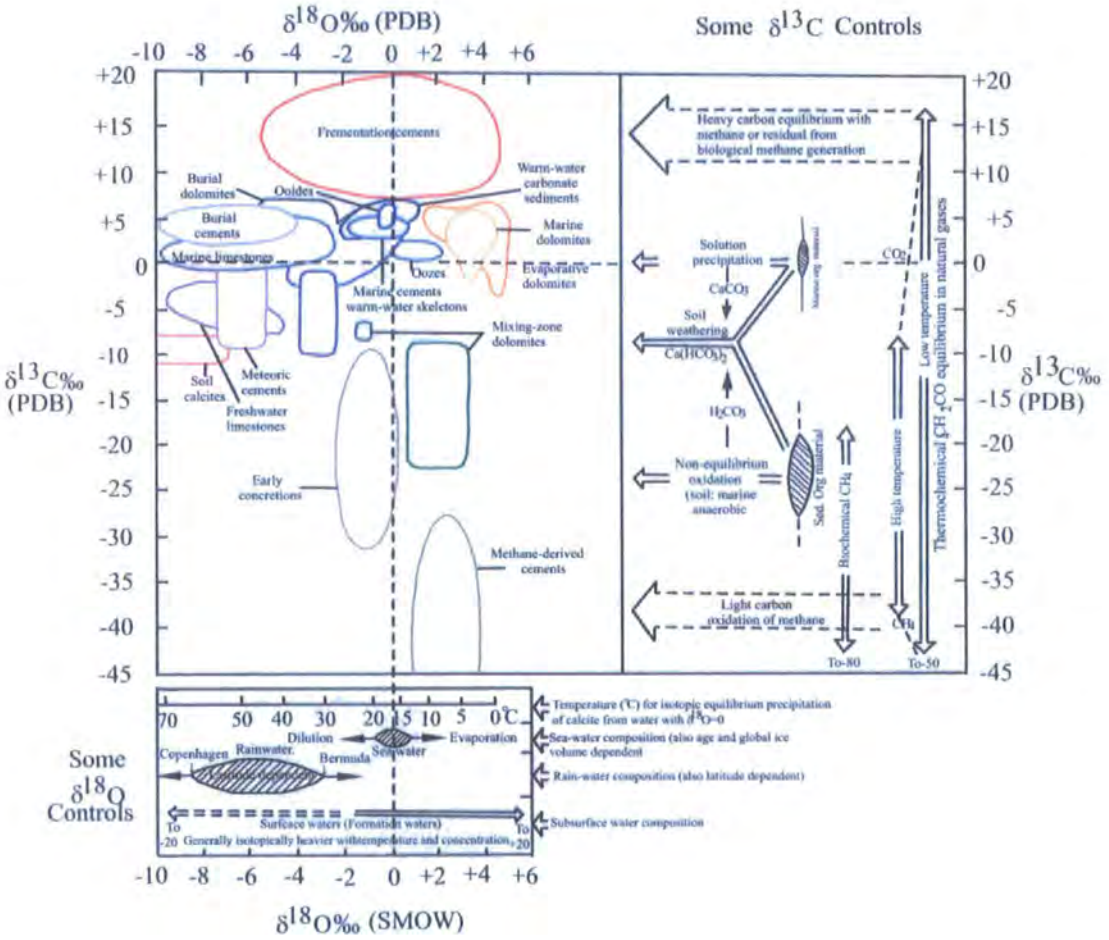

Figure 5.34. Diagram showing generalized isotope field ($\delta^{18}O$ and $\delta^{13}C$) for a selection of carbonate components, sediments, limestones, cements, dolomites and concretions and some of the factors that controls the $\delta^{18}O$ (bottom) and $\delta^{13}C$ (right) compositions of precipitated carbonates. SMOW=Standard Mean Ocean Water, the international standard used for reporting oxygen isotope variations in natural waters. Based on Hudson, 1977 and Moore, 1989) (Source, Nelson and Smith, 1996).

spectrometry (Fairchild et al. 1988). The abundance of ^{18}O and ^{13}C in sample is conventionally reported as the per mil (= mg/g or ‰) difference in delta (δ) notation ($\delta^{18}O$ and $\delta^{13}C$) between isotope ratios in the sample and those in the international Pee Dee Belemnite (PDB) standard which, by definition, has $\delta^{18}O$ and $\delta^{13}C$ values of 0‰ (Hudson, 1977). Increasingly negative, or more depleted, δ values with respect to PDB imply a relative increase in the lighter isotopes (^{18}O, ^{13}C) in the analysed samples, while more positive, or enriched, values indicate a relative increase in the heavier isotopes (^{18}O, ^{13}C). The $\delta^{18}O$ of a carbonate precipitated from water depends chiefly on the $\delta^{18}O$ composition and temperature of the water. Increasingly lighter (more negative) values tend to be associated with decreasing salinity and with increasingly higher temperatures (Hudson, 1977). The $\delta^{13}C$ composition of precipitated carbonates primary reflects the source of biocarbonate dissolved in the waters, which can include sea water ($\delta^{13}C$ near 0‰), marine shell dissolution ($\delta^{13}C$ near 0‰), soil weathering processes ($\delta^{13}C$ near -10‰), bacterial oxidation or sulphate-reduction of organic matter ($\delta^{13}C$ near -25‰), bacterial methanogenic fermentation ($\delta^{13}C$ near +15‰), oxidation of methane ($\delta^{13}C$ from -50 to -80‰), or a biotic reactions associated with thermal cracking and decarboxylation ($\delta^{13}C$ from -10 to -25‰) (Hudson, 1977; Irwin et al. 1977; Coleman, 1993 and Mozley and Burns, 1993). The $\delta^{18}O$ and $\delta^{13}C$ cross-plot was prepared by Hudson (1977), who distinguished a number of characteristic isotope field for carbonates having different origins. His diagram has been followed, adapted, and extended by many subsequent workers (Bathurst, 1981; Choquette and James, 1987; Moore, 1989; Morse and Mackenzie, 1990) (Figure 5.34).

5.5.1. RESULTS OF ISOTOPIC ANALYSES:

Isotopic analyses were performed on 10 core samples collected from three wells after petrographic study. These include 5 samples of carbonate skeletons (nummulites, discocyclina and mollusc) and 5 samples of different cements, all were extracted by drill. A summary of the isotope data for carbonate skeletons and cements is shown in Table 5.1 and Figure 5.35).

i) Carbonate skeletons:

The carbonate skeletons include nummulites and mollusc (oyster). Nummulite have negative $\delta^{18}O$ values (-3.37‰ to -4.30‰ PDB) and positive $\delta^{13}C$ values (1.17‰

to 1.60‰ PDB). Discocyclina has negative $\delta^{18}O$ value (-4.40‰ PDB) and positive $\delta^{13}C$ value (0.86‰ PDB). Mollusc fragment (oyster) has negative $\delta^{18}O$ value (-2.92‰ PDB) and positive $\delta^{13}C$ value (0.71‰ PDB). The $\delta^{13}C$ values of nummulites, discocyclina and mollusc similar to the $\delta^{13}C$ composition of Barbados marine sediments, West Indies, which are composed of skeletal reef debris, ranges from 0 to +1‰ PDB (Allan and Matthews, 1977). Nelson and Smith (1996) interpreted $\delta^{18}O$ values (0 ±2‰ PDB) and small positive $\delta^{13}C$ values (0 to +2.5‰ PDB) for bivalve shells come from fully marine formations. The $\delta^{18}O$ values from -4 to -6‰ were recorded for meteoric-derived groundwater (Lawrence and White, 1991; Hays and Grossman, 1991). The relatively depleted $\delta^{18}O$ values of fossil particles indicate that fabric component may have suffered neomorphic stabilization from freshwater dominated solutions (Shaaban, 2004).

ii) Carbonate cements:

The dominant cements in the Jdeir Formation are drusy calcite and syntaxial overgrowths around echinoderm fragments with rare coarse calcite. Stable isotopic ratios from different cement types show similar isotopic signatures, with slightly negative carbon and oxygen in coarse calcite cement. The drusy calcite cement has moderately depleted $\delta^{18}O$ values (-3.95‰ to -6.66‰ PDB) and positive $\delta^{13}C$ values (0.82‰ to 1.35‰ PDB). The overgrowth has moderately depleted $\delta^{18}O$ value (-4.48‰PDB) and positive $\delta^{13}C$ value (0.78‰ PDB). The coarse calcite has strongly depleted $\delta^{18}O$ value (-8.12‰PDB) and negative $\delta^{13}C$ value (0.25‰ PDB). The slightly depletion in oxygen suggest that these cements may have been precipitated within shallow environments under the influence of meteoric waters. A progressive increasing depletion in ^{18}O suggests that many of these cements were precipitated under conditions of increasing temperature. Increasingly $\delta^{18}O$ values (more negative) tend to be associated with decreasing salinity and with increasingly higher temperatures (Hudson, 1977).

5.6 DIAGENETIC HISTORY:

Figure 5.30 summarises paragenesis of the carbonate facies of the Jdeir Formation studied in wells A2-NC41, B7-NC41 and E1-NC41. This figure shows the diagenetic processes and their relative timing. The diagenetic sequence involved initial marine diagenesis including micritization, which has obliterated much of the

Well name	Depth	Skeleton/Cement type	$\delta^{18}O‰$ (PDB)	$\delta^{13}C‰$ (PDB)
A2-NC41	9138.0	Nummulite	-4.30	1.45
A2-NC41	9204.5	Coarse calcite	-8.12	-0.25
A2-NC41	9234.0	Mollusc (Oyster)	-2.96	0.71
A2-NC41	9262.0	Nummulite	-3.37	1.17
B7-NC41	8253.0	Drusy calcite	-6.66	1.35
B7-NC41	8429.0	Nummulite	-3.41	1.60
B7-NC41	8549.0	Syntaxial overgrowth	-4.48	0.78
B7-NC41	8570.0	Drusy calcite	-4.73	0.82
E1-NC41	8260.0	Drusy calcite	-3.95	0.96
E1-NC41	8429.0	Discocyclina	-4.40	0.86

Table 5.1. Results of oxygen and carbon isotope analyses of carbonate skeletons and cements of Jdeir Formation.

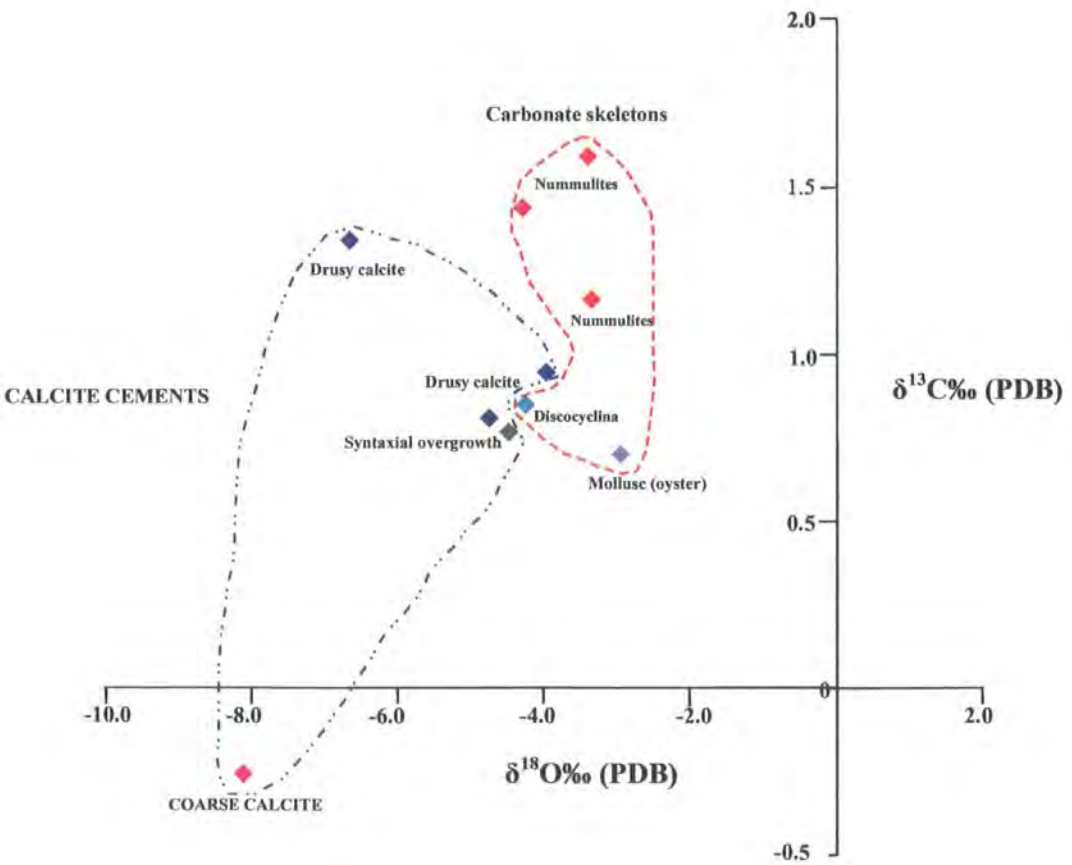

Figure 5.35. $\delta^{18}O$- $\delta^{13}C$ plots for some Jdeir Formation carbonate skeletons and cements samples.

original fabric of many skeletal grains, and the formation of micrite envelopes also occur at this time. Leaching of bioclasts and the matrix has created vuggy and mouldic porosity, which is now commonly partially or completely infilled by drusy and minor blocky calcite cements and rare kaolinite cement. Recrystallization of micrite to microspar and pseudospar is attributed to meteoric diagenesis, which has occluded some of the original porosity. The final diagenetic features include development of dissolution seams, stylolites and fractures, coarse calcite spar, dolomitization, silicification and pyrite. All these later diagenetic features are inferred to have occurred in a burial environment.

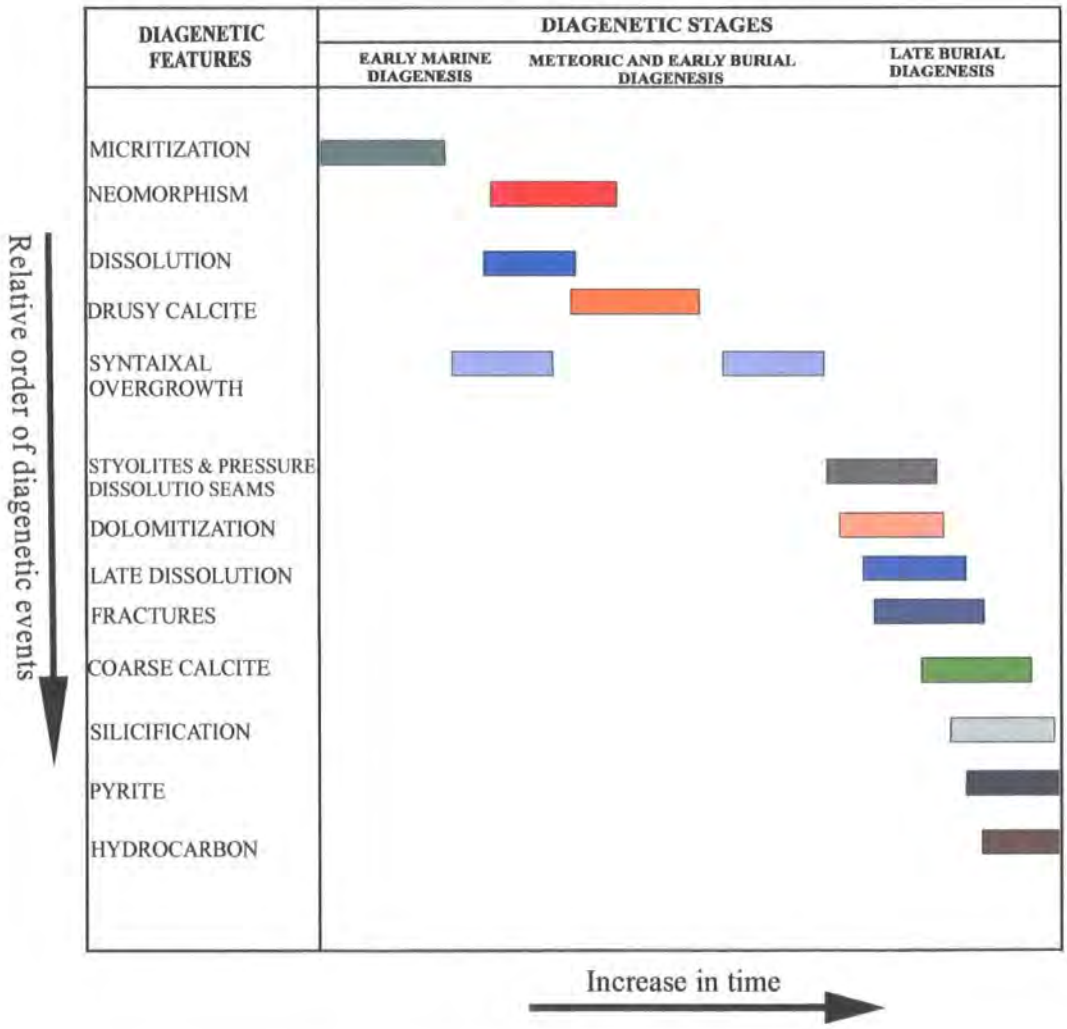

Figure 5.36 . Diagenetic History of the Jdeir Foramtion.

5.7. RESERVOIR QUAITY:

Porosity and permeability were obtained by visual estimates from thin-sections impregnated with blue resin. The common pore types in the Jdeir Formation are intergranular, mouldic, intragranular, vuggy and fractures. Porosity of the Jdeir Formation ranges from poor to very good (<1% to ~ 17%) and permeability varies from low to high. This variation in porosity and permeability is strongly related to facies variation, which was influenced by depositional environment and diagenetic processes. Good to very good porosity (17%) in the Nummulite facies is restricted to rudstone and floatstone/rudstone and decreases in the wackestone and wackestone/floatstone (<10%). Porosity in Nummulitic facies is largely of primary intragranular, intergranular and secondary vuggy types (Figures 5.24 and 5.26), and in some samples there is good connectivity between pores and moderate permeability is inferred. Mouldic porosity is also present. Cementation by drusy calcite and synatxial overgrowths has greatly reduced porosity. Coarse burial spar calcite cement is also observed filling some fracture porosity. The Nummulites occasionally have stylolitic boundaries or contacts. It is thus, concluded that compaction also reduced porosity in this facies, although permeability may have been increased. The Mollusc and echinoderm facies are characterized by poor to good porosity (<1%-12%), and included mouldic and vuggy types. Fractures are partially or completely filled by coarse calcite cement, silica cement and bitumen. The permeability of this facies is poor because the voids or pore space are isolated or not interconnected, although again permeability has been increased during burial. The *Alveolina* and peloidal-bioclastic facies are characterized by poor to fair (2%-8%) porosity and included vuggy and mouldic types. The lowest porosity values observed are in the open-marine *Discocyclina*-Nummulitic and sandy-bioclastic facies (3%-4%). Generally, cementation (syntaxial overgrowths, drusy calcite and coarse calcite spar) and compaction (Stylolite) are the main reasons for the destruction of porosity whilst extensive dissolution of Jdeir Formation during meteoric diagenesis or perhaps later burial have greatly increased or enhanced the reservoir quality (Anketell and Mriheel, 2000).

5.8. COMPARSION WITH CARBONATE NUMMULITE FROM TUNISIA:

The El Garia Formation is the time equivalent and very similar unit to the Jdeir Formation and also forms a major reservoir interval. The following explanation

of diagenetic features and their effect on reservoir equality of the El Garia Formation (Lower Eocene), offshore Tunisia is based on two references (Racey, 2001 and Moody et al., 2001). Racey, (2001) stated that primary porosity in the El Garia Formation in the *Ashtart Field* is occluded by fringing and blocky calcite cements, whilst intraskeletal porosity within nummulite tests is often preserved but is ineffective. Leaching and much later solution enhanced porosity and postdate fractures and stylolite. Porosity is generally high, ranging from 1 to 35% (average 15%), due to the large amount of ineffective intraparticle porosity present within nummulite tests. Permeability is variable and often fairly low, ranging from 0.01 to 3,400md (average 6 md). By contrast, in the *Hasdrubal field*, dolomitization is one of the main controls on reservoir quality in the El Garia Formation. Moody et al. (2001) stated that typical meteoric cements are absent in the El Garia Formation and much of the cement appears to have precipitated after compaction during a burial environment except for some early syntaxial cement around echinoderm fragments. Nummulite tests are recrystallized to microcrystalline calcite with abundant associated microporosity. Sediments in the El Garia Formation underwent extensive compaction with burial. Compaction destroyed large amounts of effective interparticle porosity. Locally, compactionally fractured nummulites connected some intraparticle pores to the remaining interparticle pore system. Where echinoderm fragments are common, syntaxial overgrowth cement is a major feature that occludes porosity. In some areas, dolomitization produced pore networks composed of intercrystalline and mouldic porosity that are quite permeable. Elsewhere baroque dolomite resulted in plugged interparticle porosity and very low to zero permeability. Most lime packstone and grainstone have moderate to high porosity ranges from 15 to 25%, but much of this porosity is ineffective and does not add to permeability. Permeability is poor to fair (less than 10 md). Moody et al. (2001) concluded that higher permeability in packstones and grainstones is favoured by low abundance of mud, high abundance of small ovate A-forms nummulites, low abundance of nummulithoclastic debris, low of abundance of echinoderm fragments, moderate sorting and minor precipitation of late burial cements and dolomitization.

5.9. SUMMARY:

Detailed petrography of 92 thin-sections, 4 samples for cathodoluminescence and 4 samples for scanning electron microscopy in wells E1, B7, and A2-NC41 reveals that the main diagenetic events which influenced in Jdeir Formation include: early marine diagenesis (micritization), meteoric and early burial diagenesis (dissolution, drusy calcite and synatxial overgrowths cements and neomorphism), and late burial diagenesis (stylolites, dolomitization, late dissolution, fractures, coarse calcite spar, silicification, pyrite and hydrocarbon migration). Cathodoluminescence (CL) analyses of four samples indicate three different types of CL zones. These zones include non-luminescent and bright-dull orange. Non-luminescence is seen in microcrystalline calcite (micrite), microsparite calcite and silica. Bright-dull orange luminescence is seen in coarse calcite and drusy calcite cements. Non-luminescent calcite is suggested to be precipitated from oxidizing pore water, whereas the variation between bright and dull cements luminescent indicates reducing pore fluid.

Isotopic analyses were performed on 10 core samples collected from three wells. The carbonate skeletons samples have negative $\delta^{18}O$ values ranging from -2.96 to -4.40‰ PDB and positive $\delta^{13}C$ values range from +0.71 to +1.60‰ PDB. Carbonate cements have negative $\delta^{18}O$ values ranging from -3.95 to -8.12 ‰ PDB and $\delta^{13}C$ values ranging from -0.25 to +1.35‰ PDB. The $\delta^{13}C$ values show marine sediments whereas the slight depletion in oxygen suggests that these cements may have been precipitated within shallow environments under the influence of fresh or meteoric waters. A progressive increase in depletion in ^{18}O suggests that many of these cements were precipitated under conditions of increasing temperature.

Variations in porosity and permeability are related to depositional environment and diagenetic processes. The observed porosity in the Jdeir Formation is commonly primary (intragranular and intergranular) or secondary, enhanced by dissolution of aragonitic bioclasts and matrix. Porosities range from zero to 17% and includes both fabric-selective and non-fabric-selective types. Fabric selective porosity is intragranular, intergranular and mouldic. Non- fabric selective porosity is vuggy and microfracture. The highest value of porosity is recorded in Nummulitic facies (bank setting), and restricted to Nummulitic rudstone (17%). This value decreases in Nummulitic wackestone and sometimes in floatstone. The lowest value is recorded in sandy-bioclastic facies (lagoonal setting) and Discocyclina-Nummulitic facies (fore-bank). Late meteoric and burial cementation and compaction are the main reason for

the reduction in porosity whilst extensive dissolution of Jdeir Formation was the reason for porosity development. By comparison, in the El Garia Formation offshore Tunisia, the porosity ranges from 1 to 35% (average 15%) and included interparticle, intraparticle, intercrystalline and mouldic types. Permeability is generally low to fair (less than 10md). The main diagenetic features which affect the El Garia Formation include syntaxial overgrowths cements, burial cementation (blocky calcite and dolomite), leaching, dolomitization and compaction.

CHAPTER SIX

6. SEQUENCE STRATIGRAPHY OF THE JDEIR FORMATION

6. SEQUENCE STRATIGRAPHY OF THE JDEIR FORMATION

6.1. INTRODUCTION:

The Jdeir Formation in the study wells is composed of eight facies that were deposited within semi-restricted lagoon, lagoon (back-bank setting), bank, fore-bank and open marine environments (see chapter 4). The sequence stratigraphic evaluation of the Jdeir Formation is based on integrating the facies data with the thirty four slabbed cores and wireline log data from three wells (A2-NC41, B7-NC41 and E1-NC41). These wells are described in detail in chapters four and five. The wireline log used in the correlation is Gamma Ray (GR). The Jdeir Formation in these wells represents shallowing and deeping-upward facies cycles. This chapter includes an introduction to sequence stratigraphy, definition of some terminology which is used in this study and a sequence stratigraphic interpretation of the Jdeir Formation. The main objective of this chapter is to assess the vertical variations in the sedimentary succession which may be controlled by relative sea-level change.

6.2. INTRODUCTION TO SEQUENCE SRATIGRAPHY:

The study of sequence straigraphy began with Sloss (1963). Brown and Fisher (1977), Mitchum (1977), and Vail et al. (1977b) used seismic data to identify genetically related packages bounded by unconformities or depositional sequences. Depositional sequences are created by changes in accommodation space, which is controlled by the rate of subsidence, rate of eustatic sea level change, and sedimentation rates (Handford and Loucks, 1993). Depositional sequences include shallowing upward and deepening upward intervals, and distinctive surfaces, such as flooding surfaces (Van Wagoner et al. (1990), Posamentier and James, (1993). Mitchum (1977), Mitchum et al. (1977), and Vail et al. (1977a, 1977b) established the basic concepts and terminology of carbonate sequence stratigraphy. Van Wagoner et al. (1988), Sarg (1988; 1992b), and Handford and Loucks (1993) summarize the concepts and terminology of sequence stratigraphy and the changes that have taken place since 1977. In a sequence stratigraphy framework, depositional sequences are predictable and can be used to help identify source, reservoir, and seal lithologies (Handford and Loucks, 1993). High-resolution stratigraphy incorporates outcrop, core, and wireline logs to construct a sequence stratigraphic framework (van Wagoner

et al. 1990). The terminology of sequence stratigraphy is complex. Mitchum (1977) defines eustatsy as a change of sea level in all the oceans, which may be caused by the ocean basin volume or a change in the volume of water in the ocean. A relative change in sea level means that the sea level is rising or falling with respect to the land on a local or regional scale (Mitchum, 1977).

The fundamental unit of a depositional sequence is the parasequence. Parasequences are small scale (1 to 10 m thick) shallowing upward cycles bounded by flooding surfaces (Heckel, 1985; Koerschner and Read, 1989; van Wagoner, 1985; Goldhammer et al., 1990; van Wagoner et al., 1990; Goldhammer et al., 1993; Handford and Loucks, 1993). Parasequence sets are a bundle of genetically related parasequences that are bounded by major flooding surfaces (van Wagoner et al., 1990). Sequence boundaries are often unconformities related to the maximum fall in sea level (van Wagoner et al., 1988; van Wagoner et al., 1990). There are two types of sequence boundaries (van Wagoner et al., 1988; van Wagoner et al., 1990). Type 1 sequence boundaries are caused by relative sea level falling faster than subsidence and their effects are often more prevalent on rimmed platforms compared with ramps. Type 2 sequence boundaries are formed when eustatic sea level fall is less than subsidence or there are minor drops of sea level that do not fall past the shelf break. These boundaries are commonly seen in ramps successions. Read (1995) summarized that unconformities can be identified by: 1) drastic changes in lithology (e.g. carbonates overlain by conglomerates, redbeds, green shale, and/or sands), 2) karstification, 3) paleosols and caliches, and 4) biostratigraphic gaps, and hardgrounds. There are several orders of cyclicity used in sequence stratigraphy (Vail et al., 1977a; Goldhammer et al., 1990). First order cycles are approximately 200 to 300 m.y. long, and are related to changes in ocean basin volume related to global tectonics (Pitman, 1978). This includes break-up of supercontinents and formation of ocean basins. Second order cycles are 10 to 50 m.y. long, and represent changes in basin evolution, such as changes in the rates of subsidence or uplift. Third order cycles are superimposed on second order cycles are approximately 0.5 to 5 m.y. long, and often result in formation-scale cycles observed in the rock record. Third order cycles are formed when changes in sea level are often less than 50 m and sedimentation rates are a few cms/k.y. Many believe that the origin of these cycles is eustatic related to ice volume (Miall, 1986; Cloetingh, 1988; Miall and Tyler, 1991;

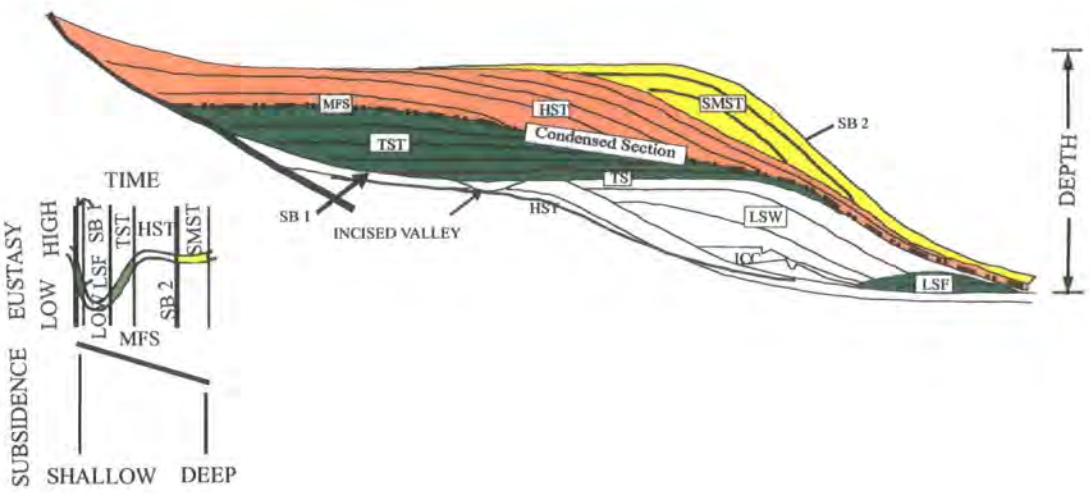

Figure 6.1. Illustration of the systems tract model (after Handford and Loucks, 1993). Abbreviations are as follows. Surface: SB1 = type 1 sequence boundary; SB2 = type 2 sequence boundary; mfs = maximum flooding surface; TS = transgressive surface. Systems tracts: HST = highstand systems tract; TST = transgressive systems tract; LSW = lowstand wedge systems tract; LSF = lowstand fan systems tract; SMST = shelf-margin systems tract; ICC = leveed channel complex.

Vail et al,. 1991). Fourth and fifth order cycles are 20 to 400 k.y. long, form parasequences, and are driven by high frequency, climatically driven changes in sea level (Heckel, 1985; Koersshner and Read, 1989; Goldhammer et al., 1990) or productivity/oxygenation (Fischer and Bottjer, 1991). Coe et al. (2002) stated that there are five orders of cycles commonly recognized in the sedimentary record: first order cycles are 50 to 200 m.y; second order cycles are 5 to 50 m.y; third order cycles are 0.2 to 5 m.y; fourth order cycles are 100 to 200 k.y and finally fifth order cycles are 10 to 100 k.y. The depositional sequence and system tracts are tools in sequence stratigraphic analysis (Fisher and Mcgowen, 1967; Brown and Fisher, 1977; Mitchum, 1977; Handford and Loucks, 1993). Systems tracts are inferred based on strata stacking patterns, position within the sequence, and types of bounding surface. Figure 6.1 illustrates the various components of the system tract model. The definition of systems tracts was gradually refined from the earlier work of Exxon scientists (Vail, 1987; Posamentier et al., 1988; Posamentier and Vail, 1988; Van Wagoner et al., 1988, 1990) based on the contributions of Galloway (1989), Hunt and Tucker

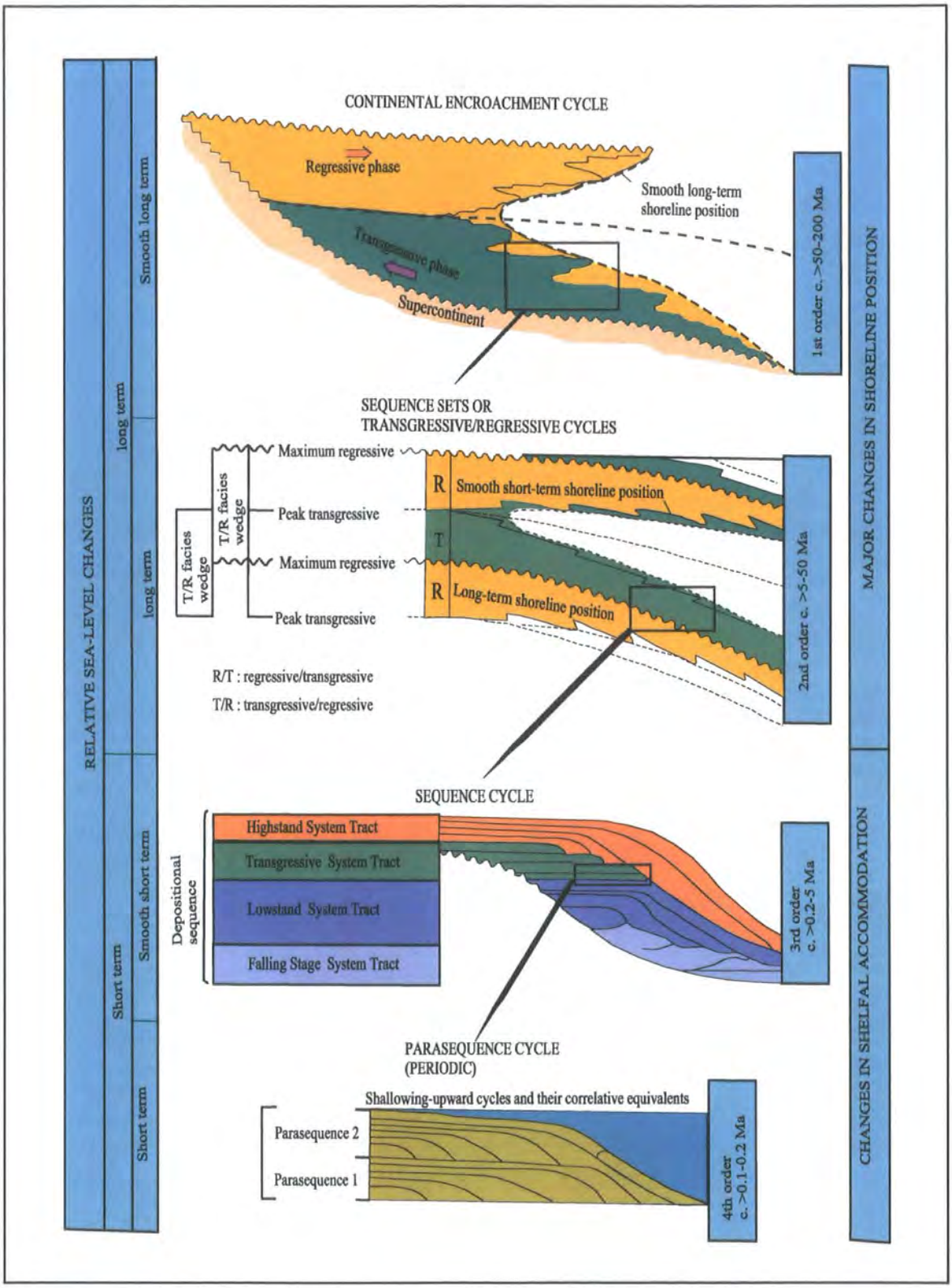

Figure 6.2. The hierarchy of stratigraphical cycles (After Coe et al., 2002).

(1995), Embry and Johannessen (1999), and Plint and Nummedal (2000). The early Exxon sequence model includes four systems tracts; the lowstand, transgressive, highstand, and shelf-margin systems tracts. These systems tracts were first defined relative to a curve of eustatic fluctuations (Posamentier et al., 1988; Posamentier and Vail, 1988), which was subsequently replaced with a curve of relative sea-level (base level) changes. The lowstand and the shelf-margin systems tracts are similar concepts, both being related to the same portion of the sea-level/base level curve, but they assume high versus low rates of sea-level/base-level fall in the shoreline area respectively. The lowstand systems tract, as defind by the Exxon school, includes a "lowstnd fan" (falling sea-level: Posamentier et al. (1988) and "lowstand wedge" (sea-level at a lowstand; Posamentier et al. (1988). The lowstand fan systems tract consists of autochthonous (shelf-perched deposits, offlapping slope wedges), and allochthonous gravity flow (slope and basin-floor fans) facies, whereas the lowstand wedge systems tract includes the aggradational fill of incised valleys, and a progradational wedge which may downlap onto the basin-floor fan (Posamentier and Vail, 1988). Hunt and Tucker (1992) redefined the lowstand fan deposits as the "forced regressive wedge systems tract". The forced regressive wedge system tract is also known as the "falling stage systems tract" (Plint and Nummedal, 2000). Four systems tracts are defined based on base level changes and sedimentation. The falling stage systems tract is the product of a forced regression. The FSST lies directly on the sequence boundary and is capped by the overlying lowstand systems tract sediments.The lowstand systems tract (LST) is deposited in the basin and slope during maximum lowstand of sea-level. Karsting, soil development, and dolomitization may all occur on exposed areas of the platform and siliciclastics may be deposited in the basin. The transgressive systems tract (TST) deposits will have a retrogradational (accommodation space greater than sedimentation rate resulting in landward stepping geometries) or progradtion (accommodation space less than sedimentation rate-stepping seaward) geometries. Cycles will be very thick and will often lack or have restricted tidal flat facies. A maximum flooding surface (MFS) documents the change from the TST to the highstand systems tract (HST). The maximum flooding surface represents the maximum landward extent of deep-water deposition. The HST is deposited during the late stage of sea-level rise, stillstand, and early sea-level fall. Accommodation space decreases due to decrease in sea-level rise and increase in

sedimentation rates. The HST has a prograding geometry that downlaps onto the MFS and parasequences are typical thin and are often dominated by peritidal facies.

6.3. SEQUENCE STRATIGRAPIC ANALYSIS OF THE JDEIR FORMATION IN THE A2-NC41, B7-NC41 AND E1-NC41 WELLS:

6.3.1. Formation-scale sequence stratigraphic analysis of the Jdeir Formation:

The Jdeir Formation is the upper unit the Farwah Group, and was deposited during the Early Eocene. Overall the Jdeir Formation is predominantly composed of shallow marine carbonates overlying the Jirani dolomites and overlain by deeper water marls. Since the underlying dolomites are associated with tidal flat deposits and formed early (Mriheel and Anketell, 1995), and the overlying deposits accumulated in deep water then the overall interpretation of the Jdeir Formation would most likely be transgressive deposits (transgressive system tract ?). However there are likely to be intra-formation smaller-scale trends most likely formed under transgressive, stillstand or regressive conditions. Lowstand sedimentation is not observed in the three wells. Bernasconi et al. (1991) stated that the uppermost nummulitic bank deposits were subjected to extensive regression compared with the intermediate and lowermost parts, due to the greater extent of the eustatic sea-level fall at the end of the Ypresian. Anketell and Mriheel, (2000) stated that dissolutional fabric was affected by the influx of meteoric waters in the upper part of the bank. This may indicate emergence of the Jdeir Formation and its exposure to subaerial processes or the influx of meteoric lenses. Reali et al. (2003) subdivided the Al Garia Formation (Jdeir FM) in southern and central parts of NC41 into transgressive system tracts and highstand system tracts. The basal part of this TST is composed of restricted lagoon facies and the upper part of HST consists of several stacked nummulitic shoals.

6.3.2. Intra-formation-scale sequence stratigraphic analysis of the Jdeir Formation:

Detailed petrographic study of three wells of the Jdeir Formation has revealed deepening and shallowing facies cycles (Figures 6.3, 6.4 and 6.5). The distribution of facies and microfacies types was analyzed for evidence of small-scale deepening and shallowing-upward deposits.

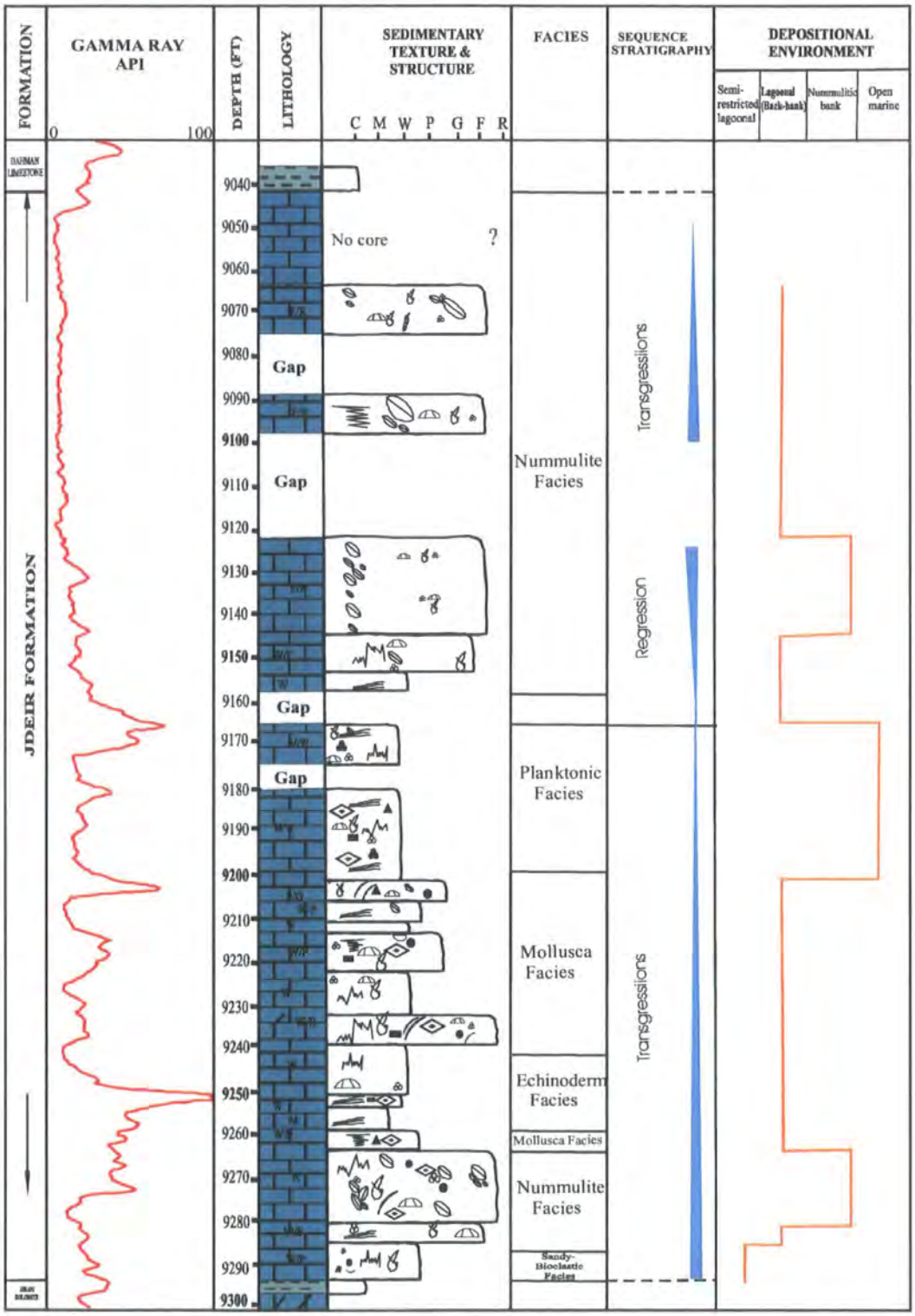

Figure 6.3. Lithological log and sequence stratigraphy of the Jdeir Formation in well A2-NC41. (see appendix for key)

A2-NC41 well: The transgressive deposits in the lower part of A2-NC41 starts with sandy-bioclastic wackestone/packstone restricted lagoon facies containing very fine to fine quartz grains, miliolids, mollusc fragments, brachiopod fragments and orbitolites. The presence of abundant miliolids suggests deposition in shallow water depth of ~ 6-10 m. This facies grades upward to nummulite bank, deposits which consist mainly of moderately sorted and large, flattened nummulites rudstone dominated by B-form. It is inferred that the water depth increased upwards on the basis of the flattened nummulites. These pass upward into wackestone/ packstone with common mollusc fragments overlain by echinoderm mudstone and wackestone/packstone, which passes up into wackestone/mudstone and packstone/grainstone with common mollusc fragments. Other grains include echinoderm fragments, nummulites fragments and minor phosphate. These grains are partially replaced by silica. The components and texture of these facies suggests deposition in lagoon environments under a range of energy conditions. These packages are interpreted as stillstand deposits. Above this package, the facies show an increase in water depth. These overlying units in the middle of the formation predominantly consists of planktonic foraminifera mudstone/wackestone containing common small echinoid fragments. Most of the bioclasts and matrix are silicified. This facies was deposited under open marine conditions and is inferred to have been deposited under deeper water conditions than the underlying mollusc rich deposits and interpreted as transgressive deposits. The upper part of the well A2-NC41 starts with wackestone and wackestone/floatstone with common small nummulites, echinoid fragments and is highly micritic. Moving upward the texture changes progressively to small and large nummulites floatstone/rudstone dominated by B and A-forms. A coarsening-upward and change in texture from wackestone to floatstone/rudstone with decrease in micrite suggest that this facies accumulated in shallower conditions than the underlying facies. These sediments were mostly deposited in a moderate to high-energy, intra or back-bank to bank environments, and are interpreted as the regressive deposits. The uppermost part of A2-NC41 is composed of whole and fragmented nummulites wackestone/ floatstone. Other bioclasts include mollusc fragments, echinoid fragments and rare miliolids. This sediment is interpreted as having been deposited in an intra or back-bank setting. The changing texture upward from floatstone/rudstone to wackestone/ floatstone and an increase in micrite upwards are indicative of lower energy. This package is interpreted as transgressive deposits.

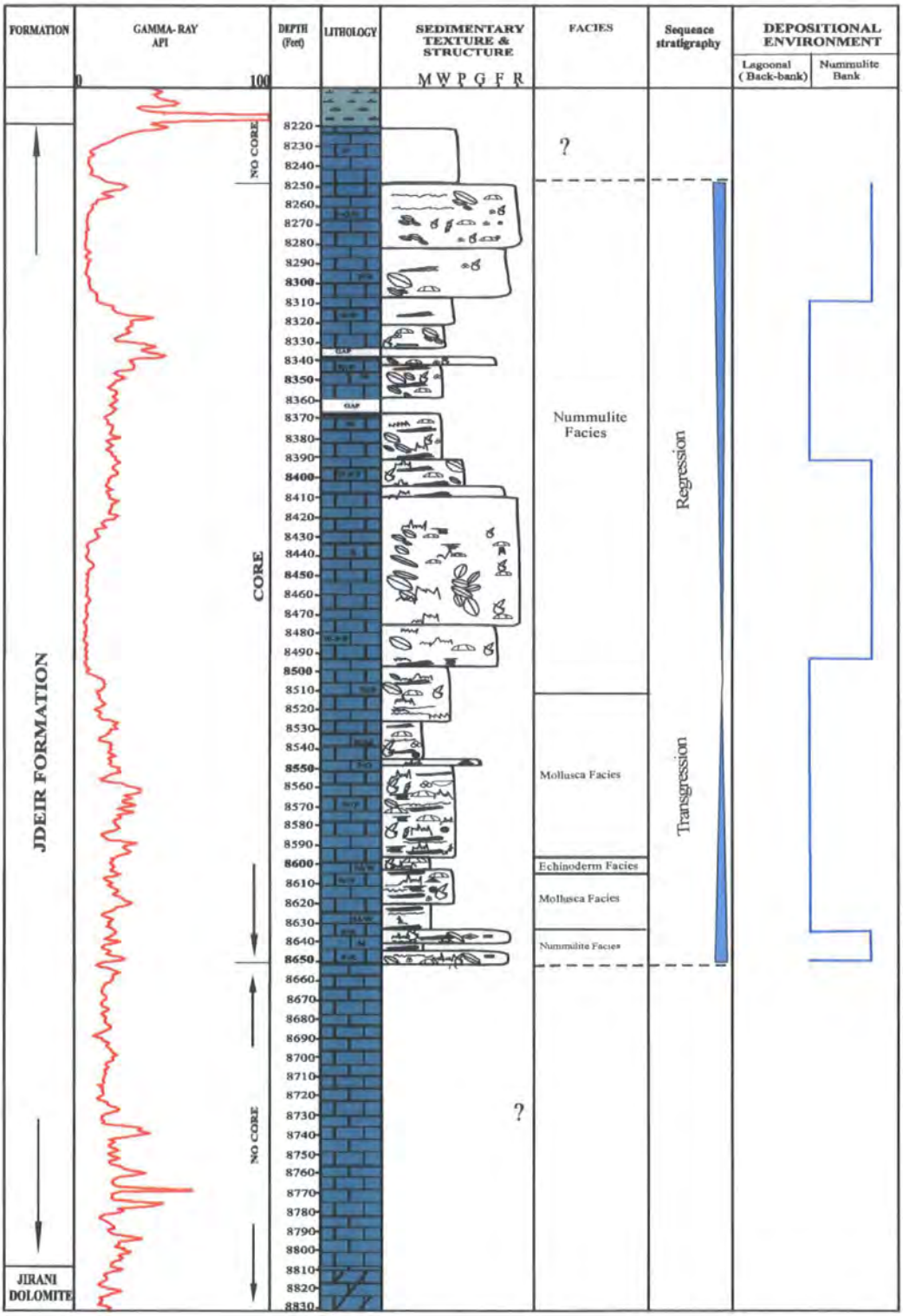

Figure 6.4. Lithological log and sequence stratigraphy of the Jdeir Formation in well B7-NC41. (See appendix for key)

B7-NC41 well: In well B7-NC41, no core data is available for the lower part of the Jdeir Formation. The middle part consists mainly of large B-form nummulites in floatstone /rudstones with minor mollusc fragments, echinoid fragments and rare miliolids. The presence of large B-form nummulite suggests deposition in moderate to deep part of the photic zone. These sediments are interpreted as forming in the lower part of a bank, which grade upward into mudstone/wackestone and wackestone/packstone with abundant mollusc and echinoid fragments overlain by nummulithoclastic debris-rich deposits grading upward into large, flat B-form nummulite rudstone. The nummulithoclastic debris is interpreted to have formed through extensive transportation and redeposition into deep areas of the Jdeir Formation These deposits were deposited in low to moderate-energy lagoonal (back-bank) and bank environments. This middle package is interpreted as transgressive deposits. The upper nummulitic facies are interpreted as regressive deposits, with shallow water facies dominated by A-B-form nummulites wackestone/floatstone grading into packstone-grainstone/rudstone. The A-form nummulites are inferred to have been deposited under shallower water condition than the large B-forms.

E1-NC41 Well: In well E1-NC41, again no core data is available in the lower part of the Jdeir Formation. The middle part is characterized by abundant *Alveolina* and peloid wackestone/packstone with common miliolids, mollusc fragments, echinoid fragments, dascycladacean algae, coralline algae, nummulites and orbitolites. The alveolina and orbitolites are interpreted as having been deposited in shallow protected back-bank environments. The presence of well preserved miliolids suggests deposition in inner shelf in water depth of 6-10 m. The occurrence of wackestone/ packstone texture suggests that these sediments were deposited in moderate energy depositional setting. This package is overlain by large, flat B-form nummulites wackestone/ floatstone grading into floatstone/rudstone with minor echinoid fragments and elongate *Discocyclina.* This facies is interpreted as lower bank setting. The uppermost unit is characterized by abundant elongate *Discocyclina* floatstone/rudstone with large B-form nummulites. This sediment is interpreted as fore-bank setting. The presence of abundant elongate *Discocyclina* suggests deposition in the deeper water part of the photic zone. This 'cycle' is interpreted as stillstand deposits in the lower part whereas coarsening and deepening upward units in the upper part of the formation are trend interpreted as transgressive deposits.

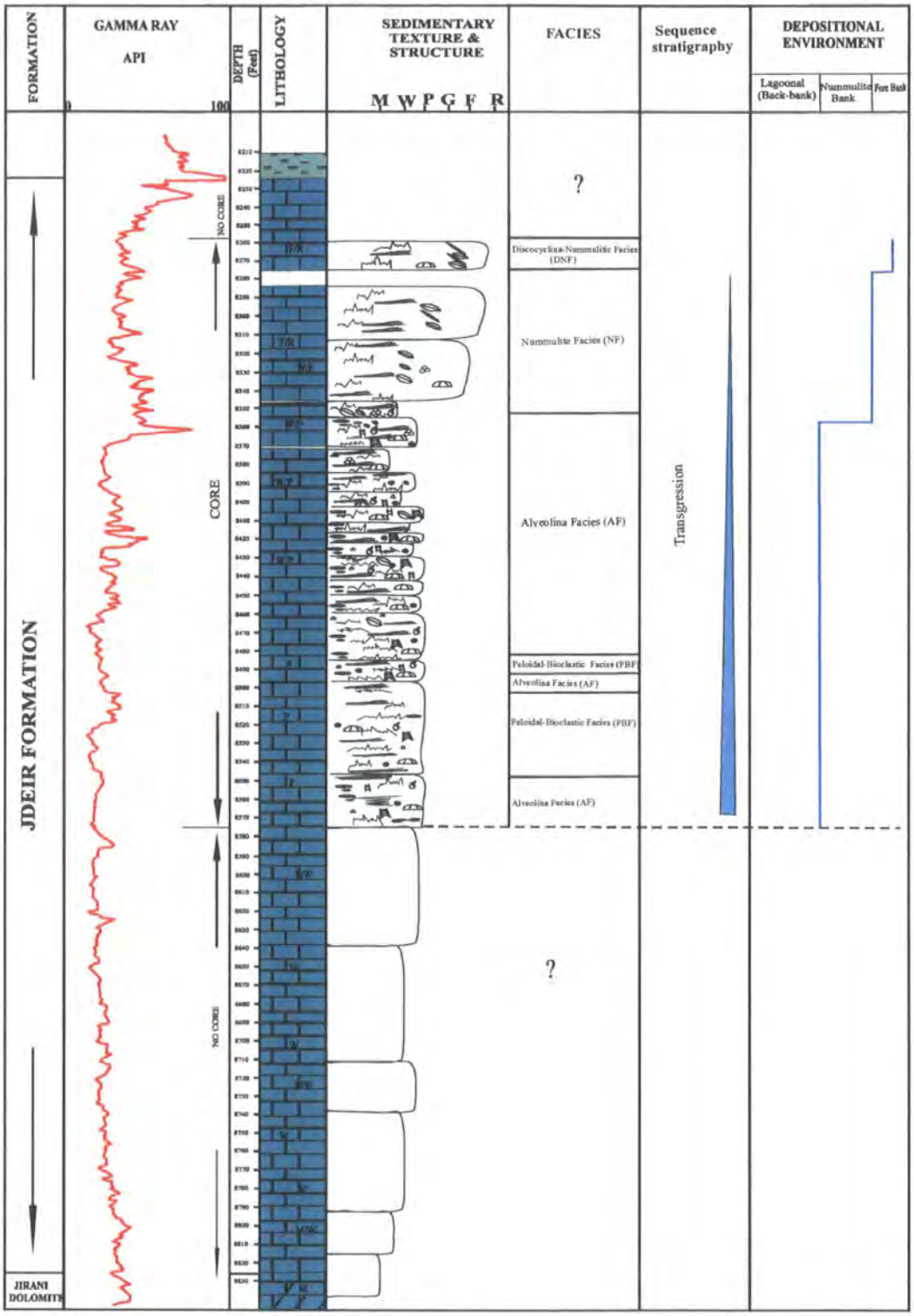

Figure 6.5. Lithological log and sequence stratigraphy of the Jdeir Formation in well E1-NC41. (see appendix for key)

6.3.3. Correlation:

Three problems were encountered in attempting to correlate between the three wells: Firstly, no core data is available in the lower part of wells E1-NC41 and B7-NC71. Secondly, there are no zone diagnostic fossils within the deposits that can be used to subdivide the wells into different correlateable time zones. Finally, there are very different facies and inferred depositional environments for the three wells. The E1-NC41 well is composed of four facies: Alveolina, peloidal-bioclastic, nummulite and discocyclina-nummulite facies. These facies are interpreted as having accumulated in lagoonal (back-bank), bank and fore-bank settings, respectively. In the B7-NC41well, three facies are recognized: mollusc, echinoderm and nummulite facies. These facies are interpreted as accumulating in lagoonal and bank settings. In comparison, four facies in A2-NC41 are recognized: sandy-bioclastic, mollusc, echinoderm, planktonic foraminifera and nummulite facies. These facies are interpreted as forming in semi-restricted lagoonal, lagoonal, open-marine and bank environments. The lagoon deposits in wells A2 and B7-NC41 are more open marine deposits than in E1-NC41. The nummulites facies in the upper part of the B7-NC41 well is characterized by the presence of A-form nummulite packstone-grainstone/rudstone which is inferred to have been deposited under shallow water conditions whereas nummulite facies in the well E1-NC41 dominated by large flat B-form floatstone/rudtsone which suggests that deposition under deep water conditions. These differences in depositional settings are the probably the result of a variable palaeogeography and palaeoenvironments setting in the Sabratah Basin and make cross-formation correlation difficult. The vertical positions and numbers of transgressive-regressive cycles in each well makes formation wide correlation problematic. In other studies, such as of the El Garia Formation authors have attempted correlation across individual nummulitic bankes (Beavington-Penny et al. 2005; Jorry et al. 2003). However, as in this study platform wide correlation was remained problematic because of the variability of facies and the shifting nature of facies belts on the nummulitic dominated platform.

6.4. SUMMARY:

The shallow-water carbonate facies of the Jdeir Formation (upper part of Farwah Group) are described from the subsurface (three wells) in northwest offshore Libya. The Jdeir Formation includes a great variety of facies and components varying

from fine to coarse grained nummulites, different bioclasts (mollusc fragments, echinoid fragments, miliolids, rotaliids, green algae, coralline algae and planktonic foraminifera), and depositional textures reflecting accumulation under of different sedimentary environments. The stacking patterns show coarsening- upward and fining-upward trends. Deepening and shallowing-upward of the vertical facies cycles often relate to decreasing and increasing water depths. In terms of relative changes in sea-level, these facies and environments might correspond to transgressive and regressive deposits. Three transgressive, stillstand and one regressive packages have been identified in A2-NC41. The basal part of this transgressive unit is composed of restricted lagoonal facies grading to coarsening-upward large, flat nummulitic facies. Nummulites are dominated by B-form which suggests deposition under deep water conditions. These facies are overlain by lagoonal facies which are interpreted as stillstand deposits. The second transgressive unit is composed of open-marine facies, dominated by planktonic foraminifera. The third transgressive unit occur in the uppermost part of the formation and is characterized by abundant nummulite fragments. The regressive deposits overlying the open-marine deposits consist of small and large nummulite bank deposits, dominated by A-B-forms, which show a shallowing upward trend.

In B7-NC41 transgressive deposits have been found in the lower to middle part of the cored interval and consist of Nummulite facies and lagoonal facies which are dominated by abundant nummulites (A-B-forms), mollusc fragment, echinoid fragments and nummulithoclastic debris. The regressive deposits are composed of packstone-grainstone/rudstone in the upper part. In contrast, in well E1-NC41, the lower lagoonal facies, which are dominated by *Alveolina*, peloids, miliolids and orbitolites, interpreted as stillstand deposits. These facies are overlain by nummulites facies and discocyclina facies which accumulated in deepening water conditions as transgressive deposits. Three problems were encountered in attempting to correlate between the three wells: Firstly, no core data is available in the lower part of wells E1-NC41 and B7-NC71. Secondly, there are no zone diagnostic fossils within the deposits that can be used to subdivide the wells into different correlateable time zones. Finally, there are very different facies and inferred depositional environments for the three wells. These differences in depositional settings are the probably the result of a variable palaeogeography and palaeoenvironments setting in the Sabratah Basin and make cross-formation correlation difficult.

CHAPTER SEVEN

7. CONCLUSION

7. CONCLUSIONS

The Lower Eocene Jdeir Formation has been studied in three wells in the NC41 concession, Sabratah Basin, Northwestern offshore Libya in the Mediterranean Sea. The core and petrographic studies provide constraints on the sedimentology, depositional environments, diagenesis and sequence stratigraphy. The conclusions of this study are outlined below:

- **Stratigrapghic and tectonic setting of the Jdeir Formation:**

  The Lower Eocene Jdeir Formation is a prolific carbonate reservoir interval and forms part of the Mesozoic-Cenozoic fill of the Sabratah Basin. The Sabratah Basin forms part of the Pelagian Block and is thought to have originated as a left-lateral pull-part basin during the Late Triassic-Early Jurassic. The oldest rocks in the area are late Triassic in age in the southern Sabratah basin. The Jdeir Formation comprises the upper part of the Farwah Group (Lower Eocene, Ypresian age) overlying the Jirani Dolomite and overlain by the Tellil Group (Middle Eocene).

- **Carbonate facies of the Jdeir Formation:**

  The Jdeir Formation is characterized by vertical and lateral facies variations. The thickness ranges from 259 feet to 600 feet thick. Based on detailed core description and petrographic analysis eight facies and twenty-four microfacies are recognized in the Jdeir Formation. These are interpreted as having been deposited in open-marine, fore-bank, lagoonal (back-bank setting) and semi-restricted lagoonal environments. Nummulitic rudstones dominated by B-forms with minor A-forms, comprise the upper part of bank depoists and floatstones/rudstones form the lower part of the bank. Abrasion and fragmentation of nummulites resulted from the extensive transport of sediments from palaeohighs and their reaccumulation into intra or back-bank environments. The discocyclina-nummulite facies is concentrated only in the uppermost part of well E1-NC41, where it accumulated in a fore-bank setting. Lagoonal deposits are highly variable and in E1-NC41 are characterized by presence of alveolina, orbitolites, miliolids, coralline algae, dasycladacean algae, peloids, mollusc and echinoderm fragments.

In contrast, lagoonal deposits from the middle and lower parts of wells B7-NC41 and A2-NC41 are characterized by abundant mollusc and echinoderm fragments.

- **Diagenetic processes and features of Jdeir Formation:**

The main diagenetic processes affecting carbonates of the Jdeir Formation occurred in early marine, meteoric and early burial and late burial diagenetic environments. Early marine diagenesis resulted in common micritization of bioclasts, whereas meteoric and early burial resulted in dissolution of aragontic bioclasts, drusy calcite cements, synatixal overgrowths around echinoderm fragments and neomorphism. Burial diagenesis resulted in coarse calcite cementation, compaction (stylolites & dissolution seams), dolomitization, silicification, and pyrite formations. Cathodoluminescence (CL) analyses indicate two types of CL zones. These zones include non-luminescent and bright-dull orange luminescence. The non-luminescence occurs in microcrystalline calcite (micrite) and microsparite calcite. Bright-dull orange luminescence present in coarse calcite, syntaxial overgrowths and drusy calcite cements. Non-luminescent calcite is suggested to be precipitated from oxidizing pore water, whereas the variation between bright and dull luminescent cements indicates reducing pore water. . The carbonate skeletons have negative $\delta^{18}O$ values ranging from -2.96 to -4.40‰ PDB and positive $\delta^{13}C$ values ranging from +0.71 to +1.60‰ PDB. Carbonate cements have negative $\delta^{18}O$ values ranging from -3.95 to -8.12 ‰ PDB and $\delta^{13}C$ values ranging from -0.25 to +1.35‰ PDB. The $\delta^{13}C$ values show marine sediments whereas the slightly depletion in oxygen suggest that theses cements may have been precipitated within shallow environments under the influence of meteoric waters. The progressive increase in depletion in $\delta^{18}O$ suggests that many of these cements were precipitated under conditions of increasing temperature.

- **Reservoir quality of Jdeir Formation:**

The depositional facies and diagenetic events affecting carbonate of the Jdeir Formation strongly influenced its reservoir quality. Mouldic, vuggy, intergranular and intragranular porosity are the main pore types observed in the Jdeir Formation. Porosity is at a maximum in the nummulitic rudstone from the bank setting (17%). This value decreases in nummulitic wackestone and sometime

floatstone. The lowest porosity is recorded in sandy-bioclastic facies planktonic foraminifera facies and discocyclina-nummulite facies (3%-4%). Late meteoric and burial cementation and compaction are the main reasons for a reduction in porosity whereas extensive dissolution of the Jdeir Formation was the reason for porosity development.

- **Sequence stratigraphy of Jdeir Formation:**

The overall interpretation of the Jdeir Formation is transgressive system tract deposits. This interpretation is on the based of shallow-marine carbonates of the Jdeir Formation overlying tidal flat deposits and associated dolomites, and being overlain by deep-marine deposits. The stacking pattern of the Jdeir Formation shows coarsening-upward and fining-upward trends, with increasing presence of coarse-grained grainstone and rudstone toward the top. Deepening and shallowing-upward of the vertical facies cycles indicate decreasing and increasing water depth during transgression and regression. The well A2-NC41 is composed of three transgressive, one stillstand and one regressive packages. The first transgressive deposits consist of restricted lagoonal facies grading to coarsening-upward large, flat nummulitic facies. Nummulites are dominated by B-form which suggests deposition under deep water conditions. These facies are overlain by lagoonal facies which are interpreted as stillstand deposits. The second transgressive unit is composed of open-marine facies, dominated by planktonic foraminifera. The third transgressive unit occurs in the uppermost part of the formation and is characterized by abundant nummulite fragments. The regressive deposits overlying the open-marine deposits consist of small and large nummulite bank deposits, dominated by A-B-forms, which show a shallowing upward trend. Transgressive deposits in B7-NC41 have been found in lower to middle part of the cored interval and consist of Nummulite facies and lagoonal facies which are dominated by abundant nummulites (A-B-forms), mollusc fragments, echinoid fragments and nummulithoclastic debris. The regressive deposits are composed of packstone-grainstone/rudstone in the upper part. The lower of lagoonal facies in well E1-NC41, which are dominated by alveolina, peloids, miliolids and orbitolites are interpreted as stillstand deposits. These facies are overlain by nummulites facies and discocyclina facies which accumulated in deepening water conditions as transgressive deposits.

- **Comparsion with similar Eocene Nummulitic deposits from Tunisia:**

The Early Eocene shallow-water carbonates in Tunisia are similar to the Jdeir Formation, in that they are commonly dominated by nummulitic facies although these are often studied in more localsed bank deposits. Lateral variation in terms of sequence thickness and facies can be related to regional variation in palaeogeographic, palaeoenvironments and structural setting. Porosity in El Garia is generally high ranging from 1 to 35% (average 15%). Intragranular porosity within nummulite tests and intercrystalline porosity are the main pore types observed in the El Garia Formation. Leaching and fracturing are partially enhanced porosity. The main diagenetic processes include dissolution, cementation, dolomitization, compaction (Stylolites), and fracturing.

REFERENCE

Adams, C. G., Lee, D. E and Rosen, B. R. (1990). Conflicting isotopic and biotic evidence for tropical sea-surface temperatures during the Tertiary. Palaeogeography, Palaeoclimatology, Palaeoecology **77,** p. 289-313.

Aigner, T. (1983) Facies and origin of nummulitic build-ups: an example from the Giza Pyramids Plateau (Middle Eocene, Egypt). Neues Jahrbuch Geol. Palaontol. **166,** p.347-368.

Al Aasm, I. S. and Veizer, J. (1986). Diagenetic stabilization of aragonite and low-Mg calcite, 1. Trace elements in rudists. J. Sediment. Petrol, **56,** p. 138-152.

Alexandersson, T. (1972) Intragranular growth of marine aragonite and Mg-calcite: Evidence of precipitation from supersaturated seawater. J. Sediment. Petrol, **42,** p. 441-460.

Alexandersson, T. (1978). Destructive diagenesis of carbonate sediments in the eastern Skagerrak, North Sea. Geology, **6,** p. 324-327.

Allan, J. R. and Matthews, R. K. (1982). Isotope signatures associated with early meteoric diagenesis. Sedimentology, v. **29,** p. 797-817

Alsharhan, A. S. and Sadd, J.. (2000) Stylolites in Lower Cretaceous carbonate reservoir, U.A.E: Middle East Model of Jurassic/Cretaceous carbonate systems.SEPM Special Publication **69,** p. 185-207.

Anderson, T. F. and Arthur, M. A. (1983). Stable isotopes of oxygen and carbon and their application to sedimentological and paleoenvironmental problems. *In*: Stable Isotopes in Sedimentary Geology. Arthur, M.A and Anderson, T.F. (Eds), SEPM short course 10: 1.1-1.151.

Anketell, J.M. (1993). Structural history of the Sirt Basin (Abstract) *In*: Sedimentary Basins of Libya, First Symposium, Geology of the Sirt Basin (ESSL), Tripoli.

Anketell, J. M. and. Mriheel, I. Y. (2000). Depositional environment and diagenesis of the Eocene Jdeir Formation, Gabes-Tripoli Basin, western offshore Libya. J. Petrol. Geol., v. **23,** p. 425-447.

Anz, J. H. and Ellouz, M. (1985). Development and operation of the El Garia reservoir, Ashtart Field, offshore Tunisia. Journal of Petroleum Technology (ETAP), Tunis, **37,** p. 481-487.

Arni, P. (1965). L'évolution des Nummulitinae en tant que facteur de modification des depots littoraux. Coloque International de Micropaléontologie (Daker), Mémoires du BRGM, **32**, p. 7-20.

Back, W., Hanshaw, B. B. and Van Driel, J.. (1984). Role of groundwater in shaping the eastern coastline of the Yucatan Peninsula, Mexico. *In*: Lafleur, R. G. (Ed), Groundwater as a Geographic Agent. p. 157-172.

Bathurst, R. G. C. (1966). Boring algae, micrite envelope and lithification of molluscan biosparite. Geological Journal, **5**, p. 15-32.

Bathurst, R. G. C. (1975). Carbonate sediments and their diagenesis. Elsevier, Amsterdam, 2nd Edition, 658p.

Bathurst, R. G. C. (1981). Early diagenesis of carbonate sediments. *In*: Parker, A and Sellwood, B. W. (Eds), Sediment diagenesis. Dordrecht, D. Reidel Publishing Company, NATO ASI series C. *Mathematical and physical sciences* 115, p. 349-377.

Beavington-Penney, S. J. (2002). Characterisation of selected Eocene Nummulites Accumulations. Ph.D. thesis. University of Wales, Cardiff.

Beavington-Penney, S. J. (2004). Analysis of the effects of abrasion on the test of *Palaeonummulites venosus*: implications for the origin of nummulithoclastic sediments. Palaios, **19**, p. 143-155.

Beavington-Penney, S. J. and Racey, A. (2004). Ecology of extant nummulitids and other larger benthonic foraminifera: applications in palaeoenvironmental analysis. Earth. Sci. Rev., **67**, p. 219-265.

Beavington-Penney, S. J., Wright, V. P. and Racey, A. (2005). Sediment production and dispersal on a foraminifera-dominated Early Tertiary ramp: the Eocene El Garia Formation, Tunisia. Sedimentology, v. **52**, p. 537-569.

Bebout, D. G. and Pendexter, C. (1975). Secondary carbonate porosity as related to Early Tertiary depositional facies, Zelten field, Libya. Am. Assoc. Pet. Geol. Bull., **59**: p. 665-693.

Ben Avraham, Z. (1978). The structure and tectonic setting of the Levant continental margin, eastern Mediterranean. Tectonophysics, **46**, p. 313-331.

Bernasconi, A., Poliani, G. and Dakshe, A. (1991). Sedimentology, petrography and diagenesis of Metlaoui Group in the offshore of Tripoli. *In*: Salem, M. J and. Belaid, M. N. (Eds), Geology of Libya, p.1907-1928.

Berner, R. A. (1970). Sedimentology pyrite formation. Am. Journ. Sci. **268**. p. 1-23.

Blondeau, A. (1972). Les Nummulites. Vuibert, Paris, 254pp.

Bowen, G. J. and Wilkinson, B. (2002) Spatial distribution of $\delta^{18}O$ in meteoric precipitation, Geology, **v. 30**, p.315-318.

Brasier, M.D. (1995). Fossil indicators of nutrient levels: 2. Evoluton and extinction in relation to oligotrophy. *In*: Bosence, D. W. J and Allison, P. A. (Eds.), Marine palaeoenvironental analysis from fossils. Geological Society of London Special Publication, v. **38**, p.133-150.

Brown, L. F. and. Fischer, W. L. (1977). Seismic-stratigraphic interpretation of depositional systems: Examples from Brazilian rift and pull-apart basin, *In*: Payton, C. E. (ed), Seismic Stratigraphy- Applications to Hydrocarbon Exploration, Am. Assoc. Pet. Geol. Bull, **26**, p. 213-248.

Caroll, D. (1958). Role of clay minerals in the transport of iron. Geochim. Cosmochim. Acta **14**, p. 1-27.

Choquette, P. W. and Pray, L. C. (1970). Geologic nomenclature and classification of porosity in sedimentary carbonates. Bull. Am. Assoc. Petrol. Geologists, **54**, p. 207-250.

Choquette, P. W. and James, N. P. (1987). Diagenesis 12. Diagenesis in limestones-3. The deep burial environment. *Geoscience Canada* **14**, p. 3-35.

Cloetingh, S. (1988). Intraplate stress: a tectonic cause for third order cycles in apparent sea level. I*n*: Wilgus, C. K., Hastings, B. S. Kendall, C. G. C., Posamentier, H. W C., Ross, A. and Van Wagoner, J. C. (Eds), Sea level Changes: An Integrated Approach. Society of Economic Paleontologic and Mineralogists Special Publication, **42**, Tulsa, OK, p. 19-30.

Coe, A., Bosence, D., Church, K., Flint, S., Howell, J. and. Wilson, C. (2002). The sedimentary record of sea-level change. The Open University, Walton Hall, 285 pp.

Coleman, M. L. (1993). Microbial processes: controls on the shape and composition of carbonate concretions. Marine geology **113**, p. 127-140.

Corfield, R. M. (1995). An introduction to the techniques, limitations and landmarks of carbonate oxygen isotope palaeothermometry. *In*: Bosence, D. V. J and Allison, P. A. (Eds), Marine palaeoenvironmental analysis from fossils. *Geological Society special publication* **83**, p. 27-42.

Craig, H. (1961) Isotopic variation in meteoric water. Science **133**, p. 1702-1703.

Cushman, J.A., Todd, R. and. Post, R. J. (1954). Recent Foraminifera of the Marshall Islands: Bikini and nearby atolls, pt. 2, Oceanography (biologic). US. Geol. Surv. Prof. Pap., 260-H: p. 319-384.

Dickson, J. A. D. (1965). A modified staining technique for carbonates in thin section. Nature, 205: 587.

Dunham, R. J. (1962). Classification of carbonate rocks according to depositional texture. *In*: Ham, W. E. (Ed), Classification of carbonate rocks. Am. Assoc. Petrol.Geologists, Tulsa, Okla, p. 108-121.

Dunham, R. J. (1971). Meniscus cements. *In*: O. P. Bricker (ed)., Carbonate cement. Am. Assoc. Petrl. Geologists. Studies in Geology, 19, John Hopkins University Press, Baltimore, p. 296-300.

Eichenseer, H. and. Luterbacher, H. (1992). The marine Paleogene of the Tremp Region (NE Spain), depositional sequence, facies history, biostratigraphy and controlling factors. Facies, **27**, p. 119-152.

Embry, A. F. and Johannessen, E. P. (1992). T-R sequence stratigraphy, facies analysis and reservoir distribution in the uppermost Triassic-Lower Jurassic succession, western Sverdrup Basin, Arctic Canada. *In*: Vorren, T. O., Bergsager, E., Dahl-Stamnes, O. A., Holter, E., Johansen, B., Lie, E and. Lund, T. B. (Eds), Arctic Geology and Petroleum Potential, v. **2.** Norwegian Petroleum Society (NPF), P. 121-146.

Fairchild, I. J. (1983). Chemical controls of cathodoluminescence of natural dolomite and calcite. Sedimentology **30**, p. 579-583.

Fairchild, I. J., Hendry, G., Quest, M and Tucker, M. (1988) Chemical analysis of sedimentary rocks. *In*: Tucker, M (Ed). Techniques in sedimentology. Oxford, Blackwell Scientific Publications. P. 274-354.

Finetti, I. (1982). Structure, stratigraphy and evolution of the Central Mediterranean. Boll. Geofis. Teor. Appl., **24**(96).

Fischer, A. G. and D. J. Bottjer, D. J. (1991). Orbital forcing and sedimentary sequences: J. Sediment. Petrol, v. **61**, p. 1063-1069.

Fischer, A. G. and. McGowen, J. H. (1967). Depositional systems in the Wilcox Group of Texas and their relationship to the occurrence of oil and gas: Gulf Coast. Association Geological Society Transcripts, v. **17**, p. 105-125.

Fletcher, T. (1985). Expansion at Ashtart: extending the life of a Mediterranean oil field. Veritas (Jan-Feb, 1985), p. 18-19.

Flugel, E. (1982). Microfacies analysis of limestones. Springer-Verlag, Berlin-Heidelburg -New York, 633p.

Flugel, E. (2004). Microfacies of carbonate rocks: Analysis, Interpretation and Application. Springer-Verlag, Berlin-Heidelburg -New York, 976p.

Fournié, D. (1975). L'analyse sequentialle et la sedimentolgie de l' Ypresien de Tunisie. Bulletin Centre Recherche, Pau-SNPA, **9**, p. 27-75.

Fournié, D. (1978). Nommenclature lithostratigraphiques des series du Crétacé supérieur au Tertiaire de Tunisie. Bull. Cent. Rech., Pau-SNPA, 2(1), 97-148.

Friedman, G. M. (1965). Terminology of crystallization textures and fabrics in sedimentary rocks. J. Sediment. Petrol, **35**, p. 643-655.

Galloway, W. E. (1989). Genetic Stratigraphic sequences in basin analysis. I. Architecture and genesis of flooding-surface bounded depositional units. Assoc. Pet. Geol. Bull., 73: p. 125-142.

Goldhammer, R. K., Dunn, P. A. and. Hardie, L. A. (1990). Depositional cycles, composite sea-level changes, cycle stacking patterns, and the hierarchy of stratigraphic forcing: Examples from Alpine Triassic carbonates: Geological Society of America Bulletin, v, **102**, p. 535-562.

Goldhammer, R. K., Harris, M. T., Dunn, P. A. and. Hardie. L. A. (1993). Chapter 14: Sequence stratigraphy and systems tract development of the Latemar Platform, Middle Triassic of the dolomites (northern Italy): Outcrop calibration keyed by cycle stacking patterns. *In*: Loucks, R. G and. Sarg, J. F. (Eds), Carbonate Sequence Stratigraphy : Recent Developments and Applications. Am. Assoc. Petrol. Geologists, Memoir **57**, p. 353-387.

Gonzalez, L.A. and. Lohmann, K. C. (1985). Carbon and oxygen isotopic composition in Holocene reefal carbonates. Geology, **13**, p. 811-814.

Gvirtzman, G. and Buchbinder, B. (1976). The desiccation events in basin around the Mediterranean during Messinian times as compared with other Miocene desiccation events in basins around the Mediterranean. Proc. 25th Congr. CIESM, Split, Yugoslavia, p. 411-420.

Hallett Don(2002). Petroleum geology of Libya. Elsevier Amsterdam, 503p.

Hallock, P (1979). Trends in test shape with depth in large, symbiont-bearing foraminifera. Journal of Foraminiferal Research **9**, p. 61-69.

Hallock, P. (1984). Distribution of larger foraminiferal assemblages on two Pacific coral reefs. Journal of Foraminiferal Research **14**, p. 250-261.

Hallock. P., Forward, L. B. and Hansen, H. J. (1986). Influence of environment on the test shape of Amphistegina. Journal of Foraminiferal Research **16**, p. 224-231.

Hallock, P. and Glenn, E. C. (1986). Larger foraminifera: a tool for paleoenvironmental analysis of Cenozoic depositional facies. Palaios **1**, p. 55-64.

Hallock, P and Hansen, H. J. (1979). Depth adaptation in Amphistegina: change in lamellar thickness. Bulletin of the Geologcal Society of Denmark **27**, p. 99-104.

Hammuda, O. S., Sbeta, A. M., Mouzughi, A. J. and Eliagoubi, B. A. (1985). Stratigraphic Nomenclature of the Northwestern Offshore of Libya. Earth Sci. Soc. Libya, 166 p.

Hammuda, O. S., van Hinte, J. E. and Nederbragt, S. (1992). Geohistory analysis mapping in central and southern Tarabulus Basin, northwestern offshore Libya. *In*: Salem, M. J., Hammuda, O. S and Eliagoubi, B. A (Eds), The Geology of Libya, p. 1657-1680.

Handford, C. R. and Loucks, R. G. (1993). Chapter 1: Carbonate depositional sequences and systems tracts-response of carbonate platforms to relative sea-level changes, *in*: Loucks, R. G and Sarg, J. F. (Eds), Carbonate Sequence Stratigraphy: Recent Developments and Applications, Am. Assoc. Petrol. Geologists, Memoir **57**, p. 3-41.

Hasler, C. A. (2004). Geometry and internal discontinuities of a Ypresian carbonate reservoir (SIT oil field, Tunisia). Terre et Environment, **45**, 230 p.

Haynes, J.R. (1965). Symbiosis wall structure and habitat in foraminifera. Special Publication-Cushman Foundation for Foraminiferal Research. **16**, p. 40-43.

Hays, P. D. and Grossman, E. L. (1991). Oxygen isotopes in meteoric calcite reduction, Smackover Formation, southeastern Mississippi salt basin. Geology, **17**, p. 441-444.

Heckel, P. H. (1985). Recent interpretations of the Late Paleozoic cyclothems: Proceedings of the Third Annual Field Conference, Mid-Content Section, Society of Economic Paleontologists and Mineralogists, p. 1-22.

Henson, F. R. S. (1950). Cretaceous and Tertiary reef formation and associated sediments in Middle East. Bull. Am. Assoc. Pet. Geol., **34**, p. 215-238.

Hmidi, Z. and Sadras, W. (1991). The Ashtart Field. Tunisia Exploration Review (ETAP), **4**, p. 1-107.

Hohenegger, J., Yordanova, E. and Hatta, A. (2000). Remarks on west Pacific Nummulitidae (Foraminifera). Journal of Foraminiferal Research **30**, p. 3-28.

Hollaus, S. S. and Hottinger, L. (1997). Temperature dependence of endosymbiotic relationships? Evidence from the depth range of Mediterranean *Amphistegina lessonii* (Foraminifera) truncated by the thermocline. Eclogae Geologicae Helvetiae **90**, p. 591-597.

Hottinger, L. and Dreher, D. (1974). Differentiation of protoplasm in Nummulitidae (Foraminifera) from Elat, Red Sea. Marine Biology. **25**, p. 41-61.

Hottinger, L. (1983). Processes determining the distribution of larger foraminifera in space and time. Utrecht Micropaleotological Bulletins **30**, p. 239-253.

Hudson, J. D. (1977). Stable isotopes and limestone lithification. Journal of the Geological Society of London 133, p. 637-660.

Hudson, J. D. and Palframan, D. F. D. (1969). The ecology and preservation of the oxford clay fauna at Woodham, Buckinghamshire. Quart. Journ. Geol. Soc. London, **124**, p. 387-418.

Hunt, D. and Tucker, M. E. (1995). Stranded parasequences and the forced regressive wedge systems tract: deposition during base-level fall. Sedimentary Geology **95**, p. 147-160.

Irwin, H.; Curtis, C. D. and Coleman, M. (1977). Isotopic evidence for the source of diagenetic carbonates in organic-rich sediments. Nature **269**, p. 209-213.

James, N. P. and Choquette, P.W. (1983). Diagenesis 6. Limestone - the sea-floor diagenetic environment. Geoscience Canada, **10**, p. 162-180.

James, N. P. and Choquette, P. W. (1984). Diagenesis 9. Limestone – the meteoric diagenetic environment. Geoscience Canada, **11**, p. 1161-194.

James, N. P. and Choquette, P. W. (1990b). Limestone – The meteoric diagenetic environment. *In*: McIlreath, A and Morrow, D. W. (Eds), Diagenesis. Geoscience Canada Reprint Series, **4**, p. 35-73.

James, N. P. and Ginsburg, R. N. (1979). The seaward margin of Belize barrier and atoll reefs. International Association of Sedimentologists, Special. Publication, **46**, p. 523-544.

Jansa, L. F. and Wade, J. A. (1975). Geology of the continental margin of Nova Scotia and Newfoundland. *In*: Offshore Geology of Eastern Canada. Geol. Surv. Can. p. 51-105.

Johnson, J. H. (1961). Limestone-building algae and algal limestone. Johnson Publishing Company, Boulder. Colo., 297 p.

Jones, R. W. (1999). Marine invertebrate (chiefly foraminifera) evidence for the palaeogeography of the Oligocene-Miocene of western Eurasia, and consequences for terrestrial vertebrate migration. *In*: Agusti, J., Andrews, P and Rook, L. (Eds.), Hominoid evolution and climatic change in Europe, v. **1**. Cambridge Univ. Press, UK, p. 274-308.

Jorry, S., Davaud, E. and Calne, B. (2003). Structurally controlled distribution of nummulite deposits: Example of the Ypresian El Garia Formation (Kersa Plateau, Central Tunisia). Journal of Petroleum Geology, **23**(6), p. 283-306.

Jorry, S. (2004). The Eocene Nummulite Carbonates (Central Tunisis and NE Libya), Sedimentology, Depositional Environments and Application to Oil Reservoir. Ph. D. thesis, Université De Genéve. Département de Géologie et de Paléontologie.

Keen, C. E. (1979). Thermal history and subsurface of rifted continental margins. Evidence from wells on the Nova Scotia and Labrador shelves. Can. J. Earth Sci., **16**, p. 505-622.

Keen, C. E. and Barrett, D. L. (1981). Thinned and subsided continental crust on the rifted margin of eastern Canada: Crustal structure, thermal evolution and subsidence history. Geophys. J.R. Astron. Soc, **65**, p. 443-465.

Kobluk, D. R. and Risk, M. J. (1977). Micritization and carbonate grain binding by endolithic algae. Bull. Am. Assoc. Pet. Geol., **61**, p. 1069-1082.

Koerschner, W. F. and Read, J. F. (1989). Field and modeling studies of Cambrian carbonate cycles, Virginia Applications: Journal of Sedimentary Petrology, v. **59**, p. 654-687.

Kulka, A. (1985). Sedimentological model in the Tatra Eocene. Kwartalnik Geologiczny, **29** (1), p. 31-64.

Langer, M. R. and Hottinger, L. (2000). Biogeography of selected larger foraminifera. Micropaleontology **26**, p. 215-126.

Lawrence, J. R. and White, J. W. (1991). The elusive climate signal in the isotopic composition of precipitation. *In*: Taylor, H. P and O'Neil, J. R (Eds), Geochemical Society special publication, **3**, p. 169-185.

Lohmann, K. C. (1988). Geochemical patterns of meteoric diagenetic systems and their application to studies of paleokarst. *In*: Paleokarst, James, N.P and Choquette, P.W (Eds), Springler-Verlag, New York, p. 58-80.

Longman, M. W. (1980). Carbonate diagenetic textures from nearshore diagenetic environments. Bull. Am. Assoc. Pet. Geol., **64**, p. 461-487.

Loucks, R. G., Moody, R. T. J., Bells, J. K. and Brown, A. A. (1998). Regional depositional setting and pore network systems of the El Garia Formation (Metlaoui Group, Lower Eocene), offshore Tunisia. *In*: MacGregor, D. S.., Moody, R. T. J and Clark-Lowes, D. D (Eds.), Petroleum Geology of North Africa. Geol. Soc., London, Special Publication **132**, p. 355-374.

Machel, H. G. and Burton, E. A. (1991). Factors governing cathodoluminescence in calcite and dolomite. *In*: Barker, C. E and Kopp, D. C (Eds), Luminescence Microscopy: Quantitative aspects. Soc. Econ. Palaeot. Miner, Short Course **25**, p. 37-57.

Machel, H. G., Krouse, H. R. and Sassen, R. (1995). Products and distinguishing criteria of bacterial and thermochemical sulfate reduction. Applied Geochemistry, **10**, p. 373-389.

Machel, H. G. (2004). Concepts and models of dolomitization: a critical reappraised. *In*: Rizzi, G., Braithwaite, C. J. R and Darke. G (Eds), The Geometry and Petrogenesis of Dolomite Hydrocarbon Reservoir. Geol. Soc., London, Special Publication **235**, P. 7-63

MacIntyre, I. G., Prufert-Bebout, L. and Reid, R. P. (2000). The role of endolithic cyanobacteria in the formation of lithified laminae in Bahamian stromatolites. Sedimentology, **47**, p. 915-921.

Marshall, J. D. 1992). Climatic and oceanographic isotopic signals from the carbonate rock record and their preservation. Geological Magazine 129, p. 143-160.

McCrossan, R.G. (1988). Geology of western offshore Libya-an introduction. In: Geology of western offshore Libya (Eds. By McCrossan, R.G and Booth, J.E). Internal report, Sirt Oil Company, prepared for the N.O.C., Libya, **1**, p. 13-18.

McIlreath, I. A. and. Morrow, D. W. (1990) Diagenesis. Geosci. Can.Rep. Ser. **4.**

Mengoli, S. and Spinicci, G. (1984). Tectonic evolution of north Africa (from Algeria to Sinai), Agip N.A.M.E., Tripoli, Internal report.

Meyers, W. J. (1978). Carbonate cements: their regional distribution and interpretation in Mississpian limestones of southwestern New Mexico. Sedimentology **25**, p. 371-400.

Meyers, W. J. (1991). Calcite cement stratigraphy: an overview. *In*: Barker, C. E. and Kopp, D. C. (Eds), Luminescence Microscopy: Quantitative and qualitative aspects. Soc. Econ. Palaeont. Miner., Short Course **25**, p. 133-148.

Miall, A. D. (1986). Eustatic sea-level changes interpreted from seismic stratigraphy: A critique of the methodology with particular reference to the North Sea Jurassic record: Am. Assoc. Pet. Geol. Bull, v. **70**, p. 131-137.

Miall, A. D. and Tyler, N. (1991). The Three-dimentional facies architecture of terrigenous clastic sediments and its implications for hydrocarbon discovery and recovery: Society of Economic Paleontologists and Mineralogists Concepts in Sedimentology and paleontology, v. **3**, 309 p.

Miller, J. (1988). Cathodoluminescence microscopy. *In*: Tucker, M. E (Ed), Techniques in Sedimentology. Blackwell, Oxford, 394p.

Milliman, J. D. (1974). Marine carbonates. Springer-Verlag, Berlin, 375pp.

Mitchum, J. R. M. (1977). Seismic stratigraphy and global changes of sea-level, Part 11: Glossary of terms used in seismic stratigraphy. *In*: Payton, C. E (Ed), Seismic Stratigraphy: Applications to Hydrocarbon Exploration: Am. Assoc. Petrol. Geologists, Memoir **26,** Tulsa, p. 205-212.

Mitchum, J. R. M., Vail, P. R. and Thompson, S, III. (1977). Seismic stratigraphy and global changes of sea-level; Pt.2, The depositional sequence as a basic unit for stratigraphic analysis. I*n*: Payton, C. E. (Ed)., Seismic Stratigraphy: Applications to Hydrocarbon Exploration: Am. Assoc. Petrol. Geologists, Memoir **26,** p. 53-62.

Montadert, L., De Chappal, D., Roberts, D. G., Guennoc, P. and Sibuet, J. (1979). Northeast Atlantic passive continental margins: Rifting and subsidence processes. *In*: Deep drilling results in the Atlantic Ocean: Continental margins and

paleoenvironments (Eds. Talwani, M., Hey, W and Ryan, W.B.F). Am. Geophys. Union, Maurice Ewing Ser, **3**, p. 154-186.

Moody, R.T. J. (1987). The Ypresian carbonates of Tunisia- a model of foraminiferal facies distribution. In: Micropalaeontology of carbonate environments. (Ed. Hart, M.B), B.M.S. Series, Ellis Horwood, Chichester, p. 82-92.

Moody, R.T. J., Loucks, R. G., Brown, A. A. and Sandman, R. I. (2001). Nummulite deposits of the Pelagian area- depositional models and diagenesis. Abstract. North Africa Research Workshop.

Moore, C. H. (1989). Carbonate diagenesis and porosity. Elsevier, 338pp.

Morse, J. and Mackenzie, F. T. (1990). Geochemistry of sedimentary carbonates. Elsevier, New York, 707pp.

Mozley, P. S. and Burns. S. J. (1993) Oxygen and carbon isotopic composition of marine carbonate concretions: an overview. Journal of sedimentry petrology **63**, p. 73-83.

Mriheel, I, Y. (1991). Diagenetic history of Early-Middle Eocene Jdeir Formation, Farwah Group, northwestern Libya offshore. Petroleum Research Journal **3**, Tripoli, p. 44-52.

Mriheel, I. Y. and Anketell, J. M. (1995). Origin of the Mid-Ypresian Jirani Dolomite-a major reservoir rock in the NW Libya offshore. Journ. Petrol. Geol., v.**18**, p. 439-452.

Mriheel, I.Y., Abugares, M. M. and Alhnaish. A. S. (1993). Depositional environment, diagenesis and reservoir quality of El Garia Formation (Jdeir Fm) at well B3-09-NC41, western Libya offshore. Technical report prepared for Agip Oil Company. (Unpublished).

Multer, H. G. (1977) Field Guide to some carbonate rock environments, Florida keys and western Bahamas, 415pp

Murray, J.W. (1987). Benthonic foraminifera assemblages: criteria for the distinction of temperate and subtropical carbonate environments. *In*: Hart, H. B (Ed), Micropalaeontology of carbonate environments. Ellis Horwood, UK, p. 9-20.

Murray, J.W. (1991). Ecology and distribution of benthonic foraminifera. *In*: Lee, J. J., Anderson, R. O. (Ed), Biology of Foraminifera. Academic Press, London, p. 221-284.

Nelson, C. S. and Smith, A. M. (1996). Stable oxygen and carbon isotope compositional fields for skeletal and diagenetic components in New Zealand

Cenozoic nontropical carbonate sediments and limestones: a synthesis and review. New Zealand Journal of Geology and Geophysics, v. **39**, p. 93-107.

Nemkov, G. I. (1962). Remarks on the palaeoecology of Nummulites. Micropaleontology **6**, p. 64-72.

Newell, N. D., Rigby, J. K., Fischer, A. G., Whiteman, A. J., Hickox, J. E. and Bradley, J. S. (1953). The Permian reef complex of the Guadalupe Mountains Region, Texas and New Mexico. A study in paleoecology. Freeman, W.H, San Franscisco, Calif., 236p.

Perkins, R. D. and Halsey, S. D. (1971). Geologic significance of microboring fungi and algae in Carolina shelf sediments. Journal of Sedimentary Petrology, **41**, p. 843-853.

Pitman, W.C. (1978). Relationship between eustasy and stratigraphic sequences on passive margins: Geology Society of America Bulletin, v. **89,** p. 1389-1403.

Pitman, W.C. and Talwani, M. (1972). Seafloor spreading in the north Atlantic. Bull. Geol. Soc. Am., 83, p.619-646.

Plint, A. G. and Nummedal, D. (2000). The falling stage systems tract: recognition and importance in sequence stratigraphic analysis: *In*: Hunt, D and Gawthorpe, R. L. (Eds), Sedimentary Response to Forced Regression, v. **172**. Geol. Soc. London Spec. Publ, p. 1-17.

Pomeral, C. (1981). Stratotypes of Paleogene stages. International Union of Geological Science, Commission on stratigraphy, Memoir 2. Bulletin d'Information des Géol. Du Bassin du Paris.

Posamentier, H. W. and James, D. P. (1993). An overview of sequence straigraphic concepts: Uses and abuses. I*n*: Posamentier, H. W., Summerhayes, C. P. (Eds), Sequence Stratigraphy and Facies Associations, Oxford, Blackwell, p. 3-18.

Posamentier, H. W. and Vail, P. R. (1988). Eustatic controls on clastic deposition. II. Sequence and systems tract models. *In*: Wilgus, C. K., Hasting, B. S., Kendall, C.G. St. C., Posamentier, H.W., Ross, C. A and Van Wagoner, J. C. (Eds), Sea Level Changes-An Integrated Approach, v. **42**. SEPM Special Publication, p. 125-154.

Posamentier, H. W., Jervey, M.T. and Vail, P.R. (1988). Eustatic controls on clastic deposition. I. Conceptual framework. *In*: Wilgus, C. K., Hasting, B. S., Kendall, C.G. St. C., Posamentier, H.W., Ross, C. A and Van Wagoner, J. C

(Eds), Sea Level Changes-An Integrated Approach, v. **42**. SEPM Special Publication, p. 110-124.

Racey, A. (1995). Palaeoenvironment significance of larger foraminiferal biofabrics from the Middle Eocene Seeb Limestone Formation of Oman: Implication for petroleum exploration. *In*: Al-Husseini, M. I. (Ed)., GEO'94 The Middle East Petroleum Geosciences, Volume II selected Middle papers from the Middle East geoscience conference, published by Gulf-Petrolink,Bahrain, p.793-810.

Racey, A. (2001). A review of Eocene Nummulite Accumulations: Structure, formation and reservoir potential. Journ. Petrol. Geol. v. **24(1)**, p. 79-100.

Read, J. F. (1995) Overview of carbonate platform sequences, cycle stratigraphy and reservoirs in greenhouse and icehouse worlds. I*n*: Read, J. F., Kerans, C. K and Weber, L. J. (Eds)., Milankovitch Sea-Level Changes, Cycles and Reservoirs on Carbonate Platforms in Greenhouse and Ice-house Worlds, SEPM Short Course Notes No. 35, Part 1, p. 1-102.

Reali, S., Ponchi, P. and Borromeo, O. (2003). Sedimentological model of the El Garia Formation (Jdeir Formation), NC41, offshore Libya. *In*: the Geology of Northwest Libya, v. **II**, p. 69-97.

Reid, R. P. and MacIntyre, I. G. (2000). Microboring versus recrystallization: Further insight into the micritization process. Journal of Sedimentary Research, **70**, p. 24-28.

Reiss, Z. and Hottinger, L. (1984). The Gulf of Aqaba. Ecological Micropaleontology. Springer-Verlag, New York.

Ross, C. A. (1972). Biology and ecology of Marginopora vertebralis (Foraminifera), Great Barrier Reef. Journal of Protozoology, **19**, p. 181-192.

Röttger, R. (1972). Die Kultur von Heterostegina depressa (Foraminifera: Nummulitidae). Marine Biology **15**, p. 150-159 (in German with English abstract).

Sarg, J. F. (1988). Carbonate sequence stratigraphy. I*n*: Wilgus, C. K., Hastings, B. S., Kendall, C. G. C., Posamentier, H. W., Ross, C. A and van Wagoner, J. C. (Eds), Sea-Level Changes- An integrated Approach, SEPM Special Publication **42**, p. 155-181.

Sbeta, A. M. (1984). Sedimentology of the Eocene sequence of the offshore northwest Libya, section I and section II. Unpbl. Rept. N.O.C. Libya.

Sbeta, A. M. (1990). Stratigraphy and lithofacies of Farwah Group and it equivalent: Offshore-NW Libya. Petrol. Res. J, **2**, p. 42-56.

Sbeta, A. M. (1991). Petrography and Facies of the Middle and Upper Eocene rocks (Tellil Group), offshore western Libya. The Geology of Libya, p.1929-1965.

Shaaban. M. N. (2004). Diagenesis of the lower Eocene Thebes Formation, Gebel Rewagen area, Eastern Desert, Egypt. Sedimentary Geology, v. **165**, p. 53-65.

Sloss, L. L. (1963). Sequences in the Cratonic Interior of the North America: Geological Society of America Bulletin, v. **74**, p. 93-114.

Trevisani, E. and Papazzoni, C. A. (1996) Paleoenvironmental control on the morphology of *Nummulites fabianii* in the Late Priabonian parasequences of the Mortisa Sandstone (Venetian Alps, northern Italy). Rivista Italiana Paleontologia Stratigrafia **102**, P. 263-366.

Tucker, M. E. (1981) Sedimentary petrology: an introduction to the origin of sedimentary rocks. Blackwell Science Publications, Oxford, 252p.

Tucker, M. E. (1991) Sedimentary petrology: an introduction to the origin of sedimentary rocks. Blackwell Science Publications, Oxford, 260p.

Tucker, M. E. (1993). Carbonate diagenesis and sequence stratigraphy. *In*: Sedimentology Review / 1, V.P. Wright, (Ed). Blackwell Science Publications, Oxford. p. 51-72.

Tucker, M. E. (2001). Sedimentary Petrology. *Third Edition.* Blackwell Science Publications, Oxford

Tucker. M. E. and Bathurst, R. G. C. (1990). Carbonate diagenesis. Reprint Series, Int. Ass. Sedimentologists, **1**, 312p.

Tucker. M. E. and Wright, V. P. (1990). Carbonate Sedimentology. Blackwell Scientific Publication, Oxford.

Vail, P. R. (1987). Seismic stratigraphy interpretation procedure. In: Bally, A. W (Ed), Atlas of Seismic Stratigraphy, v. **27.** Am. Assoc. Pet. Geol. Studies in Geology, p. 1-10.

Vail, P. R., Audemard, F., Bowman, S. A, Eisner, P. N. and Perez-Cruz, C. (1991). The stratigraphic signatures of tectonics, eustasy and sedimentology: An overview, *in*: Einsele, G., Ricken, W and Seilacher, A. (Eds), Cycles and Events in Stratigraphy, New York, Springer-Verlag, p. 617-659.

Vail, P. R., Mitchum, R. M. and Thompson, S. I. (1977a). Seismic stratigraphy and global changes of sea-level, part 3: Relative changes of sea-level from coastal

onlap. In: Payton, C. E. (Ed), Seismic Stratigraphic Application to Hydrocarbon Exploration, Am. Assoc. Petrol. Geologists, Memoir **26,** p. 63-82.

Vail, P. R., Mitchum, R. M., Todd, R.G., Widmeri, J. W., Thomson, S., Sangree, J. B., Bubb, J. N. and Hatelied, W. G. (1977b). Seismic stratigraphy and global changes of sea-level. *In*: Payton, C. E. (Ed)., Seismic Stratigraphy: Applications to Hydrocarbon Exploration, Am. Assoc. Petrol. Geologists, Memoir **26,** p. 49-212.

Van Gorsel, J. T. (1988) Biostratigraphy in Indonesia: Methods, pitfalls and new directions. Proceedings of the Indonesia Petroleum Association, 17th Ann. Convention, October, p. 275-300.

Van Wagoner, J. C., Posamentier, H. W., Campion, R. M. and Rahmanian, V. D. (1990). Siliciclastic sequence stratigraphy in well logs, cores and outcrops: Am. Assoc. Petrol. Geologists Methods in Exploration Series 7: Tulsa, 55p.

Van Wagoner, J. C., Posamentier, H. W., Mitchum, R. M., Vail, P. R., Sarg, J. F., Loutit, T. S. and Hardenbol, J.. (1988). An overview of sequence stratigraphy and key definitions, *In*: Wilgus, C. K., Hastings, B. S., Kendall, C. G. St. C., Posamentier, H. W., Ross, C. A and Van Wagoner, J. C. (Eds), Sea-Level Change: An Integrated Approach, SEPM Special Publication **42,** p. 39-45.

Van Wagoner, J. C, Mitchum, J. R. M., Campion, K. M. and Rahmanian, V. D. (1990) Siliciclastic sequence stratigraphy in well logs, core, and outcrops: concepts for high-resolution correlation of time and facies. Am. Assoc. Pet. Geol. Methods in Exploration Series 7, 55p.

Walker, K. R., Jernigan, D. G. and Weber, L. J. (1990). Petrographic criteria for the recognition of marine, syntaxial overgrowths and their distribution in geologic time. Carbonates and Evaporities, **5**: p. 141-152.

Wentworth, C. K. (1922). A scale of grade and class terms for clastic sediments. J.Geol, **30**: p. 377-392.

Wilson, J. L. (1975). Carbonate Facies in Geologic history. Springer-Verlag, Berlin, 471 p.

Wilson, M. E. J. (1995). The Tonasa limestone Formation, Sulawesi, Indonesia: Development of a Tertiary carbonate platform. Ph.D. thesis, London University, 520p.

Wilson, M. E. J. (2002). Cenozoic carbonates in SE Asia: implication for equatorial carbonate development. Sedimentary Geology, **147**, p. 295-428.

Wilson, M. E. J and Evans, M. J. (2002). Sedimentology and diagenesis of Tertiary carbonates on the Mangkalihat Peninsula, Borneo: implications for subsurface reservoir quality. Marine and Petroleum Geology, **19**, p. 873-900.

APPENDIX: TERMINOLGY

LEGEND

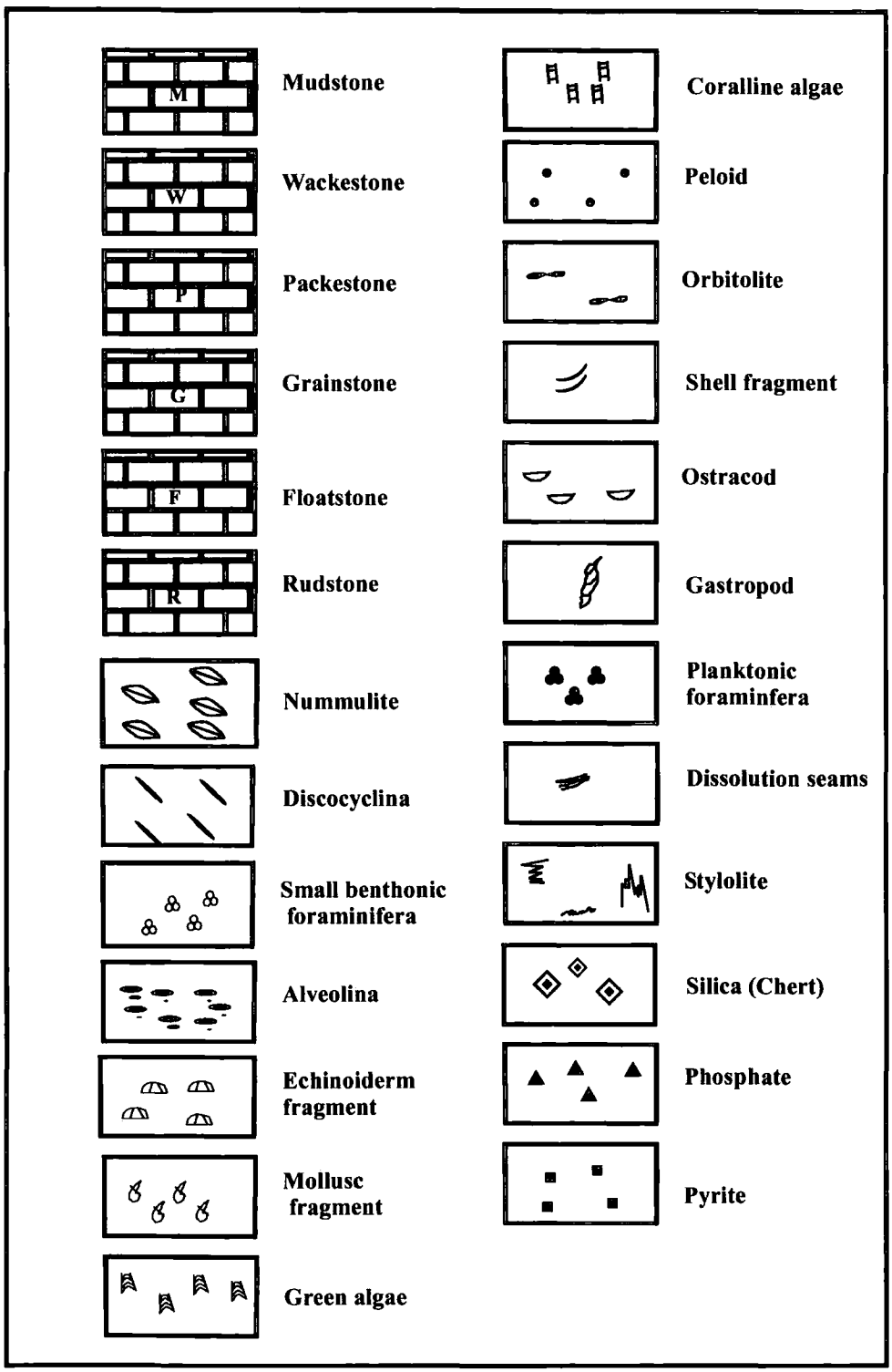

Carbonate Classification:

Dunham's classification and its modification by Embry and Klovan (1971) and James (1984) (Figures below) deal with depositional texture. For this reason, his scheme may be better suited for rock descriptions that employ a hand lens or binocular microscope. For example, if the grains of a limestone are touching one another and the sediment contains no mud, then the sediment is called a grainstone. If the carbonate is grain supported but contains a small percentage of mud, then it is known as a packstone. If the sediment is mud supported but contains more than 10 percent grains, then it is known as a wackestone, and if it contains less than 10 percent grains and is mud supported, it s known as a mudstone. Embry and Klovan (1971) and James (1984) have modified Dunham's classification to include coarse grained carbonates. In their revised scheme, a wackestone in which the grains are greater than 2mm in size is termed a floatstone and a coarse grainstone is a rudstone. Both terms are extremely useful in the description of limestones. Embry and Klovan introduced terms to more graphically reflect the role that the organisms performed during deposition by modifing the boundstone classification of Dunham to bafflestone, bindstone, and framestone.

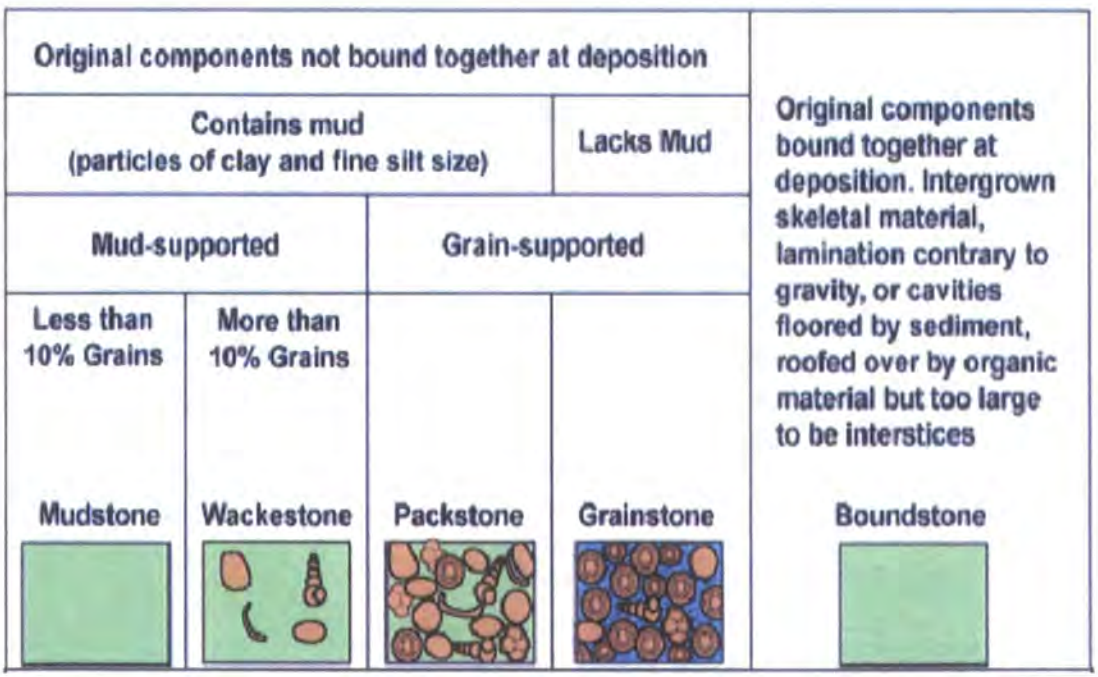

Carbonate classification (modified from Dunham, 1962)

Allochthonous		Autochthonous		
Original components not bound organically at deposition		Original components bound organically at deposition		
>10%grains>2mm				
Matrix supported	Supported by >2mm component	By organisms that act as baffles	By organisms that encrust and bind	By organisms that build a rigid framework
Floatstone	Rudstone	Bafflestone	Bindstone	Framestone

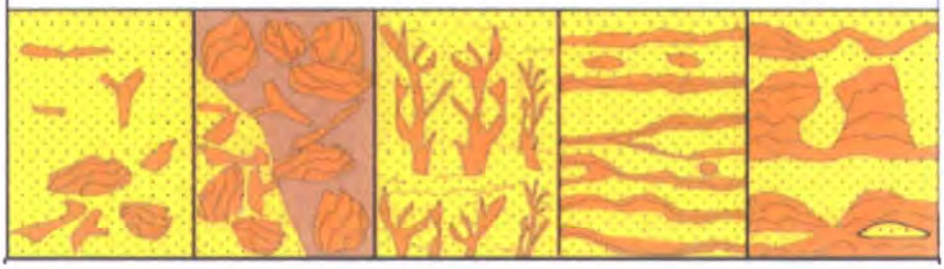

Texture classification of reef limestone (after Embery & Klovan, 1971 and James, 1984).

POROSITY:

Because of the broad-spectrum of diagenesis that affects carbonate rocks, the final porosity in carbonates may or may not be related to depositional environments. Unlike other lithologies, the original primary porosity in carbonate may be totally destroyed during diagenesis and signification new secondary porosity may be created. The types of porosities encountered are quite varied (Figure below). Interparticle, intraparticle, growth-framework, shelter and fenestral porosities are depositional porosities. Porosity formed during diagenesis may be moldic, channel, inter-crystalline, fracture or vuggy porosity.

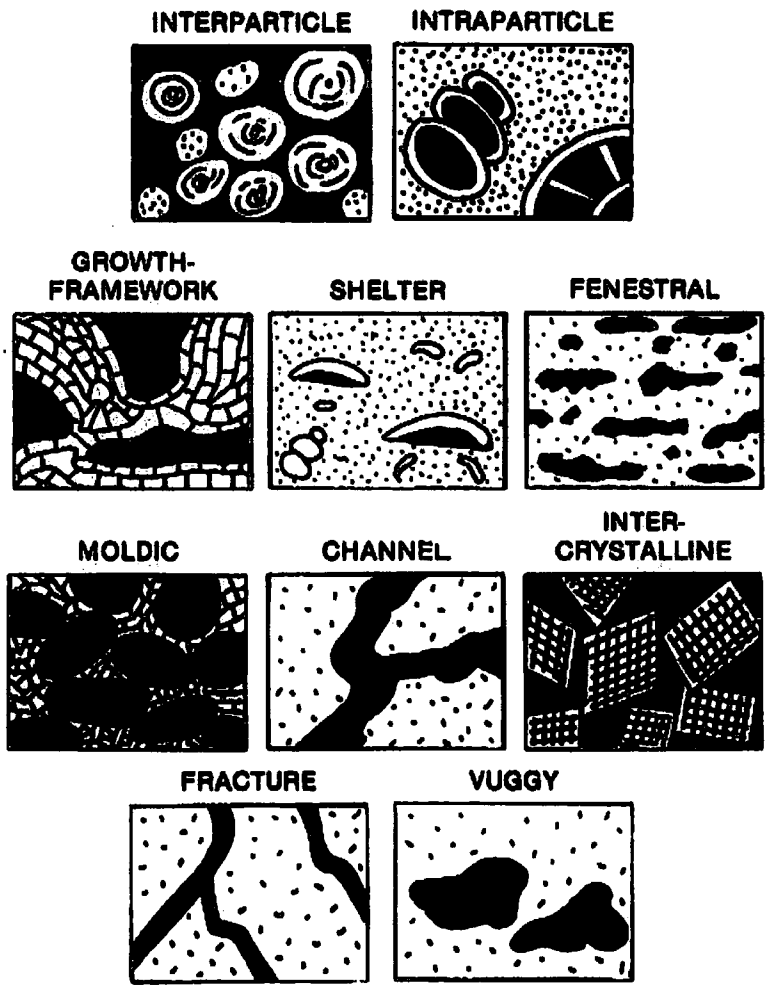

Classification of carbonate porosity (modified from Choquette and Pray, 1971).